FACULDADE DE ENGENHARIA DA UNIVERSIDADE DO PORTO

Adomian Decomposition Method, Nonlinear Equations and Spectral Solutions of Burgers Equation

Mário João Freitas de Sousa Basto

Orientador Prof. Doutor Francisco José Lage Campelo Calheiros

Coorientador Prof. Doutor Viriato Sérgio de Almeida Semião

Tese apresentada à Faculdade de Engenharia da Universidade do Porto como requisito parcial para a obtenção do grau de Doutor em Ciências da Engenharia

Dezembro de 2006
Porto

Orientador Prof. Doutor Francisco José Lage Campelo Calheiros
Departamento de Engenharia Civil
Faculdade de Engenharia
Universidade do Porto

Coorientador Prof. Doutor Viriato Sérgio de Almeida Semião
Departamento de Engenharia Mecânica
Instituto Superior Técnico
Universidade Técnica de Lisboa

AGRADECIMENTOS

Gostaria muito de agradecer ao meu orientador, Professor Francisco Lage Campelo Calheiros, e ao meu co-orientador, Professor Viriato Sérgio de Almeida Semião, por todo o apoio, sugestões e correcções propostas além da disponibilidade incondicional evidenciada.

Uma palavra de reconhecimento ao ex-Presidente do IPCA, Professor Lopes Nunes e à ex-Directora da Escola Superior de Gestão, Professora Maria José Fernandes, por me terem concedido acesso ao Prodep e pela sua amizade e incentivo. Também um agradecimento ao actual Presidente do IPCA, Professor João Carvalho e à Direcção da Escola Superior de Gestão, pelo apoio e incentivo sempre evidenciados.

Finalmente, resta a minha gratidão à minha família, muito especialmente à minha mulher e aos meus dois filhos, por todos os sacrifícios que os fiz suportar e pelo seu afecto e paciência sempre presentes.

RESUMO

Equações não lineares surgem em quase todas as áreas da Engenharia e da Física, sendo por isso de importância fundamental a existência de métodos para determinar as suas raízes. Infelizmente, como a determinação de soluções por métodos analíticos não é possivel na maioria dos casos, a construção e aplicação de métodos numéricos eficientes é essencial. O método de decomposição de Adomian tem sido aplicado com sucesso na obtenção de soluções exactas ou aproximadas de problemas lineares, não lineares, estocásticos ou determinísticos. Uma das vantagens do método é a obtenção da solução sob a forma de uma série rapidamente convergente. No entanto, isto não parece ser bem o caso quando o método é aplicado na resolução de equações não lineares, podendo-se encontrar na literatura diversas variações do método. Neste trabalho é construido um novo método iterativo baseado no método de decomposição de Adomian. A convergência e a ordem cúbica deste novo método são demonstradas.

Outra das aplicações do método de decomposição de Adomian é na resolução de equações em derivadas parciais. Sempre que a solução exacta não seja identificável a partir da série solução, a truncagem da série torna-se necessária. Uma desvantagem que daí pode advir é o raio de convergência da série ser pequeno. Aproximantes de Padé têm sido usados por diversos autores para alargar o domínio de convergência da série solução de equações diferenciais ordinárias, tendo sido obtidos bons resultados. Neste trabalho esta técnica é aplicada a equações não lineares em derivadas parciais, em particular à equação de Burgers. Só recentemente e paralelamente ao desenvolvimento deste trabalho, o uso de aproximantes de Padé aplicados à solução obtida pelo método de Adomian foi testado em equações em derivadas parciais, equações KdV e mKdV e num exemplo da equação de Boussinesq e de Burgers, onde ilustrações gráficas foram utilizadas para mostrar que a técnica pode alargar o domínio de convergência da solução, tendo sido igualmente referido que a precisão da solução podia ser melhorada pelo aumento da ordem dos aproximantes de Padé usados. Neste trabalho, além das ilustrações gráficas, são também apresentados resultados numéricos que mostram que o uso de aproximantes de Padé não só podem alargar o domínio de convergência da solução, como também podem melhorar a sua precisão. No

entanto, existe uma desvantagem ainda não referida a ter em conta no uso de aproximantes de Padé aplicados à solução obtida pelo método de Adomian: a aproximação obtida pode criar valores errados nas vizinhanças dos polos e dubletos polo/zero (Froissart) da aproximação racional sempre que a solução analítica não é obtida por este meio. É por isso conveniente tentar determinar a ordem óptima do aproximante de Padé a ser usado podendo ser conveniente reduzir a ordem deste.

A aplicação do método de Adomian após discretização espacial por diferenças finitas de uma equação em derivadas parciais, conhecido por método das linhas, é efectuada neste trabalho e mostrado que esta abordagem não tem utilidade, visto o raio de convergência da série solução poder diminuir com o número de pontos espaciais usados. De igual modo, a aplicação de aproximantes de Padé não se mostra útil neste caso.

Para valores baixos do coeficiente de viscosidade, a equação de Burgers pode desenvolver choques e descontinuidades difíceis de simular num computador. Devido ao fenómeno de Gibbs, oscilações podem ocorrer da aplicação de métodos espectrais na resolução das equações. Sob o ponto de vista dinâmico, todas estas instabilidades podem estar relacionadas com a presença de diferentes atractores e bifurcações para diferentes valores do coeficiente de viscosidade, que se podem observar na equação discretizada de Burgers por métodos espectrais. Neste trabalho é estudada a estabilidade, bifurcações e dinâmica de soluções espectrais da equação de Burgers forçada, pelo método de colocação. Na literatura está descrita para a equação de Burgers forçada, a existência de uma bifurcação de Hopf e de uma zona de atracção que surge após a perda de estabilidade das órbitas periódicas com a redução do coeficiente de viscosidade.

Neste trabalho, vários outros fenómenos são observados. Assim, são observados atractores não periódicos, torus e atractores estranhos, para valores mais baixos do coeficiente de viscosidade. Também são observadas situações de bistabilidade com dois atractores periódicos, um periódico e outro não periódico (torus ou atractor estranho) e até com dois atractores não periódicos. Neste último caso, as órbitas não periódicas parecem corresponder a movimentos quasiperiódicos. Outros pontos estáveis de equilíbrio são observados não correspondendo à solução assimptótica da equação de Burgers, podendo aí ocorrer novas bifurcaçes de Hopf, quebrando ou não a simetria que possa eventualmente estar presente no sistema considerado. A discussão sobre as condições necessárias para o surgimento destes fenómenos é também efectuada. Este tipo de comportamento indica que a equação de Burgers pode ser um bom modelo para o estudo de diferentes comportamentos dinâmicos que podem ocorrer em diferentes situações. De igual modo, este tipo de comportamento pode ser usado para o estudo e a implementação

de novas técnicas de sincronização de sistemas de elevada dimensão, dado a sua aplicação em muitas áreas tais como telecomunicações.

Condições suficientes de sincronização idêntica de equações de Burger acopladas, por intermédio de uma função de Lyapunov, são estudadas. Como aplicação para o comportamento dinâmico evidenciado pelas soluções espectrais das equações de Burgers é efectuado o estudo de soluções espectrais dessas equações acopladas unidireccionalmente, com e sem valores diferentes do parâmetro (coeficiente de viscosidade). É efectuado o acoplamento com a equação de entrada em regime estacionário, sendo o comportamento da equação de saida variável com o parâmetro de acoplamento, até estabilizar em torno da solução assimptótica. Também é confirmada a presença de sincronização idêntica ou generalizada para acoplamentos entre equações em diversos regimes assimptóticos.

Combinando a substituição parcial, técnica usada para por vezes sincronizar equações diferenciais ordinárias, e um acoplamento não linear apresentado na literatura para sistemas discretos acoplados, é construido um acoplamento não linear entre soluções espectrais da equação de Burgers, obtido por acoplamento em três diferentes posições. É observado que sincronização idêntica ou generalizada é praticamente só alcançada na posição correspondente à velocidade das ondas da equação de Burgers. É também observado o facto da sincronização ser obtida por combinação linear convexa das variáveis de entrada com as da saída, revelando que a substituição parcial pode não conduzir à sincronização do sistema, mas que isso poderá ser conseguido por este tipo de acoplamento não linear.

ABSTRACT

Nonlinear equations arise in all fields of Engineering and Physics, hence being of fundamental importance the existence of methods to find their real roots. As analytical solutions are only available in few cases, the construction of efficient numerical methods are essential. Adomian's decomposition method has been successfully applied to linear and nonlinear problems, stochastic and deterministic, obtaining an exact or approximate solution to the problem. One of its advantage is that it provides a rapid convergent solution series. However, the method applied to nonlinear equations does not seem to be fast enough to be a efficient method to solve these kind of equations and one can find in the open literature some modifications proposed by several authors. By applying the Adomian's decomposition method, a new iterative method to compute nonlinear equations is developed and is presented in this work. The convergence of the new scheme is proved herein and at least the cubic order of convergence is established.

The application of Adomian's decomposition method to partial differential equations, when the exact solution is not reached, demands the use of truncated series. But the solution's series may have small convergence radius and the truncated series may be inaccurate in many regions. In order to enlarge the convergence domain of the truncated series, Padé approximants to the Adomian's series solution have been tested and applied to ordinary differential equations, yielding promising and good results. In this thesis this technique is applied to partial differential equations, particularly to Burgers equation. Only recently, and simultaneously to the development of the work presented in this thesis, Padé approximants were implemented to the series solution given by Adomian's decomposition technique applied to partial differential equations, KdV and mKdV equations, and to an example of the Boussinesq and Burgers equation. Graphical illustrations were used to show that this technique can enlarge the domain of convergence of Adomian's solution. It is also referred that the solution accuracy can be improved by increasing the order of the Padé approximants. In this thesis, besides graphical illustrations, also numerical results are presented to show that this technique can not only enlarge the domain of convergence of the solution but also improves its accuracy even when the actual solution cannot be expressed as the

ratio of two polynomials. In addition, a disadvantage not referred can come through: the rational approximation may create inaccurate solutions near its poles when the real solution is not achieved. This drawback advises the search for the optimal order of the Padé approximant to be used, which can be of lower order.

Also, the application of Adomian's method to the ordinary differential equations set arising from the discretization of the spatial derivatives by finite differences, the so called method of lines, is performed in the present work and it is shown that this is not useful, because this technique may reduce the convergence domain of the series solution. Also, the application of Padé approximants is not useful in this case.

For low values of the viscosity coefficient, Burgers equation can develop sharp discontinuities, which are difficult to simulate in a computer. Oscillations can occur by discretization through spectral collocation methods, due to Gibbs phenomena. Under a dynamic point of view, all these instabilities may be related to the presence of different attractors and bifurcations arising to the discretized equations for different values of the viscosity coefficient. In this thesis it is studied the stability, bifurcation and dynamics of spectral collocation methods applied to forced Burgers equations, where the unknown solution of the differential equation is expanded as a global interpolant. In the open literature, it is described to the forced Burgers equation the presence of a trapping region, arising from the loss of stability of the periodic orbits arising from an Hopf bifurcation.

In this work several other phenomena are observed. In fact, it is observed the existence of nonperiodic attractors, torus and strange attractors, for lower values of the parameter below the Hopf point. Also observed is the presence of bistability with two periodic attractors, with a periodic attractor and a nonperiodic one (torus or strange attractor) and even with two nonperiodic attractors. In this last case, the nonperiodic orbits seem to correspond to quasiperiodic motions. During this work, it was verified that other stable equilibrium points can occur, diverse from the ones corresponding to the asymptotic solution of Burgers equation, and that new Hopf points can occur, breaking (or not breaking) the symmetry of the system, if present. Discussion of the necessary conditions for the emergence of these phenomena is also presented. This rich behavior indicates that Burgers equation is a good model for the study of several dynamical behaviors that can occur in many other situations. Also, this kind of behavior can be used to study and to implement new techniques of synchronization of high dimensional systems, very useful due to its application on several areas, as telecommunications.

Sufficient conditions for identical synchronization of coupled Burgers equations, by means of a Lyapunov function, is present. As an application for

the dynamics apparent by spectral solutions of forced Burgers equations, unidirectionally coupling of these equations, with and without parameter mismatch, is also studied. It is tested the unidirectionally coupling with a drive forced spatially spectral discretized Burgers equation in stationary regime and the driven equation in any motion regime. It is found out that increasing the coupling strength it is possible to carry out the suppression of the corresponding motion till the stationary solution is reached. Numerical studies show and confirm the presence of identical and generalized synchronization for different values of spacial points and different values of the viscosity coefficient in several regimes.

By combining the partial replacement used sometimes to synchronize ordinary differential equations and a nonlinear coupling presented in the literature for discrete coupled systems, a nonlinear coupling for spectral solutions of Burgers equations in three locations of the response discretized equation, is constructed. It is observed that identical or generalized synchronization is almost all the time only achieved at the position corresponding to the waves velocity, by a convex linear combination of the drive and driven variables. This point out the fact that although the partial replacement may not reach synchronization, nonlinear coupling may do it.

CONTENTS

LIST OF FIGURES

LIST OF TABLES

1. INTRODUCTION

1.1 Scope of the present work

Burgers equation [55] is one of the simplest and one of the few nonlinear partial differential equations that admits analytical solution for the initial value problem [297] [96] [97] [72] [126], having been used along the years, to test numerical methods, serving the exact solution as control. The driven equation has also been used to explore unidimensional 'turbulence' [55], in spite of this being a three-dimensional phenomenon. The turbulence in Navier-Stokes equations is incorporated in the quadratic term, the nonlinear term of convection and, therefore, Burgers equation can work as a starting point for the study of turbulence, as it possesses a nonlinear quadratic term. For low values of the viscosity coefficient, Burgers equation can develop sharp discontinuities and can be used to describe shocks and vibrations. Other phenomena as wave processes, traffic flow, acoustic transmission, gas dynamics can be studied starting from this equation [96].

To solve nonlinear differential equations, some analytical routines linearize the equations or make the assumption that the nonlinearities do not affect greatly the problem. However, the solution that one is looking for, the one that represents the physical problem, may be changed with this procedure. Perturbation methods, although providing a very useful tool in nonlinear analysis, are based on the assumption that a small parameter must exist in the equations under study, and nonlinear problems, especially those having strong nonlinearities, do not have such small parameters [119]. Usually, numerical methods are based on discretization techniques, and only approximate values of the solution are obtained and only for some values of time and space. With Adomian's decomposition method [15] [17] [16], the solution is obtained by a series expansion of the so called Adomian's polynomials, not requiring discretization of the variables, and, therefore, not being affected by errors associated to discretization. Also, this method does not require linearization or perturbation and, consequently, does not change the actual solution of the problem. As well, Adomian's decomposition method is very competent on finding an approximate or even exact solution for linear and nonlinear problems, not requiring, in many cases, large computer memory [268] [267] [269] [271] [270] [91].

It constitutes a main objective of this thesis to perform a numerical analysis of Burgers equation, studying its solution and behavior by different numerical methods, namely Adomian's decomposition method and spectral methods, viewing the possibly improvement of the solution of Burgers equation given by Adomian's decomposition method. Also, it is projected the construction of a numerical method to solve nonlinear equations, a method more efficient than Adomian's decomposition one, due to some slowness exhibited

by Adomian's method when applied to these kind of equations. Moreover, taking advantage of the behavior of Burgers equation under a low viscosity coefficient shocks development, it is intended to study its numerical solution by spectral methods, so it can bring about new insights on the behavior of higher, possibly chaotic, dimensional systems. This kind of behavior can be used to the study and to the implementation of new techniques of synchronization of high dimensional systems, very useful due to its application on several areas, as telecommunications, electronic circuits, nonlinear optics, chemical and biological systems. Hence, it is also intended to study the synchronization of coupled Burgers equation and of its coupled spectral solutions.

1.2 State-of-art

1.2.1 Burgers equation

Burgers equation [55] is a very useful equation due to the existence of analytical solution for for the initial value problem [297] [96] [97] [72] [126] and to its properties and behavior under a small viscosity coefficient [55]. Therefore, it has been used to test new numerical methods to solve partial differential equations and also to test numerical techniques to accommodate adequately discontinuities or shocks in solutions.

The one-dimensional Burgers equation is a quasi-linear parabolic partial differential equation, a simplification of the Navier-Stokes:

$$\frac{\partial u}{\partial t} + u\frac{\partial u}{\partial x} - \delta\frac{\partial^2 u}{\partial x^2} = f(x) \tag{1.1}$$

Dang-Vu and Delcarte [77], using Chebyshev collocation and Chebyshev tau methods, found out the evidence of the existence of a critical viscosity δ_c, to the spectral spatially discretized driven Burgers equation. Above that δ_c value the solution is stable and below δ_c a Hopf bifurcation takes place and the motion becomes unstable in favor of motion on a strange attractor, with the largest Lyapunov exponent positive, according to [77]. To the author's knowledge, no other studies on such motions for the spectral solutions of Burgers equations have been published in the open literature.

Numerical solutions

Several methods for both obtaining particular solutions of travelling-wave type (invariance of equations under translations) and self-similar solutions (invariance of equations under scaling transformations) have been proposed

for the vast majority of different forms of nonlinear evolution equations and Burger-type equations [79] [80] [98]. The existence of such solutions results from the invariance of those equations, respectively under translations and scale transformations, being usually difficult to implement them without numerical computations. The methods are based on the reduction of the original equations into equations with smaller number of independent variables. Many known solutions of nonlinear evolution equations are often possible to express in terms of real exponentials, which can, in turn, be recombined in powers of the tanh function. Parkes and Duffy developed a Mathematica package ATFM, Automated Tanh-Function Method [216], that allows to automate the calculations involved in the application of the so-called tanh-function method of solution [194], provided that solutions of the assumed form exist and are expressed in the form $u = \sum_{i=0}^{M} a_i \tanh^i [k(x - ct - x_0)]$, where x_0 is an arbitrary constant.

Analytical solutions and asymptotic expansions for some cases of Burgers equation on the semiline, with a flux-type boundary condition at the origin, were obtained by Biondini and Lillo [48].

Xu *et al.* proposed finite difference schemes using global discretization for convection-difusion equations [302].

Dogan [87] proposed, for the numerical solution of Burger's equation, an approach with a Galerkin finite element method and for the resolution of the resulting system of ordinary differential equations a Crank-Nicholson approach with a linear approximation of the nonlinear term. Other finite element approaches were presented in the work of [214] and [46].

A sparse-mode spectral algorithm for turbulent flows was proposed together with tests applied to the Burgers equation [202].

A technique using step integration over a small interval of the independent variable, after space discretization by finite differences, followed by the calculation of the average values for each element and repetition of the process until there is no change on the computed values was presented by Arafa [30].

A direct variational method after Hopf-Cole transformation was applied by Ozis and Özdes [215].

Finite difference schemes [170] and finite variable difference methods (FVDM) [141] [142] were proposed in the lates 90s.

An approach based on a recursive symbolic computation was introduced by [81], where the analytical solution is approximated by a discrete process in time. It has the disadvantage of easily produce overflow of the solution, requiring some filtering process to eliminate higher order negligible terms.

Multiresolution techniques and wavelets have been used in the develop-

ment of numerical schemes for the solution of partial differential equations. Muniandy and Moroz [206] present a wavelet Galerkin approximation of the Burgers equation using complex harmonic wavelets.

Wei *et al.* [295] proposed, to approximate the spatial derivatives, the method of distributed approximating functionals (GLDAF). They have tested the method with Hermite DAF, on Burgers equation uni and bidimensional $\frac{\partial U}{\partial t} + (U \cdot \nabla) U = \delta \Delta U$

$$\frac{\partial u}{\partial t} + u\frac{\partial u}{\partial x} + v\frac{\partial u}{\partial y} = \delta \left(\frac{\partial^2 u}{\partial x^2} + \frac{\partial^2 u}{\partial y^2} \right) \tag{1.2}$$

$$\frac{\partial v}{\partial t} + v\frac{\partial v}{\partial y} + u\frac{\partial v}{\partial x} = \delta \left(\frac{\partial^2 v}{\partial x^2} + \frac{\partial^2 v}{\partial y^2} \right) \tag{1.3}$$

The same authors, fall back upon other variations of this method, using Gaussian Lagrange distributed approximating functionals (LDAFs) [294]. According to the authors, the DAFs methods show enough flexibility to treat complicated geometries and boundary conditions and simultaneously they present a high precision characteristic of spectral methods.

The multiquadric (MQ) scheme, a spatial approximation scheme for solving Burgers equation, was applied by Hon and Mao [125].

The one-parameter group transformation was used in the work of [90] to calculate an exact analytical solution of Burgers equation. Burgers equation is reduced to an ordinary differential equation, which is analytically solved and the solution is obtained in closed form.

A metodology by balancing the nonlinear and dispersive effects in nonlinear evolution equations was used to obtain analytical solutions for Burgers equation, the nonlinear heat equation, the modified KDV equation and the Kuramoto-Sivashinsky equation [2].

Finite difference models based upon center manifold theory, so the discretization accurately models the dynamics, were introduced by [236]. A finite difference scheme for Burgers equation having no diffusion and a nonlinear logistic reaction term was constructed and presented in the work of [203]. A linearized implicit finite-difference scheme for the one-dimensional Burgers equation was presented by [171]. Others schemes, as quadratic splines over finite elements [171] or cubic splines over finite elements [76], a mixed method using boundary elements in association with finite differences [37] have also appeared in the open literature.

Esipov [94] derived a coupled system of viscous Burgers equations

$$\frac{\partial u}{\partial t} + u\frac{\partial u}{\partial x} = \frac{\partial^2 u}{\partial x^2} - a \cdot \left(\frac{\partial}{\partial x}(uv)\right) \tag{1.4}$$

$$\frac{\partial v}{\partial t} + v\frac{\partial v}{\partial x} = \frac{\partial^2 v}{\partial x^2} - b \cdot \left(\frac{\partial}{\partial x}(uv)\right) \tag{1.5}$$

with zero Dirichlet boundary conditions

$$u(0,t) = u(1,t) = 0 \tag{1.6}$$

$$v(0,t) = v(1,t) = 0 \tag{1.7}$$

This coupled system is a simple model of sedimentation or evolution of scaled volume concentrations of two kinds of particles in fluid suspensions, under gravity effect. Nee and Duan [210] showed that this system with initial data not too large, approach the zero equilibrium as time goes to infinity, not necessarily exponentially fast, unlike the single viscous Burgers equation.

A finite element approximation of the two-dimensional steady Burgers equation was presented by [49].

The spectral spatially discretized driven Burgers equation [77], $\frac{\partial u}{\partial t} = -u\frac{\partial u}{\partial x} + \delta\frac{\partial^2 u}{\partial x^2} + f(x)$, by Chebyshev collocation and Chebyshev tau method, provides evidence for the existence a critical viscosity δ_c, above which the solution is stable and below which a Hopf bifurcation takes place and the motion becomes unstable in favor of motion on a strange attractor. Note that spatial chaos cannot arise in steady Burgers equation, because Burgers equation with a driven term time independent is reduced to a two-dimensional dynamical system, and from Poincaré-Benidixson theorem, it can only have stable equilibria and stable limit cycles as attractors.

An implicit finite-difference scheme for the two-dimensional Burgers equation was developed by Bahadir [38].

Numerical solutions for shocks

In general, hyperbolic equations in conservative form are intimately linked to the presence of solutions with discontinuities and shocks.

Traditional finite difference schemes are based on interpolation of discrete data, using polynomials on fixed stencils, depending the order of accuracy on the width of the stencil, provided the function being interpolated is smooth inside it. For non smooth problems, this approach exhibits oscillations in the neighborhoods of the discontinuities that do not decay in magnitude when the mesh is refined. Such oscillations constitute the Gibbs

phenomenon in spectral methods, which establishes that the pointwise convergence of global approaches of discontinuous functions is at most of first order. In a neighborhood of a point of discontinuity of a function f, the convergence of the Fourier series of f cannot be uniform. Defining the oscillation of the series partial sum of order n near a discontinuity point x_0, as $w_n(x_0, \varepsilon) = \max s_n(x) - \min s_n(x)$([1]), $x \in [x_0 - \varepsilon, x_0 + \varepsilon]$, the oscillation $w_n(x_0, \varepsilon)$ does not approach the discontinuity point at x_0, but it is verified that the partial sums tend to pass the limits in the discontinuity region, being these oscillations $O(1)$ [95]. For differential equations with smooth solutions, spectral methods exhibit exponential or spectral accuracy. For problems with sharp gradients and discontinuities, the accuracy of these high order global methods deteriorates.

One way to eliminate or reduce these numerical oscillations, is to add some artificial viscosity to the problem [88]. However, such approach has the disadvantage of the dependency of the parameter that controls the size of the artificial viscosity on the problem under study.

Other forms of treating the discontinuities involve three main approaches: *shock fitting*, *front tracking* and *shock capturing* [75]. Starting from information given by the characteristics, the method of shock fitting tries to follow the discontinuities. They are usually of difficult programming and of difficult generalization for systems of equations. Following the development of the discontinuities, seeking for more accuracy in their location, but also of difficult programming, are the methods of front tracking. The methods that obtained larger acceptance in the scientific community are the shock capturing ones. Such methods are appropriate to eliminate the oscillations and do not demand any special treatment of the discontinuity, consist of applying limiters to eliminate the oscillations, known by total variation diminishing (TVD) [114].

The TDV schemes were generalized since 1987, to the essentially non-oscillatory schemes (ENO), with the classic work of Harten *et al.* [116], and later to the weighted essentially non-oscillatory schemes (WENO) [116] [248] [115] [60] [247], schemes of higher order accuracy, having been built to solve problems with piecewise smooth functions, with discontinuities of first kind, as the ones that appear in the shock surfaces in conservation laws. These schemes allow to solve discontinuities without numerical oscillations, avoiding the Gibbs phenomenon (these oscillations occur because the stencils actually contain the discontinuous cell) and are suitable especially for problems containing both shocks and complicated smooth flow structures, such those occurring in shock interactions with a turbulent flow [247]. The

[1] $(s_n)_n$ is the Fourier series partial sum sequence of f

ENO schemes involve the reconstruction of the solution (starting from cell averages or point values), using an adaptative stencil, that vary with the space location, avoiding when possible the inclusion of the cells containing discontinuities in the stencil.

The WENO schemes [191] involve a linear convex combination of all candidate stencils, instead of just one as in the above mentioned ENO schemes. More recently, optimized WENO schemes [266] were developed to increase their order of precision, robustness and efficiency. The temporal discretization fall back upon the TVD Runga-Kutta schemes and more recently to the Lax-Wendroff type schemes [233].

An essentially nonoscillatory Fourier method, for first order nonlinear hyperbolic equations, based on the formulation by cell averages, was presented by Cai *et al.* in [60]. The method consists of adding step functions to the base functions used in the spectral approximation, in the process of reconstruction of point values starting from the cell averages, in a way that the Gibbs phenomenon is eliminated. An extension of this method for the case of multiple discontinuities was presented in [209].

A new method of cell average spectral Chebyshev approximation (CAC) for first order hyperbolic equations in conservation form, and the formulae between the pointwise data at the collocation points and the cell averaged quantities, can be consulted in the work of [59]. The spectral algorithm of Crossley *et al.* [74], for the numerical solution of partial differential equations, is based on the observation that it is enough to add step functions to the series approximants smooth functions to represent functions with discontinuities, differing essentially from the method exposed by [60] for doing this in the physical space rather than in the transformed space. It makes use of Harten's method about subcellular resolution, in the sense that the cell-averages of a discontinuous piecewise-smooth function contain information about the exact location of the discontinuity within a cell [115].

Other nonoscillatory spectral methods possessing the properties of both upwind difference schemes and ENO, efficient in the capture of shocks, and of the spectral methods, as methods of high order, were presented in [61].

A tool for shock capturing was proposed by a single-sided locally averaged adaptative coupling scheme for the synchronization of spatially extended systems [293].

The application of the differential quadrature method (DQM) has been employed to approximate spatial partial derivatives, requiring interpolation in space. This interpolation can be obtained through the use of Lagrange polynomials, but there are advantages of using *sinc* functions to solve initial boundary value problems characterized by oscillating behaviors in space, due to the spectral approximation properties [44] [300]. A method to solve

nonlinear evolution equations involving steep gradients, the linearized and rational approximation method (LRAM) was presented by [300].

1.2.2 Adomian's decomposition method

In the beginning of years 1980s, a new method for exactly solving nonlinear functional equations of various kinds has been proposed by Adomian, the so called Adomian decomposition method (ADM) [15] [17] [16] [19] [22]. Over the past twenty years, it has been applied to solve and to obtain formal and approximate solutions to a wide class of problems, both deterministic and stochastic, linear and nonlinear, arising from Physics, Chemistry, Biology, Engineering, etc. for all types of boundary or initial conditions. Nonlinear phenomena play a crucial role in Applied Mathematics and Physics, Mechanics, Biologics, and, therefore, explicit solutions to the nonlinear equations are of fundamental importance to preserve the actual physical character of the problem and to understand deeply the described process. Calculating exact and numerical solutions, in particular traveling wave solutions of nonlinear equations in mathematical physics, plays an important role in soliton [2] theory [14]. Several methods for obtaining explicit solutions of nonlinear evolution equations are described in the literature, like the similarity methods [245], the generalized separation of variables, the tanh method, the sine-cosine method, the Painlevé method, the Darboux transformation, the inverse scattering transform (IST), which allows transforming nonlinear evolution equations, into linear ones [181] [232] [14], the Bäcklund transformation (like the Hopf-Cole transformation in the Burgers equation [126], [72]) among others [78] [232]. For both linear and nonlinear problems, Adomian's approach has revealed great results for obtaining an exact or approximate analytical solution, with very fast convergence to the actual solution, high accuracy, minimal calculation, and does not need linearization, weak nonlinearity assumptions or perturbation theory to be applied, avoiding physical unrealistic assumptions [15] [19] [17] [22].

The technique uses a decomposition of the nonlinear operator as a series function. Each term is a generalized polynomial called *Adomian polynomial*. Adomian introduced formulae to generate these polynomials for all kind of nonlinearities [17] [15] [19] [22].

[2] A soliton is a solitary traveling nonlinear wave solution that obeys a superposition-like principle (solitons passing throught one another emerge unmodified) [299]

Advantages of the method

Advantages of the Adomian's decomposition method applied to many linear and nonlinear problems are emphasized by many authors. Common analytical procedures, to solve nonlinear differential equations, linearize the system or assume that the nonlinearities are relatively small, transforming the physical problem into a purely mathematical one with an available solution. This procedure may change the real solution of the mathematical model which represents the physical reality. Generally, the numerical methods are based on discretization techniques, and permit only to calculate the approximate solutions for some values of time and space variables, which has the disadvantage of causing overlooking for some important phenomena occurring in very small time and space intervals, such as chaos and bifurcations. Perturbation methods may only be applied when nonlinear effects are very small.

Adomian's method does not require discretization of the variables. Hence, the solution is not affected by computation roundoff errors and the necessity of large computer memory. Moreover it does not require linearization or perturbation, and, therefore it does not need any modification of the actual model that could change the actual solution, being very efficient on determining an approximate or even exact solution in a closed form, on both linear and nonlinear problems, minimizing in many cases the computational work [268] [267] [269] [271] [270] [91].

Another advantage of Adomian's decomposition technique is that it provides a fast accurate convergent series, attribute manifested by several authors [69] [22] [6] [7] [8] [10] [68], being this the reason why it is only necessary a small number of terms to obtain an approximate solution with high accuracy [143] [145] [92] [67].

A particular phenomenon noticed by Adomian and Rach [25], is the existence of the "self-canceling noise terms" for a decomposition series solution, where the summation vanishes at the limit. The noise terms are identical terms with opposite signs that may appear in various components u_k of the series solution of $u(x)$. The authors concluded that those noise terms appear for every nonhomogeneous partial differential equation, whereas the homogeneous equations show no noise terms. Such conclusions were based on observations made when the authors were working on specific examples. Wazwaz extended the previous study to nonhomogeneous ordinary differential and integral equations, showing that this conclusion is not always correct, exhibiting the nonhomogeneous behavior as a necessary condition but not sufficient [269]. The author also thinks that, for the appearance of effective noise terms, the exact solution must be included in the zeroth component u_0

of the series solution of $u(x)$ [269] [288]. This phenomenon does not appear with homogeneous equations, but provides a major advantage of the method.

Comparisons with other numerical methods have been investigated by several authors. Bellomo and Monaco [45] compared Adomian's method with perturbation techniques, emphasizing the efficiency of Adomian's method in contrast with the exhaustive work required by application of perturbation techniques. In the work of [234] the relatively simple computation required by the decomposition method is compared with that of Picard iterative method, exhibiting the last one a fast growing computational complexity. Comparisons with a wavelet-Galerkin method (WGM) for the solution of integro-differential equations [91] show that the Adomian's decomposition method is efficient, easy to use, and, moreover, it minimizes the computational calculus and supplies quantitatively reliable results, which can be obtained in explicit form. Wazwaz compared Adomian's method with the Taylor series method [270], concluding that the decomposition method is efficient, produces reliable results with few iterations, is easy to use from a computational viewpoint minimizing the computational difficulties of the Taylor series, and handles nonlinear problems in a similar manner as linear problems, overcoming thus the deficiency of linearization or perturbation. Guellal [107] deduced that the graphical results obtained by Adomian's method applied to Lorenz's equations are similar to those obtained by Runga-Kutta discretization, but with faster convergence of Adomian's technique. The results were similar, but with less subdivisions of the time interval $[0, T = 20]$ for Adomian's method (20 against 400 subdivisions for the Runga-Kutta method). Shawagfeh and Kaya [246] presented a numerical comparison between Adomian's decomposition technique and a fourth-order Runga-Kutta method for solving systems of ordinary differential equations, concluding that Adomian's technique is very powerful, quite accurate, readily implemented and efficient in finding analytical as well as numerical solutions. Vadasz and Olek [261] doing a more comprehensive study of the same equation concluded that the Adomian's method is more precise than the Runga-Kutta one.

Applications of the method

Applications of the Adomian's decomposition method and its modifications have roused the attention of several researchers, so it could be possible to solve a great diversity of both ordinary as well as partial linear and nonlinear differential equations, deterministic and also stochastic.

One can find in the open literature, among other studies, applications to stochastic problems [20] [21], wave equation [271] [67], nonlinear advection equation [267], Lorenz equations [107] [261], heat equation [18] [111],

Burgers equation [22] [149], two-dimensional Burgers equation (STDBE) $\frac{\partial \overrightarrow{u}}{dt} + (\overrightarrow{u} \cdot \nabla)\overrightarrow{u} = \mu \Delta^2 \overrightarrow{u}$ [92] [150], Korteweg-de-Vries and Korteweg-de-Vries-Burger type equations [23] [284] [145] [144], combined Korteweg-de-Vries-Modified Korteweg-de-Vries (KdV-MKdV) equation [148], Volterra and Fredholm integral type equations [292] [287], Thomas-Fermi equation [24] [274], systems of partial differential equations [278], boundary value problems of higher order [277] [282], problems with singular points like Lane-Emden type equations [280] [286], Fisher and Fisher type equations [290], Burger's-Huxley and Burger's-Fisher equations [130], the model of dispersive nonlinear waves proposed by Boussinesq [285], nonlinear dispersive equations which exhibit compactons $\frac{\partial u}{\partial t} + \frac{\partial u^m}{\partial x} + \frac{\partial^3 u^n}{\partial x^3} = 0$, $m > 1$, $1 \leq n \leq 3$, equations denoted by $K(m, n)$ [283], generalization of the KdV equation to two space variables, Kadomtsev-Petviashvili equation [279], coupled Schrödinger-Korteweg-de Vries equation [146], achievement of known results of special functions of mathematical physics as the hypergeometric function and Bessel functions [86], integrals by reformulation into differential equations [112], ordinary differential equations with discontinuities [63], nonlinear and systems of nonlinear equations [7] [34].

According to Liu [190] and He [118], the problem of solving nonlinear boundary partial differential equations, by using Adomian's decomposition method, is the impossibility that appears in satisfying all its boundary conditions, leading to an error at its boundary. Following Wazwaz [276], with the proper investment on Adomian's method, the conclusion drawn by Liu and by He is not quite exact, and the exact solution can be obtained for some boundary value problems on closed form solutions, or a rapid convergent series solution is always attainable [19]. On the formulation of boundary value problems, it is possible to have an unknown function or parameter that is determined later by imposing the other boundary condition [281].

Initial-boundary value problems have been usually solved based only on the imposition of the initial conditions with the nonimposed boundary conditions being naturally satisfied. To solve some PDEs by imposing both initial and boundary conditions, Ngarhasta *et al* [211], suggested taking in account both initial and boundary conditions in the canonical form, by choosing the first term of Adomian's series verifying all conditions. Also, to overcome this problem, by imposing both initial and boundary conditions, Adomian [16] proposed a new approach to solve the initial boundary heat linear one-dimensional differential equation. Due to some wrong limits obtained, Lesnic [182] [183] [184] proposed a modification of Adomian's approach to solve linear initial-boundary problems, referring that it could be extended to higher-dimensional, inhomogeneous and nonlinear problems.

Adomian's method modifications

A modification of Adomian method is proposed by [263] to overcome the computational difficulties arising when obtaining the solution of differential equations containing radicals while inverting the operator, particularly when the initial approximation is not a constant. It is proposed the expansion of the nonlinear term in the equation involving radicals in a power series, followed by its Padé approximant [39].

Wazwaz [272] proposed a modification of the Adomian's decomposition method in order to simplify the calculations and accelerate the rapid convergence of the series solution, the modified technique, the method being validated through several examples. He proposed a small modification for the first two components, u_0 and u_1. The function f, that represents u_0 by the classic method, is divided into two parts $f = f_1 + f_2$, with f_1 the new zeroth component u_0, whereas the remaining part f_2 is combined with the other terms of u_1. The main reason for this modification is that Adomian's polynomials depend considerably on u_0, and therefore, the reduction of its number of terms could make easier the calculation of Adomian's polynomials, as it can be seen in the work of [274] where the difficulties appeared with the nonlinear term given by the exponent of a radical, or in the work of [277] and [282] where the difficulties from the high order of differential and integrate-differential equations are surpassed with the modified technique.

A new modification proposed by the same author was introduced in [289], where the function f that represents u_0 by the classic method is expressed in Taylor series, and a new recursive relationship is suggested.

For nonlinear oscillatory systems, as the solution given by Adomian's method did not exhibited periodicity, Venkatarangan and Rajalakshmi [263] modified the Adomian's solution making it periodic, using a technique suggested by Nayfeh [208]. The authors applied the Laplace transform to the Adomian's truncated series, followed by Padé approximants and finally the inverse Laplace transform, which yielded a better and also periodic solution.

There are some disadvantages on the Adomian's decomposition method. The solution's series may have small convergence radius and the truncated series solution may be inaccurate in some regions [132] [65] [93]. One way of improving the mathematical structure, enlarging the convergence domain of the truncated series solution, can be achieved by defining Padé approximants (PAs), converting the polynomial approximation into a ratio of two polynomials, a rational function [29] [274] [273] [274] [132] [4] [5] [43]. Padé approximants, generally, may enlarge the convergence domain of the truncated Taylor series and improve the convergence rate of the truncated series [132]. Also, Padé approximants will converge on the entire real axis if the

function is free of real singularities. An aftertreatment technique (AT) by using Padé approximants to modify Adomian's series solution, applied to ordinary differential equations with initial conditions, is proposed by [132].

Cheng *et al.* [65] suggest a piecewise solution technique, by dividing the solution space into regions, to overcome the divergent difficulties arising from small convergence radius.

In the work of [93] the Adomian's method approximated to the first two terms is applied to the Riccati matrix differential equation in a recursive form, in n subintervals on the time horizon, which can be used to obtain the solution for the entire time interval considered. The authors named the method as the multistage Adomian's decomposition method (MADM), being based on the fact that the first two terms give a good approximation for the Riccati matrix equation, only in the neighborhood of the initial time. The accuracy of the method can be increased either by choosing a smaller time interval or by adding more terms.

To solve the Burgers equation, Abbasbandy and Darvishi [13] proposed transforming the equation into a nonlinear ordinary differential one, by means of time discretization, solving it then by Adomian's method.

To solve nonlinear equations by Adomian's decomposition method, some modifications are proposed in the open literature. By rearranging the problem in such a way that the order of convergence of Adomian's method is improved [32], Babolian and Biazar proposed a method to solve nonlinear equations [33]. Other modifications of standard Adomian's method can be found in the work of Abbasbandy [12] and Babolian and Javadi [35]. In the approach of Abbasbandy [12], to solve the nonlinear equation $f(x) = 0$, three terms of Adomian's series solution applied to a second order Taylor expansion of the nonlinear function f are kept, so a iterative method is constructed. In the approach of Babolian and Javadi [35], an algorithm named as the restarted Adomian method, is proposed to solve nonlinear equations of the type $x = F(x) + c_0$, by applying Adomian's approximated series to the equation, and restarting successively with a new starting point. Choosing x_0 close enough to the exact solution, the truncated series $\sum_{k=0}^{n} x_k$ will be a good approximation for the solution of the equation for a moderate value of n. Starting with an initial value $x_0 = c_0$, by application of Adomian's method, a solution x_1 is obtained and then making $x = F_1(x) + x_1$ with $F_1(x) = F(x) - (x_1 - x_0)$. The process is repeated until the difference between the last two consecutive values of x satisfies a given tolerance ε [35].

1.2.3 Coupling and synchronization

Identical synchronization

Synchronization of periodic signals is a well-known phenomenon in Physics, Engineering and many other scientific areas. Synchronization has a fundamental importance in telecommunication, electronic circuits, nonlinear optics, and chemical and biological systems. In spite of being natural to associate synchronization with periodic signals, chaotic systems also can synchronize [99] [227]. Synchronization of chaotic systems has been studied due to its interest and applicability. Chaos synchronization has reached a great interest because of its potential applications in the transmission of secure information [159], control and suppression of chaos, anticontrol of chaos and estimation of model parameters from time series. Since 1993 that researchers have realized that chaotic systems can be synchronized, by the numerical observation of the phenomenon in a lattice of diffusively coupled chaotic systems [99].

A definition for *identical synchronization* is the following [227]:

Definition 1: Two dynamical systems are said to be identical synchronized if both trajectories $\mathbf{x}_t$ and $\mathbf{y}_t$ are bounded and $\lim_{t\to\infty} |\mathbf{x}_t - \mathbf{y}_t| = 0$. The equality $\mathbf{x}_t = \mathbf{y}_t$ defines a dynamical behavior restricted to an invariant hyperplane in the phase space, called synchronization manifold.

A possible definition for an attractor is given by Milnor [204] [205]:

Definition 2: A closed subset $A \subset M$, M invariant manifold, is an attractor of F, if it satisfies the following two conditions:

- its **basin of attraction** $\beta(A)$, consisting of all points $x \in M$, for which all its limit points with $t \to \infty$ belong to A, has strictly positive Lebesgue measure, and
- there is no strictly smaller closed set $A' \subset A$ such that $\beta(A') = \beta(A)$ up to a set of measure zero.

An attractor is said to be minimal if no proper subset is an attractor.

Studying synchronization requires the find out of the *invariant synchronization manifold* in the phase space and then the determination of its stability. In a coupled system, the property of having a synchronization manifold is independent of the motion attraction to that manifold when it started away from it. This property is related to stability, and, therefore, it is important to determine whether perturbations transverse to the invariant subspace damp out or are amplified. This means that one has to determine if

the invariant subspace is an attractor. If perturbations damp out, the motion is restricted to the synchronization manifold. Many different types of synchronization schemes are possible in both unidirectional and bidirectional coupling schemes [227].

Pecora *et al.* [227] analyzed and review several synchronization schemes of chaotic systems, with great potential for applications in communications systems. They considered the case of synchronization of two identical systems, showing that different initial conditions often drive to identical chaotic synchronization. Also for certain coupling schemes, the synchronization is robust under disturbances in the parameters of the systems of the drive or of the response [133].

In the presence of *identical synchronization*, which is revealed by the equality of the components of both systems, the synchronization manifold is an hyperplane. Assuming that the hyperplane contains the origin of the coordinates (since this is just a simple translation that keeps the geometry) then the transverse space, the space orthogonal to the synchronization manifold, must have zero coordinates when the motion is on the synchronization manifold.

The stability of the invariant synchronization manifold is guaranteed if perturbations transversal to this manifold damp out. The most general criterion, and it appears also the minimal condition for stability, used to study the stability of the synchronization manifold of coupled chaotic oscillators was proposed by Fujisaka and Yamada [99]. It consists of having all the Lyapunov exponents associated to the transverse subsystem negative. Such study was made starting from the variational equations of the system that supply the dynamics of the transverse disturbances to the synchronization manifold [99] [121] [227]. However, this is only a necessary criterion for stability, due to the fact that large desynchronizations bursts can be observed in spite of the largest negative Lyapunov exponent [120] [227] [102]. This is explained by the fact that the Lyapunov exponents are only ergodic means over the attractor. One would have to show that all of the Lyapunov exponents are negative for all the measures of the dynamics. Gauthier and Bienfang [102] suggest as sufficient condition to quickly estimate the range of coupling strengths that result in high-quality coupled chaotic oscillators, not interrupted irregularly by large (comparable to the size of the attractor) and brief desynchronization events (bubbling attractor), by investigating the time derivative of the Lyapunov function $\mathcal{L}(\mathbf{x}_\perp) = |\delta\mathbf{x}_\perp(t)|^2$, $\mathbf{x}_\perp(t) = \mathbf{x}^{(1)}(t) - \mathbf{x}^{(2)}(t)$.

In the presence of two identical chaotic systems, with an *unidirectionally coupling* scheme (*master-slave configuration*), Pecora *et al.* named as *complete replacement* [224] [225] [227] the substitution of one or more of the components of the response system by the corresponding components of the

drive system (for instance, a transmitted signal from the drive to the response as being a subsystem from the drive), which reduces the dimension of the response system:

$$\begin{bmatrix} \frac{d\mathbf{u}^{(1)}}{dt} \\ \frac{d\mathbf{v}^{(1)}}{dt} \end{bmatrix} = \begin{bmatrix} F_1\left(\mathbf{u}^{(1)}, \mathbf{v}^{(1)}\right) \\ F_2\left(\mathbf{u}^{(1)}, \mathbf{v}^{(1)}\right) \end{bmatrix} \tag{1.8}$$

$$\left[\frac{d\mathbf{v}^{(2)}}{dt}\right] = \left[F_2\left(\mathbf{u}^{(1)}, \mathbf{v}^{(2)}\right)\right] \tag{1.9}$$

In the previous equations, equation (1.8) is the drive and equation (1.9) the response.

Identical synchronization takes place if $\lim_{t\to\infty}\left|\mathbf{v}^{(1)} - \mathbf{v}^{(2)}\right| = 0$, being $\mathbf{u}^{(1)}$ the components of equation (1.8) that drive the response equation (1.9) by complete replacement, named *synchronization driven* by $\mathbf{u}^{(1)}$.

A dynamical system is said to be *absolutely synchronizing* if synchronization takes place for every $\mathbf{u}^{(1)}$. A dynamical system is said to be *resynchronizable* if there are, at least, two synchronizing coordinates. Similarly, one defines as *absolutely resynchronizing,* a system possessing at least two absolutely synchronizing coordinates [256]. An example of a resynchronizing dynamical system are the Lorenz equations. The study of the stability of the synchronization manifold is made by making recourse to the Lyapunov exponents from the variation subsystem $d\left(\mathbf{v}^{(1)} - \mathbf{v}^{(2)}\right)/dt$ [224], named by Pecora and Caroll [225] as *conditional Lyapunov exponents*, because they depend on the trajectory of $\mathbf{u}^{(1)}$. In [227] complete replacement is exemplified with two chaotic Lorenz systems, where the driven signal is the first component x. In other words, the x component from the response system is substituted by the respective component of the drive system:

$$\begin{bmatrix} \frac{dx^{(1)}}{dt} \\ \frac{dy^{(1)}}{dt} \\ \frac{dz^{(1)}}{dt} \end{bmatrix} = \begin{bmatrix} \sigma\left(y^{(1)} - x^{(1)}\right) \\ rx^{(1)} - y^{(1)} - x^{(1)}z^{(1)} \\ x^{(1)}y^{(1)} - bz^{(1)} \end{bmatrix} \tag{1.10}$$

$$\begin{bmatrix} \frac{dx^{(1)}}{dt} \\ \frac{dy^{(2)}}{dt} \\ \frac{dz^{(2)}}{dt} \end{bmatrix} = \begin{bmatrix} \sigma\left(y^{(2)} - x^{(1)}\right) \\ rx^{(1)} - y^{(2)} - x^{(1)}z^{(2)} \\ x^{(1)}y^{(2)} - bz^{(2)} \end{bmatrix} \tag{1.11}$$

the parameters σ, r and b being real and positive. In chaotic regime, identical synchronization is observed. The dynamics is then restricted to the three-dimensional hyperplane $y^{(1)} = y^{(2)}$ and $z^{(1)} = z^{(2)}$ defined on a five-dimensional space. To study the stability, a change of coordinates is made,

$y_{\shortparallel} = y^{(1)} + y^{(2)}$, $y_{\perp} = y^{(1)} - y^{(2)}$ and $z_{\shortparallel} = z^{(1)} + z^{(2)}$, $z_{\perp} = z^{(1)} - z^{(2)}$, three coordinates belonging to the synchronization manifold $\left(x^{(1)}, y_{\shortparallel}, z_{\shortparallel}\right)$ and two to the transverse manifold $(y_{\perp}, z_{\perp})$. One needs to have $y_{\perp}$ and $z_{\perp}$ approaching zero as $t \to \infty$. Thus, the zero point $(0, 0)$ in the transverse manifold must be a fixed point within that manifold. So, the dynamical transverse subsystem $\frac{dy_{\perp}}{dt}$ and $\frac{dz_{\perp}}{dt}$ must be stable at the $(0, 0)$ point, which requires the negativity of the largest Lyapunov exponent of the variational equations for the response subsystem,

$$\begin{bmatrix} \frac{dy_{\perp}}{dt} \\ \frac{dz_{\perp}}{dt} \end{bmatrix} \approx \mathbf{D}F_2 \cdot \begin{bmatrix} y_{\perp} \\ z_{\perp} \end{bmatrix} \tag{1.12}$$

where $\mathbf{D}F_2$ is the Jacobian of F_2 calculated in the attractor, in the synchronization manifold. This is equivalent to requiring the response subsystem $y^{(2)}$ and $z^{(2)}$ to have negative Lyapunov exponents. Lorenz system driven by the component y is also synchronized, being the subsystem (x, z) asymptotically stable [224], which means that the Lorenz system has two synchronizing coordinates and is, therefore, resinchronizable.

The replacement of one or more components from the drive system into the driven one, can also be done in a partial manner [109] [108] [227] step that is named as *partial replacement*. In the partial substitution approach a response variable is replaced with the drive counterpart only in certain locations, depending on which replacements will cause stable synchronization and which of them are accessible in the physical device that one is interested in building.

From a more general viewpoint one can synchronize two chaotic unidirectionally coupled systems by *diffusive coupling*, also called *negative feedback control*, where the above technique of complete replacement is a special case [227]. It consists of adding a damping term to the response system, a difference between the drive and response variables:

$$\frac{d\mathbf{x}^{(1)}}{dt} = F\left(\mathbf{x}^{(1)}\right) \tag{1.13}$$

$$\begin{aligned} \frac{d\mathbf{x}^{(2)}}{dt} &= F\left(\mathbf{x}^{(2)}\right) + \alpha E \cdot \left(\mathbf{x}^{(1)} - \mathbf{x}^{(2)}\right) \\ &= \left(F\left(\mathbf{x}^{(2)}\right) - \alpha E\right) \cdot \mathbf{x}^{(2)} + \alpha E \cdot \mathbf{x}^{(1)} \end{aligned} \tag{1.14}$$

In the previous equations, E is the matrix that determines the linear combination of the components that will be used in the difference and α determines the strength of the coupling. The Lyapunov exponents are determined by the variational equation $\frac{d\mathbf{x}_{\perp}}{dt} = [DF - \alpha E]\,\mathbf{x}_{\perp}$. In [227] this type

of coupling is exemplified with two chaotic Rössler systems, where $E_{ij} = 0$, except $E_{11} = 1$:

$$\begin{bmatrix} \frac{dx^{(1)}}{dt} \\ \frac{dy^{(1)}}{dt} \\ \frac{dz^{(1)}}{dt} \end{bmatrix} = \begin{bmatrix} -\left(y^{(1)} + z^{(1)}\right) \\ x^{(1)} + ay^{(1)} \\ b + z^{(1)}\left(x^{(1)} - c\right) \end{bmatrix} \tag{1.15}$$

$$\begin{bmatrix} \frac{dx^{(2)}}{dt} \\ \frac{dy^{(2)}}{dt} \\ \frac{dz^{(2)}}{dt} \end{bmatrix} = \begin{bmatrix} -\left(y^{(2)} + z^{(2)}\right) + \alpha\left(x^{(1)} - x^{(2)}\right) \\ x^{(2)} + ay^{(2)} \\ b + z^{(2)}\left(x^{(2)} - c\right) \end{bmatrix} \tag{1.16}$$

In the same way as before, the negativity of the largest Lyapunov exponent of the system $\frac{d\mathbf{x}_\perp}{dt}$, $\lambda_{\max}^{\perp}$, gives a necessary condition for stability. This exponent is a function of α. The effect of adding coupling is, at first, to decrease the largest Lyapunov exponent occurring for most coupling situations of chaotic systems [121]. However, at larger values of α, $\lambda_{\max}^{\perp}$ becomes positive and the synchronous state looses its stability [121] [223]. At extremely large values of α, particularly for $\alpha \to \infty$, the synchronization approaches the complete replacement method of synchronization [227], being these conclusions also valid for *bidirectionally couplings* [121] [223] (unidirectionally and bidirectional coupling are at least locally equivalent [134]). Hence, diffusive, unidirectionally coupling and complete replacement are related and the asymptotic value of $\lambda_{\max}^{\perp}$ indicates whether the complete replacement works. Conversely, the asymptotic value of $\lambda_{\max}^{\perp}$ is determined by the stability of the subsystem that remains uncoupled from the drive. For the study of the stability of bidirectionally coupled systems, one can also end with the variational equations [227].

It is important to notice that even if the largest Lyapunov exponent is negative, bursts may occur, because this exponent is only an ergodic average over the attractor, and invariant sets maybe still unstable. The bursts can be directly associated with unstable periodic orbits (UPOs) [120] [227].

Sometimes several or even all drive variables are desired at the response system when only send one signal can be sent. Techniques of *synchronous substitution* [227] permit a great range of coupled chaotic systems to synchronize. There are described extensions of this technique that allow the so-called hyperchaotic systems to synchronize (systems with more than one positive Lyapunov exponent).

One variation of this method, based on a decomposition of the given systems into active and passive parts, was reported by Kocarev and Parlitz [159] and may be viewed as a generalization of the complete replacement method of Pecora and Carroll [224] [227]: starting from a chaotic autonomous system $\frac{d\mathbf{x}}{dt} = F(\mathbf{x})$ and rewriting it as a nonautonomous one $\frac{d\mathbf{x}}{dt} = G(\mathbf{x}, s(t))$,

with some driving $s(t) = h(\mathbf{x})$, in such a way that this nonautonomous system tends to a fixed point when not driven. The authors called this decomposition, given by an active function h that defines the driving signal and a passive function asymptotically stable G, an *active-passive decomposition* (APD) of the original dynamical system. The freedom to choose the active function h leads to a large flexibility in applications. This is different from the complete replacement synchronization method of Pecora and Carroll [224] [227] where only a finite number of possible couplings exists, which is given by the number of stable subsystems of the dynamical system.

Another scheme of unidirectionally chaotic coupled systems can be consulted in the work of [240]. Applications of Lie derivatives in chaos synchronization and localization of periodic orbits are discussed by [164].

Coupling of two systems can be generalized to a chain of chaotic systems where each output acts as a drive signal for the next system, with applications in secure communications [227].

The method BK [228] is another possible configuration. The key feature of BK technique is to provide for m-dimensional systems, $2m$ adjustable coupling parameters. From a chaotic system $\frac{d\mathbf{x}^{(1)}}{dt} = F\left(\mathbf{x}^{(1)}\right)$, to generate the transmission signal u, one defines it as $u(t) = K^T\mathbf{x}^{(1)}(t)$, where K is a constant column vector and $\mathbf{x}^{(1)}(t)$ the drive system state vector. Similarly, the response state vector $\mathbf{x}^{(2)}(t)$ is used to generate a second scalar signal, $v(t) = K^T\mathbf{x}^{(2)}(t)$. The difference between the two scalars is multiplied by a second constant vector B, and subtracted directly from the vector field F of the response subsystem. The response system becomes

$$\frac{d\mathbf{x}^{(2)}(t)}{dt} = F\left(\mathbf{x}^{(2)}(t)\right) - BK^T \cdot \left(\mathbf{x}^{(2)}(t) - \mathbf{x}^{(1)}(t)\right) \tag{1.17}$$

With this method, systems with more than one positive Lyapunov exponent can be synchronized with a scalar transmitted signal [228]. The problem of synchronization consists on finding an adequate combination BK with negative Lyapunov exponents on the driven system.

In [133], theBK method is used to obtain and maintain excellent synchronization between a drive and a response system even when there is large parameter mismatch between them ($F\left(\mathbf{x}^{(i)}\right) \equiv F\left(\mathbf{x}^{(i)}, \mu_{\mathbf{x}^{(i)}}\right)$. Particularly when other techniques of coupling used, as in [262], intermittent burstings of desynchronization are observed, even in the presence of small parameter mismatch. Numerical experiments showed that varying the drive parameter and keeping constant the driven parameter, modifications were produced in the dynamics of both systems, from bifurcations to chaos, showing a high synchronization degree, with reproduction in the driven system of the dynamics of the drive system. It must be emphasized that, when the systems

are not identical, it is not in general possible to obtain identical synchronization. In this case the possible synchronization is the so-called generalized synchronization [220] [250].

Many coupling schemes, either for periodic or chaotic systems, consist on adding linear combinations to the coordinates of N identical oscillators, running:

$$\begin{aligned}
\frac{d\mathbf{x}^{(0)}}{dt} &= F\left(\mathbf{x}^{(0)}\right) + \alpha E \cdot G^0\left(\mathbf{x}^{(0)}, \mathbf{x}^{(1)}, ..., \mathbf{x}^{(N-1)}\right) \\
\frac{d\mathbf{x}^{(1)}}{dt} &= F\left(\mathbf{x}^{(1)}\right) + \alpha E \cdot G^1\left(\mathbf{x}^{(0)}, \mathbf{x}^{(1)}, ..., \mathbf{x}^{(N-1)}\right) \\
&\vdots \\
\frac{d\mathbf{x}^{(N-1)}}{dt} &= F\left(\mathbf{x}^{(N-1)}\right) + \alpha E \cdot G^{N-1}\left(\mathbf{x}^{(0)}, \mathbf{x}^{(1)}, ..., \mathbf{x}^{(N-1)}\right)
\end{aligned} \tag{1.18}$$

where $F : \mathbb{R}^n \to \mathbb{R}^n$ is the vector field controlling the dynamics of a single oscillator and $\mathbf{x}^{(i)} \in \mathbb{R}^n$ is a individual oscillator coordinates. The coupling between oscillators is described by the coupling functions $G^i : \mathbb{R}^{nN} \to \mathbb{R}^n$, and $E = diag\,(\gamma_1, ..., \gamma_n)$ is a diagonal matrix that determines the linear combination of the coordinates of $\mathbf{x}$ that will be used in coupling. Eventually, α is a scalar coupling constant, which determines the coupling strength.

For coupled dynamical oscillators, exhibiting *shift-invariant symmetry*, coupling configuration does not vary from one oscillator to the next and the oscillators can be considered to occupy points on a one-dimensional lattice with periodic boundary conditions. The shift-invariance of the coupling is expressed algebraically as:

$$\begin{aligned}
G^i\left(\mathbf{x}^{(j)}, \mathbf{x}^{(j+1)}, ..., \mathbf{x}^{(j+N-1)}\right) &= G^{i+1}\left(\mathbf{x}^{(j-1)}, \mathbf{x}^{(j)}, ..., \mathbf{x}^{(j+N-2)}\right) \\
i, j &= 0, 1, ..., N-1 \,(\mathrm{mod}\, N)
\end{aligned} \tag{1.19}$$

In [121] the chaotic synchronization problem is studied for this type of restricted, but representative class of coupled dynamical oscillators, for those that exhibit shift-invariant symmetry, property shared by many coupled oscillator systems. To ensure that any solution for a single oscillator is also a solution of the coupled system, the coupling functions G^i must vanish when the oscillators are synchronized. Common examples of shift-invariant coupling is the *nearest-neighbor diffusive coupling*, having coupling functions of the form $G^i = \mathbf{x}^{(i-1)} - 2\mathbf{x}^{(i)} + \mathbf{x}^{(i+1)}$, and the *global coupling*, with coupling functions typically having the form $G^i = \sum_{k=0}^{N-1} g\left(\mathbf{x}^{(k)} - \mathbf{x}^{(i)}\right)$, where g is a vector function satisfying $g\,(0) = 0$. Common examples of *non-shift-invariant*

coupling are nearest-neighbor coupling cases with fixed or free-end conditions [121].

The stability of the synchronization manifold is insured if the variations transverse to the synchronization manifold damp out with time. For systems with shift-invariant symmetry, the variational equations can always be changed by a convenient transformation [121], like the spatial discrete Fourier transform [212], whose jacobian is block diagonal, so that the transverse and nontransverse variations to the synchronization manifold ($\mathbf{x}^{(0)} = \mathbf{x}^{(1)} = ... = \mathbf{x}^{(N-1)}$, which represent $n\,(N-1)$ constraint equations, so that the synchronization manifold has dimension $nN - n\,(N-1) = n$, which is the phase space dimension of a single oscillator) decompose naturally, and the transverse variational equations typically come in independent, lowdimensional sets, usually the dimension of a single oscillator. In general, the synchronization problem can be studied by reducing a highdimensional set of variational equations to a lowdimensional set.

By application of the discrete Fourier transform, the transverse variational equations for diffusive coupling are given by ($\frac{N}{2}+1$ distinct modes for N odd) [121],

$$\frac{d\eta^{(k)}}{dt} = \left[\mathbf{D}F - 4\alpha \sin^2\left(\frac{k\pi}{N}\right) E\right] \eta^{(k)}, \quad k = 1, 2, ...N-1 \tag{1.20}$$

being $\eta^{(k)} = \mathbf{x}^{(k)} - s\,(t)$, where $s\,(t)$ represents the synchronized state. For the case where the coupling is done through all the coordinates, where $G^i = E\left(\mathbf{x}^{(i-1)} - 2\mathbf{x}^{(i)} + \mathbf{x}^{(i+1)}\right)$ and $E = diag\,(\gamma_1, ..., \gamma_n)$, $\gamma_i = 1$, the transverse Lyapunov exponents are given by [121] [99],

$$\lambda_i^k = \lambda_i^0 - 4\alpha \sin^2\left(\frac{k\pi}{N}\right), \quad k = 1, 2, ..., N-1 \tag{1.21}$$

being λ_i^k the transverse Lyapunov exponents and λ_i^0 the Lyapunov exponents in the synchronized state. The largest transverse Lyapunov exponent is then given by $\lambda_{\max} = \lambda_{\max}^0 - 4\alpha \sin^2\left(\frac{\pi}{N}\right)$, where $\lambda_{\max}^0$ is the largest Lyapunov exponent of a single oscillator. Therefore, it is possible to have a stable synchronized chaotic solution, provided the coupling constant α is large enough. Note that the modes do not lose stability at the same time.

For global coupling, $G^i = \sum_{k=0}^{N-1} g\left(\mathbf{x}^{(k)} - \mathbf{x}^{(i)}\right)$, with $g\,(0) = 0$, $\mathbf{D}g\,(0) = \gamma \cdot I_n$, the transverse Lyapunov exponents are given by [121],

$$\lambda_i^k = \lambda_i^0 - \alpha\gamma, \quad k = 1, 2, ..., N-1 \tag{1.22}$$

and all the modes lose stability simultaneously.

In case there are nil entries in E, the synchronized state can be broken for larger values of the coupling strength α, and the study of the chaotic synchronization can be related with complete replacement when the value of the parameter α tends to infinity [121].

Increasing the coupling parameter α does not necessarily guarantee synchronization. Often, the synchronized motion is stable only over a finite range of coupling values as it is seen with a Rössler-like circuit system coupled diffusively with the x coordinate, equations (1.15), (1.16) [227]. If there exists a value for the coupling α above which desynchronization takes place, the highest-order mode will then go unstable first. Pecora *et al.* [122] [223] call this a *short-wavelength bifurcation*. It is a desynchronizing bifurcation that sometimes occurs in diffusively-coupled arrays of oscillators and is caused by increasing the coupling. It means that the smallest spatial wavelength will be the first to desynchronize and is excited to cause the system to desynchronize. This type of bifurcation can occur in any coupled system where each oscillator or node has internal dynamics that are not coupled directly to other nodes. In the example with the coupled chaotic Rössler system, using x coordinate for coupling, y and z coordinates are internal dynamical variables. This phenomenon of desynchronization bifurcation can also take place in a coupled array of limit cycle oscillators [223]. However, some coupling schemes do not allow a straight-forward wavelength interpretation [223].

Besides, when there are desynchronization bifurcations in chaotic arrays, there is an upper limit, a size limit, to the number of chaotic oscillators that can be added to the array while keeping the synchronized state stable [122] [227] [223]. Heagy *et al.* [122] showed that this maximum number can be calculated if one knows the stability diagram. This occurs when the highest frequency mode becomes unstable before the lowest frequency mode becomes stable as the coupling increases. This is due to a scale phenomenon of the variational equations for each mode that, for the case of the nearest-neighbor diffusive coupling runs as: $\mathbf{D}F - 4\alpha \sin^2\left(\frac{k\pi}{N}\right) E = \mathbf{D}F - 4\left[\alpha \frac{\sin^2\left(\frac{k\pi}{N}\right)}{\sin^2\left(\frac{\pi}{N}\right)}\right] \sin^2\left(\frac{\pi}{N}\right) E$. Thus, computing the Lyapunov exponents for the first mode as a function of the coupling parameter α, yields automatically the exponents for the mode k. In the case of limit cycles, this situation is not verified, considering that the maximum Lyapunov exponent of each mode in the absence of coupling, $\alpha = 0$, is zero and not a positive value [122] [223].

Rewriting the coupled linear system (1.18) as $\frac{d\mathbf{x}}{dt} = F(\mathbf{x}) + \alpha (G \otimes E)\mathbf{x}$, where $F(\mathbf{x})$ has $F\left(\mathbf{x}^{(i)}\right)$ for the i-th node block, the matrix $G \in \mathcal{M}_N$ defines the linear combination of the nodes and $E \in \mathcal{M}_n$ operates on the nodes individually to determine which of the oscillator components are coupled,

Pecora [223] showed that, for $F(\mathbf{x})$ and E fixed, the stability of many linear symmetric coupling schemes of identical oscillators personified by the matrix G, limit cycles or chaotic systems, may be evaluated from another linear symmetric coupling scheme with coupling matrix G', with possible different number of oscillators. Thus, if the matrices G and G' can be diagonalized, the stability diagram given by the Lyapunov exponents (or Floquet multipliers) are related by the identity $\lambda_{\max}^{k}(\alpha) = \lambda_{\max}^{q}\left(\frac{\gamma_k}{\gamma'_q}\alpha\right)$ where γ_k is the eigenvalue of G associated to the k-th mode and γ'_q is the eigenvalue of G' associated to the q-th mode.

A rigorous criterion for synchronization is presented by Brown and Rulkov [54] [53] which guarantees, if satisfied, that the coupling scheme will yield synchronization linearly stable to perturbations for identical chaotic (or not) systems coupled in a drive response manner. The dynamics of the driving system is given by $\frac{d\mathbf{x}^{(1)}}{dt} = \mathbf{F}\left(\mathbf{x}^{(1)}, t\right)$ and the dynamics of the response system given by $\frac{d\mathbf{x}^{(2)}}{dt} = \mathbf{F}\left(\mathbf{x}^{(2)}, t\right) + \mathbf{E}\left(\mathbf{x}^{(1)} - \mathbf{x}^{(2)}\right)$, where $\mathbf{E}$ is a vector function, and represents the coupling between the systems. It is assumed that $\mathbf{E}(\mathbf{0}) = \mathbf{0}$ so synchronization occurs on the invariant manifold given by $\mathbf{x}^{(1)} = \mathbf{x}^{(2)}$. Depending on the choice of $\mathbf{F}$ and $\mathbf{E}$, synchronous motion may only occur within a finite range of coupling strengths and it may not occur for coupling strength too small or too large, or it may never occur. Using the linearized equations of motion transverse to the synchronization manifold, $\mathbf{w}_\perp = \mathbf{x}^{(2)} - \mathbf{x}^{(1)}$, $\frac{d\mathbf{w}_\perp}{dt} = \left[\mathbf{DF}\left(\mathbf{x}^{(1)}, t\right) - \mathbf{DE}(\mathbf{0})\right]\mathbf{w}_\perp$, where $\mathbf{DF}\left(\mathbf{x}^{(1)}, t\right)$ is the Jacobian of $\mathbf{F}$ evaluated at $\mathbf{x}^{(1)}$ at time t, and $\mathbf{DE}(\mathbf{0})$ is the Jacobian of $\mathbf{E}$ evaluated at $\mathbf{w}_\perp = \mathbf{0}$, the goal is to reach the asymptotic behavior of $\mathbf{w}_\perp(t)$, because if $\lim_{t\to\infty} \|\mathbf{w}_\perp(t)\| = 0$ then the synchronization manifold is linearly stable. This study was made by Brown and Rulkov [54] [53] by dividing $\mathbf{DF}\left(\mathbf{x}^{(1)}, t\right) - \mathbf{DE}(\mathbf{0})$ into a time independent part $\mathbf{A}$, and an explicitly time dependent part $\mathbf{B}(\mathbf{x}, t)$, decomposition not unique since one may add and subtract constant terms to $\mathbf{A}$ and $\mathbf{B}$

$$\mathbf{DF}\left(\mathbf{x}^{(1)}, t\right) - \mathbf{DE}(\mathbf{0}) \equiv \mathbf{A} + \mathbf{B}(\mathbf{x}, t) \tag{1.23}$$

Assuming that $\mathbf{A}$ can be diagonalized one has $\mathbf{D} = \mathbf{P}^{-1}\mathbf{A}\mathbf{P}$. Being Λ_M the eigenvalue of $\mathbf{A}$ with larger real part $R(\Lambda_M)$, the optimal decomposition found for equation (1.23) was [54] [53]:

$$\mathbf{A} \equiv \langle \mathbf{DF} \rangle - \mathbf{DE}(\mathbf{0}) \tag{1.24}$$

$$\mathbf{B}(\mathbf{x}, t) \equiv \mathbf{DF}\left(\mathbf{x}^{(1)}, t\right) - \langle \mathbf{DF} \rangle \tag{1.25}$$

where $\langle\cdot\rangle$ denotes time average, $\langle \mathbf{DF} \rangle = \lim_{t\to\infty} \frac{1}{t-t_0} \int_{t_0}^{t} \mathbf{DF}\left[\mathbf{x}^{(1)}(s), s\right] ds$.

Finally, the condition for linear stability of the invariant trajectory in the synchronization manifold is [54] [53]:

$$-R(\Lambda_M) > \left\langle \left\| \mathbf{P}^{-1} \left[\mathbf{B}(\mathbf{x}, t)\right] \mathbf{P} \right\| \right\rangle \tag{1.26}$$

This criterion can be used to design couplings that guarantee linearly stable synchronization, being only sufficient, but not necessary. Thus, one can expect that it is possible for a coupling scheme to fail this criterion and still produce stable synchronization.

An approximate and quick criterion, non rigorous, to determine whether or not synchronization will occur for a particular coupling scheme is $R(\Lambda_M) < 0$ according to [54]. But although a linear stability analysis may seem to guarantee stable synchronization, noise and nonlinear effects may prevent long term synchronous behavior.

To get synchronization beyond the transformations of the driving signal, Tresser *et al.* [257] showed that it is possible to get driven synchronization in dynamical systems by a linear change of variables.

Another type of unidirectionally coupling consists of sending the drive signal in discrete moments of time, *occasional driving*, sometimes being able to produce synchronization where the continuous driving does not. In [110] the authors introduced a new method for synchronizing chaotic systems with positive conditional Lyapunov exponents, systems that do not synchronize by the complete replacement method of Pecora and Carroll [224]. A copy of the drive system (1.8) is considered as the response system,

$$\left[\begin{array}{cc} \frac{d\mathbf{u}^{(2)}}{dt} & \frac{d\mathbf{v}^{(2)}}{dt} \end{array} \right]^T = \left[\begin{array}{cc} F_1\left(\mathbf{u}^{(2)}, \mathbf{v}^{(2)}\right) & F_2\left(\mathbf{u}^{(2)}, \mathbf{v}^{(2)}\right) \end{array} \right]^T \tag{1.27}$$

and the following driving signal formed by a convex combination of the drive and response systems as the new driving signal,

$$\overline{\mathbf{u}}^{(2)}\left(\mathbf{u}^{(1)}, \mathbf{u}^{(2)}\right) = \mathbf{u}^{(2)} + \varepsilon\ \delta_{\Delta t,t}\left(\mathbf{u}^{(1)} - \mathbf{u}^{(2)}\right) = \left(1 - \varepsilon\ \delta_{\Delta t,t}\right)\mathbf{u}^{(2)} + \varepsilon\ \delta_{\Delta t,t}\mathbf{u}^{(1)} \tag{1.28}$$

where $\delta_{\Delta t,t}$ is a Kronecker delta and ε is the combination parameter, taking values between 0 and 1. This new signal is injected into the response system at time steps Δt. For $\varepsilon = 0$ the dynamics of both systems are independent and for $\varepsilon = 1$, establishes one the complete replacement of Pecora and Carroll [224].

It was reported by [196] that chaotic systems can be stabilized by applying proportional pulses to the system variables. Thus, the component associated with the response system, $\left(1 - \varepsilon\ \delta_{\Delta t,t}\right)\mathbf{u}^{(2)}$, applies proportional pulses to

the system variables at time steps Δt acting as a chaos suppression method, and for some values of the parameter ε, these perturbations stabilize the dynamics of the response system, obtaining a fixed point. The component associated with the drive, $\varepsilon\ \delta_{\Delta t,t}\mathbf{u}^{(1)}$, is the connecting term that induces the behavior of the chaotic drive into the stabilized response system.

A coupling for arbitrary pairs of identical systems that makes use of the contraction properties of the underlying flow, suppressing the exponential divergence of the dynamics transversal to the synchronization manifold, and thus fulling exploiting the contraction properties of the flow of the given systems, was presented by Junge *et al.* [217] [137].

Chaotic systems possessing invariant manifolds of lower dimension than that of the full phase space can exhibit several classes of phenomena. In chaotic systems with an invariant subspace M, where a chaotic attractor A exists, like the synchronization manifold of coupled chaotic systems, basins of positive measure but containing no open sets, have been observed. These basins, called *riddled basins* [28] [178] [31], were first studied theoretically for discrete maps by Alexander *et al.* [28]. They are characterized by any point chosen at random from any disk having a positive probability of being in $\beta\,(A)$ (basin of attraction of the attractor A) and a positive probability of not being. The normal Lyapunov exponents must be negative, indicating that A attracts points with positive probability [28]. Also A must repel sufficiently many points. For riddling to occur it is then necessary to have a dense set of points in the invariant subspace with zero Lebesgue measure and transversely unstable. Lai and Grebogi [177] argue that the existence of a chaotic attractor in the invariant manifold is not necessary for riddling to occur, only being necessary the existence of a chaotic invariant set in the invariant manifold M, which can be a chaotic attractor or a nonattracting chaotic saddle. This is what occurs in periodic windows near a parameter value at which the chaotic attractor is observed, where there are both a stable periodic attractor and a nonattracting chaotic saddle in the invariant subspace, and, unlike chaotic attractors where riddling disappears when the attractor becomes transversely unstable [28] [178], in a periodic window riddling (in a generalized sense) can occur regardless the chaotic saddle is transversely stable or unstable [177] [174]. Globally, the basin of attraction of the periodic attractor in the invariant subspace contains both an open set and a set of measure zero with structures of the riddled type with holes belonging to the basin of another attractor, being this base named by Lai [174] as *pseudo-riddled basin*. A stronger property, called *intermingled basins* [28] [85], can occur when there is, in the invariant subspace M, more than one chaotic attractor with basins of attraction riddled and dense. Any point chosen at random from any disk has a positive probability of being in each of the basins of attraction. No

finite computation can determine the fate of a given initial condition, even if that initial condition is given with a precision of infinity [85].

Lai and Winslow [180] demonstrated that dynamical systems may also exhibit sensitive dependence of asymptotic attractors on system parameters. They showed that a class of spatiotemporal chaotic systems, modeled by globally coupled maps, exhibit riddled parameter space. This means that for every point in the chaotic parameter space, there are parameter values arbitrarily nearby that lead to nonchaotic attractors. A consequence is an extremely sensitive parameter dependence characterized by a significant probability of error in numerical computations of asymptotic attractors, regardless the precision specified for the parameters.

To characterize and quantify dynamical invariants for the sensitivity in phase space or parameter space, one can appeal to the *uncertainty exponents* γ [180] [31] [106]. One randomly chooses many different pairs of phase points in phase space or parameter space r_0, and $r_0+\delta$, being δ a small perturbation. If the final state of the system for each value of each pair are on different attractors, the initial conditions or parameters are called uncertain initial conditions or uncertain parameter values. For δ fixed, one calculates the fraction of uncertain initial conditions or uncertain parameter values $f(\delta)$. Typically, there is a scaling relation, $f(\delta) \sim \delta^{\gamma}$, where γ is the uncertain exponent.

In the work of [117] several phenomena linked to the synchronization of discrete chaotic systems are discussed using as example of two coupled skew tent maps, $f : [0,1] \to [0,1]$, dependent on a parameter a, for $0.5 \leq a < 1$.

$$f(x) = \begin{cases} \frac{x}{a}, & 0 \leq x \leq a \\ \frac{1-x}{1-a}, & a < x \leq 1 \end{cases} \tag{1.29}$$

By application of Birkhohff theorem, the asymptotic distribution of almost every trajectory is uniform. The synchronization was studied starting from the determination of the natural Lyapunov exponent transversal to the synchronization manifold, $S = \{(x,y) \in \mathbb{R} : 0 \leq x = y \leq 1\}$, for two different cases, one of linear coupling

$$\begin{array}{l} x_{n+1} = f(x_n) + \delta(x_n - y_n) \\ y_{n+1} = f(y_n) + \varepsilon(x_n - y_n) \end{array}, n = 0, 1, 2, \ldots \tag{1.30}$$

and one of nonlinear coupling

$$\begin{array}{l} x_{n+1} = f(x_n + \delta(x_n - y_n)) \\ y_{n+1} = f(y_n + \varepsilon(x_n - y_n)) \end{array}, n = 0, 1, 2, \ldots \tag{1.31}$$

being δ and ε real parameters. According to [117], the global dynamic behavior is quite different particularly when the ideal system is perturbed by

parameter mismatch or noise. A necessary condition for synchronization to take place is that the transversal natural Lyapunov exponent is negative (meaning that almost all of the trajectories that begin close to S are by S attracted, or, in other words, almost all synchronized trajectories are transversally attracting), which means that the synchronization manifold S is an attractor in the weak Milnor sense.

In the nonlinear case, there are values of the coupling parameters, for which all synchronized trajectories are transversally attracting, the transversal Lyapunov exponent for all trajectories is negative, so the synchronization manifold is an asymptotically stable attractor. In the presence of noise or small parameter mismatch, the synchronization error is asymptotically and uniformly bounded. When the transversal natural Lyapunov exponent is negative, but the basin of attraction is locally riddled (there are initial conditions that generate trajectories with positive transversal Lyapunov exponents), the synchronization manifold is not Lyapunov stable and in the presence of noise or small parameter mismatch, intermittent desynchronization bursts, of larger amplitude for the linear case, are observed [117].

Coupled discrete dynamical systems are called of *coupled map lattices (CML)*. This type of lattices differ from cellular automata, because the state is continuous and not discrete.

In the work of [188] is presented a complete numerical description for the synchronization of coupled map lattices making recourse to the logistic function $f : (0,1) \to (0,1)$, $f(x_n) = \gamma\ x_n(1-x_n)$, $\gamma \in [\gamma_\infty \approx 3.57, 4]$, in chaotic regime. The one dimensional model is given by

$$x_i^{n+1} = f(x_i^n) + \alpha \left[f\left(x_{i+1}^n\right) + f\left(x_{i-1}^n\right) - 2f(x_i^n) \right], i = 1, 2, \ldots, N \quad (1.32)$$

with periodic boundary conditions $f(x_0^n) = f(x_N^n)$, $f\left(x_{N+1}^n\right) = f(x_1^n)$. The bidimensional model is, in turn, given by

$$\begin{aligned} x_{(i,j)}^{n+1} &= f\left(x_{i,j}^n\right) + \\ &+ \alpha \left[f\left(x_{i+1,j}^n\right) + f\left(x_{i-1,j}^n\right) + f\left(x_{i,j+1}^n\right) + f\left(x_{i,,j-1}^n\right) - 4f\left(x_{i,j}^n\right) \right] \\ &i, j = 1, 2, \ldots, N \end{aligned} \quad (1.33)$$

with periodic boundary conditions in both dimensions $f\left(x_{0,j}^n\right) = f\left(x_{N,j}^n\right)$, $f\left(x_{N+1,j}^n\right) = f\left(x_{1,j}^n\right)$, $f\left(x_{i,0}^n\right) = f\left(x_{i,N}^n\right)$, $f\left(x_{i,N+1}^n\right) = f\left(x_{i,1}^n\right)$.

A rigorous proof for synchronization in the case of one-dimensional coupled map lattice (1.32), with lattice sizes $n = 2, 3$ for $\gamma \in [\gamma_\infty \approx 3.57, 4]$ and $n = 4$ for $\gamma \in [\gamma_\infty \approx 3.57, 3.82]$ is given by [188]. A rigorous proof for synchronization in the case of one-dimensional coupled map lattice (1.32), with lattice size $n = 4$ for $\gamma \in [\gamma_\infty \approx 3.57, 4]$ in the chaotic regime, is given by [189].

The loss of chaos synchronization is associated with transverse bifurcations of unstable periodic orbits embedded in the synchronous chaotic attractor (SCA), which constitute the skeleton of any typical chaotic attractor [153] [155]. These bifurcations are described in the work of [153] [155]. Hence, following [153] [155], if all such unstable periodic orbits are transversely stable against perturbations transverse to the invariant subspace, the synchronous chaotic attractor becomes asymptotically stable, and one has strong synchronization. When the coupling parameter passes through a threshold value, a *riddling bifurcation* can occur. Before the bifurcation, all the periodic orbits embedded in the chaotic attractor are saddles, and when the bifurcation takes place in the first periodic saddle embedded in the synchronous chaotic attractor, usually of low period, it loses its transverse stability and weak synchronization in the Milnor sense takes place [153] [155]. Then, a typical trajectory may have repelling segments exhibiting positive local transverse Lyapunov exponents, with the average transverse Lyapunov exponent negative, and the trajectories starting from these segments will be repelled from the synchronous chaotic attractor. The global dynamics will depend on the existence or not of an absorbing area inside the basin of attraction. If it exists, the locally repelled trajectories exhibit a transient *intermittent bursting* from the synchronous chaotic attractor, and the basin of attraction is said to be *locally riddled*. For this case, the synchronous chaotic attractor is transversely stable because its transverse Lyapunov exponent is negative, and the bursts will tend to stop [153] [155]. When there is no absorbing area, the locally repelled trajectories will go to another attractor or will diverge to infinity, and the basin of attraction becomes *globally riddled*. With further variation of the coupling parameter, eventually a *blowout bifurcation* takes place and the weak stable synchronous chaotic attractor loses its transverse stability, a complete desynchronization occurs and the transverse Lyapunov exponent becomes positive [153] [155].

From this point, if the global dynamics is bounded and there is no attractor outside the invariant subspace, a new *asynchronous attractor* appears by means of a supercritical (or soft) blow-out bifurcation, and an intermittent bursting, called *on-off intermittency* takes place, where long periods of motion near the invariant subspace (off state) are occasionally interrupted by short burstings away from it (on state) [185] [157]. But if the global dynamics is unbounded or there exists another attractor outside the invariant subspace, then a subcritical (or hard) blow-out bifurcation takes place and an abrupt disappearance of the synchronized chaotic state occurs, and typical trajectories near the synchronization subspace are attracted to another asynchronous attractor or diverge to infinity [185] [157].

Kim *et al.* [153] [155] investigated the bifurcation mechanism from strong

to weak synchronization in unidirectionally coupled systems without symmetry and found out a mechanism for direct transition to global riddling where an absorbing area disappears, leading to divergent trajectories, through a transcritical contact bifurcation between a periodic saddle embedded in the synchronous chaotic attractor and a repeller on the boundary of its basin of attraction. This bifurcation mechanism is different from the one occurring in coupled chaotic systems with symmetry, where the basin becomes globally riddled through a pitchfork or period doubling bifurcation [178]. The effect of asymmetry of coupling on the loss of chaos synchronization was studied by [152].

In real situations, a small parameter mismatch or the presence of noise is inevitable. In the regime of weak synchronization, a small parameter mismatch or noise results in the prosecution of the intermittent bursting, intermittent loss of synchronization, transforming the chaotic attractor into a bubbling attractor, called *attractor bubbling* [120] [262] [102] [227] or results in a chaotic transient with a finite lifetime, depending on the case, bubbling or riddling. Hence, for the study on the loss of chaos synchronization the effect of a parameter mismatch or noise must be taken into account. In both cases, bubbling and riddling, the quantity of interest is the average time τ that a trajectory spends near the synchronous chaotic attractor (the average interburst interval or the average lifetime of the chaotic transient) [156]. How τ scales with the mismatch parameter and the noise intensity in unidirectionally coupled one-dimensional maps was studied by [156]. To measure quantitatively the degree of parameter or noise sensitivity on the weak chaotic synchronization, a quantifier, called the *parameter sensitivity exponent* was introduced by [131] [154] in two coupled one-dimensional maps. The extension of this method to bidimensional coupled invertible systems such as the coupled Henon maps and coupled pendula was made by Kim and co-workers [185] [187] [186]. It was found that the scaling exponent μ for the *average characteristic time* (the average interburst time and the average chaotic transient lifetime for both the bubbling and riddling cases) is given by the reciprocal of the parameter sensitivity exponent, as in the case of a system of coupled unidimensional maps.

Generalized synchronization

A more general kind of synchronization can occur for non identical coupled chaotic systems, connecting through a function or relation the dynamical variables of one system to the variables of another system [26]. The term *generalized synchronization* was first introduced by Rulkov *et al.* [244] for unidirectionally coupled chaotic systems. This type of synchronization

leads to richer behaviors than the simple identical synchronization, implying a collapse onto a subspace of the overall evolution of the dynamics. Sometimes, knowing the state of one system allows one to know the state of the other, being even possible in certain cases, to predict the state of one system starting from the knowledge of the state of the other, including for totally different systems. For practical applications, predictability is the most important feature. Falling back on Lyapunov functions, one can show that completely different systems can GS [160] [165]. Almost all the studies in the open literature have been concentrated on unidirectionally coupled systems. Many examples of non synchronization due to parameter mismatch are actual examples of generalized synchronization [161].

Basically, there are two types of generalized synchronization for coupled systems described in the literature. There is a stronger notion, that corresponds to the existence of a continuous mapping between the systems [160] [165] (or differentiable for [26]):

Definition 3: Given the systems $\frac{d\mathbf{x}}{dt} = F(\mathbf{x}, \mathbf{y})$ and $\frac{d\mathbf{y}}{dt} = G(\mathbf{x}, \mathbf{y})$, $\mathbf{x} \in \mathbb{R}^n$, $\mathbf{y} \in \mathbb{R}^m$, one says that the system possess the property of generalized synchronization (GS) if there exists an invertible continuous function $\phi : \mathbb{R}^n \to \mathbb{R}^m$, a manifold $M = \{(\mathbf{x}, \mathbf{y}) : \mathbf{y} = \phi(\mathbf{x})\}$ and a subset $B \supset M$, such that for all $(\mathbf{x}, \mathbf{y}) \in B$, $(\mathbf{x}, \mathbf{y}) \underset{t \to \infty}{\longrightarrow} M$.

In the case of unidirectionally coupled systems the function ϕ does not need to be invertible. Except for special cases, it will not be possible to exhibit explicitly the function ϕ. However, the set of synchronization can show complex structures [220] [250] and it is possible that no function ϕ exists in its exact sense, but only as a multivalued relation. A more general definition of generalized synchronization, for unidirectionally coupled systems, where ϕ does not need to be a function but can be a multivalued relation [3] [220] [250] is:

Definition 4: Given the systems $\frac{d\mathbf{x}}{dt} = F(\mathbf{x}, \mathbf{y})$, $\frac{d\mathbf{y}}{dt} = G(\mathbf{x}, \mathbf{y})$, $\mathbf{x} \in \mathbb{R}^n$, $\mathbf{y} \in \mathbb{R}^m$, one says that the system possess the property of generalized synchronization (GS) if there exists a synchronous open basin $B \subset \mathbb{R}^n \times \mathbb{R}^m$ such that for all $(\mathbf{x}_0, \mathbf{y}_{01}), (\mathbf{x}_0, \mathbf{y}_{02}) \in B$, $\|\mathbf{y}(t, \mathbf{x}_0, \mathbf{y}_{01}) - \mathbf{y}(t, \mathbf{x}_0, \mathbf{y}_{02})\| \underset{t \to \infty}{\longrightarrow} 0$, in other words, if the response system is asymptotically stable with respect to the drive $\mathbf{x}$.

Typically, a continuous function ϕ exists if the response system is asymptotically stable when driven by the coupling signal and no subharmonic entrainment occurs [220]. Subharmonic entrainment means that exist points on the drive attractor which are not mapped uniquely to the response attractor.

A general theory of generalized synchronization in unidirectionally coupled systems was presented in [160] [165] [161]. The authors argued that with the dynamics of the driving system invertible, a functional relation occurs if the response system is asymptotically stable or if all the conditional Lyapunov exponents of the response are negative (in the case of generalized synchronization, the jacobian of the vector field for the calculation of the Lyapunov exponents is determined with bases on the states of the driven system, unlike what would be done for the identical synchronization, for which the state of the drive system could be used). These conclusions hold for aperiodic orbits and for periodic oscillations with entertainment ratio equal to unity [220].

Experimentally, Rulkov [241] believes that the onset of synchronized chaos is accompanied by phase locking of pairs of unstable periodic orbits existing in the chaotic attractors of the uncoupled driving and response systems.

In the case of strong high-quality synchronization, all the unstable periodic orbits (UPO) of the driving attractor, must have stable periodic responses in the driven system (PO). Although such fact seems to be a sufficient condition to confirm the stability of identical synchronization, it is not sufficient to confirm stability of generalized synchronization of chaos, particularly in the case of subharmonic entrainment of chaotic oscillations, as it was shown by [243].

The proprieties of the multivalued relation that occurs between the drive and the response systems when the synchronization is achieved with other than one to one frequency ratio was studied by [242].

Generalized synchronization of unidirectionally coupled dynamical systems, may occur not only for pairs of different systems but also for identical systems as it was shown through the use of an example in the work of [221] [219].

Close to the onset of generalized synchronization, intermittent generalized synchronization (IGS) has been detected by Hramov and Koronovskii *[128].*

In physical experiments, only synchronization phenomena that are described with stable and robust manifolds can be observed. A manifold is said to be robust, if it shows persistence of its properties, such as smoothness of the invariant manifold and quantitative bounds for deformations of the synchronization manifold, under small arbitrary perturbations and under small noise [163].

An invariant manifold is k-normal hyperbolic if the rate of normal contraction to the manifold is k times larger than the tangential one, if the rate at which trajectories are attracted towards the manifold is k times greater than the rates of contraction or expansion within the manifold. The conditions for stability and normal hyperbolicity can be expressed in terms of Lyapunov

exponents [163]. The invariant manifold is stable if the largest normal Lyapunov exponent is negative, and the stable manifold is normally hyperbolic if the largest normal Lyapunov exponent is smaller than the smallest tangential Lyapunov exponent, which means that the contraction towards the synchronization manifold is sufficiently strong. Normal hyperbolicity is a necessary and sufficient condition for the synchronization manifold to be smooth and persistent under small perturbations [218] [163], but in real applications, when parameter mismatches are not arbitrarily small, normal hyperbolicity is not sufficient to give quantitative bounds for deformations of the synchronization manifold, *i.e.*, normal hyperbolicity is not sufficient to guarantee a small synchronization error, and two almost identical systems may cause large synchronization errors [163] [218].

Bounds on the synchronization error for the case of nearly identical nonlinear systems that are unidirectionally coupled were presented in [129].

Phase and lag synchronization

Another type of synchronization called *phase synchronization* was first reported for chaotic systems by Rosenblum *et al.* [237]. Periodic systems are called synchronized if either their phases or frequencies are locked. Stable periodic oscillations of an autonomous dissipative dynamical system are represented by a stable limit cycle in its phase space [230]. Following the definition presented by Pikovsky *et al.* [230] the phase is a variable that corresponds to the motion along the limit cycle, along the direction where neither contraction nor expansion of the phase volume occurs. Therefore, this direction in the phase space and, respectively, the phase of oscillations corresponds to the zero Lyapunov exponent. Amplitudes are all other variables of the dynamical system that are locally transversal to the cycle, corresponding to the negative Lyapunov exponents. Therefore, weakly perturbed amplitude will tend to its stable value, whereas a small perturbation of the phase does not grow or decay.

For chaotic systems, the notion of frequency or phase is, in general, not well defined except for some class of chaotic systems where a phase variable can be introduced. Phase synchronization is better observed when a well defined phase variable can be identified in both coupled systems. Any autonomous continuous dynamical system with chaotic behavior possesses one zero Lyapunov exponent that corresponds to shifts along the flow, and, therefore, the notion of phase can be generalized for this case as well. The phase variable of a chaotic oscillator can be introduced by some techniques as proposed by [239] [230]. For strange attractors that spiral around some particular point in a two dimensional projection of the attractor, a phase angle

$\phi(t)$ can be defined that decreases or increases monotonically [222]. Phase synchronization occurs if the difference $|n\phi - m\varphi|$, for arbitrary integers n and m, between the corresponding phases, is bounded by some constant, which means $|n\phi - m\varphi| < const$, occurring when a zero Lyapunov exponent of the response system becomes negative [237] [219], due to weak interaction of non-identical chaotic oscillators [239]. One may then define a mean rotation frequency as $\Omega = \lim_{t\to\infty} \phi(t)/t$. This mean rotation frequency of the drive and the response system coincide, if phase synchronization is present, with the amplitudes of both systems varying chaotically and being completely uncorrelated [222] [219].

An experimental observation of phase synchronization and generalized synchronization of a system of two unidirectionally coupled Rössler systems was performed by [222]. In this case, a close relation between phase synchronization and generalized synchronization was established, with generalized synchronization leading to phase synchronization.

A counterintuitive phenomenon observed by Liu *et al.* [193] refers that the dynamics of coupled chaotic oscillators can become more complex due to coupling and this fact does not seem to depend on the way through which the oscillators are coupled. In the weakly coupling regime (before phase synchronization), on a system of N coupled chaotic attractors with multiple scrolls, a subset of null Lyapunov exponents in the absence of coupling can become positive as the coupling is increased. Liu *et al.* [193] argued that this phenomenon is expected to be quite general, as it can occur for typical chaotic attractors with multiple scrolls in the phase space, such as the Lorenz attractor.

On-off intermittency was observed from the transition from phase unlocking status to phase locking [303].

Rosemblum *et al.* [238] studied synchronization transitions in a system of two symmetrically coupled nonidentical chaotic oscillators. Increasing the coupling strength, the system undergoes the transition to phase synchronization and, with further increase of coupling, a lag in time synchronous regime was observed, where both states coincide, but shifted in time, $\mathbf{x}^{(1)}(t) = \mathbf{x}^{(2)}(t+\tau)$. Further increase of coupling decreased the time shift τ and the systems tended to be completely synchronized. These transitions were traced in the Lyapunov spectrum by Rosemblum *et al.* [238]. *Lag synchronization* is then a phenomenon that can be observed for two coupled nonidentical chaotic oscillators where the dynamical variables are synchronized with a time delay relative to each other. In physical systems where noise is inevitable, lag synchronization is typically destroyed when the noise level is comparable to the amount of average system mismatch and, at small noise

levels lag synchronization occurs in an intermittent fashion [252]. Increasing the coupling strength often leads to a transition to complete synchronization.

Generalized time-lagged synchronization was observed by [304] for unidirectionally coupled systems in the presence of large parameter mismatch.

1.2.4 Coupling extended dynamical systems

A fundamental observation in nonlinear dynamics is the low-dimensional characteristic of the asymptotic chaotic invariant sets, that occur in many high-dimensional systems *[175].* Lai *et al. [175]* argued and provided numerical evidence that a high-dimensional dynamical system exhibiting low-dimensional chaotic behavior is generally associated with chaos synchronization, identical or generalized.

Coupling spatially extended dynamical systems is also possible. It has been shown that it is possible to synchronize not only low-dimensional chaotic dynamical systems, but also high-dimensional ones [166] [167] [168] [254]. The *synchronization manifold* is defined in a similar way as those for the other dynamical systems. As an example, for the unidirectionally coupled of two arrays of N coupled ordinary differential equations (CODEs), one gets for two systems of type of those decribed by equations (1.18)

$$\frac{d\mathbf{x}^{(i)}}{dt} = F\left(\mathbf{x}^{(i)}\right) + \alpha E \cdot G^i\left(\mathbf{x}^{(0)}, \mathbf{x}^{(1)}, ..., \mathbf{x}^{(N-1)}\right) \tag{1.34}$$

$$\frac{d\mathbf{y}^{(i)}}{dt} = F\left(\mathbf{y}^{(i)}\right) + \alpha E \cdot G^i\left(\mathbf{y}^{(0)}, \mathbf{y}^{(1)}, ..., \mathbf{y}^{(N-1)}\right) + \beta I \ \left(\mathbf{x}^{(i)} - \mathbf{y}^{(i)}\right) \tag{1.35}$$

In the previous equations β is the coupling parameter between the driving and driven systems.

The identical synchronization manifold is given by,

$$M = \left\{\left(\mathbf{x}^{(i)}, \mathbf{y}^{(i)}\right) \in \mathbb{R}^n \times \mathbb{R}^n : \mathbf{x}^{(i)} = \mathbf{y}^{(i)},\ i = 0, 2, ..., N-1\right\} \tag{1.36}$$

being defined in a similar way the other cases of coupled spatially extended systems.

A general method for synchronizing pairs of unidirectionally arrays of N coupled ordinary differential equations with spatiotemporal chaotic dynamics was introduced by [162]. The synchronization is achieved by discrete time coupling of individual cells of the arrays. At the moments $t_{i,n} = iT_1 + (n-1)\,NT_2$, $i = 1, 2, ..., N$, $n = 1, 2, ...$, (*sporadic coupling*) one of the state variables of the i^{th} cell of the driven system is replaced by the corresponding state of the the drive system (complete substitution). For $T_1 = 0$, all the cells are simultaneously coupled. Whenever the coupled individual

cells in the limit of continuous time lead to an asymptotically stable subsystem, then there exists a critical value of time τ_c such that, for all $\tau_n < \tau_c$ sporadically coupled systems synchronize. Following the work of [162], this type of synchronization of sporadically coupled individual cells can be applied to pairs of unidirectional coupled arrays where the synchronization mechanism of the local elements or cells is known. It can be applied to various pairs of coupled systems including two or three dimensional arrays, nonhomogeneous arrays and arrays with different internal couplings. The authors stressed also that it can be applicable not only to arrays, but also in the case of PDEs. They also discussed the possible applications in communications and anticontrol and control of chaos.

Most of the coupling schemes applied to ordinary differential equations or finite difference equations are very difficult to verify experimentally for partial differential equations. Generalization of the coupling schemes of arrays of coupled ordinary differential equations to partial differential equations is more complex, because there are no longer isolated cells to couple for PDEs, but one has to couple in spacial areas separated by small infinitesimal spaces.

Kocarev *et al.* [168] showed analytically (following the arguments of Heagy *et al. [121]*) and numerically that a large class of pairs of unidirectionally coupled of spatially extended dynamical systems with spatiotemporal chaotic dynamics can synchronize, and for the case of PDEs this is achieved by driving the response system only at a finite number of space points, through time discrete points [167] [168]. At each moment $t = kT$ $(k \in \mathbb{Z})$, the space points v_i, from the response PDE $\mathbf{v}_t = F(\mathbf{v}, \mathbf{v}_x, \mathbf{v}_{xx}, ...)$, $x \in [0, L]$, are simultaneously driven and their values are set to new values according to the equation $v_i(kT) = v_i(kT^-) + \alpha[u_i(kT) - v_i(kT^-)]$[3], being $\mathbf{u}_t = F(\mathbf{u}, \mathbf{u}_x, \mathbf{u}_{xx}, ...)$, $x \in [0, L]$, the drive PDE. The synchronization is verified by determining the local error in space and time $e_j(x,t) = |u_j(x,t) - v_j(x,t)|$ and the global error $e(t) = \sqrt{\frac{1}{L}\int_0^L \|\mathbf{u}(x,t) - \mathbf{v}(x,t)\|^2 dx}$. These authors also pointed out that two PDEs can synchronize by sporadic coupling [168].

Junge and co-workers [135] [138] considered the problem of controlling and synchronizing spatially extended systems, with only a few driving signals from local regions. They took the solution u of the one dimensional PDE, $u_t = F(u, u_x, u_{xx}, ...)$, $x \in [0, L]$, not at singular points in space x (which is impossible for experiments), but the local spatial average of the observable u, which is measured by N sensors $\overline{u}_n$ that take averaged values from local

[3] $v_i(kT^-)$ is the value of v_i in the immediately former instant to kT.

regions of width p at some time t

$$\overline{u}_n(t) = \frac{1}{p}\int_{nd-p/2}^{nd+p/2} u(y,t)\,dy,\ n = 1, ..., N. \tag{1.37}$$

being $d = L/(N+1)$ the distance between the sensors.

To synchronize a pair of PDEs, besides the N sensors $\overline{u}_n$ in the driving system, identical number of sensors $\overline{v}_n$ at same positions were measured in the driven system and a locally diffusive coupling term was used

$$f(u,v,x) = \begin{cases} \alpha(\overline{u}_n - \overline{v}_n),\ nd - p/2 \le x \le nd + p/2 \\ 0,\ elsewhere \end{cases} \tag{1.38}$$

being necessary a minimum value N of coupling signals for the synchronization to take place, which depended on the coupling strength α and the width p of the sensors . An examination of the synchronization properties of two coupled Kuramoto-Sivashinski equations was performed (the discretization scheme used was an explicit Euler scheme):

$$\begin{aligned} u_t &= -2uu_x - u_{xx} - u_{xxxx}, \quad x \in [0, L] \\ v_t &= -2vv_x - v_{xx} - v_{xxxx} + f(u,v,x) \end{aligned} \tag{1.39}$$

with boundary conditions $u = u_x = 0$ for $x = 0$ and $x = L$.

As the chaotic behavior in space destroys the spacial correlations at an exponential speed, the distance d between two sensors can not be arbitrarily large and must have more sensors for larger values of L. Also the sensor coupling improves the pinning control because less coupling signals are needed [135] [138]. It was confirmed by the authors of the works [135] [138] that the extensive Lyapunov dimension of the attractor D_L grows linearly with the system size L (because equation (1.39) shows extensive and microextensive chaos [253]). The synchronization mechanism was studied by computing the six largest transversal Lyapunov exponents (TLE) [4]. As applications, the synchronization of chaotic systems used for controlling purposes and suppression of chaos and the estimation of model parameters were presented by [135] [138]. The transition to high quality synchronization as a function of the number of sensors N occurred via spatiotemporal intermittency, although all transversal Lyapunov exponents were negative [254]. An extensive numerical study for a coupling of this type, applied to Ginzburg-Landau equation, with

[4] PDEs have infinite dimension and, therefore, there is also an infinite number of Lyapunov exponents. Determining only a number N of exponents, they are the N largest with probability one, because the components of the eighenspaces corresponding to the largest eighenvalues grow much faster.

similar results, was performed by Junge *et al.* [136], through the use of an implicit Crank-Nicholson discretization.

Wei [293] proposed a single-sided locally averaged adaptative coupling scheme for extended dynamical systems. The author showed that this scheme can suppress and control spatiotemporal oscillations, providing an approach for shock capturing. For the case of two identical systems, described by partial differential equations $u_t = F(u, u_x, u_{xx}, ...)$ and $v_t = F(v, v_x, v_{xx}, ...) + c(u, v)$, considering the adaptively coupling $c(u, v) = \varepsilon(|v_x|)\ (v - \overline{u})$, $\overline{u}(x, t) = \frac{1}{p}\int_{x-p/2}^{x+p/2} u(y, t)\, dy$, where the coupling strength ε is a nondecreasing function of the gradient measurement $|v_x|$, Wei [293] noticed an oscillation suppression occurring near the shocks, which appear, for example, in Burgers equation at low viscosity. These spurious oscillations were eliminated by coupling two Burgers equations, one of low viscosity and the other of a higher viscosity, and by coupling two exactly inviscid identical systems. The scheme became more dissipative as the size of local average was enlarged, as indicated by solving the inviscid Burgers equation with a Riemann-type initial value.

1.3 Contributions of the present work

Nonlinear equations arise in all fields of Engineering and Physics, hence being of fundamental importance the existence of methods to find their real roots. As analytical solutions are only available in few cases, the construction of efficient numerical methods are essential. Adomian's decomposition method has been successfully applied to linear and nonlinear problems, stochastic and deterministic [15] [17] [16], obtaining an exact or approximate solution to the problem. This method has the advantage of not requiring discretization, linearization or perturbation techniques, providing a rapid convergent solution series [69] [22] [6] [7] [8] [10] [68]. However, the method applied to nonlinear equations does not seem to be fast enough to be a efficient method to solve these kind of equations and one can find in the open literature some modifications proposed by several authors [33] [12] [35]. By applying the Adomian's decomposition method, a new iterative method to compute nonlinear equations is developed and is presented in this work. This new method [40] is based on the proposals of Abbasbandy to improve the order of accuracy of Newton-Raphson method [12] and on the proposals of Babolian and Biazar to improve the order of accuracy of Adomian's decomposition method [32]. The convergence of the new scheme is proved herein and at least the cubic order of convergence is established.

The application of Adomian's decomposition method to partial differential equations, when the exact solution is not reached, demands the use of

truncated series. But the solution's series may have small convergence radius being the truncated series only accurate in a small region. In order to enlarge the convergence domain of the truncated series, Padé approximants (PAs) to the Adomian's series solution have been tested and applied to ordinary differential equations, yielding promising and good results [29] [274] [273] [132]. In this thesis this technique is applied to partial differential equations, particularly to Burgers equation. Only recently, and simultaneously to the development of the work presented in this thesis, Padé approximants were implemented to the series solution given by Adomian's decomposition technique applied to partial differential equations (KdV and mKdV equations) [4] and to an example of the Boussinesq and Burgers equation [5]. Graphical illustrations were used to show that this technique can enlarge the domain of convergence of Adomian's solution. It is also referred by [4] [5] that the solution accuracy can be improved by increasing the order of the Padé approximants. In this thesis, besides graphical illustrations, also numerical results are presented to show that this technique can not only enlarge the domain of convergence of the solution but also improves its accuracy even when the actual solution cannot be expressed as the ratio of two polynomials. In addition, a disadvantage not referred by [4] [5], can come through: the rational approximation may create inaccurate solutions near its poles when the real solution is not achieved. This drawback advises the search for the optimal order of the Padé approximants to be used, which can be of lower order. Also, the application of Adomian's method to the ordinary differential equations set arising from the discretization of the spatial derivatives by finite differences, the so called method of lines, is performed in the present work and it is shown that this is not useful, because this technique may reduce the convergence domain of the series solution [43].

New behaviors are found for the numerical solution of the driven Burgers equation by collocation spectral methods [42]. For low values of the viscosity coefficient, Burgers equation can develop sharp discontinuities, which are difficult to simulate in a computer. Oscillations can occur by discretization through spectral collocation methods, due to the Gibbs phenomena. Under a dynamic point of view, all these instabilities may be related to the presence of different attractors and bifurcations arising to the discretized equation for different values of the viscosity coefficient. In this thesis it is studied the stability, bifurcation and dynamics of spectral collocation methods applied to forced Burgers equations, where the unknown solution of the differential equation is expanded as a global interpolant. Besides the trapping region found by Dang-Vu and Delcarte [77], arising from the loss of stability of the periodic orbits arising from an Hopf bifurcation, other phenomena are observed. In fact, it is observed the existence of nonperiodic attractors,

torus and strange attractors, for lower values of the parameter below the Hopf point, before the dynamics becomes unbounded [42] [41].

Also observed is the presence of bistability with two periodic attractors, with a periodic attractor and a nonperiodic one (torus or strange attractor) and even with two nonperiodic attractors. In this last case, the nonperiodic orbits seem to correspond to quasiperiodic motions on torus type attractors [41]. During this work, it was verified that other stable equilibrium points can occur, diverse from the ones corresponding to the asymptotic solution of Burgers equation, and that new Hopf points can occur, breaking (or not breaking) the symmetry of the system, if present. Discussion of the necessary conditions for the emergence of these phenomena is also presented. This rich behavior indicates that Burgers equation is a good model for the study of several dynamical behaviors that can occur in many other situations. Also this kind of behavior can be used to study and to implement new techniques of synchronization of high dimensional systems.

Sufficient conditions for identical synchronization of coupled Burgers equations, by means of a Lyapunov function, is presented. As an application for the dynamics apparent by spectral solutions of forced Burgers equation, unidirectionally coupled equations with and without parameter mismatch are also studied. It is tested the unidirectionally coupling with a drive forced spatially spectral discretized Burgers equation in stationary regime and the driven equation in any motion regime. It is found out that increasing the coupling strength it is possible to carry out the suppression of the corresponding motion through periodic and nonperiodic windows till the stationary solution is reached. Numerical studies show and confirm the presence of identical and generalized synchronization for different values of spacial points and different values of the viscosity coefficient δ in several regimes. Also, by combining the partial replacement [109] [108] [227] of one or more components of coupled ODEs and the nonlinear coupling presented in [117] for discrete coupled systems, a nonlinear coupling is constructed in the three locations of the response discretized equation, waves velocity v, $\frac{\partial v}{\partial x}$ and $\frac{\partial^2 v}{\partial x^2}$, by replacing the response variable discretized v by $u + \alpha\,(u - v)$, where u represents the drive and α the coupling parameter. It is observed that coupling at the position corresponding to the waves velocity v, by a convex linear combination of the drive and driven variables with $\alpha < 1$, identical or generalized synchronization is achieved, only allowing values of α around 1 in very few cases. This point out the fact that although the partial replacement may not reach synchronization, nonlinear coupling with $\alpha < 1$ may do it. Coupling at $\frac{\partial v}{\partial x}$, synchronization is only observed in very few cases and with low values of the coupling parameter α, whereas at $\frac{\partial^2 v}{\partial x^2}$ synchronization is not achieved [41].

1.4 Structure of the thesis

The present thesis is structured as follows:

Chapter 1, the present chapter, constitutes the Introduction.

In chapter 2 a review of some important concepts related to partial differential equations and the development of singular solutions is made.

In chapter 3 a description of the Adomian's decomposition method and its convergence is made. A new iterative method to compute nonlinear equations is presented and the numerical improvement of Adomian's method applied to Burgers equation by Padé approximants is performed. Also, the application of Adomian's method to the ordinary differential equations set arising from the application of the method of lines, is studied.

In chapter 4 an introduction to some notions of dynamical systems, such as bifurcations and chaos and related instruments, like Lyapunov exponents, is presented. Also a brief introduction to spectral methods is made. The study of spectral solutions of several forced Burgers equations is performed together with its discussion.

In chapter 5 a discussion of the synchronization of a linear coupled Burgers equation, by means of a Lyapunov function, is presented. Also a study of unidirectionally coupled forced spectral solutions of Burgers equations with and without parameter mismatch is performed.

In chapter 6 conclusions are withdrawn and suggestions for further work are made.

2. PARTIAL DIFFERENTIAL EQUATIONS

Some partial differential equations can develop discontinuities in its solutions, so a brief review of some concepts related to PDEs are very important to fully understand how to define such solutions. It is imperative to generalize the concept of solution of a differential equation and to introduce concepts that allows one to define solutions that exist from the point of view of applications, but that are not sufficiently smooth to be solutions from the strict or classic point of view.

Burgers equation [55] is a PDE that admits analytical solution for the initial value problem [297] [96] [97] [72] [126] and can develop such singular solutions, solutions that in the classic sense do not exist [55]. This one is the PDE worked out in this thesis, hence, a brief review of the relation between this equation, Navier-Stokes and heat equation is presented here.

2.1 The classification of partial differential equations

A wide variety of problems arising from Engineering, Physics, Chemistry, Finance, Biology, and all other science subjects, are characterized by partial differential equations (PDEs). In particular, among those, the second order equations possess a major importance in applications. To study and to correctly implement numerical methods, classification of partial differential equations is of great matter. There are three different basic categories for second order linear partial differential equations, with mathematical and physical different properties, describing three types of different physical phenomena [95]. Being u the dependent variable, such categories are:

The *wave equation* (associated with oscillatory processes)

$$u_{tt} = c^2 \Delta u \tag{2.1}$$

The *heat equation* (associated with diffusion processes)

$$u_t = \alpha^2 \Delta u \tag{2.2}$$

The *potential equation* or *Poisson equation* (associated with stationary processes)

$$\Delta u = -\frac{1}{\varepsilon_0}\rho \tag{2.3}$$

being ρ a given function, and c^2, α^2 and ε_0 representing, generally, physical constants. The potential equation is transformed into the *Laplace equation* for $\rho = 0$.

$$\Delta u = 0 \tag{2.4}$$

These equations are also classified, according to their mathematical properties, into, respectively, hyperbolic, parabolic and elliptic equations, possessing two, one and zero real characteristics (on the plane).

The second order quasilinear partial differential equations are of the form $a(x,t)u_{xx} + b(x,t)u_{xt} + c(x,t)u_{tt} = f(x,t,u,u_x,u_t)$, being the classification made as a function of the sign of the discriminant $b^2 - 4ac$. The equation is hyperbolic if $b^2 - 4ac > 0$, is parabolic if $b^2 - ac = 0$ and is said to be elliptic if $b^2 - 4ac < 0$. As the functions a, b and c depend on x and t, the sign of the discriminant may fluctuate for different values of x and t, and so the same equation may be classified in different way according to the range under consideration [78] [200].

As far as their application is concerned, hyperbolic equations are generally adequate to model transport phenomena, parabolic equations are more appropriate to model diffusion phenomena and elliptic equations generally model equilibrium or permanent phenomena.

Generally, both parabolic and elliptic equations exhibit regular solutions, whereas singular solutions are more common for hyperbolic equations. This is a fundamental issue on the development of numerical schemes [75] [101].

2.2 Sobolev spaces

Many nonlinear equations develop discontinuities. This has as consequence the inexistence of a solution in the classic sense. Sobolev spaces are the replacement for the classic space C^k of solutions of partial differential equations of order k [201] [235].

Consider Ω a nonempty open set belonging to $\mathbb{R}^n$, the Banach space $L^p(\Omega) = \left\{u : \Omega \to \mathbb{R} : \int_\Omega |u|^p < \infty\right\}$, $1 \leq p < \infty$, with the associated norm $||u||_{L^p(\Omega)} = \left(\int_\Omega |u|^p\right)^{1/p}$ and $L^p_{loc}(\Omega) = \{u \in L^p(K)$, for all compact subset of K of $\Omega\}$. For $p = 2$, $L^2(\Omega)$ is an Hilbert space for the usual scalar product $(u,v) = \int_\Omega u(x)v(x)\,dx$. The space of all functions belonging to $C^\infty(\Omega)$ with support compact in Ω, is called the space of test functions $\mathcal{D}(\Omega)$, and is dense in $L^p(\Omega)$ for $1 \leq p < \infty$. The following notion of convergence is associated: a sequence of test functions (φ_ν) converges to zero, when the support of all functions φ_ν belong to a fix compact K, and when for every $\alpha \in \mathbb{N}^n$, the sequence $(D^\alpha \varphi_\nu)$ converges to zero uniformly in K, where $\alpha = (\alpha_1, \alpha_2, ..., \alpha_n) \in \mathbb{N}^n$ and $D^\alpha \equiv \frac{\partial^{|\alpha|}}{\partial x_1^{\alpha_1} \partial x_2^{\alpha_2} \cdots \partial x_n^{\alpha_n}} = \frac{\partial^{\alpha_1+\alpha_2+\ldots+\alpha_n}}{\partial x_1^{\alpha_1} \partial x_2^{\alpha_2} \cdots \partial x_n^{\alpha_n}}$. A sequence of test functions (φ_ν) converges to φ when $(\varphi_\nu - \varphi)$ converges to zero. The dual space $\mathcal{D}'(\Omega)$ of all continuous functionals T, defined on $\mathcal{D}(\Omega)$, is called the *distribution space* on Ω.

One calls *generalized derivative* or *derivative in the sense of distributions*

of order α of u, to the function $v \in L^1_{loc}$ such that

$$\int_\Omega u(x) D^\alpha \varphi(x) dx = \int_\Omega (-1)^{|\alpha|} v(x) \varphi(x) dx \quad \forall \varphi \in \mathcal{D}(\Omega)$$

where $|\alpha| = \alpha_1 + \alpha_2 + ... + \alpha_n$. One says that $D^\alpha u = v$ in the sense of distributions.

The Sobolev space $W^{m,p}(\Omega)$ consists of all functions u belonging to the Lebesgue space $L^p(\Omega)$, $1 \leq p < \infty$, having generalized derivatives of all orders, up to the order m in $L^p(\Omega)$. One defines the norm $||u||^\Omega_{m,p} = \left(\sum_{|\alpha| \leq m} \int_\Omega |D^\alpha u(x)|^p \, dx \right)^{1/p}$, $1 \leq p < \infty$, being the Sobolev space $W^{m,p}(\Omega)$ a Banach space. The particular case of $p = 2$ is very useful in applications and one represents $W^{m,p}(\Omega)$ by $H^m(\Omega)$.

When $m = 0$, $W^{0,p}(\Omega) = L^p(\Omega)$, and although $\mathcal{D}(\Omega)$ is dense in $L^p(\Omega)$ it is not true that $\mathcal{D}(\Omega)$ is always dense in $W^{m,p}(\Omega)$, $m \geq 1$. Due to that one represents $W^{m,p}_0(\Omega)$ as the closure of $\mathcal{D}(\Omega)$ with respect to the norm $|| \cdot ||^\Omega_{m,p}$, *i.e.* the closure of $\mathcal{D}(\Omega)$ with respect to $W^{m,p}(\Omega)$. For $p = 2$, one represents $W^{m,p}_0(\Omega)$ by $H^m_0(\Omega)$ [201] [235].

2.3 Conservation laws

Conservation laws describe a conservation principle of some basic physical quantities of a system. In fluid mechanics the equations of motion are of the type, *conservation hyperbolic equations* [88] [101]

$$\frac{\partial u}{\partial t} + \nabla \cdot F(u) = S(u) \tag{2.5}$$

being F the correspondent total flux u per unit time.

If u is smooth and $S(u) = 0$, equation (2.5) becomes

$$\frac{\partial u}{\partial t} = -\left(F'(u)\right) \frac{\partial u}{\partial x} \tag{2.6}$$

Generalized inviscid Burgers equation is obtained substituting $F(u) = \left(\alpha + \frac{\beta}{2} u\right) u$ in equation(2.6), which yields:

$$\frac{\partial u}{\partial t} + \alpha \frac{\partial u}{\partial x} + \beta u \frac{\partial u}{\partial x} = 0 \tag{2.7}$$

Equations of this type admit solutions with spontaneous singularities, developing discontinuities. This means that, in the classic sense, solutions of

such equations do not exist. The solutions that we look for are weak solutions $u \in L^1_{loc}$.

For $\alpha = 0$ and $\beta = 1$, equation (2.7) becomes the *standard inviscid Burgers equation*

$$\frac{\partial u}{\partial t} + u\frac{\partial u}{\partial x} = 0 \tag{2.8}$$

Using the method of characteristics [78], one can study and even obtain the solution of equation (2.6) with given initial conditions. Equation (2.6) reveals that the vector field $(x, t, u) \mapsto (F'(u), 1, 0)$, must be tangent to the integral surface. Introducing an auxiliary variable λ, the following set of three equations is obtained [27] [197] [78]:

$$\begin{bmatrix} \frac{dx}{d\lambda} \\ \frac{dt}{d\lambda} \\ \frac{du}{d\lambda} \end{bmatrix} = \begin{bmatrix} F'(u) \\ 1 \\ 0 \end{bmatrix} \tag{2.9}$$

In the previous set of equations its integral curves are the *characteristics curves* for equation (2.6). The integral surface that satisfies the initial condition $(x, t, u)_{\lambda=0} = (\tau, 0, u_0(\tau))$ is

$$\begin{bmatrix} \frac{dx(\tau,\lambda)}{d\lambda} \\ t(\tau, \lambda) \\ u(\tau, \lambda) \end{bmatrix} = \begin{bmatrix} F'(u(\tau, 0)) \\ \lambda + t(\tau, 0) \\ u(\tau, 0) \end{bmatrix} \tag{2.10}$$

$$\begin{bmatrix} x(\tau, \lambda) \\ t(\tau, \lambda) \\ u(\tau, \lambda) \end{bmatrix} = \begin{bmatrix} F'(u(\tau, 0))\lambda + x(\tau, 0) \\ \lambda + t(\tau, 0) \\ u(\tau, 0) \end{bmatrix} = \begin{bmatrix} F'(u_0(\tau))\lambda + \tau \\ \lambda \\ u_0(\tau) \end{bmatrix} \tag{2.11}$$

Therefore , one gets the implicit solution given by $u = u_0(x - F'(u) \cdot t)$. For each value of τ, the curves $\lambda \mapsto (x(\tau, \lambda), t(\tau, \lambda))$, projections on $u = 0$ of the characteristic curves, called *characteristics base curves* or *simply characteristics* (plane solution curves), along which the initial conditions propagate, are straight lines $x - F'(u_0(\tau)) \cdot t = \tau$, that have as slope [197] [88] [101] [78]:

$$\frac{dt}{dx} = \frac{1}{F'(u_0(x))} \tag{2.12}$$

Discontinuous solutions for a Cauchy problem for a nonlinear conservation partial differential equation are settled either as *shock type solutions* or as *fan type solutions* [78] [88]. As they do not admit a single weak solution, it becomes necessary to apply some selection principle to identify the physically relevant solution from all possible solutions. A form of doing this is to impose the *entropy condition of Lax* to the weak solution, which establishes that a

shock solution occurs when characteristics carrying conflicting information collide. The discontinuities in the solution then appear, being created the shock surfaces, in which $u(x,t)$ takes several values, that is a phenomenon frequent in hyperbolic nonlinear equations [78] [88].

For a weak solution u of equation (2.6), which possesses a jump discontinuity along a curve c, but is smooth on either side of the curve, the propagation velocity $\frac{dx}{dt}$ should satisfy the *Rankine-Hugoniot relation* for the speed of the shock wave [232] [78] [88] [78]

$$\frac{dx}{dt}\left(u^{+}-u^{-}\right)=F\left(u^{+}\right)-F\left(u^{-}\right) \tag{2.13}$$

One solution of this type is as a shock type solution, being c the *shock curve*. Discontinuities transmit along these shock curves.

The conservation law is said to be *genuinely nonlinear* if $F''(u)\neq 0$. If, for example, $F(u)=a(x,t)\,u(x,t)$, then $F'(u)=a(x,t)$ and the conservation equation is linear, reducing the Rankine-Hugoniot relation (2.13) to $\frac{dx}{dt}=a(x,t)$. This means that, in this case, the shock curve is just a characteristic curve for the PDE. There are some important differences between linear and nonlinear initial value problems [88] [78]. For linear problems and for all smooth initial data, there is a smooth global solution, which is uniquely determined by the equation and the initial data. Moreover, discontinuities in the initial data propagate along characteristics curves and solutions are invariant under smooth transformations and equivalent equations have the same smooth solutions. On the other hand, for nonlinear problems, it may not exist any global classical solution even for smooth initial data. Although global weak solutions exist, they are not uniquely determined by the equation and the initial data. In addition, discontinuities can arise spontaneously and are propagated along noncharacteristic curves called shock curves. Also, weak solutions are not invariant under smooth transformations and equations that are algebraically equivalent may not have the same weak solutions. Particular care is required in the variable changes used in the resolution of nonlinear equations, because in spite of the smooth transformations of the conservation equations, they lead to equivalent equations as far as smooth solutions are concerned, but the weak solutions are in general different, which means that the shocks are in general different.

One classic form of obtaining the solution of the conservation equation (2.6) $\partial u/\partial t+\partial F(u)/\partial x=0$ is to make recourse to the equation disturbed by some viscosity $\partial u/\partial t+\partial F(u)/\partial x=\delta\,\partial^2 u/\partial x^2$. As this equation admits analytical solution for all initial conditions belonging to $L^2(\mathbb{R})$ [126], making $\delta\to 0$ one hopes to obtain the relevant physical solution of the original equation without viscosity. This method of studying the conservation equation

(2.6) is called *parabolic regularization* [88] [78].

2.4 Navier-Stokes and Burgers equations

The equations that govern the laminar flux, Newtonian fluids, are the Navier-Stokes equations [89] for compressible fluids.

$$-\nabla p + \delta\left(\nabla^2 \mathbf{v}\right) + \frac{1}{3}\delta\left[\nabla\left(\nabla \cdot \mathbf{v}\right)\right] + \rho\mathbf{b} = \rho\dot{\mathbf{v}} \tag{2.14}$$

For incompressible fluids, the Navier-Stokes equation take the form:

$$-\nabla p + \delta\left(\nabla^2 \mathbf{v}\right) + \rho\mathbf{b} = \rho\dot{\mathbf{v}} \tag{2.15}$$

In the previous equations, $\mathbf{v}$ is the particle velocity vector, p is the pressure, ρ is the density, δ is the fluid viscosity and $\mathbf{b}$ is the body force vector. The time derivative of the fluid velocity, $\dot{\mathbf{v}}$, is the *material* or *transport derivative*, defined as

$$\dot{\mathbf{v}} \equiv \frac{\partial \mathbf{v}}{\partial t} + \mathbf{v} \cdot \nabla \mathbf{v} \tag{2.16}$$

Burgers equation can be considered as a simplification of the Navier-Stokes equations, by neglecting the terms of pressure and body force as both Navier-Stokes and Burgers equations contain nonlinear terms of the same type and higher-order terms multiplied by a small parameter:

$$\frac{\partial u}{\partial t} + u\frac{\partial u}{\partial x} - \delta\frac{\partial^2 u}{\partial x^2} = 0 \tag{2.17}$$

However, Burgers equation with high Reynolds number[1], or equivalently, small values for the viscosity coefficient, develops waves with sharp slopes. This phenomenon is responsible for the appearance of discontinuities for values $\delta \to 0$, yielding difficulties to obtain a solution. For $\delta = 0$ the inviscid Burgers equation is an hyperbolic equation type:

$$\frac{\partial u}{\partial t} + u\frac{\partial u}{\partial x} = 0 \tag{2.18}$$

Burgers equation can be transformed into the linear heat equation by the *Hopf-Cole transformation* [126] [72] [232], so exact solutions to Burgers equation with initial conditions can be obtained. Burgers equation is connected to the heat equation

$$\frac{\partial v}{\partial t} = \delta\frac{\partial^2 v}{\partial x^2} \tag{2.19}$$

[1] Reynolds number, a nondimensional number, determines the flux type, either laminar or turbulent, $R = \frac{\rho V D}{\delta}$, being V the velocity and D the carachteristic lengh.

by the Bäcklund transformation [232]

$$\frac{\partial v}{\partial x}+\frac{1}{2\delta}vu=0 \tag{2.20}$$

$$\frac{\partial v}{\partial t}+\frac{1}{2}\frac{\partial\left(vu\right)}{\partial x}=0 \tag{2.21}$$

Relation (2.20) may be rewritten as the following differential substitution:

$$u=-\frac{2\delta}{v}\frac{\partial v}{\partial x}=-2\delta\frac{\partial}{\partial x}\log v \tag{2.22}$$

This formula is called the *Hopf-Cole transformation* [126], [72] [232]. A solution can be obtained for the Burgers equation (2.17) to the Cauchy problem

$$\begin{aligned}\frac{\partial u}{\partial t}+u\frac{\partial u}{\partial x}&=\delta\frac{\partial^2 u}{\partial x^2},\quad x\in\mathbb{R},\ t>0\\ u\left(x,0\right)&=f\left(x\right)\end{aligned} \tag{2.23}$$

Eliminating u from (2.20) and (2.21) one obtains the heat equation (2.19), or, using Hopf-Cole transformation (2.22) [232]:

$$\begin{aligned}&\frac{\partial u}{\partial t}+u\frac{\partial u}{\partial x}-\delta\frac{\partial^2 u}{\partial x^2}=\\ &=-2\delta\frac{v_{xt}}{v}+2\delta\frac{v_t v_x}{v^2}+4\delta^2\frac{v_{xx}v_x}{v^2}-4\delta^2\frac{\left(v_x\right)^3}{v^3}+\\ &\quad+2\delta^2\frac{v_{xxx}}{v}-2\delta^2\frac{v_{xx}v_x}{v^2}-4\delta^2\frac{v_{xx}v_x}{v^2}+4\delta^2\frac{\left(v_x\right)^3}{v^3}=\\ &=-2\delta\frac{v_{xt}}{v}+2\delta\frac{v_t v_x}{v^2}+2\delta^2\frac{v_{xxx}}{v}-2\delta^2\frac{v_{xx}v_x}{v^2}=\\ &=-\frac{\partial}{\partial x}\left[\frac{2\delta}{v}\left(\frac{\partial v}{\partial t}-\delta\frac{\partial^2 v}{\partial x^2}\right)\right]=0\end{aligned} \tag{2.24}$$

where $v\left(x,t\right)$ is the solution of the linear heat equation (2.19). Then, if v satisfies the heat equation (2.19), u satisfies Burgers equation (2.23). The initial conditions for the heat equation must be similarly transformed, being given by the solution of the ordinary differential equation $u\left(x,0\right)=f\left(x\right)=-\frac{2\delta}{v(x,0)}\frac{\partial v(x,0)}{\partial x}$, having as solution:

$$v\left(x,0\right)=K\exp\left(-\frac{1}{2\delta}\int_0^x f\left(s\right)ds\right) \tag{2.25}$$

The heat equation (2.19) with initial condition (2.25) has the following solution [78] [95]:

$$v\left(x,t\right)=\frac{1}{\sqrt{4\delta\pi t}}\int_{-\infty}^{+\infty}\exp\left(-\frac{\left(x-y\right)^{2}}{4\delta t}\right)v\left(y,0\right)\ dy \tag{2.26}$$

It becomes apparent that the zeros of the heat equation correspond to singularities of the Burgers equation [139]. Finally, the solution for Burgers equation (2.23) is:

$$u\left(x,t\right)=\frac{\int_{-\infty}^{+\infty}\left(x-y\right)\exp\left(-\frac{\left(x-y\right)^{2}}{4\delta t}-\frac{1}{2\delta}\int_{0}^{y}f\left(s\right)ds\right)\ dy}{t\int_{-\infty}^{+\infty}\exp\left(-\frac{\left(x-y\right)^{2}}{4\delta t}-\frac{1}{2\delta}\int_{0}^{y}f\left(s\right)ds\right)dy} \tag{2.27}$$

This transformation rules out stochastic behavior, and exclude, in principle, Burgers equation for modeling of turbulence.

3. ADOMIAN'S DECOMPOSITION METHOD

3.1 Adomian's decomposition method

Adomian's method has been applied to solve and to obtain formal and approximate solutions to a wide class of problems, arising from Physics, Chemistry, Biology or Engineering. For both linear and nonlinear problems, Adomian's decomposition method allows one to obtain an exact analytical solution, or when that is not possible, to obtain an approximate solution with very fast convergence to the actual solution. Also the method does not need discretization, linearization or perturbation theory to be applied [15] [19] [17] [22].

In this chapter, a description of Adomian's method and its convergence is present, followed by two sections where two different applications of Adomian's method are studied. The first study concerns an application to nonlinear equations, where a efficient iterative method to solve these kind of equations is constructed. The second one concerns the numerically improvement of the solution of Burgers equation by Adomian's method.

3.1.1 Description of the method

For the sake of generality it is described the method applied to a nonlinear differential equation $Fu = g$, where F represents a nonlinear differential operator. The technique consists on decomposing the linear part of F in $L + R$, where L is an operator easily invertible and R is the remaining part. Representing the nonlinear term by N, the equation in *canonical form* runs

$$Lu + Ru + Nu = g \tag{3.1}$$

Representing the inverse of the invertible operator L by L^{-1}, one gets the following equivalent equation:

$$L^{-1}Lu = L^{-1}g - L^{-1}Ru - L^{-1}Nu \tag{3.2}$$

Being L the operator derivative of order n, L^{-1} represents the n-fold integration operator. Thus, $L^{-1}Lu = u + a$, containing a the terms achieving from the integration. We look for a series solution $u = \sum_{n=0}^{\infty} u_n$. Identifying u_0 as $L^{-1}g - a$, equation (3.2) yields:

$$u = u_0 - L^{-1}Ru - L^{-1}Nu \tag{3.3}$$

The rest of the terms u_n, $n > 0$, will further be settled by a recursive relation. The key of the method is to decompose the nonlinear term in the

equation Nu, into a particular series of polynomials $Nu = \sum_{n=0}^{\infty} A_n$, being A_n the so called *Adomian polynomials*. Each polynomial A_n depends only on the independent variables and on $u_0, u_1, \ldots, u_n$, for each n. Adomian introduced formulae to generate these polynomials for all kinds of nonlinearities [17] [15] [19] [22]. It has also been shown that the sum of the Adomian polynomials is a generalization of Taylor series in a neighborhood of a function u_0 rather than a point,

$$Nu = \sum_{n=0}^{\infty} A_n = \sum_{n=0}^{\infty} \frac{1}{n!} (u - u_0)^n N^{(n)} (u_0) \tag{3.4}$$

tending the general term of the series to zero very fast, as $\frac{1}{(mn)!}$, due to the optimal choice of the initial term, for m terms and n order of L [69] [22].

Substituting $u = \sum_{n=0}^{\infty} u_n$ and $Nu = \sum_{n=0}^{\infty} A_n$ into equation (3.3) one gets:

$$\sum_{n=0}^{\infty} u_n = u_0 - L^{-1} R \sum_{n=0}^{\infty} u_n - L^{-1} \sum_{n=0}^{\infty} A_n \tag{3.5}$$

To determine the components $u_n(x,t)$, $n = 0, 1, 2, ...$, one employs the following recursive relation:

$$\begin{aligned} u_1 &= -L^{-1} R\ u_0 - L^{-1} A_0 \\ u_2 &= -L^{-1} R\ u_1 - L^{-1} A_1 \\ &\vdots \\ u_{n+1} &= -L^{-1} R\ u_n - L^{-1} A_n \\ &\vdots \end{aligned} \tag{3.6}$$

Adomian polynomials were formally introduced by [15] [17] [19] [68] [6] as follows:

$$A_n (u_0, u_1, \ldots, u_n) = \frac{1}{n!} \left[\frac{d^n}{d\lambda^n} N \left(\sum_{i=0}^{\infty} \lambda^i u_i \right) \right]_{\lambda=0} \tag{3.7}$$

This formula is achieved by introducing, for convenience, the parameter λ, and writing

$$u(\lambda) = \sum_{n=0}^{\infty} \lambda^n u_n \tag{3.8}$$

$$N(u(\lambda)) = \sum_{n=0}^{\infty} \lambda^n A_n \tag{3.9}$$

Expanding in a Taylor series $N \circ v$ in a neighborhood of $\lambda = 0$ one gets

$$\begin{aligned} N\left(v\left(\lambda\right)\right) &= \sum_{n=0}^{\infty} \frac{1}{n!} \left[\frac{d^n}{d\lambda^n} N\left(u\left(\lambda\right)\right)\right]_{\lambda=0} \lambda^n \\ &= \sum_{n=0}^{\infty} \frac{1}{n!} \left[\frac{d^n}{d\lambda^n} N\left(\sum_{i=0}^{\infty} \lambda^i u_i\right)\right]_{\lambda=0} \lambda^n \end{aligned} \tag{3.10}$$

From the previous equation, equation (3.7) follows immediately.

Practical methods have been developed for the calculation of Adomian's polynomials A_n [6] [8] [10] [9]. The next theorem [6] [64], allows the infinite series representing the Adomian's polynomials A_n to be substituted by a finite sum, fact that allows its computation.

Theorem 5: Adomian's polynomials A_n may be computed by the formula

$$A_n = \frac{1}{n!} \left[\frac{d^n}{d\lambda^n} N\left(\sum_{i=0}^{n} \lambda^i u_i\right)\right]_{\lambda=0} \tag{3.11}$$

For systems of differential or algebraic equations, the nonlinear terms N, may be of the form $N = N\left(v_1, v_2, ..., v_k, ...\right)$, $v_k = \sum_{i=0}^{\infty} v_{ki}$. From a similar way [64], the Adomian's polynomials can be calculated through equation (3.12).

$$\begin{aligned} A_n &= \frac{1}{n!} \left[\frac{d^n}{d\lambda^n} N\left(\sum_{i=0}^{\infty} \lambda^i u_{1i}, \sum_{i=0}^{\infty} \lambda^i u_{2i}, ..., \sum_{i=0}^{\infty} \lambda^i u_{ki}, ...\right)\right]_{\lambda=0} \\ &= \frac{1}{n!} \left[\frac{d^n}{d\lambda^n} N\left(\sum_{i=0}^{n} \lambda^i u_{1i}, \sum_{i=0}^{n} \lambda^i u_{2i}, ..., \sum_{i=0}^{n} \lambda^i u_{ki}, ...\right)\right]_{\lambda=0} \end{aligned} \tag{3.12}$$

The polynomials may also be computed with the formulae expressed by equations (3.13) and (3.14) [6] [8],

$$A_0\left(u_0\right) = N\left(u_0\right) \tag{3.13}$$

$$A_n\left(u_0, u_1, \ldots, u_n\right) = \sum_{\substack{\alpha_1+...+\alpha_n=n \\ \alpha_1 \geq \alpha_2 \geq ... \geq \alpha_n}} N^{(\alpha_1)}\left(u_0\right) \frac{u_1^{(\alpha_1-\alpha_2)}}{(\alpha_1-\alpha_2)!} \cdots \frac{u_{n-1}^{(\alpha_{n-1}-\alpha_n)}}{(\alpha_{n-1}-\alpha_n)!} \frac{u_n^{\alpha_n}}{\alpha_n!}, \tag{3.14}$$

$$n \geq 1 \tag{3.15}$$

or by expressing the series solution as a function of the first term of the series that is always known [8]

$$A_n(u_0) = \sum_{\substack{\alpha_1+\ldots+\alpha_n=n \\ \alpha_1\geq\alpha_2\geq\ldots\geq\alpha_n}} C_{\alpha_1,\alpha_2,\ldots,\alpha_n} \left[N(u_0)\right]^{n+1-\alpha_1} \left[N'(u_0)\right]^{\alpha_1-\alpha_2} \cdots \cdots \left[N^{(n-1)}(u_0)\right]^{\alpha_{n-1}-\alpha_n} \left[N^{(n)}(u_0)\right]^{\alpha_n}, \quad n \geq 1 \tag{3.16}$$

where

$$C_{\alpha_1,\alpha_2,\ldots,\alpha_n} = \frac{n!}{(\alpha_1-\alpha_2)!\cdots(\alpha_{n-1}-\alpha_n)!\alpha_n!\,(1!)^{\alpha_1-\alpha_2}\cdots(n-1)^{\alpha_{n-1}-\alpha_n}(n+1-\alpha_1)!} \tag{3.17}$$

Generalizations of these formulae to polynomials on several variables may be consulted in [10].

A technique to calculate Adomian's polynomials by using only algebraic operations, trigonometric identities and Taylor series was introduced by [275]. The application of this algorithm with the Mathematica software may be consulted in [71].

3.1.2 Convergence of Adomian's method

One important observation is that the series solution of Adomian's decomposition technique usually converges very fast to the exact solution, if one exists, and to one of the solutions, if several exist, tending the general term of the series solution to zero very fast, as $\frac{1}{(mn)!}$, for m terms and n order of L [69] [22].

The convergence of Adomian's method has been subject of investigation by several authors [66] [70] [68] [6] [7] [100] [8] [10] [69] [36].

Following Cherruault [66], the Adomian's decomposition method applied to the functional equation $u = f + N(u)$, where N is a nonlinear operator from a Hilbert space H into H and f is a given function in H, is equivalent to determining the sequence $(S_n)_n = (u_1 + u_2 + \ldots + u_n)_n$ by using the iterative scheme $S_{n+1} = N(u_0 + S_n)$, $S_0 = 0$, which converges if N is a contraction. This scheme may be associated with the functional equation $S = N(u_0 + S)$, which, in turn, is susceptible of being solved by Adomian's technique.

Abbaoui and Cherrault [8], with new formulae for calculate the Adomian's polynomials used in decomposition method, gave a proof of convergence of the Adomian's decomposition technique applied to the functional equation

$u = f + N(u)$. Following Abbaoui and Cherrault [8], one has the following results:

Theorem 6: If $N \in C^\infty$ in a neighborhood of u_0 and $\left\|N^{(n)}(u_0)\right\| \leq M'$, $\forall n \in \mathbb{N}$ (the derivatives of N are bounded in norm in a neighborhood of u_0), and if $\|u_i\| \leq M$, $i = 1, 2, ...$, where $\|\cdot\|$ is the norm in the Hilbert space H, then the series $\sum_{n=0}^{\infty} A_n$ is absolutely convergent and, furthermore, $\|A_n\| \leq M' M^n \exp\left(\pi\sqrt{\frac{2}{3}n}\right)$

Theorem 7: If $N \in C^\infty$ in a neighborhood of u_0 and $\left\|N^{(n)}(u_0)\right\| \leq M < 1$, $\forall n \in \mathbb{N}$, then the decomposition series $\sum_{n=0}^{\infty} u_n$ is absolutely convergent and, furthermore, $\|u_{n+1}\| = \|A_n\| \leq M^{n+1} n^{\sqrt{n}} \exp\left(\pi\sqrt{\frac{2}{3}n}\right)$

The following results are due to Cherruault [66] and Mavoungou and Cherruault [198]. Consider the Hilbert space H, defined by $H = L^2((\alpha, \beta) \times [0, T])$, the set of applications:

$$u : (\alpha, \beta) \times [0, T] \to \mathbb{R} \quad \text{with} \quad \int_{(\alpha,\beta)\times[0,T]} u^2 ds d\tau < +\infty \tag{3.18}$$

and the scalar product

$$(u, v)_H = \int_{(\alpha,\beta)\times[0,T]} uv \; ds d\tau < +\infty \tag{3.19}$$

and the associated norm

$$\|u\|_H^2 = \int_{(\alpha,\beta)\times[0,T]} u^2 ds d\tau < +\infty \tag{3.20}$$

Consider the differential equation

$$Lu + Ru + Nu = g \tag{3.21}$$

with

$$Tu = Ru + Nu \tag{3.22}$$

Consider the following hypotheses:

(H_1) There exists a constant $k > 0$, such that for every $u, v \in H$, the following inequality holds $(T(u) - T(v), u - v) \geq k \|u - v\|^2$

(H_2) Whatever may be $M > 0$, there exists a constant $C(M) > 0$, such that for every $u, v \in H$ with $\|u\| \leq M$, $\|v\| \leq M$, one has $(T(u) - T(v), w) \leq C(M) \|u - v\| \|w\|$ for every $w \in H$

If the above hypotheses are satisfied, the Adomian's method is convergent according to [66] [198].

Other results of convergence are described in the literature. Sufficient conditions to obtain convergence of Adomian's method were presented by [11] [123]. In the work of [213], sufficient conditions of convergence for Adomian's technique applied to algebraic equations were put forward. Convergence of the Adomian's method applied to linear and nonlinear diffusion equations (partial differential equations) were proved by [211].

3.2 A new iterative method to compute nonlinear equations

One of the most and generalized process to find accurate roots of nonlinear equations is the Newton-Raphson iterative method [231] [113], a method with quadratic convergence. Alternatively, other well known methods of higher order, the Householder [127] and the Halley [62] methods, methods with cubic convergence, can also be used. One of the applications of Adomian's decomposition method is to solve these kind of equations. It has been proved that this method leads to accurate solutions [7] [213]. However, in spite of Adomian's series be in most cases a rapid convergent series, the method applied to nonlinear equations does not seem very efficient to be a generalized method to solve nonlinear equations.

In this section one constructs a new efficient iterative method to solve nonlinear equations [40]. This method behaves better than the Adomian's decomposition one and equally or better than other methods derived from Adomian's technique or other usual methods. The convergence of the new scheme is proved and at least the cubic order of convergence is established. Several examples are presented and compared to other methods, showing the accuracy and fast convergence of this new method. Also, it is shown that the modified Adomian's method developed by Babolian and Biazar [33] to solve nonlinear equations should be slightly modified, due to the fact that convergence of Adomian's method does not ensure convergence of the modified method. An example illustrates this fact, which, unlike what is claimed by the authors, does not converge with their method, but with a simple different choice of the zero component becomes convergent.

Adomian's technique applied to nonlinear equations, consists, in the first place, in transforming the equation $f(x) = 0$ into the canonical form

$$x = x_0 + F(x) \tag{3.23}$$

where x_0 is a constant and F a nonlinear function. The solution is given in a series form, running:

$$x = \sum_{n=0}^{\infty} x_n \tag{3.24}$$

Identified x_0, the rest of the terms x_n, $n \geq 1$, will further be settled by a recursive relation. The nonlinear function $F(x)$ is decomposed into the following particular series of polynomials:

$$F(x) = \sum_{n=0}^{\infty} A_n \tag{3.25}$$

A_n being the so called Adomian polynomials. For each n, the polynomial A_n depends only on $x_0, x_1, \ldots, x_n$. Adomian introduced formulae to generate these polynomials for all kind of nonlinearities [15], [17], [19] and [22].

Substituting equations (3.24) and (3.25) into equation (3.23) gives rise to:

$$\sum_{n=0}^{\infty} x_n = x_0 + \sum_{n=0}^{\infty} A_n \tag{3.26}$$

To determine the components x_n, $n = 1, 2, ...$, one employs the recursive relation:

$$x_{n+1} = A_n \tag{3.27}$$

Practical methods for the calculation of Adomian's polynomials A_n have been developed and published in the open literature [6], [8], [10], [9] and [64].

Following Cherruault [66] and Babolian [33], the Adomian's decomposition method applied to equation (3.23), is equivalent to determining the sequence $(S_n)_n = (x_1 + x_2 + ... + x_n)_n$ by using the iterative scheme:

$$\begin{aligned} S_0 &= 0 \\ S_{n+1} &= F(x_0 + S_n) \end{aligned} \tag{3.28}$$

On the other hand, the associated functional equation $S = F(x_0 + S)$, can be solved by Adomian's decomposition method.

Babolian [33] proposed a modification of Adomian's method in order to increase the order of convergence of the solution obtained by application of the Adomian's method to the nonlinear equation (3.23). Instead of solving the nonlinear equation (3.23), one can solve the following functional equation:

$$S = F(x_0 + S) \tag{3.29}$$

making recourse to the following scheme:

$$s_0 = 0 \tag{3.30}$$

$$s_{n+1} = A_n\left(s_0, s_1, ..., s_n\right) \tag{3.31}$$

and obtaining an approximation to the solution of equation (3.29) given by a truncated series $\sum_{k=0}^{n} s_k$, which in turn supplies an approximation to the solution of the equation $x = x_0 + F\left(x\right)$, given by $x_0 + \sum_{k=0}^{n} s_k$.

To improve the order of convergence of the sequence $\left(S_n\right)_n$ as given by [32], instead of solving equation (3.29), Babolian and Biazar [33] proposed the following equation for the S^* solution of equation (3.29):

$$S = G\left(x_0 + S\right) = \frac{-F'\left(x_0 + S^*\right)S + F\left(x_0 + S\right)}{1 - F'\left(x_0 + S^*\right)} \tag{3.32}$$

based on the fact that $G'\left(x_0 + S^*\right) = 0$. Equation (3.32) was obtained by adding $-F'\left(x_0 + S^*\right)S$ to both sides of equation (3.29). Because one does not possess the solution $x = x_0 + S^*$ of equation (3.23), Babolian and Biazar [33] proposed an approximation, by choosing $x \approx x_0$.

It should be noted at this point that it is known the sensitivity of Adomian's method on the zero component [8] [11] [47], and the method may fail when this zero component drives the solution to a divergent series. Also, equations (3.29) and (3.32) are different and, therefore, for the same starting value s_0, one can converge and the other diverge. Besides, if one solves equation (3.29) or (3.32) with Adomian's decomposition method, it may fail because the series of solution has small convergence radius. Thus, concerning the above statements, an application of Adomian's method to the equation (3.29) or (3.32) should start with a point close enough to the real solution.

To illustrate this, one recalls the first example presented by [33]

$$x^3 + 4x^2 + 8x + 8 = 0 \tag{3.33}$$

In opposition to that claimed by the authors, the application of Adomian's method (3.30) and (3.31) to equation (3.32) fails for $s_0 = 0$, because the series obtained is divergent.

Writing equation (3.33) in canonical form as done by [33],

$$x = -1 - \frac{x^2}{2} - \frac{x^3}{8} \tag{3.34}$$

and applying the scheme expressed by equation (3.32), one obtains:

$$S = \frac{\left(\left(S^* - 1\right) + \frac{3}{8}\left(S^* - 1\right)^2\right)S - \frac{1}{2}\left(S - 1\right)^2 - \frac{1}{8}\left(S - 1\right)^3}{1 + \left(\left(S^* - 1\right) + \frac{3}{8}\left(S^* - 1\right)^2\right)} \tag{3.35}$$

Following [33], and choosing $S^* - 1 \approx -1$, the functional equation (3.35) becomes

$$S = -\frac{5}{3}S - \frac{4}{3}(S-1)^2 - \frac{1}{3}(S-1)^3 \tag{3.36}$$

Figures 3.1 and 3.2 show the truncated series solution $x_0 + \sum_{k=1}^{n} s_k$ obtained as a function of the number of iterations n, by applying Adomian's method to equation (3.36) with $s_0 = 0$. As it can be seen, Babolian's method diverges, in spite of the fact that, after one iteration, the correct solution of the equation (3.33), $x = x_0 + s_1 = -2$ has been reached, as claimed by the authors in their work [33].

If one takes the real value of $S^* = -1$, the functional equation (3.35) becomes

$$S = -S - (S-1)^2 - \frac{1}{4}(S-1)^3 \tag{3.37}$$

The solution of such equation also diverges, although more slowly, as it can be seen in figure 3.3.

As it has been mentioned above, to obtain the real solution one should modify equation (3.36), so that the zero component s_0 has a value closer to the exact value $S^* = -1$. Adding and subtracting $s_0 = a$ to equation (3.36), the following equation is obtained:

$$S = -\frac{5}{3}S - \frac{4}{3}(S-1)^2 - \frac{1}{3}(S-1)^3 + a - a \tag{3.38}$$

The principle of increasing the order of convergence maintains and a convergent series can be reached. Figure 3.4 shows the result for $a = -\frac{1}{2}$.

3.2.1 The method

An algorithm based on Newton-Raphson method and Adomian's decomposition method was presented by [12]. Considering the nonlinear equation $f(x) = 0$, and writing f in limited Taylor expansion around x, one obtains:

$$f(x+h) = f(x) + hf'(x) + \frac{h^2}{2}f''(x) + O\left(h^3\right) \tag{3.39}$$

Supposing $f'(x) \neq 0$, one searches for a value of h such that

$$f(x+h) = 0 \approx f(x) + hf'(x) + \frac{h^2}{2}f''(x) \tag{3.40}$$

This is equivalent to saying that one looks for the following h value:

$$h \approx -\frac{f(x)}{f'(x)} - \frac{h^2}{2}\frac{f''(x)}{f'(x)} \tag{3.41}$$

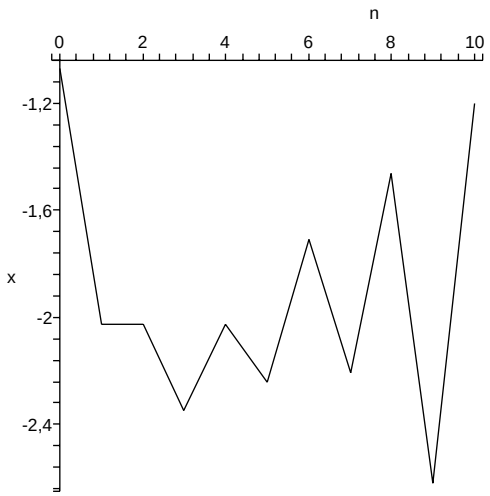

Fig. 3.1: The truncated series solution of equation (3.33), by Babolian's method, as a function of $0 \leq n \leq 10$.

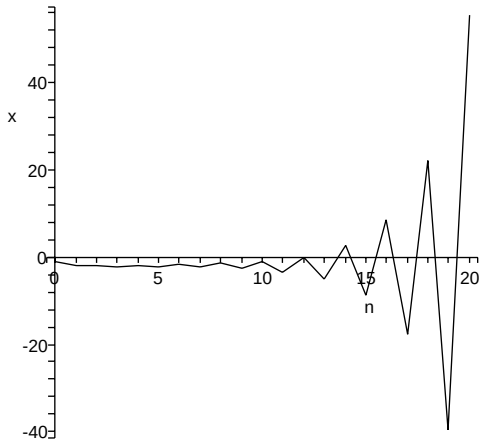

Fig. 3.2: The truncated series solution of equation (3.33), by Babolian's method, as a function of $0 \leq n \leq 20$.

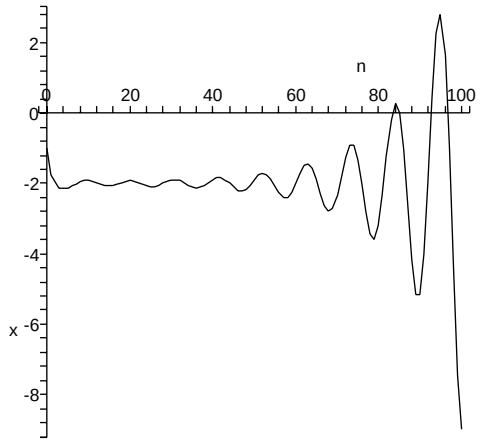

Fig. 3.3: The truncated series solution of equation (3.33), by Babolian's method with the correct value of S^*, as a function of $0 \leq n \leq 100$.

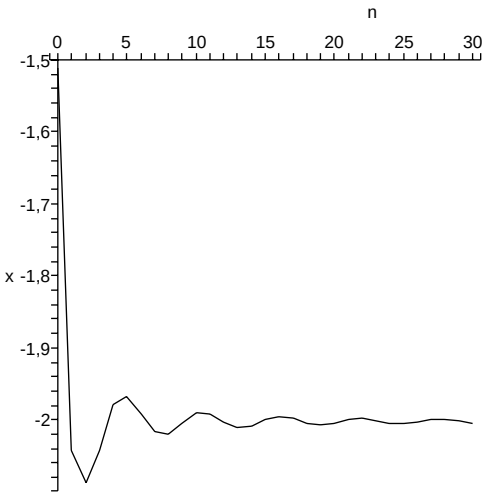

Fig. 3.4: The truncated series solution of equation (3.33), by adding and subtracting to Babolian's scheme $\frac{1}{2}$, taking $s_0 = -\frac{1}{2}$, as a function of $0 \leq n \leq 30$.

$$h = c + N(h) \tag{3.42}$$

where $c = -\frac{f(x)}{f'(x)}$ is a constant and $N(h) = -\frac{h^2}{2}\frac{f''(x)}{f'(x)}$ is a nonlinear function. Abbasbandy [12] applied Adomian's decomposition method to approximate the value of h, obtaining a new scheme.

Applying equation (3.32) to equation (3.43), equation (3.44) is obtained

$$S = N(c + S) \tag{3.43}$$

$$S = \frac{-N'(c + S^*)S + N(c + S)}{1 - N'(c + S^*)} \tag{3.44}$$

For x close enough to the real solution of $f(x) = 0$, $S^* \approx 0$. Applying Adomian's method to equation (3.44) with $c + S^* \approx c$, one obtains:

$$s_0 = 0 \tag{3.45}$$

$$A_0 = \frac{-\frac{1}{2}\left[\frac{f(x)}{f'(x)}\right]^2 \frac{f''(x)}{f'(x)}}{1 - \frac{f(x)}{f'(x)}\frac{f''(x)}{f'(x)}} = -\frac{[f(x)]^2 f''(x)}{2[f'(x)]^3 - 2f(x)f'(x)f''(x)} \tag{3.46}$$

$$s_1 = A_0 \tag{3.47}$$

$$A_1 = 0 \tag{3.48}$$

$$s_2 = 0 \tag{3.49}$$

After two iterations, one gets for h:

$$h = c + s_1 + s_2 = -\frac{f(x)}{f'(x)} - \frac{[f(x)]^2 f''(x)}{2[f'(x)]^3 - 2f(x)f'(x)f''(x)} \tag{3.50}$$

The new iterative method is then constructed and given by:

$$x_{n+1} = x_n - \frac{f(x_n)}{f'(x_n)} - \frac{[f(x_n)]^2 f''(x_n)}{2[f'(x_n)]^3 - 2f(x_n)f'(x_n)f''(x_n)} \tag{3.51}$$

3.2.2 Convergence analysis

Consider the iteration function g as expressed by equation (3.52).

$$g(x) = x - \frac{f(x)}{f'(x)} - \frac{[f(x)]^2 f''(x)}{2[f'(x)]^3 - 2f(x)f'(x)f''(x)} \tag{3.52}$$

The following theorem of convergence holds:

Theorem 8: Let x^* be a solution of the equation $f(x) = 0$, $f \in C^3$. If $f'(x^*) \neq 0$ then there exists an interval I containing x^* such that for $x_0 \in I$, the iterative scheme (3.51) converges to the only solution of $f(x) = 0$ belonging to I.

Proof:

The statements $f(x^*) = 0$, $f'(x^*) \neq 0$ and $f \in C^3$ imply that $g(x^*) = x^*$ and g is continuous differentiable in $x = x^*$. Fulfilling some easy computations the following result is reached: $|g'(x^*)| = 0 < 1$.

So, one concludes that there exists an $\varepsilon > 0$ such that for $x \in (x^* - \varepsilon, x^* + \varepsilon)$, $|g'(x)| < 1$, and, by the Fixed Point Theorem, the iterative scheme $x_{n+1} = g(x_n)$ converges to the unique solution in that interval.

End of proof.

Definition 9: Let $e_n = x^* - x_n$ be the truncation error in the n^{th} iterate. If there exists a number $p \geq 1$ and a constant $c \neq 0$ such that

$$\lim_{n \to \infty} \frac{|e_{n+1}|}{|e_n|^p} = c \tag{3.53}$$

then p is called the order of convergence of the method.

The following theorem holds:

Theorem 10: Consider the nonlinear equation $f(x) = 0$. Suppose $f \in C^5$. Then, for the iterative method defined by equation (3.51), the convergence is at least of order 3.

Proof:

Consider equation (3.52)

$$g(x) = x - \frac{f(x)}{f'(x)} - \frac{[f(x)]^2 f''(x)}{2[f'(x)]^3 - 2f(x) f'(x) f''(x)}$$

Executing some computations one gets to the following derivatives:

$$g'(x^*) = g''(x^*) = 0 \tag{3.54}$$

and

$$g'''(x^*) = -\frac{f'''(x^*)}{f'(x^*)} \tag{3.55}$$

From Taylor limited expansion of $g(x_n)$ around x^*, one gets, for $\min(x_n, x^*) < \xi_n < \max(x_n, x^*)$ the following relation:

$$\begin{aligned} x_{n+1} - x^* &= g(x_n) - g(x^*) \\ &= g'(x^*)(x_n - x^*) + \frac{g''(x^*)}{2}(x_n - x^*)^2 + \frac{g'''(\xi_n)}{6}(x_n - x^*)^3 \end{aligned} \tag{3.56}$$

that, according to equation (3.54) and for $x_n \neq x^*$, is equivalent to:

$$\frac{x_{n+1} - x^*}{(x_n - x^*)^3} = \frac{g'''(\xi_n)}{6} \tag{3.57}$$

The statement $f \in C^5$ implies that $g \in C^3$ in the neighborhood of interest of $x = x^*$. Hence for $g'''(x^*) \neq 0$

$$\lim_{n\to\infty} \frac{x_{n+1} - x^*}{(x_n - x^*)^3} = \frac{g'''\left(\lim_{n\to\infty} \xi_n\right)}{6} = \frac{g'''(x^*)}{6} \neq 0 \tag{3.58}$$

End of proof.

3.2.3 Numerical examples

The examples presented by [12] and [33] are considered in order to parallel their results with those obtained with the new proposed scheme. Also, Newton-Raphson method and Adomian's method are performed for comparisons purposes. The solutions prospected for each example are the ones indicated below, through examples 7 to 10.

Example 11: $x^3 + 4x^2 + 8x + 8 = 0$ with $x_0 = -1$. The exact solution prospected is $x = -2$.

Example 12: $x - 2 - e^{-x} = 0$ with $x_0 = 2$. The exact solution prospected is $x = 2.120028239$.

Example 13: $x^2 - (1 - x)^5 = 0$ with $x_0 = 0.2$. The exact solution prospected is $x = 0.345954816$.

Example 14: $e^x - 3x^2 = 0$ with $x_0 = 0$ for Adomian's and Babolian's methods and $x = 0.5$ for the remainder. The exact solution prospected is $x = 0.910007573$. With $x_0 = 0$, the exact solution prospected for Newton-Raphson, Abbasbandy and new iterative method (3.51), is $x = -0.458962268$.

Tab. 3.1: Number of iterations and solution obtained by the different methods. The exact solution prospected is $x = -2$.

Method	**Example 11**	
	Number iterations	*Obtained solution*
Newton-Raphson	1	-2.000000000
Adomian		slow convergence
Babolian		divergence
Abbasbandy	2	-2.003987741
New method (3.51)	3	-2.000100903

Tab. 3.2: Number of iterations and solution obtained by the different methods. The exact solution prospected is $x = 2.120028239$.

Method	**Example 12**	
	Number iterations	*Obtained solution*
Newton-Raphson	3	2.120028239
Adomian	6	2.120013306
Babolian	4	2.120016168
Abbasbandy	2	2.120028239
New method (3.51)	2	2.120028239

Tab. 3.3: Number of iterations and solution obtained by the different methods. The exact solution prospected is $x = 0.345954816$.

Method	**Example 13**	
	Number iterations	*Obtained solution*
Newton-Raphson	3	0.345953774
Adomian	10	0.340622225
Babolian	5	0.346021366
Abbasbandy	2	0.345954646
New method (3.51)	2	0.345952189

Tab. 3.4: Number of iterations and solution obtained by the different methods for the starting point $x_0 = 0$. The exact solution prospected is $x = 0.910007573$. (*)For Newton-Raphson, Abbasbandy and the new iterative method (24), the starting point is $x_0 = 0.5$.

Method	**Example 14**	
	Number iterations	*Obtained solution*
Newton-Raphson(*)	4	0.910007662
Adomian	10	0.904938647
Babolian	6	0.903257054
Abbasbandy(*)	4	0.910007573
New method (3.51)(*)	3	0.910007573

Tab. 3.5: Number of iterations and solution obtained by the different methods, for the starting point $x_0 = 0$. The exact solution prospected is $x = -0.458962268$.

Method	**Example 14**	
	Number iterations	*Obtained solution*
Newton-Raphson	5	-0.458962274
Abbasbandy	5	-0.458964191
New method (3.51)	2	-0.458992962

The results, similar to the ones presented in [12], are presented in tables 3.1 to 3.4.

The values for the number of iterations and corresponding solution, obtained by Adomian's method for the example 11, are not presented, due to the very slow convergence exhibited when the zero component is $x_0 = -1$, as it is clearly shown in figure 3.5. Choosing a value of x_0 closer to the real solution $x^* = -2$ (by adding and subtracting a constant to the equation), one would have an improvement on the rate of convergence.

Also, for example 14, the start value for Newton-Raphson and Abbasbandy method must not be $x_0 = 0$ in opposition to the statement of [12], because iterations converge to the negative root $x = -0.458962268$ for that start point. Table 3.5 presents a comparison between these two methods and the new proposed iterative method (3.51) starting at $x_0 = 0$.

Figures 3.6 to 3.10, show the evolution of the solution in terms of the number of iterations n.

As it can be seen from these examples, the new iterative method (3.51) exhibits equal or faster convergence to the exact solution than the other compared methods, exception made for example 11 where the solution is

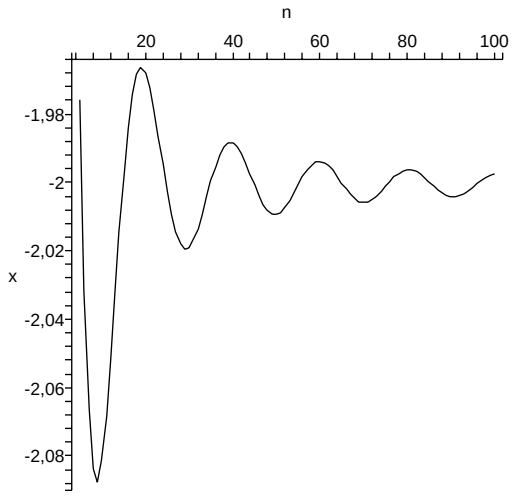

Fig. 3.5: Solution obtained by Adomian's method applied to example 11, in terms of the number of iterations $5 \leq n \leq 100$, evidencing the slow convergence.

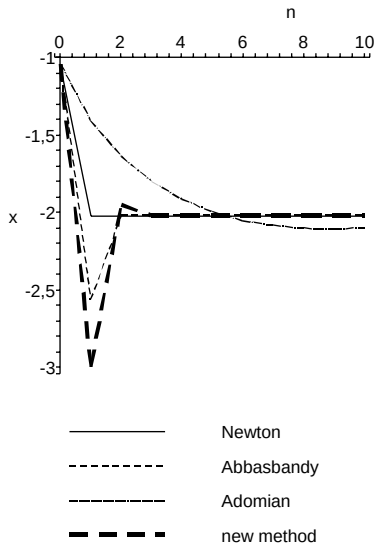

Fig. 3.6: Comparison between the solutions obtained for the different methods, applied to example 11, in terms of the number of iterations $0 \leq n \leq 10$.

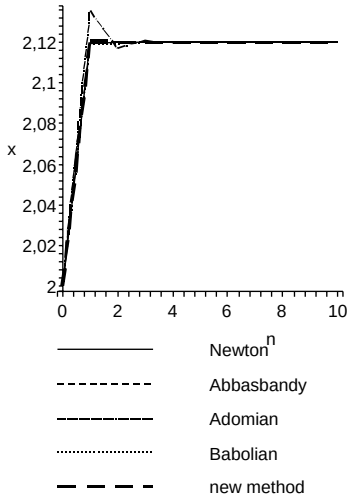

Fig. 3.7: Comparison between the solutions obtained for the different methods, applied to example 12, in terms of the number of iterations $0 \leq n \leq 10$.

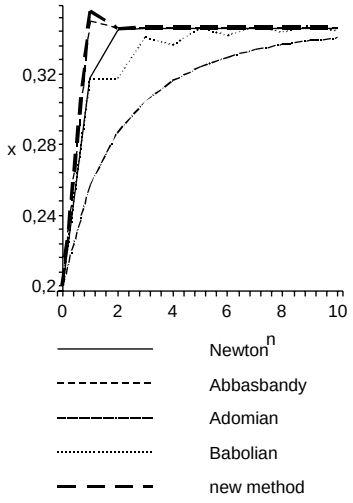

Fig. 3.8: Comparison between the solutions obtained for the different methods, applied to example 13, in terms of the number of iterations $0 \leq n \leq 10$.

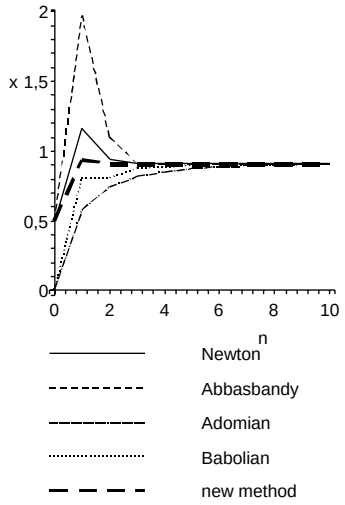

Fig. 3.9: Comparison between the solutions obtained for the different methods, applied to example 14, in terms of the number of iterations $0 \leq n \leq 10$.

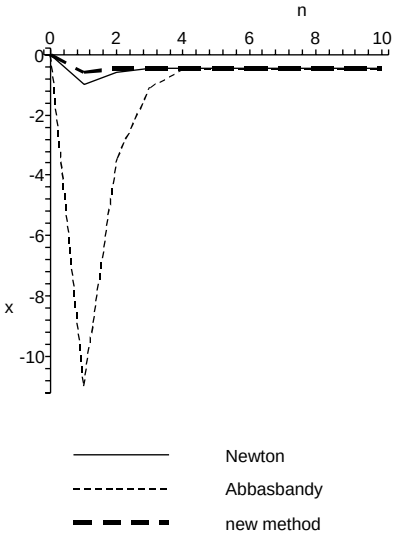

Fig. 3.10: Comparison between the solutions obtained for Newton-Raphson, Abbasbandy and the new iterative method (3.51), applied to example 14, for $x_0 = 0$, in terms of the number of iterations $0 \leq n \leq 10$.

Tab. 3.6: Number of correct decimals of the positive root of equation (3.59) for the different methods and for different number of iterations. The golden ratio is obtained by adding 0.5 to this solution. Starting point is $x0 = 1$

	Number of iterations					
Method	1	2	3	4	5	6
Newton-Raphson	1	3	6	12	25	51
Householder	2	6	21	63	191	575
Halley	3	10	33	100	304	913
Abbasbandy	2	7	24	73	221	663
New method (3.51)	2	6	21	63	191	575

reached faster by the Newton-Raphson method. But this fact has a simple explanation. The function f for example 11 has an inflexion point at $x = -\frac{4}{3}$, a point between the exact solution $x = -2$ and the starting point $x = -1$. Purely by chance, the tangent line at $x = -1$ to the graph of f, intersects the x-axis at the point corresponding to the exact solution $x = -2$, and the exact solution is obtained in only one iteration. For any other value of the starting point that would not occur and the new method would exhibit a better performance. The new method is also of easy computation, revealing among the compared methods, the best alternative to the Newton-Raphson one to solve nonlinear equations.

Next, a comparison with other well known methods of higher order, the Householder [127] and the Halley [62] methods, methods with cubic convergence, is performed by computing the Golden Ratio $\varphi = \frac{1+\sqrt{5}}{2}$. To carry out this comparison, the positive root of the following equations is prospected by different methods, and the number of correct decimals is calculated:

$$\frac{1}{x^2} - \frac{4}{5} = 0 \tag{3.59}$$

$$x^2 - x - 1 = 0 \tag{3.60}$$

The results are shown in tables 3.6 to 3.9, where Newton-Raphson and Abbasbandy methods are also included, this last one due to its cubic order of convergence.

As it can be seen the new iterative method (3.51) behaves quite well, and its high order of convergence is patent.

The computations associated with the examples discussed above were performed by using the software *Maple*.

Tab. 3.7: Number of correct decimals of the positive root of equation (3.59) for the different methods and for different number of iterations. The golden ratio is obtained by adding 0.5 to this solution. Starting point is $x0 = 1.5$

	Number of iterations					
Method	1	2	3	4	5	6
Newton-Raphson	0	0	2	4	8	17
Householder	0	1	6	18	55	165
Halley	1	6	21	67	202	608
Abbasbandy	0	2	7	21	64	194
New method (3.51)	0	3	10	30	92	278

Tab. 3.8: Number of correct decimals of the positive root of equation (3.60) for the different methods and for different number of iterations. Starting point is $x0 = 1.1$

	Number of iterations					
Method	1	2	3	4	5	6
Newton-Raphson	0	1	3	7	16	32
Householder	0	1	6	19	60	181
Halley	0	4	13	41	125	378
Abbasbandy	0	2	10	44	177	712
New method (3.51)	1	7	32	132	532	2132

Tab. 3.9: Number of correct decimals of the positive root of equation (3.60) for the different methods and for different number of iterations. Starting point is $x0 = 2$

	Number of iterations					
Method	1	2	3	4	5	6
Newton-Raphson	1	2	6	12	26	52
Householder	1	5	18	57	172	519
Halley	1	6	21	67	202	608
Abbasbandy	2	9	41	165	663	2652
New method (3.51)	2	12	52	213	855	3423

3.2.4 Further developments

Other iterative methods may be constructed either by conserving more terms in the series solution obtained by Adomian's modified method, or by considering Taylor expansions of higher order for f, or both.

Now, considering Taylor expansion as expressed by equation (3.39) and conserving one more term in the series solution obtained by Adomian's modified method, the following result are obtained:

$$s_0 = 0 \tag{3.61}$$

$$A_0 = -\frac{[f(x)]^2 f''(x)}{2[f'(x)]^3 - 2f(x) f'(x) f''(x)},\ s_1 = A_0 \tag{3.62}$$

$$A_1 = 0,\ s_2 = 0 \tag{3.63}$$

$$A_2 = -\frac{[f''(x)]^3 [f(x)]^4}{8f'(x)\left[[f'(x)]^2 - f''(x) f(x)\right]^3},\ s_3 = A_2 \tag{3.64}$$

After three iterations, the following expression is obtained:

$$\begin{aligned} h =& c + s_1 + s_2 + s_3 \\ =& -\frac{f(x)}{f'(x)} - \frac{[f(x)]^2 f''(x)}{2[f'(x)]^3 - 2f(x) f'(x) f''(x)} \\ & - \frac{[f''(x)]^3 [f(x)]^4}{8f'(x)\left[[f'(x)]^2 - f''(x) f(x)\right]^3} \end{aligned} \tag{3.65}$$

The iterative method is then constructed, given by:

$$\begin{aligned} x_{n+1} = x_n & - \frac{f(x_n)}{f'(x_n)} - \frac{[f(x_n)]^2 f''(x_n)}{2[f'(x_n)]^3 - 2f(x_n) f'(x_n) f''(x_n)} \\ & - \frac{[f''(x_n)]^3 [f(x_n)]^4}{8f'(x_n)\left[[f'(x_n)]^2 - f''(x_n) f(x_n)\right]^3} \end{aligned} \tag{3.66}$$

Consider the iteration function g associated to (3.66). One has $g'(x^*) = g''(x^*) = 0$ and $g'''(x^*) = -\frac{f'''(x^*)}{f'(x^*)}$, where x^* is the solution of the equation $f(x) = 0$.

If one more term in Taylor expansion is conserved,

$$f(x+h) = f(x) + hf'(x) + \frac{h^2}{2} f''(x) + \frac{h^3}{6} f'''(x) + O\left(h^4\right) \tag{3.67}$$

Applying Adomian's modified method described above, one gets:

$$s_0 = 0 \tag{3.68}$$

$$A_0 = \frac{[f(x)]^2 [3 f''(x) f'(x) - f'''(x) f(x)]}{3f'(x) \left[-2 [f'(x)]^3 + 2 f''(x) f'(x) f(x) - f'''(x) [f(x)]^2\right]}, \; s_1 = A_0 \tag{3.69}$$

$$A_1 = 0, \; s_2 = 0 \tag{3.70}$$

After two iterations the iterative method is constructed and given by

$$x_{n+1} = x_n - \frac{f(x_n)}{f'(x_n)} + \frac{[f(x_n)]^2 [3 f''(x_n) f'(x_n) - f'''(x_n) f(x_n)]}{3f'(x_n) \left[-2 [f'(x_n)]^3 + 2 f''(x_n) f'(x_n) f(x_n) - f'''(x_n) [f(x_n)]^2\right]} \tag{3.71}$$

Considering the iteration function g associated to equation (3.71), one has $g'(x^*) = g''(x^*) = 0$ and $g'''(x^*) = 3\left(\frac{f''(x^*)}{f'(x^*)}\right)^2 - \frac{2f'''(x^*)f'(x^*)+3[f''(x^*)]^2}{[f'(x^*)]^2} + 2\frac{f'''(x^*)}{f'(x^*)}$, where x^* is the solution of the equation $f(x) = 0$.

For the above description, the order of convergence for both schemes (3.66) and (3.71), appears not to increase. Also, it is clear that they bring about much more computations, appearing to evidence not to have advantages over the new iterative method (3.51), which has already proved to be very efficient.

Summing up, in this section an efficient iterative method to solve nonlinear equations was built up. The convergence of the scheme has been proved and the order of convergence established. The algorithm exhibits at least a cubic convergence, and, illustrated by some examples, the performance has been compared with other methods and showed that it behaves equally or better than them. Among the methods derived from Adomian's technique, this new method exhibits one of the best performance and also reveals to be a very good alternative to other methods, such the Newton-Raphson or the Householder and Halley methods.

3.3 Numerical study of modified Adomian's method applied to Burgers equation

Finding explicit solutions to nonlinear differential equations is of fundamental importance to fully understand the problem under analysis. Adomian's decomposition method appears as a useful tool to find analytical or

approximate solutions to many problems. The advantages of the method are almost always emphasized in the literature. However, some embarrassments may appear that are not quite stressed. The good results presented include exact Taylor series solutions identified from the truncated series. This is achieved either because it is easy to identify the exact solution from the truncated series or because the real solution derived by other methods is known in advance [291] [145] [147] or because the presence of the so called noisy terms [269] [145] [147]. Otherwise, it would not be so straightforward the finding of such closed form solutions. Moreover, the series solution may have small convergence radius and the truncated series solution may be inaccurate in some regions, as described by [132] [65] [93] [4] [5].

Therefore, when the series solution given by Adomian's decomposition method applied to differential equation does not allow the identification of the exact analytical solution, the use of truncated series becomes necessary. To overcome the possible small convergence radius exhibited by Adomian's series solution, Padé approximants (PAs) to the Adomian's series solution have been tested and applied to ordinary differential equations [29] [274] [273] [132] and more recently to partial differential equations [4] [5]. Also, a piecewise solution technique, the multistage Adomian's decomposition method (MADM), a technique that consists in dividing the solution space into regions, was applied to try to bypass the small convergence radius of Adomian's series solution [65] [93].

In the present section, Padé approximants, both in x and t directions, are implemented to the series solution given by Adomian's decomposition technique applied to nonlinear partial differential equations, in particular to Burgers equation. Numerical and graphical illustrations show that this technique can improve the accuracy and enlarge the domain of convergence of the solution, even when the actual solution cannot be expressed as the ratio of two polynomials. There is however a disadvantage on using Padé approximants applied to the series solution of partial differential equations. When the real solution is not obtained by the use of Padé approximants, which means that the real solution is not a rational polynomial function with respect to the variable considered in the Padé approximation or the order of the Padé approximant used is lower than the one of the real solution, inaccurate solutions near its poles can occur.

Another way of trying to overcome the limitations of the small convergence radius of Adomian's method, which has not yet been tested, would be to develop a time analytical and spacial numerical method, approximating the spatial derivatives by finite differences and then solve analytically the resulting set of ordinary differential equations by applying Adomian's decomposition method and Padé approximants or by applying the multistage

Adomian's decomposition method (MADM). However, it is shown in this section, that the application of Adomian's method to the ordinary differential equations set arising from the discretization of the spatial derivatives by finite differences, the method of lines, may reduce the convergence domain of the solution's series [43].

3.3.1 Convergence

The convergence of Adomian's method was deeply investigated by several authors [66] [70] [198] [68] [6] [7] [100] [8] [10] [69] [36].

Consider the Hilbert space $H = L^2((\alpha,\beta)\times[0,T])$ defined by the set of applications

$$u : (\alpha,\beta)\times[0,T] \to \mathbb{R} \quad \text{with} \quad \int_{(\alpha,\beta)\times[0,T]} u^2(s,\tau)\,dsd\tau < +\infty \tag{3.72}$$

Consider the differential equation

$$Lu + Ru + Nu = g \tag{3.73}$$

with

$$Tu = Ru + Nu \tag{3.74}$$

As already stated, if the following hypothesis are satisfied, the Adomian's method is convergent [66] [198] [199]:

(H_1) $(T(u) - T(v), u - v) \geq k\|u - v\|^2,\ k > 0,\ \forall u, v \in H$

(H_2) $\forall M > 0, \exists C(M) > 0 : \|u\| \leq M, \|v\| \leq M \Longrightarrow (T(u) - T(v), w) \leq C(M)\|u - v\|\|w\|, \forall\ w \in H$

These hypothesis applied to Burgers equation can be verified using the same scheme of proof of [198] [199] [211] [147] [148].

Theorem 15 (sufficient condition of convergence): The Adomian's decomposition method applied to the Burgers equation

$$\frac{\partial u}{\partial t} = -u\frac{\partial u}{\partial x} + \delta\frac{\partial^2 u}{\partial x^2} \tag{3.75}$$

without initial and boundary conditions, converges towards a particular solution.

Proof:

For the equation (3.75) let $Lu = \frac{\partial u}{\partial t}$, $Ru = u\frac{\partial u}{\partial x}$ and $Nu = -\delta\frac{\partial^2 u}{\partial x^2}$. One has then:

$$Tu = u\frac{\partial u}{\partial x} - \delta\frac{\partial^2 u}{\partial x^2} \tag{3.76}$$

This operator T is hemicontinuous.

Verification of hypothesis H_1:

$$\begin{aligned} T(u) - T(v) &= \left(u\frac{\partial u}{\partial x} - v\frac{\partial v}{\partial x} \right) - \delta \frac{\partial^2}{\partial x^2}(u-v) \\ &= \frac{1}{2}\frac{\partial}{\partial x}\left(u^2 - v^2\right) - \delta \frac{\partial^2}{\partial x^2}(u-v) \end{aligned} \tag{3.77}$$

$$\begin{aligned} &(T(u) - T(v), u - v) \\ &\quad = \left(\frac{1}{2}\frac{\partial}{\partial x}\left(u^2 - v^2\right) - \delta \frac{\partial^2}{\partial x^2}(u-v), u - v \right) \\ &\quad = \left(-\delta \frac{\partial^2}{\partial x^2}(u-v), u - v \right) + \frac{1}{2}\left(\frac{\partial}{\partial x}\left(u^2 - v^2\right), u - v \right) \end{aligned} \tag{3.78}$$

In addition, there exists $\alpha, \sigma > 0$ such that :

$$\left(-\frac{\partial^2}{\partial x^2}(u-v), u - v \right) \geq \alpha \|u - v\|^2 \tag{3.79}$$

$$\left(\frac{\partial}{\partial x}\left(u^2 - v^2\right), u - v \right) \leq \sigma \|u + v\| \|u - v\|^2 \leq 2M\sigma \|u - v\|^2 \tag{3.80}$$

where $\|u\| \leq M$, $\|v\| \leq M$.

Therefore

$$(T(u) - T(v), u - v) \geq (\alpha\delta - 2M\sigma) \|u - v\|^2 \tag{3.81}$$

Setting $k = \alpha\delta - 2M\sigma$ (with $\alpha\delta > 2M\sigma$), hypothesis H_1 is verified.

For hypothesis H_2:

$$\begin{aligned} (T(u) - T(v), w) &= \left(\frac{1}{2}\frac{\partial}{\partial x}\left(u^2 - v^2\right) - \delta \frac{\partial^2}{\partial x^2}(u-v), w \right) \\ &= \frac{1}{2}\left(\frac{\partial}{\partial x}\left(u^2 - v^2\right), w \right) + \delta \left(-\frac{\partial^2}{\partial x^2}(u-v), w \right) \\ &\leq M \|u - v\| \|w\| + \delta \|u - v\| \|w\| \\ &\leq (M + \delta) \|u - v\| \|w\| \end{aligned} \tag{3.82}$$

being $C(M) = M + \delta$ and therefore hypothesis H_2 is verified.

End of proof.

3.3.2 Application of Padé approximants to Burgers equation

Padé approximants are tested herein and applied to the series solution given by Adomian's decomposition technique for Burgers equation. Padé approximations are usually superior to Taylor expansions when functions contain poles, because the use of rational functions allows them to be well-represented. One will compute essentially the symmetric Padé approximant, because the diagonal approximants are the most accurate ones [274]. Numerical and graphical applications illustrate the study.

Consider Burgers equation (3.75) with the following initial and Dirichlet boundary conditions

$$u(x,0) = u_0(x) \tag{3.83}$$

$$u(0,t) = f_0(t), \quad u(1,t) = f_1(t) \tag{3.84}$$

Following Adomian, the linear operators expressed by equations (3.85) are defined.

$$L_t(\cdot) = \frac{\partial}{\partial t}(\cdot), \quad L_{xx}(\cdot) = \frac{\partial^2}{\partial x^2}(\cdot) \tag{3.85}$$

Applying the inverse operator of $L_t(\cdot) = \frac{\partial}{\partial t}(\cdot)$, $L_t^{-1}(\cdot) = \int_0^t (\cdot)\, dt'$, to both sides of equation (3.75) one obtains:

$$u(x,t) = u_0(x) + L_t^{-1}\left(-u\frac{\partial u}{\partial x} + \delta\frac{\partial^2 u}{\partial x^2}\right) \tag{3.86}$$

According to Adomian's method, one assumes that the unknown function $u(x,t)$ can be expressed by an infinite sum of components of the form,

$$u(x,t) = \sum_{n=0}^{\infty} u_n(x,t) \tag{3.87}$$

and the nonlinear term $u\frac{\partial u}{\partial x}$ into the following infinite series of Adomian's polynomials:

$$u\frac{\partial u}{\partial x} = \sum_{n=0}^{\infty} A_n \tag{3.88}$$

Substituting equations (3.87) and (3.88) into equation (3.86) one obtains:

$$\sum_{n=0}^{\infty} u_n = u_0(x) + L_t^{-1}\left(\delta\frac{\partial^2}{\partial x^2}\sum_{n=0}^{\infty} u_n - \sum_{n=0}^{\infty} A_n\right) \tag{3.89}$$

To determine the components of $u_n(x,t)$, $n = 0, 1, 2, ...$, Adomian's technique can employ the recursive relation defined by:

$$u_0 = u_0(x) \tag{3.90}$$

$$u_1 = L_t^{-1}\left(\delta\frac{\partial^2}{\partial x^2}u_0 - A_0\right) \tag{3.91}$$

$$u_2 = L_t^{-1}\left(\delta\frac{\partial^2}{\partial x^2}u_1 - A_1\right) \tag{3.92}$$

$$\vdots$$

$$u_n = L_t^{-1}\left(\delta\frac{\partial^2}{\partial x^2}u_{n-1} - A_{n-1}\right) \tag{3.93}$$

$$\vdots$$

The Adomian's polynomials depend on the particular nonlinearity. In this case, the A_n polynomials are given by:

$$A_0 = u_0\frac{\partial}{\partial x}u_0 \tag{3.94}$$

$$A_1 = u_0\frac{\partial}{\partial x}u_1 + u_1\frac{\partial}{\partial x}u_0 \tag{3.95}$$

$$A_2 = u_0\frac{\partial}{\partial x}u_2 + u_1\frac{\partial}{\partial x}u_1 + u_2\frac{\partial}{\partial x}u_0 \tag{3.96}$$

$$A_3 = u_0\frac{\partial}{\partial x}u_3 + u_1\frac{\partial}{\partial x}u_2 + u_2\frac{\partial}{\partial x}u_1 + u_3\frac{\partial}{\partial x}u_0 \tag{3.97}$$

$$\vdots$$

Applying Adomian's decomposition method in the x direction

$$u(x,t) = u(0,t) + x\frac{\partial}{\partial x}u(0,t) + \frac{1}{\delta}L_{xx}^{-1}\left[\frac{\partial u}{\partial t} + u\frac{\partial u}{\partial x}\right] \tag{3.98}$$

with $L_{xx}^{-1}(\cdot) = \int_0^x dx' \int_0^{x'} (\cdot)\, dx''$. The series solution is given by:

$$\sum_{n=0}^{\infty} u_n = u(0,t) + x\frac{\partial}{\partial x}u(0,t) + \frac{1}{\delta}L_{xx}^{-1}\left(\frac{\partial}{\partial t}\sum_{n=0}^{\infty}u_n + \sum_{n=0}^{\infty}A_n\right) \tag{3.99}$$

To determine the components of $u_n(x,t)$, $n = 0, 1, 2, ...$, Adomian's technique can define the following recursive relation:

$$u_0 = u(0,t) + x\frac{\partial u}{\partial x}(0,t) \tag{3.100}$$

$$u_1 = \frac{1}{\delta}L_{xx}^{-1}\left[\frac{\partial}{\partial t}u_0 + A_0\right] \tag{3.101}$$

$$u_2 = \frac{1}{\delta}L_{xx}^{-1}\left[\frac{\partial}{\partial t}u_1 + A_1\right] \tag{3.102}$$

$$\vdots$$

$$u_n = \frac{1}{\delta}L_{xx}^{-1}\left[\frac{\partial}{\partial t}u_{n-1} + A_{n-1}\right] \tag{3.103}$$

$$\vdots$$

In the following examples the truncated series solution $\phi_n(x,t) = \sum_{k=0}^{n} u_k(x,t)$ is considered.

Example 1

Consider Burgers equation (3.75) with the particular initial and Dirichlet homogeneous boundary conditions given by:

$$u_0(x) = \sin(\pi x) \tag{3.104}$$

$$u(0,t) = u(1,t) = 0 \tag{3.105}$$

The exact solution is given by [78]:

$$u(x,t) = \frac{4\pi\delta\sum_{k=1}^{\infty} kI_k\left(\frac{1}{2\pi\delta}\right)\sin(k\pi x)\exp(-k^2\pi^2\delta t)}{I_0\left(\frac{1}{2\pi\delta}\right) + 2\sum_{k=1}^{\infty} I_k\left(\frac{1}{2\pi\delta}\right)\cos(k\pi x)\exp(-k^2\pi^2\delta t)} \tag{3.106}$$

being I_k the modified Bessel functions of first kind.

Consider $\delta = 1$. For such δ one can find, as an illustrative example, the first four terms of the Adomian's series solution:

$$\begin{aligned}
u_0 =& \sin(\pi x)\\
u_1 =& -\sin(\pi x)(\pi + \cos(\pi x))\pi t\\
u_2 =& \frac{1}{2}\sin(\pi x)\left(\pi^2 + 6\cos(\pi x)\pi + 3(\cos(\pi x))^2 - 1\right)\pi^2 t^2\\
u_3 =& -\frac{1}{6}\sin(\pi x)\pi^3 t^3\left[28\pi^2\cos(\pi x) + \pi^3 - 15\pi\right.\\
&\left.+51(\cos(\pi x))^2\pi + 16(\cos(\pi x))^3 - 10\cos(\pi x)\right]
\end{aligned}$$

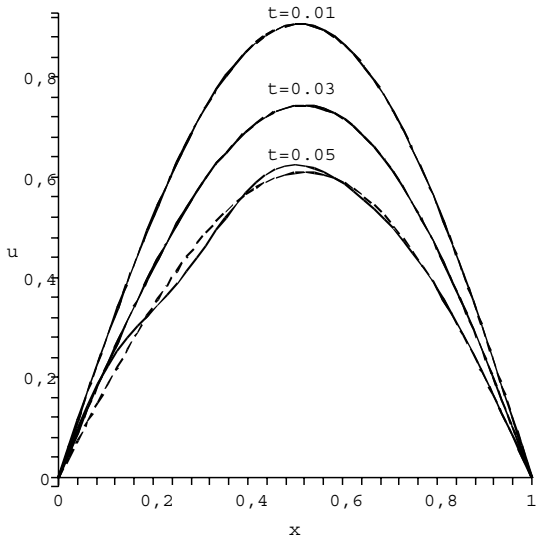

Fig. 3.11: Example 1: Results obtained for the exact solution (dashed line) and the one obtained by application of Adomian's method (solid line) with $n = 10$.

Figures 3.11 and 3.12 show the results for the exact solution and the one obtained by application of Adomian's method with $n = 10$ and $n = 14$. Figure 3.13 shows the three-dimensional plot for the solution obtained by Adomian's method for $n = 20$. One can see that the solution diverges for values of t greater than a value elsewhere between $t = 0.03$ and $t = 0.04$.

Figures 3.14, 3.15 and 3.16 show the results for the exact solution and the one obtained by application of Padé approximants [5/5], [5/4] and [7/7] to Adomian's solution. Figure 3.17 show the three-dimensional plot for the solution obtained by a [7/7] Padé approximant.

Tables 3.10 and 3.11 show the errors (difference between the exact solution and the approximate solution) for the solution given by Adomian's method with $n = 14$, and for the solution modified by Padé approximant [7/7].

The more accurate solution and the improved region of convergence is patent by using Padé approximants. However, a drawback of using Padé approximants that can be clearly seen in figure 3.14 and also in figure 3.16, occur due to the existence of poles in the rational approximation.

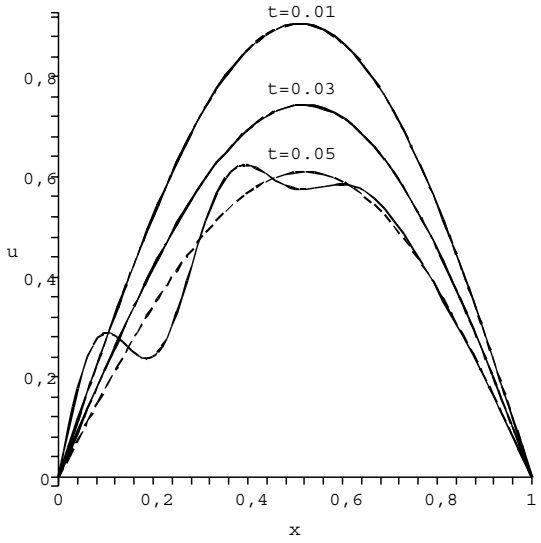

Fig. 3.12: Example 1: Results obtained for the exact solution (dashed line) and the one obtained by application of Adomian's method (solid line) with $n = 14$.

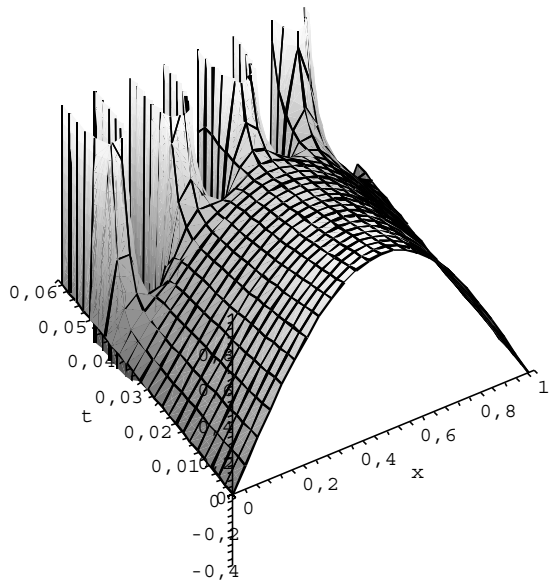

Fig. 3.13: Example 1: Three-dimensional plot for the solution obtained by Adomian's method for $n = 20$.

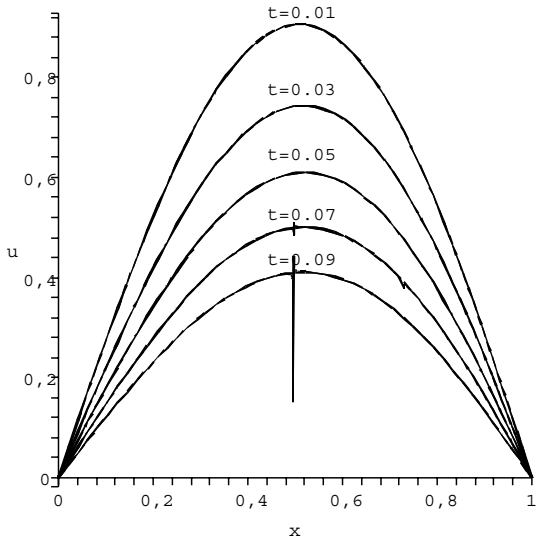

Fig. 3.14: Example 1: Results obtained for the exact solution (dashed line) and the one obtained by application of a Padé approximant [5/5] to Adomian's series solution (solid line).

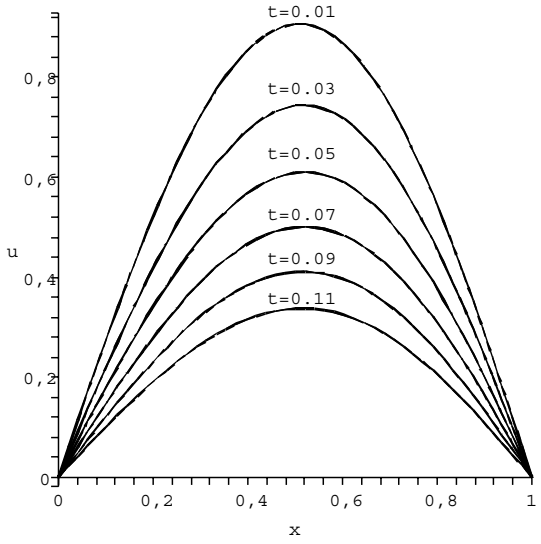

Fig. 3.15: Example 1: Results obtained for the exact solution (dashed line) and the one obtained by application of a Padé approximant [5/4] to Adomian's series solution (solid line).

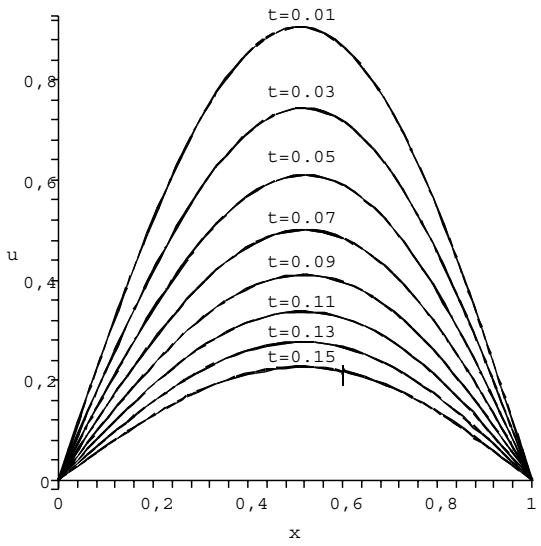

Fig. 3.16: Example 1: Results obtained for the exact solution (dashed line) and the one obtained by application of a Padé approximant [7/7] to Adomian's series solution (solid line).

Tab. 3.10: Example 1: Errors, differences between the exact solution and the approximate solution, given by Adomian's method with $n = 14$.

$t_i \backslash x_j$	0.05	0.15	0.25	0.35	0.45
0.1	-7.51745E-12	8.46701E-13	4.91018E-12	-4.38956E-12	4.50247E-13
0.2	-1.98818E-07	1.75001E-08	1.35282E-07	-1.15055E-07	6.11515E-09
0.3	-7.30473E-05	5.18810E-06	5.09930E-05	-4.18427E-05	7.06584E-07
0.4	-4.71039E-03	2.75777E-04	3.34633E-03	-2.67247E-03	-2.88965E-05
0.5	-1.17644E-01	5.76254E-03	8.46449E-02	-6.61789E-02	-2.16060E-03
0.6	-1.61678E+00	6.69537E-02	1.17453E+00	-9.02702E-01	-4.54042E-02
0.7	-1.47351E+01	5.19643E-01	1.07855E+01	-8.17325E+00	-5.30109E-01
$t_i \backslash x_j$	0.55	0.65	0.75	0.85	0.95
0.1	1.54630E-12	-8.34916E-13	-1.34394E-13	2.16168E-13	1.83671E-14
0.2	4.43314E-08	-2.12349E-08	-5.21332E-09	6.05034E-09	9.07751E-10
0.3	1.70554E-05	-7.46111E-06	-2.35344E-06	2.27028E-06	4.52373E-07
0.4	1.13185E-03	-4.60881E-04	-1.72366E-04	1.47078E-04	3.49075E-05
0.5	2.88133E-02	-1.10676E-02	-4.68945E-03	3.66155E-03	9.79461E-04
0.6	4.01285E-01	-1.46841E-01	-6.84936E-02	4.99722E-02	1.45870E-02
0.7	3.69265E+00	-1.29695E+00	-6.53125E-01	4.51534E-01	1.40891E-01

Tab. 3.11: Example 1: Errors, differences between the exact solution and the approximate solution, given by application of a Padé approximant [7/7] to Adomian's series solution.

$t_i \backslash x_j$	0.05	0.15	0.25	0.35	0.45
0.1	7.72079E-17	4.15110E-16	-4.60375E-15	1.85715E-15	-3.08566E-15
0.2	6.64533E-13	2.97967E-12	4.79233E-11	1.15523E-11	-2.68941E-11
0.3	8.83448E-11	3.53281E-10	2.15023E-09	1.18129E-09	-3.97138E-09
0.4	2.24271E-09	8.27523E-09	3.44407E-08	2.41130E-08	-1.24531E-07
0.5	2.35585E-08	8.18779E-08	2.72689E-07	2.11025E-07	-1.92525E-06
0.6	1.43608E-07	4.76656E-07	1.36455E-06	1.10350E-06	-2.77392E-05
0.7	6.06647E-07	1.94200E-06	4.97574E-06	4.09749E-06	2.09511E-04
0.8	1.97133E-06	6.13120E-06	1.44267E-05	1.19450E-05	1.68476E-04
1.0	1.20971E-05	3.60752E-05	7.51463E-05	6.19395E-05	3.97112E-04
1.5	1.90141E-04	5.37610E-04	9.53013E-04	7.69280E-04	2.52636E-03
2.0	8.60069E-04	2.38495E-03	3.93444E-03	3.15794E-03	7.90138E-03
3.0	3.99455E-03	1.09768E-02	1.71344E-02	1.38859E-02	2.73590E-02
4.0	8.34046E-03	2.29107E-02	3.50999E-02	2.87099E-02	5.12215E-02
$t_i \backslash x_j$	0.55	0.65	0.75	0.85	0.95
0.1	3.12547E-15	4.52255E-16	-4.48250E-16	-9.95009E-16	-8.52856E-15
0.2	1.51485E-11	2.45257E-12	-2.64229E-12	-8.25245E-12	6.56919E-11
0.3	1.28440E-09	2.10130E-10	-2.48538E-10	-1.00155E-09	3.02544E-09
0.4	2.25029E-08	3.53289E-09	-4.64875E-09	-2.28691E-08	4.31081E-08
0.5	1.73013E-07	2.51916E-08	-3.75399E-08	-2.17176E-07	2.93990E-07
0.6	8.08725E-07	1.06053E-07	-1.83231E-07	-1.21422E-06	1.25877E-06
0.7	2.72097E-06	3.11320E-07	-6.43426E-07	-4.79189E-06	3.94343E-06
0.8	7.26666E-06	6.96330E-07	-1.79757E-06	-1.48379E-05	9.91050E-06
1.0	3.24437E-05	1.73659E-06	-8.88349E-06	-8.77082E-05	4.00941E-05
1.5	3.05102E-04	-2.56678E-05	-1.14953E-04	-1.73076E-03	3.24537E-04
2.0	1.01625E-03	-2.84541E-04	-5.55498E-04	-1.69520E-02	1.02811E-03
3.0	3.04366E-03	-2.95330E-03	-3.65196E-03	6.38294E-02	3.43774E-03
4.0	3.77849E-03	-1.00792E-02	-1.08112E-02	6.11860E-02	6.22718E-03

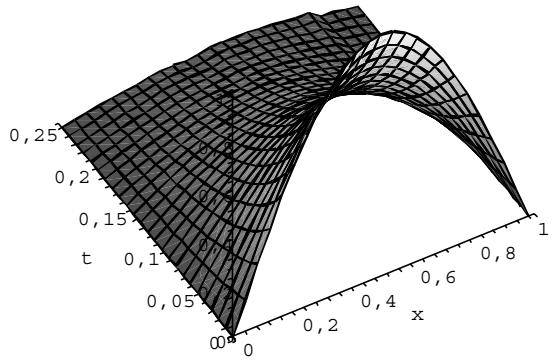

Fig. 3.17: Example 1: Three-dimensional plot for the solution obtained by application of a Padé approximant [7/7] to Adomian's series solution.

Example 2

Consider Burgers equation (3.75) with initial and boundary conditions given by:

$$u(x,1) = x - \pi \tanh\left(\frac{\pi x}{2\delta}\right) \tag{3.107}$$

$$u(0,t) = 0, \quad \frac{\partial}{\partial x}u(0,t) = \frac{1}{t} - \frac{\pi^2}{2\delta t^2} \tag{3.108}$$

The exact solution is

$$u(x,t) = \frac{x}{t} - \frac{\pi}{t}\tanh\left(\frac{\pi x}{2\delta t}\right) \tag{3.109}$$

This example was worked by [149]. By Adomian's decomposition method applied in the x direction, the solution is given by:

$$u(x,t) = u(0,t) + x\frac{\partial}{\partial x}u(0,t) + \frac{1}{\delta}L_{xx}^{-1}\left[\frac{\partial u}{\partial t} + u\frac{\partial u}{\partial x}\right] \tag{3.110}$$

being $L_{xx}^{-1}(\cdot) = \int_0^x dx' \int_0^{x'} (\cdot)\, dx''$.

So, as performed by [149] one obtains:

$$u_0 = \frac{x}{t} - \frac{x\pi^2}{2\delta\, t^2} \tag{3.111}$$

$$u_1 = \frac{\pi^4 x^3}{24\delta^3 t^4} \tag{3.112}$$

$$u_2 = -\frac{\pi^6 x^5}{240\delta^5 t^6} \tag{3.113}$$

$$u_3 = \frac{17\pi^8 x^7}{40320\delta^7 t^8} \tag{3.114}$$

$$u_4 = -\frac{31\pi^{10} x^9}{725760\delta^9 t^{10}} \tag{3.115}$$

The series obtained is the Taylor expansion of the real solution (3.109) around $x = 0$.

The expansion of the function $\tanh(x)$ being:

$$\tanh(x) = \sum_{n=1}^{\infty} B_{2n} \frac{4^n\,(4^n - 1)}{(2n)!} x^{2n-1}, \qquad |x| < \frac{\pi}{2} \tag{3.116}$$

one gets for the real solution (3.109) expanded in Taylor series around $x = 0$ the following equation (3.117).

$$\frac{x}{t} - \frac{\pi}{t}\tanh\left(\frac{\pi x}{2\delta t}\right) = \frac{x}{t} - \sum_{n=1}^{\infty} B_{2n} \frac{4^n\,(4^n - 1)}{(2n)!} \left(\frac{\pi}{t}\right)^{2n} \left(\frac{x}{2\delta}\right)^{2n-1}, \qquad |x| < \delta t \tag{3.117}$$

In the previous equation, B_n are the Bernoulli numbers. This expansion coincides with the one obtained by Adomian's method:

$$\begin{aligned} \frac{x}{t} - \frac{\pi}{t}\tanh\left(\frac{\pi x}{2\delta t}\right) = \frac{x}{t} - \frac{\pi^2 x}{2\delta\, t^2} + \frac{\pi^4}{24\delta^3 t^4} x^3 - \frac{\pi^6}{240\delta^5 t^6} x^5 \\ + \frac{17\pi^8}{40320\delta^7 t^8} x^7 - \frac{31\pi^{10}}{725760\delta^9 t^{10}} x^9 + \ldots \end{aligned} \tag{3.118}$$

Keeping this in mind, one can conclude that the Adomian's truncated series solution is only a good approximation for the real solution when $|x| < \delta t$, diverging for all other values of x and t. Representing the truncated series solution by $\phi_n = \sum_{k=0}^{n} u_k$, the numerical comparison for $\delta = 0.1$, performed by [149] for the truncated series ϕ_{20} given by Adomian's method with the analytical solution (3.109) is not accurate. For this value of δ, one should have $10x < t$ and the values taken by those authors were $0.1 \leq t_i \leq 0.5$ and

Tab. 3.12: Example 2: The true results obtained for the error between the exact solution and the one obtained by application of Adomian's method with $n = 20$.

$t_i \backslash x_j$	0.01	0.02	0.03	0.04	0.05
0.1	2.00000E+01	7.03687E+13	1.31303E+21	1.82050E+26	1.74903E+30
0.2	1.81899E-12	1.00000E+01	2.29652E+08	3.51844E+13	3.56543E+17
0.3	3.65567E-20	2.47351E-07	6.66667E+00	1.13138E+06	1.22236E+10
0.4	1.21644E-25	9.09495E-13	2.71528E-05	5.00000E+00	5.73412E+04
0.5	6.76623E-30	5.33595E-17	1.69846E-09	3.31983E-04	4.00000E+00

$0.01 \leq x_j \leq 0.05$. Table 3.12 shows the precise results obtained for the error between the exact solution and the one obtained by application of Adomian's method with $n = 20$, for $\delta = 0.1$. For the majority of those values one can see that the solution diverges. In order to be accurate, the values presented by Kaya and Yokus [149] should obey to the relation $\max x_j < \delta \min t_i$, that is, those authors may have performed their calculations for $\delta > 0.5$.

Consider again $\delta = 0.1$. Figure 3.18 shows the results obtained for the exact solution and the one obtained by application of Adomian's method with $n = 20$. Figure 3.19 shows the results obtained for the exact solution and the one obtained by application of Padé approximant [10/10] to Adomian's series solution. The results obtained for the error between the exact solution and the one obtained by application of Padé approximant [10/10] to Adomian's series solution are shown in table 3.13. The more accurate solution and the improved region of convergence is patent by using Padé approximants.

Example 3

Consider once more Burgers equation (3.75) with the following particular initial and boundary conditions:

$$u(x,1) = \frac{x}{1 + e^{\frac{x^2}{4\delta}}} \tag{3.119}$$

$$u(0,t) = 0, \quad u(1,t) = \frac{1}{t\left(1 + \sqrt{t}e^{\frac{1}{4\delta t}}\right)} \tag{3.120}$$

The exact solution, which can be verified by direct substitution in Burgers equation (3.75), is:

$$u(x,t) = \frac{x}{t\left(1 + \sqrt{t}e^{\frac{x^2}{4\delta t}}\right)} \tag{3.121}$$

Tab. 3.13: Example 2: Results obtained for the error between the exact solution and the one obtained by application of a Padé approximant [10/10] to Adomian's series solution.

$t_i \backslash x_j$	0.01	0.02	0.03	0.04	0.05
0.1	-7.80799E-15	-1.08753E-09	-4.15470E-07	-1.63449E-05	-1.99498E-04
0.2	-5.74753E-21	-3.66689E-15	-4.69991E-12	-5.09706E-10	-1.48886E-08
0.3	-9.38304E-25	-1.03846E-18	-2.24700E-15	-3.82994E-13	-1.66668E-11
0.4	-1.65326E-27	-2.34680E-21	-6.73391E-18	-1.49469E-15	-8.24634E-14
0.5	-1.06739E-29	-1.72494E-23	-5.83936E-20	-1.53467E-17	-9.92477E-16
$t_i \backslash x_j$	0.06	0.07	0.08	0.09	0.10
0.1	-1.22003E-03	-4.78901E-03	-1.39084E-02	-3.26205E-02	-6.54008E-02
0.2	-1.94092E-07	-1.47243E-06	-7.60301E-06	-2.95326E-05	-9.23204E-05
0.3	-3.11483E-10	-3.28583E-09	-2.29811E-08	-1.18092E-07	-4.77972E-07
0.4	-1.91039E-12	-2.45529E-11	-2.06381E-10	-1.26007E-09	-5.99905E-09
0.5	-2.66083E-14	-3.91240E-13	-3.72707E-12	-2.55932E-11	-1.36165E-10
$t_i \backslash x_j$	0.11	0.12	0.13	0.14	0.15
0.1	-1.16485E-01	-1.89345E-01	-2.86389E-01	-4.08878E-01	-5.56990E-01
0.2	-2.43553E-04	-5.61274E-04	-1.15936E-03	-2.18899E-03	-3.83582E-03
0.3	-1.60074E-06	-4.59913E-06	-1.16494E-05	-2.65664E-05	-5.54553E-05
0.4	-2.34166E-08	-7.77501E-08	-2.25780E-07	-5.85883E-07	-1.38180E-06
0.5	-5.90685E-10	-2.16882E-09	-6.93288E-09	-1.97193E-08	-5.07715E-08

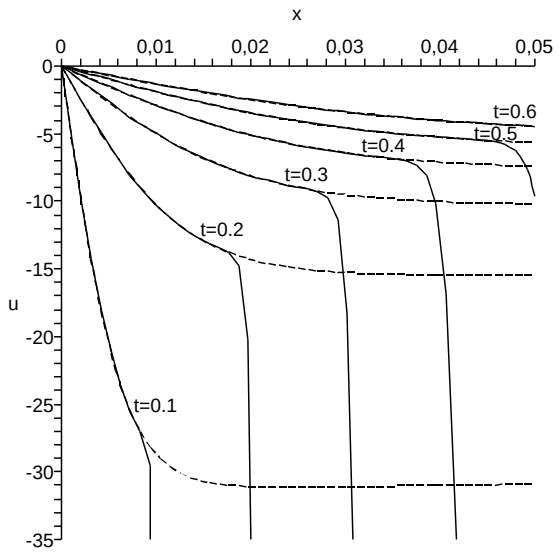

Fig. 3.18: Example 2: Results for $t = 0.1$, $t = 0.2$, $t = 0.3$, $t = 0.4$, $t = 0.5$ and $t = 0.6$, obtained for the exact solution (dashed line) and the one obtained by application of Adomian's method with $n = 20$ (solid line).

Consider $\delta = 0.1$. Figures 3.20 and 3.21 show the three-dimensional results for the solution obtained by application of Adomian's method with $n = 10$ and the one obtained by application of a Padé approximant [3/3] to Adomian's series solution. The symmetric Padé approximant correspondent to $n = 10$ is a [5/5] Padé approximant, but the much too demanding computation associated to it led one to use instead the less demanding [3/3] Padé approximant.

Table 3.14 shows the results obtained for the error between exact solution and the one obtained by application of Adomian's method with $n = 10$. The results obtained for the error between the exact solution and the one obtained by application of Padé approximant [3/3] to Adomian's series solution is shown in table 3.15.

The most accurate solution and the improved region of convergence is patent by using Padé approximants in spite of the comparison being performed between a [3/3] Padé approximant and the series solution with $n = 10$. Only for small values of time t and in the neighborhoods of $x = 0.8$ this is not true, because of the appearance of poles in the solution near $x = 0.8$, as it is shown in figures 3.21 and 3.22.

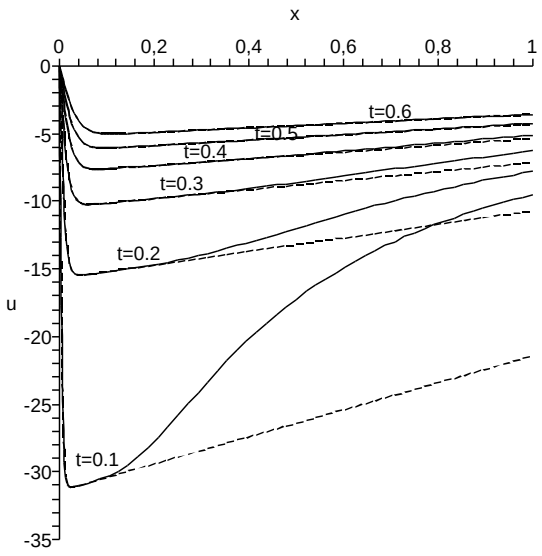

Fig. 3.19: Example 2: Results for $t = 0.1$, $t = 0.2$, $t = 0.3$, $t = 0.4$, $t = 0.5$ and $t = 0.6$, obtained for the exact solution (dashed line) and the one obtained by application of a Padé approximant [10/10] to Adomian's series solution (solid line).

Tab. 3.14: Example 3: Results obtained for the error between the exact solution and the one obtained by application of Adomian's method with $n = 10$.

$t_i \backslash x_j$	0.1	0.2	0.3	0.4	0.5
0.1	2.43833E-01	2.61487E-01	-1.53871E-01	-4.21187E-01	-9.57961E-02
0.3	5.14780E-03	7.11723E-03	1.86708E-03	-9.74435E-03	-1.25352E-02
0.5	7.61650E-05	1.09543E-04	4.59579E-05	-1.20577E-04	-2.16753E-04
0.7	1.97159E-07	2.88136E-07	1.39259E-07	-2.78553E-07	-5.76015E-07
0.9	8.64972E-13	1.27512E-12	6.60120E-13	-1.13337E-12	-2.53511E-12
1.1	-7.07303E-13	-1.04838E-12	-5.65256E-13	8.78828E-13	2.06821E-12
1.3	-1.05975E-07	-1.57665E-07	-8.73234E-08	1.26589E-07	3.08767E-07
1.5	-2.53072E-05	-3.77535E-05	-2.13128E-05	2.93269E-05	7.34644E-05
1.7	-9.04018E-04	-1.35142E-03	-7.73855E-04	1.02270E-03	2.61537E-03
1.9	-1.28341E-02	-1.92170E-02	-1.11263E-02	1.42377E-02	3.70166E-02
$t_i \backslash x_j$	0.6	0.7	0.8	0.9	1.0
0.1	2.59384E-01	2.08289E-01	-5.01249E-02	-1.33354E-01	-4.61523E-02
0.3	3.31525E-03	1.34845E-02	3.18653E-03	-6.41433E-03	-4.46725E-03
0.5	-2.30201E-05	2.22107E-04	1.22349E-04	-9.01966E-05	-1.03979E-04
0.7	-1.59242E-07	5.48580E-07	4.25550E-07	-1.80266E-07	-3.14395E-07
0.9	-9.40572E-13	2.25722E-12	2.11536E-12	-5.71407E-13	-1.45578E-12
1.1	8.89948E-13	-1.74225E-12	-1.84047E-12	3.25633E-13	1.20793E-12
1.3	1.45327E-07	-2.48709E-07	-2.85370E-07	3.25616E-08	1.80701E-07
1.5	3.67200E-05	-5.70584E-05	-6.95540E-05	4.79428E-06	4.28002E-05
1.7	1.36483E-03	-1.97130E-03	-2.51681E-03	8.79493E-05	1.51269E-03
1.9	1.99534E-02	-2.72113E-02	-3.60346E-02	3.06051E-04	2.12348E-02

Tab. 3.15: Example 3: Results obtained for the error between the exact solution and the one obtained by application of a Padé approximant [3/3] to Adomian's series solution.

$t_i \backslash x_j$	0.1	0.2	0.3	0.4	0.5
0.1	-8.60461E-03	-4.13796E-02	-1.79268E-01	-2.61018E-02	2.20208E-01
0.3	-4.73900E-05	-1.66618E-04	-8.16442E-04	-8.71155E-04	1.31269E-03
0.5	-6.84560E-07	-2.13900E-06	-8.94407E-06	-1.08418E-05	8.03014E-06
0.7	-4.94078E-09	-1.44641E-08	-5.37449E-08	-6.72593E-08	2.37770E-08
0.9	-7.70704E-13	-2.16225E-12	-7.37029E-12	-9.34334E-12	1.14841E-12
1.1	3.13951E-13	8.54371E-13	2.72755E-12	3.48157E-12	1.06377E-13
1.3	3.16534E-10	8.41686E-10	2.55197E-09	3.27169E-09	4.60525E-10
1.5	5.71408E-09	1.49182E-08	4.33790E-08	5.57863E-08	1.25124E-08
1.7	3.26833E-08	8.40620E-08	2.36098E-07	3.04354E-07	8.83149E-08
1.9	1.09029E-07	2.76943E-07	7.55334E-07	9.75586E-07	3.35335E-07
3.0	2.69059E-06	6.53941E-06	1.60435E-05	2.08624E-05	1.09247E-05
4.0	9.42320E-06	2.23926E-05	5.19886E-05	6.78483E-05	4.14633E-05
6.0	3.26520E-05	7.56064E-05	1.64632E-04	2.15799E-04	1.53060E-04
$t_i \backslash x_j$	0.6	0.7	0.8	0.9	1.0
0.1	2.26184E-01	1.75848E-01	2.57468E-01	-2.01302E-01	-6.01716E-02
0.3	6.15424E-03	1.41896E-02	1.73301E+00	-1.00293E-02	-6.03234E-03
0.5	8.59361E-05	4.13946E-04	-7.93718E-04	-2.41646E-04	-2.11008E-04
0.7	5.15066E-07	4.31281E-06	-3.70338E-06	-1.84955E-06	-1.98855E-06
0.9	6.75362E-11	9.98495E-10	-4.20469E-10	-2.64645E-10	-3.20265E-10
1.1	-2.38213E-11	-8.06939E-10	1.31928E-10	9.47361E-11	1.22714E-10
1.3	-2.13499E-08	1.13939E-05	1.06848E-07	8.33902E-08	1.12384E-07
1.5	-3.49795E-07	1.19630E-05	1.60163E-06	1.32262E-06	1.82453E-06
1.7	-1.84535E-06	3.42814E-05	7.81115E-06	6.71618E-06	9.39248E-06
1.9	-5.74947E-06	7.53380E-05	2.26973E-05	2.01117E-05	2.83473E-05
3.0	-1.11354E-04	6.34877E-04	3.33750E-04	3.21491E-04	4.55076E-04
4.0	-3.45297E-04	1.42551E-03	8.85082E-04	8.79852E-04	1.23382E-03
6.0	-1.04284E-03	3.08856E-03	2.21164E-03	2.26387E-03	3.11921E-03

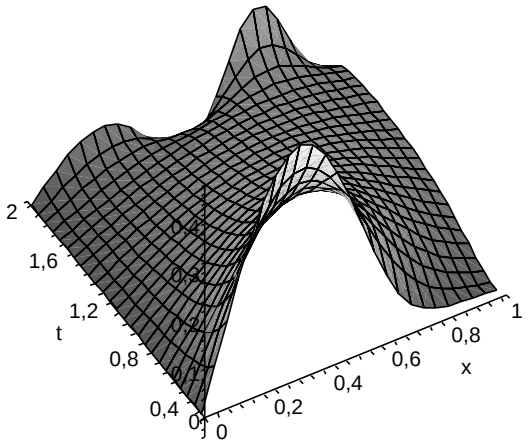

Fig. 3.20: Example 3: Three-dimensional plot, for $t = 0.3$ to $t = 2$, for the solution obtained by Adomian's method for $n = 10$.

3.3.3 The method of lines

Another possible way of trying to bypass the small convergence radius of Adomian's method would be to develop a time analytical and space numerical method, approximating the spatial derivatives by finite differences and then solve analytically the resulting set of ordinary differential equations by applying Adomian's decomposition method and Padé approximants or by applying the multistage Adomian's decomposition method (MADM). It is shown herein, illustrated by an example, that the application of Adomian's method to the ordinary differential equations set, arising from the discretization of the spatial derivatives by finite differences, may reduce the convergence domain of the solution series and, therefore, the above bypassing approach becomes useless. Actually, the convergence radius of the series solution may decrease with the number of discretization points, and, although the numerical results obtained by application of Padé approximants to the Adomian's solution series enlarge the convergence domain, this improvement also decreases with the number of spatial discretization points.

Consider Burgers equation (3.75) with initial and Dirichlet boundary con-

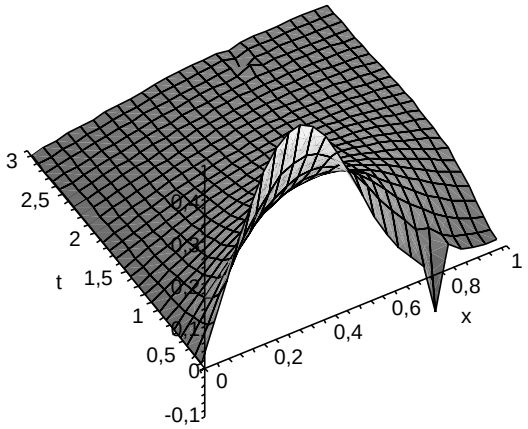

Fig. 3.21: Example 3: Three-dimensional plot,, for $t = 0.3$ to $t = 3$, for the solution obtained by application of a Padé approximant [3/3] to Adomian's series solution.

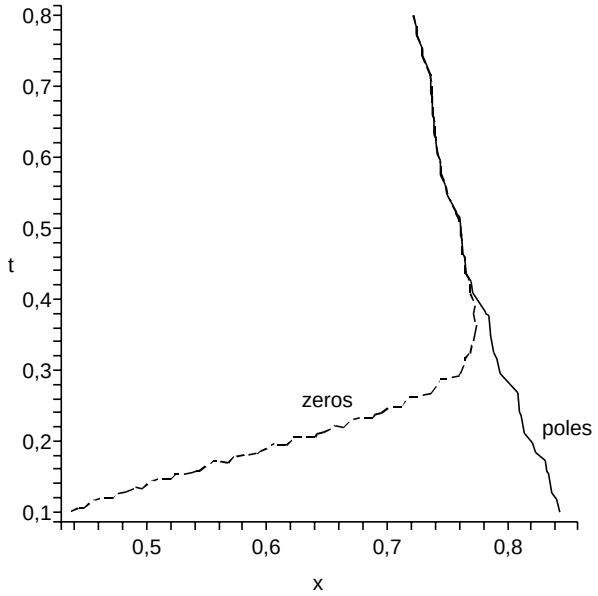

Fig. 3.22: Example 3: Zeros and poles for the solution obtained by application of a Padé approximant [3/3] to Adomian's series solution.

ditions given by:

$$u(x,0) = \sin(\pi x) \tag{3.122}$$

$$u(0,t) = u(1,t) = 0 \tag{3.123}$$

Consider a uniform grid with $\Delta x = x_{j+1} - x_j$, and approximate the first and second spatial derivatives by the following difference schemes of second order:

$$\frac{\partial u}{\partial x} = \frac{u_{j+1} - u_{j-1}}{2\Delta x} \tag{3.124}$$

$$\frac{\partial^2 u}{\partial x^2} = \frac{u_{j+1} + u_{j-1} - 2u_j}{\Delta x^2} \tag{3.125}$$

By applying the finite differences (3.124) and (3.125) to Burgers equation (3.75) with initial and boundary conditions (3.122) and (3.123), one gets for $N-1$ points the following equation:

$$\frac{\partial u_j}{\partial t} = \frac{1}{2\Delta x}\left(u_j u_{j-1} - u_j u_{j+1}\right) + \frac{\delta}{\Delta x^2}\left(u_{j+1} + u_{j-1} - 2u_j\right), \tag{3.126}$$
$$1 < j < N-1$$

Alternatively, in conservative form, equation (3.126) may be written as:

$$\frac{\partial u_j}{\partial t} = \frac{1}{4\Delta x}\left(u_{j-1}^2 - u_{j+1}^2\right) + \frac{\delta}{\Delta x^2}\left(u_{j+1} + u_{j-1} - 2u_j\right), \quad 1 < j < N-1 \tag{3.127}$$

Adomian's polynomials are given, respectively, by (the superscript of u represents the spatial discretization):

$$A_n^j = \frac{1}{n!}\left[\frac{d^n}{d\lambda^n}\left(\sum_{i=0}^{n}\lambda^i u_i^j\right)\left(\sum_{i=0}^{n}\lambda^i u_i^{j-1}\right)\right]_{\lambda=0} \tag{3.128}$$

$$A_n^j = \frac{1}{n!}\left[\frac{d^n}{d\lambda^n}\left(\sum_{i=0}^{n}\lambda^i u_i^j\right)\left(\sum_{i=0}^{n}\lambda^i u_i^j\right)\right]_{\lambda=0} \tag{3.129}$$

Consider $\delta = 1$. For the solution given by Adomian's method with $n = 20$ ($n+1$ terms conserved in Adomian's solution series) applied to system (3.127) with initial and boundary conditions given by equations (3.122) and (3.123), for different values of N, considering the convergence radius $r(N)$ the largest value of t for which the difference for all of the considered points, between the exact values of the solution given by (3.106) and the ones obtained by the truncated series applied to the discretized system (3.127), is inferior to 10^{-2}, one obtains the values showed in table 3.16. One can see that the convergence radius $r(N)$ and/or the rate of convergence of the series solution, decreases with the number of subintervals N. The conclusions applied to system (3.126) are similar.

This behavior is not due to the dimension of the system, but it seems to be related to the way the solution series of Adomian's method is constructed. To determine the components $u_n^j(x,t)$, $n = 0, 1, 2, ...$, $j = 1, 2, ..., N-1$, applied to system (3.127), Adomian's technique employs the recursive relation defined by:

$$\begin{aligned}
u_0^j &= u(x_j, 0)\\
u_1^j &= \int_0^t \left(\frac{1}{4\Delta x}\left[A_0^{j-1} - A_0^{j+1}\right] + \frac{\delta}{\Delta x^2}\left[u_0^{j+1} + u_0^{j-1} - 2u_0^j\right]\right)\\
u_2^j &= \int_0^t \left(\frac{1}{4\Delta x}\left[A_1^{j-1} - A_1^{j+1}\right] + \frac{\delta}{\Delta x^2}\left[u_1^{j+1} + u_1^{j-1} - 2u_1^j\right]\right)\\
&\vdots\\
u_n^j &= \int_0^t \left(\frac{1}{4\Delta x}\left[A_{n-1}^{j-1} - A_{n-1}^{j+1}\right] + \frac{\delta}{\Delta x^2}\left[u_{n-1}^{j+1} + u_{n-1}^{j-1} - 2u_{n-1}^j\right]\right)\\
&\vdots
\end{aligned} \tag{3.130}$$

Tab. 3.16: Experimental convergence radius in function of the number of subintervals.

N	$r(\mathbf{N})$	N	$r(\mathbf{N})$
20	0.013575	100	0.000563
30	0.006024	200	0.000137
40	0.003461	300	0.000062
50	0.002307	400	0.000034
70	0.001161	500	0.000021

For the sake of clarity, the solution for $n = 2$ of the i^{th} equation written in terms of the zero's term of Adomian's series solution (the subscript zero has been omitted), is:

$$\begin{aligned}\sum_{k=0}^{2} u_k^i = &\left[\frac{1}{2}u_{i+2} + 3u_i + \frac{1}{2}u_{i-2} - 2u_{i-1} - 2u_{i+1}\right] t^2 \frac{\delta^2}{\Delta x^4} \\ &+ \left[-\frac{1}{2}u_{i+2}^2 - u_{i+1}u_i + 3u_{i+1}^2 - u_{i+1}u_{i+2}\right. \\ &\left. + u_{i-1}u_i - 3u_{i-1}^2 + u_{i-1}u_{i-2} + \frac{1}{2}u_{i-2}^2\right] \frac{t^2}{4}\frac{\delta}{\Delta x^3} \\ &+ \left[16u_{i+1} + 16u_{i-1} - 32u_i\right] \frac{t}{16}\frac{\delta}{\Delta x^2} \\ &+ \left[u_{i+1}u_{i+2}^2 - u_{i+1}u_i^2 - u_{i-1}u_i^2 + u_{i-1}u_{i-2}^2\right] \frac{t^2}{16}\frac{1}{\Delta x^2} \\ &+ \left[u_{i-1}^2 - u_{i+1}^2\right] \frac{t}{4}\frac{1}{\Delta x} + u_i \end{aligned} \tag{3.131}$$

Increasing the number of subintervals N, Δx diminishes, the absolute values of the expressions between brackets in equations (3.130) and (3.131) should also diminish and the values of the powers of $\frac{1}{\Delta x}$ increase. It seems that the powers of $\frac{1}{\Delta x}$ may have a deeper influence on the convergence radius of the series solution, as shown below. Consider the powers of $\frac{1}{\Delta x^2}$. If one has αN subintervals ($\alpha > 1$), $\frac{1}{\Delta x^2}$ equals $\alpha^2 N^2$, which is α^2 times larger than that of $\frac{1}{\Delta x^2}$ if one had N subintervals. Therefore, the convergence radius may decrease as a function of α^2. Considering that it decreases α^2 times, this means that $r(\alpha N) = \frac{1}{\alpha^2} r(N)$ or $r(y) = \frac{N^2}{y^2} r(N)$. Fixing the value of $N = 20$, the one found in table 3.16, one gets the values showed in table 3.17 that are almost the same as those showed in table 3.16.

However, in some particular problems, the behavior can be quite different. Consider Burgers equation (3.75) with $\delta = 1$ and initial and Dirichlet

Tab. 3.17: Theoretical convergence radius in function of the number of subintervals.

N	$r(\mathbf{N})$	N	$r(\mathbf{N})$
20	0.013575	100	0.000543
30	0.006033	200	0.000136
40	0.003394	300	0.000060
50	0.002172	400	0.000034
70	0.001108	500	0.000022

boundary conditions given by:

$$u(x,0) = x \tag{3.132}$$

$$u(0,t) = 0, \quad u(1,t) = \frac{1}{1+t} \tag{3.133}$$

In this case one has at $x = 1$ a boundary condition not nil. Hence, the computations may become quite hard or even impossible to carry on, due to the successive analytical integrations performed by Adomian's method. Nevertheless, one can substitute $\frac{1}{1+t}$ by its Taylor series $\sum_{k=0}^{\infty} (-1)^k t^k$ and constructing the Adomian's series through the standard procedure, the corresponding terms in both series are identical. This way the computations become easier to perform, and, in this particular case, the solution is independent of the number of lines used, since the solution series obtained is the exact solution given by $x \sum_{k=0}^{\infty} (-1)^k t^k$.

One can say, as conclusions, that when it is not possible to know the explicit solution given by Adomian's method applied to nonlinear partial differential equations, the series obtained may be adequate only in a small region. Techniques to enlarge and/or improve this region may be necessary.

Moreover, in order to prove numerically whether the application of Padé approximants to Adomian's series solution of Burgers equation leads to better accuracy and larger convergence region, the numerical solution of some examples with and without Padé approximants were evaluated. From the worked examples, it is clear that Padé approximants improve the convergence region and the accuracy of the solution, except in the neighborhood of poles that can appear in the rational approximation and are not present in the real solution. This drawback warns one to look for the optimal Padé approximant to be applied, which can be of lower order. It was also shown that the application of Adomian's method to the ordinary differential equations set arising from the discretization of the spatial derivatives by finite

differences may reduce the convergence domain of the solution series, behavior that seems to be related to the presence of powers of $\frac{1}{\Delta x}$ that are larger when the spatial interval grid is smaller.

4. DYNAMICAL SYSTEMS AND BURGERS EQUATION

4.1 Dynamical systems: theory

Up to a certain level it is possible to predict the behavior of many physical, biological or economical systems by knowing their present state and the laws governing their evolution, provided these laws do not change in time. The set of all possible states of a system, the state space (often called phase space), and the laws of its evolution, is called a dynamical system. Formally, a dynamical system is a triple (T, X, φ^t), where T is a time set, X a state space and $\varphi^t : X \to X$ is a family of evolution operators parametrized by $t \in T$ and satisfying the properties $\varphi^0 = I$, which implies that the system does not change its state spontaneously, and $\varphi^{t+s} = \varphi^t \circ \varphi^s$, which means that the behavior of the system does not change in time [172] [52]. An *orbit* is an order subset of the state space X starting at a particular state x_0, that is, it is the evolution of a particular state of a dynamical system. Orbits of a discrete-time system are sequences of points in the state space X, that arise from the successive iteration of φ. A continuous-time dynamical system usually arises as a solution of a differential equation. The dynamical system is called a flow if the time t ranges over $\mathbb{R}$, and a semiflow if it ranges over $\mathbb{R}_0^+$ [172] [52].

A point $x^0 \in X$ is an *equilibrium point* if $\varphi^t x^0 = x^0$ for all $t \in T$. Being L_0 a *cycle* or periodic orbit, for each point $x_0 \in L_0$, $\varphi^{t+T_0} x_0 = \varphi^t x_0$ for some $T_0 > 0$ and for all $t \in T$. The minimal value of T_0 satisfying this property is called the period of the cycle L_0. Thus, each point $x_0 \in L_0$ of this orbit is a fixed point of φ^{T_0} [172] [52].

Consider a continuous-time dynamical system defined by the equation

$$\frac{dx}{dt} = f(x),\ x \in \mathbb{R}^n \tag{4.1}$$

being f a smooth function. An equilibrium point x_0 of the system, $f(x_0) = 0$, is called *hyperbolic*, if there are no eigenvalues of the Jacobian matrix of f evaluated at x_0 on the imaginary axis [172] [52].

Consider a discrete-time dynamical system $x = f(x)$, where the map f is a diffeomorphism. A fixed point x_0 of the system, $f(x_0) = x_0$, is called hyperbolic, if there are no eigenvalues of the Jacobian matrix of f on the unit circle [172] [52] [82].

4.1.1 Periodic orbits and Poincaré maps

Consider a continuous-time dynamical system defined by the differential equation (4.1), being f a smooth function, and possessing a periodic orbit L_0. Let $x_0 \in L_0$ and Σ a cross-section to the cycle at that point. The cross-section Σ is a smooth hypersurface of dimension $n-1$, intersecting L_0 at

a nonzero angle, being the simplest choice of Σ a hyperplane orthogonal to the cycle L_0 at x_0. One says that the hypersurface Σ is of codimension 1. The cycle L_0 is an orbit that starts at a point on Σ and returns to Σ at the same point. By the existence and uniqueness and smooth dependence on their initial conditions, an orbit starting at a point $x \in \Sigma$ sufficiently close to x_0 also returns to Σ at some point $\widetilde{x} \in \Sigma$ near x_0. Thus, a map, called a *Poincaré map*, associated with the cycle L_0 is constructed [172]:

$$\begin{aligned} P &: \Sigma \to \Sigma \\ \widetilde{x} &\hookrightarrow P(x) \end{aligned}$$

The Poincaré map P is locally defined and is invertible near x_0, being the intersection point x_0 a fixed point of the Poincaré map P.

As described by Kuznetsov [172] by introducing local coordinates $\xi = (\xi_1, \xi_2, \ldots, \xi_{n-1})$ on Σ, the stability of the cycle L_0 is equivalent to the stability of the fixed point ξ_0 corresponding to the point x_0. The cycle is stable if all eigenvalues $\mu_1, \mu_2, \ldots, \mu_{n-1}$ of the Jacobian matrix of P at the point ξ_0 are located inside the unit circle. These eigenvalues are independent on the choice of the point x_0 on L_0, the cross-section Σ, and the local coordinates ξ.

Let one see the relation between these eigenvalues and the differential equation (4.1) that defines the dynamical system having the cycle L_0 according to [172]. Let $\gamma(t)$ be a periodic solution of (4.1), $\gamma(t + T_0) = \gamma(t)$, corresponding to a cycle L_0. Being $u(t)$ an arbitrary solution, the deviation from the periodic solution is given by $w(t) = u(t) - \gamma(t)$. If f is twice continuously differentiable and w is small, one can expand f into a Taylor series yielding:

$$\frac{dw}{dt}(t) = \frac{du}{dt}(t) - \frac{d\gamma}{dt}(t) = f(\gamma(t) + w(t)) - f(\gamma(t)) = A(t)\, w(t) + O\left(\|w(t)\|^2\right)$$

where $A(t) = \frac{\partial f}{\partial x}(\gamma(t))$. The linearization of this equation, $\frac{dw}{dt}(t) = A(t)\, w(t)$ is called the variational equation about the cycle L_0, which represents the evolution of perturbations near the cycle. The stability of the cycle depends on the properties of the variational equation. This equation admits a unique global solution, $w(t) = M(t)\, w(0)$, where $M(t)$ satisfies $\frac{dM}{dt}(t) = A(t)\, M(t)$ with the initial condition $M(0) = I_n$, $M(t)$ being therefore its fundamental matrix. By Floquet theorem there exists a constant matrix B such that $M(T_0) = \exp(BT_0)$, and so the solution of the variational equation can be written as $w(t) = P(t) \exp(Bt)\, w(0)$. Since $P(t)$ is periodic, the asymptotic behavior of the solution depends only on B. The eigenvalues of B are called the *characteristic exponents* and the eigenvalues of $\exp(BT_0)$ are the

characteristic multipliers, being exponential functions of the characteristic exponents times T_0. The linear stability of L_0 is related to the behavior of these eigenvalues. Poincaré maps permit to reduce the problem of the dynamics of the cycle L_0 to a simpler one.

Theorem 16: The characteristic multipliers of the periodic orbit L_0 are given by 1 and by the $n-1$ eigenvalues of the Poincaré map associated with the cycle L_0 [172] [151].

By studying the Poincaré map, one obtains a complete characterization of the dynamics in a neighborhood of the periodic orbit.

4.1.2 Bifurcations and hyperbolicity

A dynamical system $(T, \mathbb{R}^n, \varphi^t)$ is called topologically equivalent to another dynamical system $(T, \mathbb{R}^n, \psi^t)$ if there is a homeomorphism $h : \mathbb{R}^n \to \mathbb{R}^n$ mapping orbits of the first system onto orbits of the second system, preserving the direction of time. Two equivalent systems have the same number of equilibria and cycles of the same stability types. The relative position of these invariant sets and the shape of their regions of attraction are also similar, which means that two dynamical systems are equivalent if their phase portraits are qualitatively similar, if one can be obtained from another by a continuous map [82] [172] [52].

The asymptotic properties of a dynamical system may change when one or more parameters are continuously changed. Consider a dynamical system that depends on parameters, $\frac{dx}{dt} = f(x, \alpha)$, $x \in \mathbb{R}^n$, $\alpha \in \mathbb{R}^m$, for continuous systems, or $x = f(x, \alpha)$, $x \in \mathbb{R}^n$, $\alpha \in \mathbb{R}^m$, for discrete systems. As the parameters vary, the phase portrait also varies, and either the system remains topologically equivalent to the original one, or its topology changes. The appearance of a topologically nonequivalent phase portrait under variation of parameters is called a *bifurcation.* Thus, a bifurcation is a change of the topological type of the system as its parameters pass through a critical value [82] [172] [151].

There are bifurcations that can be detected fixing any small neighborhood of the equilibrium. Such bifurcations are called local. Those bifurcations of limit cycles which correspond to local bifurcations of the associated Poincaré maps are called local bifurcations of cycles. There are also bifurcations that cannot be detected by looking at small neighborhoods of equilibrium or fixed points or cycles. Such bifurcations are called global, such as the heteroclinic or the homoclinic bifurcations [172] [82].

Under a small parameter variation, if the equilibrium is hyperbolic, it moves slightly, but remains hyperbolic. By varying further one or more parameters, if the hyperbolicity condition is violated, there is a qualitative change of the system and a bifurcation occurs. As described by [172] for a continuous-time dynamical system, the lost of hyperbolicity of an equilibrium happens, generally, by the approach to zero of a simple real eigenvalue of the variational equation (tangent or fold bifurcation) or by a pair of simple complex eigenvalues crossing the imaginary axis (Andronov-Hopf bifurcation). For a discrete-time dynamical system the hyperbolicity condition can be violated, generally, by the approach to the unit circle of a simple positive multiplier (tangent or fold bifurcation) or by a simple negative multiplier (flip or period-doubling bifurcation) or by a pair of simple complex multipliers (Neimark-Sacker or torus bifurcation). The combination of the Poincaré map and the center manifold theorem (that allows one to reduce the dimension of a system near a local bifurcation), allows these results to be applied to the study of limit cycle bifurcations in n-dimensional continuous-time dynamical systems [172].

According to [172] continuous time dynamical systems with phase-space dimension $n > 2$ can have invariant tori. An invariant torus appears through a generic Neimark-Sacker bifurcation. For example, a stable cycle can lose stability when a pair of complex conjugate multipliers crosses the unit circle. Then, provided the normal form coefficient is negative, a smooth, stable, invariant torus bifurcates from the cycle.

4.1.3 Chaos and Lyapunov exponents

Definition 17: For a probability space $(X, \mathcal{A}, \mu)$, a transformation $F : X \to X$ is said to be measure preserving or μ is said to be an $F-$invariant measure, if F is measurable and $\mu\left(F^{-1}(A)\right) = \mu(A)$ for all $A \in \mathcal{A}$ [264] [195].

Definition 18: For a probability space $(X, \mathcal{A}, \mu)$, a measure preserving transformation F is said to be *ergodic* or the $F-$invariant measure μ is said to be ergodic, if for all set $A \in \mathcal{A}$ with $F^{-1}(A) = A$ (A is $F-$invariant), $\mu(A) = 0$ or $\mu(A) = 1$ [264] [195].

By other words, an invariant measure is ergodic if the dynamics cannot be decomposed into different pieces that are themselves invariant.

Definition 19: $\varphi^t : X \to X$ is said to be topologically transitive, if for any pair of open sets $U, V \subset X$, there exists $t_k > 0$ such that $\varphi^{t_k}(U) \cap V \neq \phi$ (the dynamics cannot be decomposed into two or more invariant subsystems) [82].

Definition 20: $\varphi^t : X \to X$ has sensitive dependence on initial conditions if there is $\varepsilon > 0$, such that for every $x \in X$ and $\delta > 0$, there are $y \in X$ and $t_k > 0$ for which $d(x, y) < \delta$ and $d(\varphi^{t_k}(x), \varphi^{t_k}(y)) > \varepsilon$ [82].

Sensitive dependence on initial conditions means that minor changes in initial conditions lead to dramatically different long-term behavior (unpredictability).

There is no universal agreement on the definition of chaos, being generally agreed that a chaotic dynamical system should exhibit sensitive dependence on initial conditions. One possible definition of chaos is the one adopted by Devaney [82]:

Definition 21: $\varphi^t : X \to X$ is said to be chaotic on X if φ^t has sensitive dependence on initial conditions, φ^t is topologically transitive and periodic orbits are dense in X (unpredictable, indecomposability and with dense orbits).

Due to the impossibility of characterizing exactly a chaotic dynamics, one needs a statistical description, making use of properties of the attractor that should be independent *a.e.* on the initial conditions [73].

One of the most common modes of measuring the sensibility on the initial conditions, and consequently to deduce the eventual presence of a chaotic situation, consists on the determination of the *Lyapunov exponents*, which measure the exponential average growth rate of tangent vectors along trajectories, that is, measure the average rate of convergence or divergence in the phase space of nearby trajectories. Positive values are indicators of instability or chaos, being an important invariant of nonlinear systems.

For a discrete time dynamical system, $\mathbf{x}_{k+1} = F(\mathbf{x}_k)$, $F : \mathbb{R}^n \to \mathbb{R}^n$, v non-zero vector belonging to $\mathbb{R}^n$, one defines the Lyapunov exponent $\lambda(\mathbf{x}, v)$ [52] [73] [117] as:

$$\lambda(\mathbf{x}, v) = \lim_{k\to\infty} \frac{1}{k} \log \left\| \frac{dF^k(\mathbf{x})}{d\mathbf{x}} \cdot v \right\| \tag{4.2}$$

In $\mathbb{R}^n$ there are n Lyapunov exponents λ_i, $1 \leq i \leq n$, which measure the exponential growth rate of tangent vectors according to the eigenspaces directions of the matrix $\Lambda_{\mathbf{x}} = \left[J_k^T J_k\right]^{\frac{1}{2k}}$ for large t_k, being J_k the jacobian matrix of F^k ([1]), given by the logarithm of their eigenvalues [73].

For the unidimensional case λ is given by:

$$\lambda = \lim_{k\to\infty} \frac{1}{k} \log \left| \frac{df^k(x_0)}{dx} \right| = \lim_{k\to\infty} \frac{1}{k} \sum_{j=0}^{k-1} \log |f'(x_j)| \tag{4.3}$$

[1] $J_k(\mathbf{x}_0) = J(\mathbf{x}_{k-1}) \cdots J(\mathbf{x}_1) J(\mathbf{x}_0)$.

For a continuous time dynamical system n dimensional, $\frac{d\mathbf{x}}{dt} = F(\mathbf{x})$, v non-zero vector belonging to $\mathbb{R}^n$, the Lyapunov exponent $\lambda(\mathbf{x}, v)$ runs [73]:

$$\lambda(\mathbf{x}, v) = \lim_{t\to\infty} \frac{1}{t} \log \|M(\mathbf{x},t) \cdot v\| \tag{4.4}$$

being $M(\mathbf{x},t)$ the matrix satisfying the system $\frac{dM}{dt} = \mathbf{D}F \cdot M$ and $\mathbf{D}F$ the jacobian matrix of F. The Lyapunov exponents are calculated, in a identical manner, as being the logarithm of the eigenvalues of the positive and symmetric matrix $\Lambda_{\mathbf{x}} = \left[M^T(\mathbf{x},t)\ M(\mathbf{x},t)\right]^{\frac{1}{2t}}$ for large t.

The existence of the limit in equation (4.3) and its independence on the trajectory considered for almost all initial conditions, are guaranteed by the Birkohff ergodic theorem [264] [195] [117].

Theorem 22 (Birkhoff): Suppose $(X, \mathcal{A}, \mu)$ is a probability space, $f : X \to X$ is a measure preserving function and $g \in \mathcal{L}^1(X)$. Then,

- $\frac{1}{k}\sum_{j=0}^{k-1} g(f^j(x))$ converges a.e. in X to a function $g^* \in \mathcal{L}^1(X)$
- $g^* \circ f(x) = g^*(x)$ a.e. in X
- $\int_X g^* d\mu = \int_X g\ d\mu$.

For the multidimensional case, the existence of the Lyapunov exponents and their independence on the trajectory considered for almost all initial conditions, are guaranteed by the *Oseledec multiplicative ergodic theorem* [264] [195] [117].

Lyapunov spectrum, consists on the calculation of all Lyapunov exponents in decreasing order.

From the Lyapunov spectrum we can derive some quantities as the *Kolmogorov entropy and the Lyapunov dimension*.

The entropy measures the uncertainty of a possible outcome. In a system with N possible and independent results with probabilities p_i, the entropy S or information of the system is $S = -\sum_{i=1}^{N} p_i \log p_i$. The Kolmogorov entropy h measure the precision of a prediction for the nth iterate, and decreases with n due to the possible sensitive dependence on initial conditions. The Kolmogorov entropy h is bounded by the sum of the positive Lyapunov exponents $h \leq \sum_{\lambda_i>0} \lambda_i$ [73].

The geometry of a chaotic attractor can be characterized by a non-integral dimension, being the structure called a *fractal*. The *capacity* is a simple way

of defining a non-integral dimension. If in a m-dimensional space, one covers a set A, whose dimension one wants to find, with equal size m-cubes of side ε, and obtain N_ε m-cubes containing points of the set A, *capacity* or *box counting dimension* is defined, with $N_\varepsilon \sim \varepsilon^{-D_c}$, as [73]:

$$D_c = \lim_{\varepsilon \to 0} \frac{\log N_\varepsilon}{\log \epsilon^{-1}} \tag{4.5}$$

Hausdorff dimension D_H, another form purely geometric, is often equal to the capacity, but gives more reasonable answers in some special cases [73]. *Generalized dimensions* are an attempt to take into account the measure of the attractor, that is, the number of times the dynamics visits different regions of the phase space.

Dimensions are a static characterization of the attractor. An attempt to address this issue is given by Kaplan and Yorke [140], proposing a dimension based on the Lyapunov exponents, the *Lyapunov dimension (Kaplan-Yorke dimension)*, given by:

$$D_L = \nu + \frac{1}{|\lambda_{\nu+1}|} \sum_{i=1}^{\nu} \lambda_i \tag{4.6}$$

where ν is the largest integer for which the sum $\sum_{i=1}^{\nu} \lambda_i > 0$ (if ν equals the dimension of the phase space, then $D_L = \nu$). Recall that the Lyapunov exponents are always ordered by decreasing magnitude. Lyapunov dimension gives an estimate of the dimension of the space volume that neither grows nor decays [73].

4.1.4 Lyapunov spectrum

Probably the most important property of chaotic systems is given by its sensitive dependence on initial conditions. This sensitivity can be quantified by the largest Lyapunov exponent.

Several methods are described in the literature for the calculation of the Lyapunov spectrum, computing all exponents on decreasing order. A usual method consists of following two nearby orbits, one being the reference orbit and the other the test orbit, separated by a sufficiently small phase space distance d_0 at a time t_0. The difficulty in the calculation appears as a consequence of the following reasoning: for any initial displacement of the test orbit $\overrightarrow{v}$, the component with the maximal expansion rate dominates, so the component in the direction of the largest Lyapunov exponent is largely amplified comparatively to the other components. Hence, the displacement quickly becomes almost parallel to that direction, turning more difficult the

calculation of the other Lyapunov exponents [298]. To avoid this situation one falls back upon reorthonormalization methods.

To compute only the largest Lyapunov exponent [298] [207] [251], one consider the two described orbits, one being the reference orbit and the other the test orbit, separated by a sufficiently small phase space distance d_0 at a time t_0. At time t one has the distance between the two orbits given by $d(t) \approx d_0 e^{\lambda(t)(t-t_0)}$ and defines the *instantaneous largest Lyapunov exponent* as $\lambda(t) = \frac{1}{t-t_0} \log \frac{d(t)}{d_0}$. The largest Lyapunov exponent λ, can be computed by the formula:

$$\lambda = \lim_{t \to \infty} \frac{1}{t - t_0} \log \frac{d(t)}{d_0} \tag{4.7}$$

In practice one computes the value of the instantaneous largest Lyapunov exponent, for t sufficiently large, so it can be a valid approach of its asymptotic value. In the case of chaotic orbits, infinitesimal variations grow quickly at an exponential rate and the distance between the two nearby orbits $d(t)$ quickly saturates. Therefore, one must periodically renormalize the orbit separation whenever the distance $d(t)$ passes beyond a small enough value, so that the linear regime keeps valid, where the linearized equations of motion are an accurate description. This way, one determines the largest Lyapunov exponent, computing the reference orbit for a sufficiently long period and computing at each discrete time t_k, the linearized perturbations $\overrightarrow{d_k}$, being then adjusted by the factor $\frac{d(t_{k-1})}{d(t_k)}$. Summarizing, being $\overrightarrow{R}$ the reference vector of the phase space and $\overrightarrow{r}$ the test vector, the adjustment is made in the appropriate direction in the phase space at each instant t_k according to the equation $\overrightarrow{r} \leftarrow \overrightarrow{R} + \overrightarrow{d_k} \frac{d(t_{k-1})}{d(t_k)}$. For the computation of the largest Lyapunov exponent one uses the formula [298] [207] [251]:

$$\lambda_n = \frac{1}{t_n - t_0} \sum_{k=1}^{n} \log \frac{d(t_k)}{d(t_{k-1})} \tag{4.8}$$

One must ignore the first values to guarantee that the orbits are oriented in the direction of larger expansion.

The sensitive dependence on initial conditions brings about the amplification of small numeric errors, which establishes the importance of a larger attention on the implementation of numeric methods in these cases.

In [103] different discrete and continuous methods for computing the Lyapunov exponents are proposed, based on the QR decomposition, Q being an orthogonal matrix and R an upper triangular matrix with positive diagonal elements, or based on the singular value decomposition. The discrete methods iteratively approximate the Lyapunov exponents in a finite number of

time steps and, therefore, apply to iterated maps and continuous dynamical systems where the linearized flow map is evaluated at discrete times. The continuous methods are applied when all relevant quantities are obtained as solutions of ordinary differential equations, *i.e.,* continuous methods can only be formulated for continuous dynamical systems, not for maps. Discrete methods based on the QR decomposition may be performed by the Gram-Schmidt orthonormalization procedure (GS) or a sequence of Householder transformations. The continuous methods show several disadvantages, as they need much more computer time, exhibit loss of orthogonality of the matrices Q or U, the computation of only the largest k exponents is not necessarily cheaper than the determination of the whole spectrum and the continuous singular value method diverges for attractors with (almost) degenerate Lyapunov spectra ($\lambda_i \simeq \lambda_{i+1}$ for at least one $1 \leq i \leq n-1$) which very often occur in dynamical systems [103].

An efficient and numerically stable method to determine all the Lyapunov exponents of a discrete n-dimensional dynamical system, based on a modification of the HQR algorithm, factorization QR by Householder transformations, was developed by Bremen *et al.* [51]. The adaptation of this method to the computation of only the largest $p \leq n$ Lyapunov exponents was presented by [260].

In the work of Udawadia *et al.* [258] an approach for computing the Lyapunov exponents for continuous dynamical systems based on the QR decomposition that preserves the orthogonality of the matrix Q was presented. However, the method was adapted only to systems with small dimensions, till $n = 3$. Without this inconvenient, a method based on the Cayley transform, preserving the orthogonality of the matrix Q and requiring, for large n, only the solution of about half the number of differential equations was presented by [259].

4.2 Extended dynamical systems: theory

Many nonlinear phenomena are modeled by spatiotemporal systems of infinite or very high dimension, denominated spatially extended dynamical systems. Spatiotemporal behavior includes periodic patterns, frozen and traveling interfaces, intermittency, spirals and synchronization. Extended dynamical systems appear in various areas of science like Biology, Physics, Engineering, Chemistry or any other area related to spatiotemporal behavior. Often, the complex interaction between time and space gives rise to spatiotemporal chaos. Spatiotemporal chaos can be defined by the existence of a temporally chaotic wave $u(x,t)$ for which the time series $\{u(x_1,t)\}_t$ and

$\{u(x_2,t)\}_t$ become statistically independent as the distance from x_1 to x_2 increases [58]. From the Lyapunov spectrum it is possible to estimate bounds for the effective number of degrees of freedom of the system, the dimension of the attractor. This is presently an area of intensive research, particularly pertaining to communications systems, chaos control, estimation of model parameters and model identifications.

The most common models are based on a local dynamics and in a coupled one, which operates in the space directions. These systems can be seen as collections of many sub-systems, identical or similar, that interact amongst themselves. Frequently the complex interaction between time and space, between the local and the coupled dynamics, leads to the denominated chaos spatiotemporal. Control of spatiotemporal chaos may be consulted in the work of [166] and [158].

Basic models for spatially extended systems are coupled ordinary differential equations (CODEs), coupled map lattices (CML) and partial differential equations (PDEs).

4.2.1 Lyapunov spectrum

The computation of the entire Lyapunov spectrum for extended dynamical systems may be a very time-consuming task, according to the dimension of the systems. It is possible to approximately reconstruct the Lyapunov spectrum from the spectrum of a subsystem of smaller dimension N_s, by a suitable rescaling. One technique to estimate the Lyapunov spectrum is to consider a relatively small system with dimension N_s and with exactly the same dynamical equations as the original system N-dimensional. In a wide range of spatiotemporal systems the Lyapunov spectrum for the small system converges to the spectrum of the original system under appropriate rescaling [57].

One method to approximate quantities derived from the Lyapunov spectrum, like the Lyapunov dimension D_L and the Kolmogorov entropy h, is obtained by defining intensive quantities, *i.e.*, independent from the subsystem size, from the extensive ones, using the corresponding densities, $\rho_d(N_s) = \frac{D_L}{N_s}$ and $\rho_h(N_s) = \frac{h}{N_s}$. The estimates of the extensives quantities are taken by the linear relation $Q(V) = V \times q$, where Q is the extensive quantity to be estimated, q the corresponding intensive one and V the size of the system. This method relies on the linear increase of the Lyapunov dimension and the Kolmogorov entropy with the system size [249] [57]. A physical interpretation of this phenomenon can be given in terms of the thermodynamic limit of the system. For many spatiotemporal chaotic systems there is a typical finite correlation length ξ such that the system can be seen as the union of

several almost independent subsystems of size ξ. One expects that, in the limit of a large number of degrees of freedom and small correlation length, the Lyapunov spectrum repeats itself in each of the subsystems and, as a consequence, the fractal dimension of the system attractor scales linearly with the volume of the system. This generally fails if the size N_s is too small, often due to boundary conditions that become stronger as the system size is decreased [249] [57]. Because the Lyapunov exponents are not extensive quantities, to estimate the largest Lyapunov exponent for the whole system one could take the value of the largest Lyapunov exponent of the subsystem considered. In the work of [57] a new method was proposed, that the authors believe to be more accurate, to estimate the Lyapunov quantities. The method consists of taking the Lyapunov spectrum of the subsystem, rescaling it, and then extrapolating a curve through it to obtain an approximation to the whole Lyapunov spectrum, and only then the quantities are computed. Gonzalez and Bünner [56] showed that, for spatially extended chaotic systems, the relation $Q(V) = V \times q$ must be corrected by the inclusion of a system dependent constant $V_0 > 0$, being the new relation given by $Q(V) = (V - V_0) \times q$ for $V > V_0$. The presence of such a constant emerges from the observation that, when computing the Lyapunov spectrum from a subsystem, there is a transition from chaos to order parametrized by the subsystem size when the subsystem size is decreased below a certain critical size V_0, which means that if the dimension of a subsystem is smaller than V_0, it does not give any information about the quantity Q.

Another way of reconstructing the Lyapunov spectrum from a smaller subsystem of dimension N_s, is obtained by truncating the original system and considering only a small subset of variables, taking into account only a portion of the information of the entire system. Only a subset N_s of the N variables is used to build the Jacobian, and so the underlying dynamics of the original system is not changed [57]. Gonzalez *et al.* [57] noticed that, for consecutive subsystem sizes N_s and $N_s + 1$, the Lyapunov exponents interleave. They also presented a new rescaling method, by using the ratio of volumes $\frac{N+1}{N_s+1}$ instead of the conventional one $\frac{N}{N_s}$, reasoning that this new rescaling method gives a better fitting to the original Lyapunov spectrum.

The extension of the notion of Lyapunov exponent to an potential infinite extended dynamical system, which exhibits space-time chaotic behavior, is not always straightforward. In a system with few degrees of freedom, it is not particularly important what Lyapunov vector is choosed initially (initial perturbation), because after an initial transient, the component with the maximal growth rate dominates over almost all initial vectors. This may not be true for infinitely extended systems, since the transient time can be, formally, infinite [229]. If the initial Lyapunov vector is homogeneous in

space, one can expect this homogeneity to be conserved at least in a statistical way during the evolution in time. With this approach, the computation of Lyapunov exponents appears to be the closest analogue for systems with a finite number of degrees of freedom. Also, there is a second limit tending to infinity, the thermodynamic limit, corresponding to the system size L, that must be taken together with the limit of the time T. By investigating the convergence properties of both limits, Pikovsky and Politi [229] found the optimal strategy to determine the largest Lyapunov exponent. The order of magnitude of the optimal time T_0 for a fixed L is then given by $T_0 \approx L^{\frac{3}{2}}$.

4.2.2 Unstable dimension variability

The dynamics on a chaotic attractor is said to be *hyperbolic* if at each point of any trajectory the phase space can be splitted into an expanding subspace and a contracting one and the angle between them is bounded away from zero. Furthermore, along each trajectory, the expanding subspace evolves into the expanding one and the contracting subspace evolves into the contracting one. Otherwise, the set is said to be nonhyperbolic. For hyperbolic chaotic systems, numerical trajectories can be shadowed by true trajectories for an arbitrarily long time, a property that is not present in nonhyperbolic chaotic systems, which cause difficulties in the study of such systems [179].

By investigating systems of coupled chaotic oscillators, theoretical and computational reasoning were presented by [176] [179], defending that chaotic high-dimensional dynamical systems may impose severe modelling difficulties, as no model is able to produce reasonably long solutions that exist in nature. Coupled oscillators arise in many situations of Physics and Biology and from spatial discretization of nonlinear partial differential equations. The collective behavior of all oscillators can range from steady state to periodic oscillations and chaotic or turbulent motions. The justification put forward by the authors that support the modelling difficulties is the phenomenon known as *unstable dimension variability* [176] [179], a type of nonhyperbolicity behavior, characterized by a trajectory that may have a different number of unstable directions in different regions of the phase space, and, consequently, there is no continuous decomposition of the tangent space at each trajectory point into stable and unstable subspaces. The number of unstable directions of any unstable periodic orbit is determined by the local chaotic dynamics and the coupling strength. These conclusions are also applied to the integration of partial differential equations where discretization is used, yielding a system of coupled ordinary differential equations. Lai *et al.* [179] argue that unstable dimension variability can arise on coupled systems for small values

of the coupling parameter, but severe modelling difficulties, where the models do not accurately represent the deterministic evolution of the real systems, can occur only for reasonable coupling when the unstable dimension variability is appreciable. Often, in these cases, the only results that can be trusted are statistical invariants obtained from a large numbers of trajectories of the model. This phenomenon is believed to arise commonly in high-dimensional chaotic systems, but the Liu *et. al.* [192] showed that noise can induce unstable-dimension variability even in low dimensional chaotic systems.

4.3 Spectral methods

The generic outline of differential equations discretization, known as method of weighted residuals (MWR), consists of seeking a solution expanded in truncated series of basis functions, denominated trial, expansion or approximating functions, and test or weight functions, used to ensure, by minimizing the residual, that the differential equation is satisfied as closely as possible by the truncated series expansion. Spectral methods can be referred as methods of this nature but much more developed. The basis functions used in spectral methods are functions with global support, infinitely differentiable, characteristics that distinguish them from finite element or finite difference methods that use functions with local support where the expansion involves local interpolants such as piecewise polynomials [105]. For problems with smooth solutions, convergence rates of spectral methods are superior, with convergence rates of $O\left(c^N\right)$, $0 < c < 1$, where N is the number of degrees of freedom in the expansion. In contrast, finite element or finite difference methods yield convergence rates that are only algebraic in N, $O\left(N^{-m}\right)$. This property of superior accuracy of spectral methods is commonly called *spectral accuracy* or *exponential convergence* [50] [255] [105]. There are, however, some disadvantages in using a spectral method instead of a finite element or a finite difference method, due to the fact that sparse matrices are replaced by full matrices, and also due to the fact that it is not easily adaptable for problems posed on irregular domains. Nevertheless, provided the solution is sufficiently smooth, the rapid convergence of spectral methods often compensates these disadvantages [296] [105].

The most commonly used spectral methods are the Galerkin, Tau and collocation methods. These methods differ for the choice of the test functions. In Galerkin methods the test functions are the same as the trial functions, which must individually satisfy the boundary conditions. Tau methods are similar to Galerkin methods, except in the fact that none of the trial functions needs to satisfy the boundary conditions. In collocation methods (also

known as pseudospectral methods), the test functions are shifted Dirac delta functions centered at the so-called collocation points.

For the sake of clarity, and as an example, let one obtain the solution of the partial differential equation $\frac{\partial u}{\partial t} = f(u)$, with homogeneous Dirichlet boundary conditions. As far as the method of weighted residuals is concerned, the test functions are the following shifted Dirac delta functions [105],

$$\psi_j(x) = \delta(x - x_j), \ j = 1, 2, \ldots, N-1 \tag{4.9}$$

where the x_j are distinct collocation points in the interval $(-1, 1)$. The standard method of weighted residuals condition impose that,

$$\int_{-1}^{1} \left[\frac{\partial u^N}{\partial t} - f\left(u^N\right) \right] \psi_j(x)\, dx = 0, \ j = 1, 2, \ldots, N-1 \tag{4.10}$$

or, equivalently,

$$\frac{\partial u^N}{\partial t} - f\left(u^N\right)|_{x=x_j} = 0, \ j = 1, 2, \ldots, N-1 \tag{4.11}$$

The boundary conditions are achieved by restricting the interpolants to those satisfying $u^N(1,t) = u^N(-1,t) = 0$.

Fourier series are not always a good choice for the trial functions. They are only appropriate for problems with periodic boundary conditions. Chebyshev polynomials constitute a more versatile set of trial functions. Chebyshev polynomials are defined on the interval $[-1, 1]$ by equation (4.12).

$$T_k(x) = \cos(k \cdot \arccos x), \ k = 0, 1, 2, \ldots \tag{4.12}$$

Choosing for trial functions the Chebyshev polynomials T_k, the approximate solution, interpolating the solution in $N+1$ points is

$$u^N(x,t) = \sum_{k=0}^{N} \widehat{u}_k(t) \cdot T_k(x) \tag{4.13}$$

A particularly convenient choice for the collocation points are the Gauss-Lobatto points (Chebyshev points of the second kind, the extreme points on $[-1, 1]$), defined by equation (4.14) [105] [50] [255],

$$x_j = \cos\frac{\pi j}{N}, \ \ j = 0, ..., N \tag{4.14}$$

which produces highly accurate approximations and is, simultaneously, economical since $\phi_k(x_j) = \cos\frac{\pi jk}{N}$.

The finite series defined by equation (4.13) is not simply the truncation of the Chebyshev infinite series, so the expansion coefficients $\widehat{u}_k(t)$ are different. The expansion coefficients are given by the following expression [105] [50] [255],

$$\widehat{u}_k(t) = \frac{2}{N \cdot \overline{c_k}} \sum_{j=0}^{m} \frac{1}{\overline{c_j}} \; u(x_j, t) \; T_k(x_j) \tag{4.15}$$

where $\overline{c_j} = \begin{cases} 2 & j = 0, N \\ 1 & 1 \leq j \leq N-1 \end{cases}$.

The concept of a differentiation matrix for spectral collocation methods for solving boundary value problems has proven to be a very useful tool in the numerical solution of differential equations [296], and is based on weighted interpolants of the form,

$$f(x) \approx p_N(x) = \sum_{j=0}^{N} \frac{\alpha(x)}{\alpha(x_j)} f(x_j) \, \phi_j(x) \tag{4.16}$$

where the points $\{x_j\}_{j=0}^{N}$ are a set of distinct interpolation nodes, $\alpha(x)$ is a weight function and the set of interpolating functions $\{\phi_j(x)\}_{j=0}^{N}$ satisfies $\phi_j(x_k) = \delta_{kj}$. The n^{th} derivative operator may be represented by the differentiation matrix with entries defined by equation (4.17).

$$D_{k,j}^{(n)} = \frac{d^n}{dx^n} \left[\frac{\alpha(x)}{\alpha(x_j)} \phi_j(x) \right]_{x=x_k} \tag{4.17}$$

The numerical differentiation process may also be performed as a matrix-vector product. By applying the Fast Fourier Transform (FFT), the matrix-vector product can be computed in $O(N \log N)$ operations rather than $O(N^2)$ operations that the direct computation requires. The matrix approach defined by equation (4.17) is, for many situations, preferred to the FFT as, for small values of N the matrix approach is faster than the FFT. On the other hand, for the FFT to be optimally efficient, $N+1$ has to be a power of 2, otherwise the matrix approach may not be much slower in practice even for large N [296].

The boundary conditions are established by adding additional equations or by restricting the interpolants to those that satisfy them.

4.4 Dynamics in spectral solutions of Burgers equation

An important issue in nonlinear dynamics is to understand how the asymptotic properties of a dynamical system evolve when one or more parameters are continuously changed. By varying one parameter the resulting

system may or may not remain topologically equivalent to the original one. If not, there is a qualitative change of the system and a bifurcation occurs.

Burgers equation used for high Reynolds number, or equivalently, for small values for the viscosity coefficient $\delta = \frac{1}{R}$, develops waves with sharp slopes, leading to the appearance of discontinuities for values $\delta \to 0$. Such discontinuities are the cause of difficulties that arise in obtaining a solution, fact that led several authors to propose several numerical solutions [302] [202] [87] [142] [206] [295] [294]. Oscillations can occur by discretization through spectral collocation methods, due to Gibbs phenomena. Under a dynamic point of view, these instabilities may be related to bifurcations arising to the discretized equation.

Dang-Vu and Delcarte [77] provided numerical studies of the following Dirichlet problem for Burgers equation with homogeneous boundary conditions, by Chebyshev collocation and Chebyshev Tau spectral methods,

$$\frac{\partial u}{\partial t} + u\frac{\partial u}{\partial x} = \delta\frac{\partial^2 u}{\partial x^2} + f(x), \quad -1 \leq x \leq 1 \tag{4.18}$$

with $f(x) = \pi \sin(\pi x)[\cos(\pi x) + \delta\pi]$ [77] and found out a critical value of the viscosity δ for equation (4.18), where a Hopf bifurcation took place and a periodic orbit around the critical point arose, with frequency given by the absolute value of the imaginary part of the pair of complex eigenvalues at the critical point. As δ continued to decrease they found out that the limit cycles lost their stability and a trapping region was obtained, *i.e.*, a bounded region of phase space to which all sufficiently close trajectories from the basin of attraction were asymptotically attracted. The positive values found by the authors for the largest Lyapunov exponent provided support for the existence of chaotic motion [77]. Numerical studies were made for $N = 16$, 20 and 24, but it was referred that the same behavior was repeated for higher values of N. However, in this chapter, further studies are carried out, such as the improvement of the accuracy on the calculation of the largest Lyapunov exponents, the identification of many bifurcations implicated, the observation of orbits in real time, the change of coordinates in time and Poincaré maps. The results show that, in several cases, the value of the largest Lyapunov exponent may be compatible with the nil value, indicating that attractors classified as chaotic are actuality not. Moreover, the results show that, in many cases, the attractors are really torus type attractors, quasiperiodic motions, seeming to be chaotic only for some situations.

In this chapter, it is studied the stability, bifurcation and dynamics of spectral collocation methods applied to Burgers equation (4.18), where the unknown solution of the differential equation is expanded as a global interpolant. The Tau and Galerkin methods are alternatives to the collocation

method, but the latter is typically easier to implement, particularly for non-constant coefficients or nonlinear problems. The following equation with $N-1$ degrees of freedom is obtained by discretization of equation (4.18) with $N+1$ points x_j, $0 \leq j \leq N$, by Chebyshev collocation method,

$$\frac{du_i}{dt} = -u_i D^{(1)} u + \delta D^{(2)} u + f_i, \quad 1 \leq i \leq N-1 \tag{4.19}$$

where $u_1 = u(x_1, t)$, $u_2 = u(x_2, t)$, ..., $u_{N-1} = u(x_{N-1}, t)$, $u = [u_1, u_2, ..., u_{N-1}]^T$, $f_i = f(x_i)$ and $D^{(i)}$, $1 \leq i \leq 2$ are the Chebyshev differentiation matrices of order i. The problem is then reduced to a system of ordinary differential equations of order $N-1$.

To begin, one choses the same example used by [77] with the same function f, so that an asymptotic solution is given by $u(x,t) = \sin(\pi x)$. Studies are also made for other forced Burgers equation (4.18) with different function f, in order to allow for a fruitful discussion of results.

Besides the trapping region found by Dang-Vu and Delcarte [77], arising from the loss of stability of the periodic orbits emerging from Hopf bifurcation, other phenomena are observed. In fact, it is observed the existence of torus type attractors or strange attractors, for lower values of δ, before the dynamics becomes unbounded.

Also, bistability is observed, which means the coexistence of two final states, attractors, for a given set of parameters. Multistability, or in particular, bistability behavior is found in a variety of systems from different disciplines of science, like Physics, Chemistry, Neuroscience and Laser Physics. The long term behavior of such systems becomes more involved, because it may exist a nontrivial relationship between these coexisting asymptotic states and their basins of attraction. Given the initial conditions, it is not clear at which attractor the dynamics will finally settle down. In this case, both the coexistence of two periodic attractors, a periodic and a nonperiodic one (torus type or strange attractor), and even two nonperiodic attractors are observed. In this last case, the nonperiodic orbits seem to correspond to quasiperiodic motions. In addition, other stable equilibrium points can occur, diverse from the ones corresponding to the asymptotic solution of Burgers equation.

For different degrees of freedom, some differences were noticed. For the example used by [77], the main difference found, when there was an odd number of degrees of freedom (with N even) and when there was an even number of degrees of freedom (with N odd), is that all the motion in the periodic and nonperiodic attractors, in the first case, is restricted to the invariant subspace of the example studied, while in the second case, this did

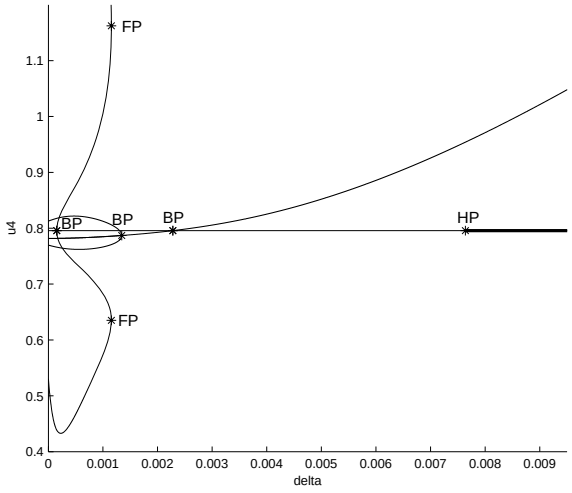

Fig. 4.1: Equilibrium solutions for Chebyshev spectral solution of Burgers equation for $N = 16$. HP represents the point where the Hopf Bifurcation takes place. BP represents a branch point. FP represents a fold point. The bold segments represent the stable solutions.

not occur. The symmetry of the system is broken in this last case. This is more evident for values of x away from the boundaries.

Positive values yielded by the largest Lyapunov exponent for some non-periodic motions, provide evidence of chaotic attractors.

For this study, Chebyshev collocation method is considered, with low and higher values of N, such as $N = 16$, $N = 17$, $N = 50$ and $N = 51$. The tools used to perform this study were MATLAB [1] and MATCONT [83] [84].

4.4.1 Numerical results

Consider the same example used by [77] with $f(x) = \pi \sin(\pi x)[\cos(\pi x) + \delta\pi]$, so that an asymptotic solution is given by $u(x,t) = \sin(\pi x)$.

- *Dynamics for N=16*

In this case the Dirichlet problem admits an odd number of degrees of freedom. Figure 4.1 shows the equilibrium solutions as a function of u_4, where HB represents a Hopf Bifurcation, BP branch points and FP fold points. The bold segments represent the stable critical solutions.

As the value of δ is decreased, a supercritical Hopf bifurcation takes place at $\delta_H \simeq 0.007638903$ and simultaneously the stable asymptotic solution loses

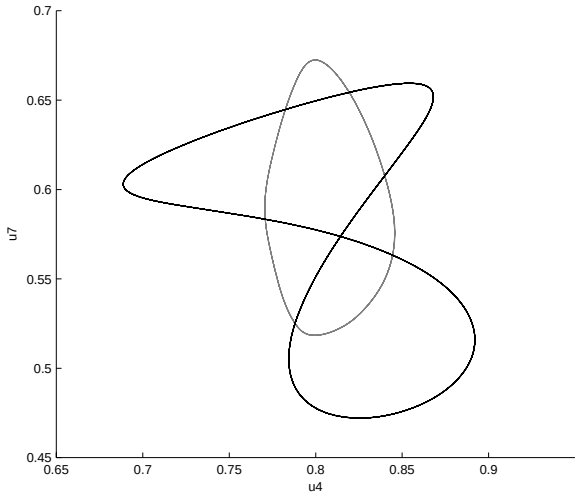

Fig. 4.2: $N = 16$. Bistability for $\delta = 0.007$, with two stable periodic orbits.

its stability, and a stable periodic orbit appears. The period of such orbit at the onset of the bifurcation is around 4.1991798. As a stable limit cycle emerges, the bifurcation is supercritical. Eventually, the limit cycle arising from the Hopf bifurcation loses its stability at $\delta \simeq 0.006867718$ where a Neimark-Sacker bifurcation occurs, in fact, there is a conjugate pair of complex multipliers with modulus equal to one. As the normal form coefficient is positive, a stable torus does not bifurcates from the cycle. After this point the cycle becomes unstable.

Before this limit cycle loses its stability, one found the coexistence of another stable periodic orbit for $\delta \lesssim 0.007373201$. The two periodic orbits can be seen in figure 4.2, projection onto the $u_4 - u_7$ space, being the new one the orbit with a eight shape. This phenomenon is called bistability, *i.e.*, there is a coexistence of two attractors for a given set of parameters. Depending the initial conditions belonging to the basin of attraction of one or other, depends where the asymptotic trajectories go.

When this new periodic orbits loses its stability which happens at $\delta \simeq 0.006727808$, by a Neimark-Sacker bifurcation with a negative normal form coefficient, a stable invariant torus type attractor bifurcates from the limit cycle. The improvement on the accuracy of the calculation of the largest Lyapunov exponent, shows that the largest Lyapunov exponent for this new attractor is compatible with zero. Figure 4.3 and 4.4 show for $\delta = 0.0065$ and $\delta = 0.0061$ respectively, the attractor and a Poincaré map projected onto different coordinates. Figure shows the same for . The Poincaré maps are

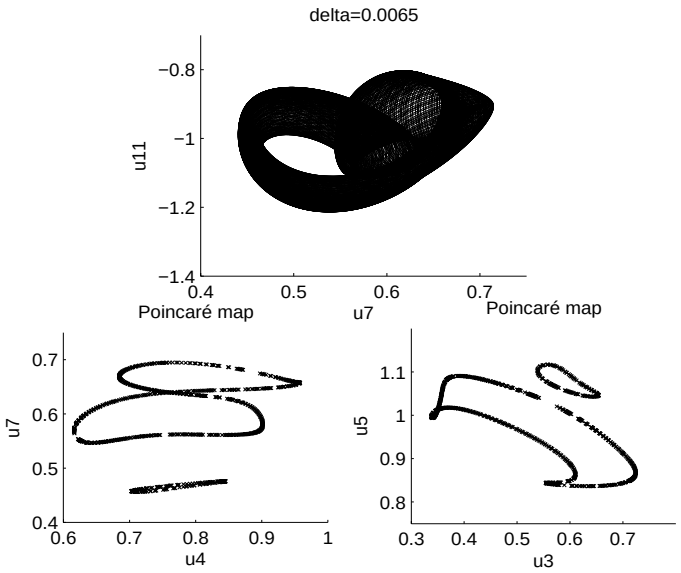

Fig. 4.3: $N = 16$. The attractor for $\delta = 0.0065$ and a Poincaré map projected onto different coordinates.

compatible with the attractor to be a torus type. The Poincaré maps have been computed by allowing an error less than 10^{-6} between any point of the orbit and the hyperplane orthogonal to a vector defined by two close points on the attractor.

With the variation of the parameter of the system δ, the orbit structure appears to change, resulting in a system topologically nonequivalent. Hence, for lower values of $\delta \lesssim 0.00603$, the orbits of the system seem to start loosing its density, which appears to indicate that the system begins to generate long period cycles instead of dense orbits. This bifurcation from quasiperiodic motions to periodic ones is called a phase locking [172]. Figure 4.5 shows a possible long period cycle for $\delta = 0.006015$. This attractor looses its stability for lower values of δ and disappears for a value of $\delta \simeq 0.006$.

Another phenomenon of bistability is observed for some values of $\delta \lesssim 0.006409616$, where a new asymptotically stable periodic orbit is observed as it can be seen in figure 4.6. For values of $\delta \lesssim 0.005801757$ this periodic orbit loses its stability by a Neimark-Sacker bifurcation.

Another periodic orbit, with approximately the triple of the period of this last one, is present for values of $0.00583 \lesssim \delta \lesssim 0.00585$, and so, another phenomenon of bistability of two periodic orbits can be observed. For lower values, $\delta \lesssim 0.00583$, and also by a Neimark-Sacker bifurcation, this limit cycle looses its stability, and a stable torus type attractor arises. Lowering δ,

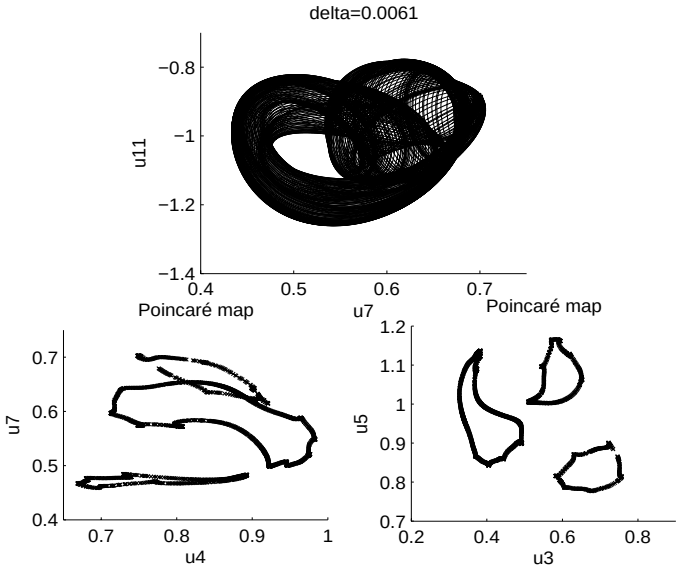

Fig. 4.4: $N = 16$. The attractor for $\delta = 0.0061$ and a Poincaré map projected onto different coordinates.

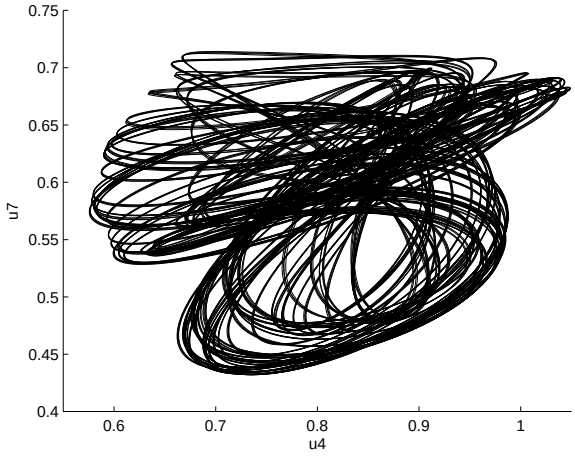

Fig. 4.5: $N = 16$. The attractor, for $\delta = 0.006015$, projected onto the $u4 - u7$ space.

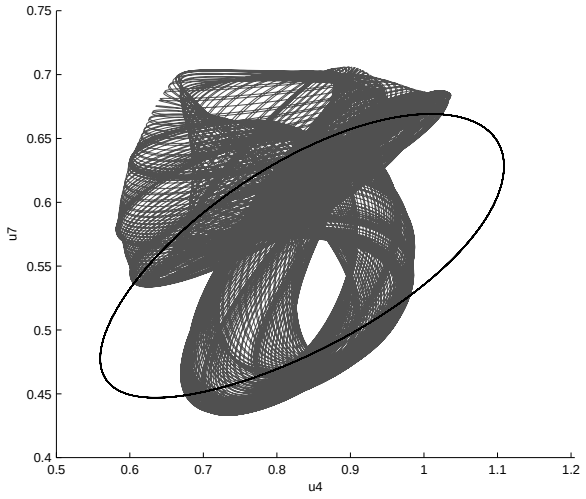

Fig. 4.6: $N = 16$. Bistability for $\delta = 0.0061$, with a periodic orbit and a torus type attractor.

the attractor appears to pass over a periodic orbit of long period that gives rise to a strange chaotic attractor for values of $\delta \lesssim 0.00579$, evidenced by a positive largest Lyapunov exponent. This progression can be seen in figures 4.7 to 4.10.

Figure 4.11 shows the resume of the dynamics described above.

- *Dynamics for N=17*

In this case the Dirichlet problem admits an even number of degrees of freedom. Figure 4.12 shows the equilibrium solutions as a function of u_7. The bold segments represent the stable critical solutions.

Decreasing the value of δ, a supercritical Hopf bifurcation takes place at $\delta_H \simeq 0.0065513413$ and simultaneously the stable asymptotic solution loses its stability, and a stable periodic orbit appears. The period of such orbit at the onset of the bifurcation is around 1.0326709. Eventually, the limit cycle arising from the Hopf bifurcation loses its stability at $\delta \simeq 0.004665232$ by means of a branch point cycle.

The coexistence of another stable periodic orbit is found for $\delta \lesssim 0.006089687$. The two periodic orbits can be seen in figure 4.13, projection onto the $u_4 - u_7$ space, being the new one depicted at bold. A Neimark-Sacker bifurcation takes place at a value of δ around 0.0048780813 and this new periodic orbit loses its stability. As the normal form coefficient is negative a stable

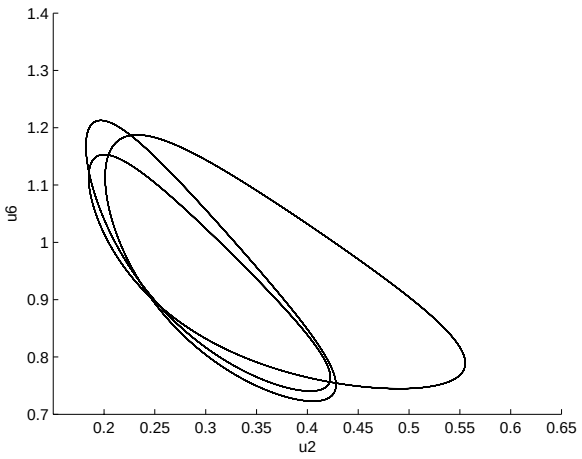

Fig. 4.7: $N = 16$. A periodic attractor for $\delta = 0.00584$, projected onto the $u2 - u6$ space.

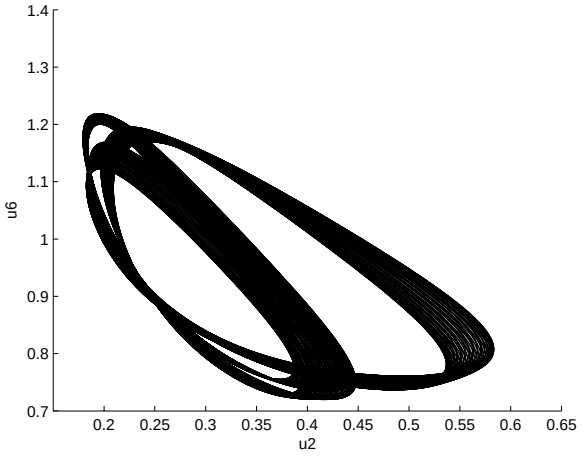

Fig. 4.8: $N = 16$. A torus type attractor for $\delta = 0.00582$, projected onto the $u2 - u6$ space.

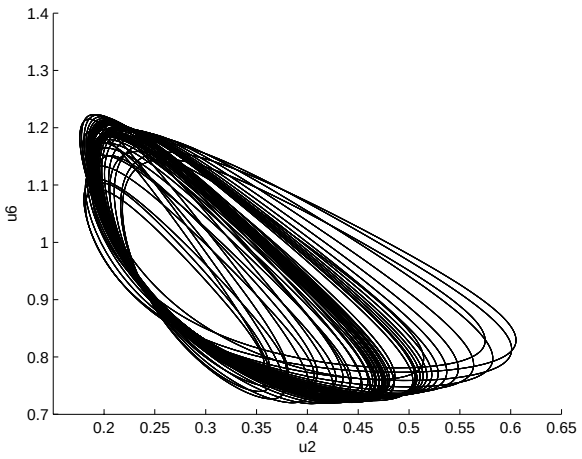

Fig. 4.9: $N = 16$. A likely long periodic attractor for $\delta = 0.00580$, projected onto the $u2 - u6$ space.

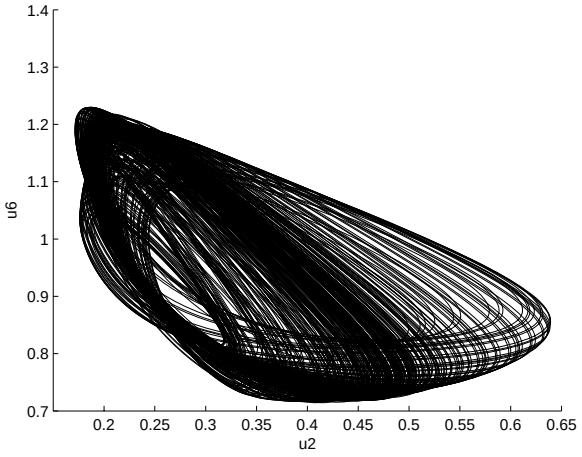

Fig. 4.10: $N = 16$. Chaotic attractor for $\delta = 0.00577$, projected onto the $u2 - u6$ space. The large Lyapunov exponent is ≈ 0.132.

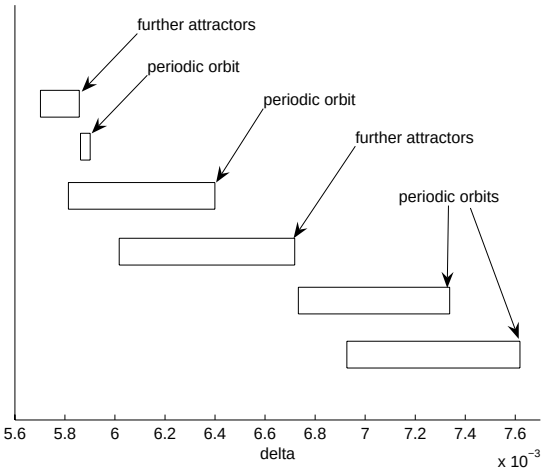

Fig. 4.11: Resume for the dynamics for $N = 16$.

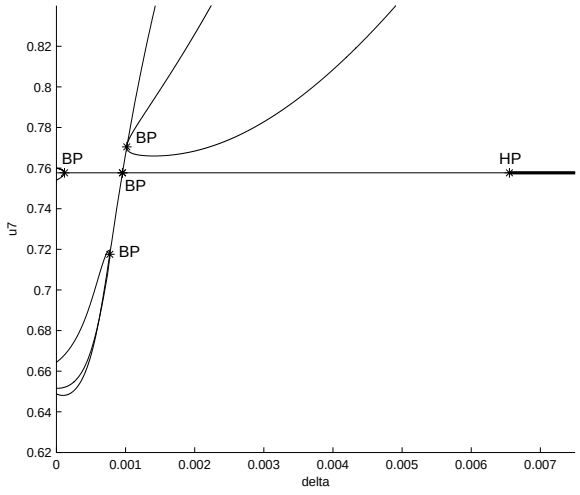

Fig. 4.12: Equilibrium solutions for Chebyshev spectral solution of Burgers equation for $N = 17$. HP represents the point where the Hopf Bifurcation takes place. BP represents a branch point. The bold segments represent the stable solutions.

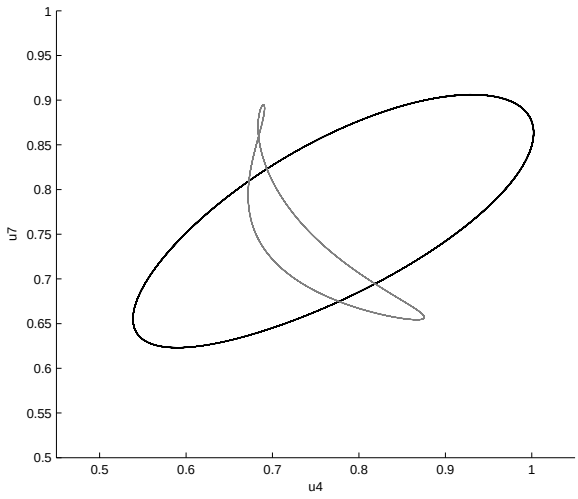

Fig. 4.13: $N = 17$. Bistability for $\delta = 0.0054$, with two stable periodic orbits.

torus type attractor emerges. Lowering δ, the maximum Lyapunov exponent keeps compatible with the nil value, becoming only positive for values of $\delta \lesssim 0.00473$, before loosing stability for a value of δ around 0.00468. Hence, other phenomena of bistability can be observed, where the limit cycle arose from Hopf bifurcation has not yet lost its stability, and so, a torus type attractor coexist with a stable periodic orbit and a chaotic one with a stable periodic one, as it can be seen in figure 4.14.

As already described, the limit cycle arising from Hopf bifurcation loses its stability at $\delta \simeq 0.004665232$, a branching point cycle, bifurcating into two stable limit cycles. Figure 4.15 show these two periodic orbits for $\delta = 0.00465$. For lower values of $\delta \simeq 0.004639949$, these two periodic orbits lose their stability by a period doubling bifurcation and a new strange attractor witharises with a particular behavior in phase space. Its motion approaches and leaves the unstable saddle periodic orbits, jumping between them. This behavior can be seen in figure 4.16 where different visualizations over different short periods of time are displayed, so that the trajectories can be distinguished in the phase space.

Figure 4.17 shows the resume of the dynamics described.

- *Dynamics for N=50 and N=51*

For the cases of $N = 50$ *and* $N = 51$ the equilibrium solutions found are presented in figures 4.18 and 4.19, respectively.

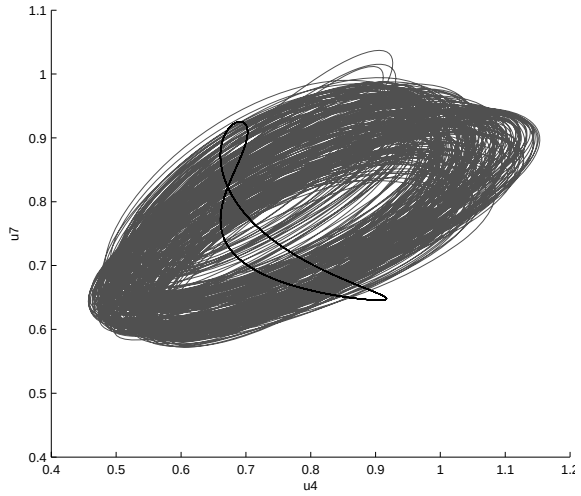

Fig. 4.14: $N = 17$. Bistability for $\delta = 0.0047$, with a periodic stable attractor and a strange chaotic one.

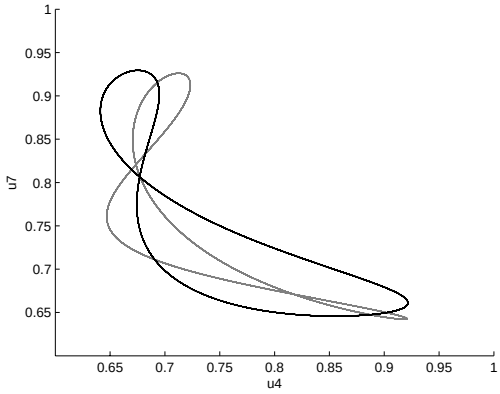

Fig. 4.15: $N = 17$. Bistability for $\delta = 0.00465$, with two stable periodic orbits.

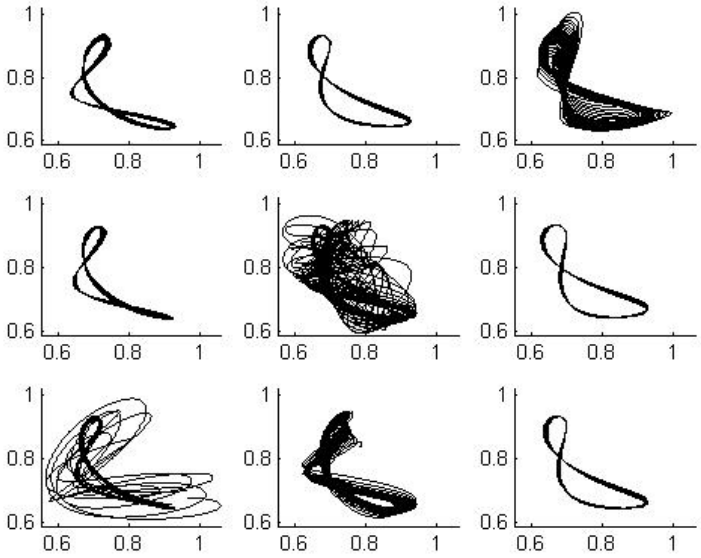

Fig. 4.16: $N = 17$. Strange attractor projected onto the $u4 - u7$ space, over different short periods of time, for $\delta = 0.0046$.

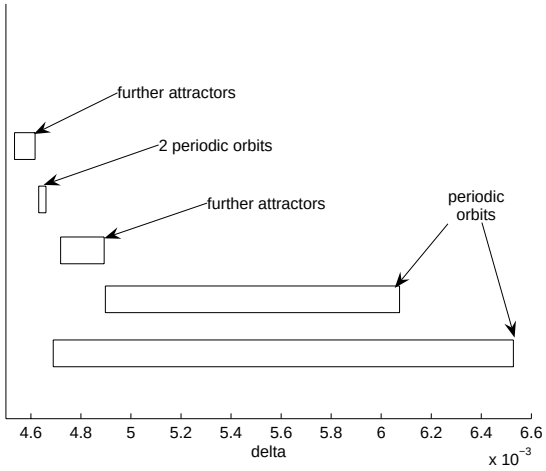

Fig. 4.17: Resume for $N = 17$.

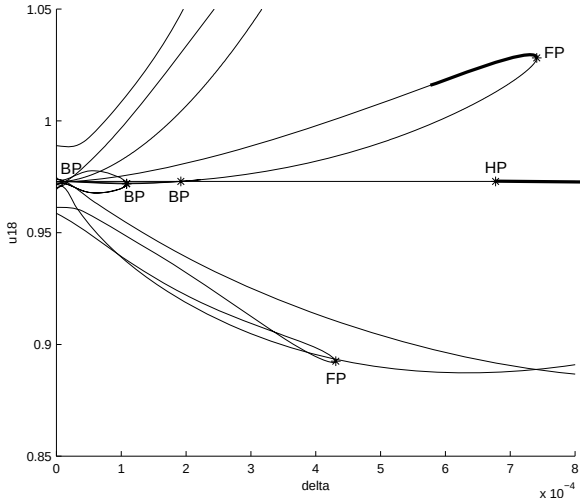

Fig. 4.18: Equilibrium solutions for Chebyshev spectral solution of Burgers equation for $N = 50$. HP represents the point where the Hopf Bifurcation takes place. BP represents a branch point. FP represents a fold point. The bold segments represent the stable solutions.

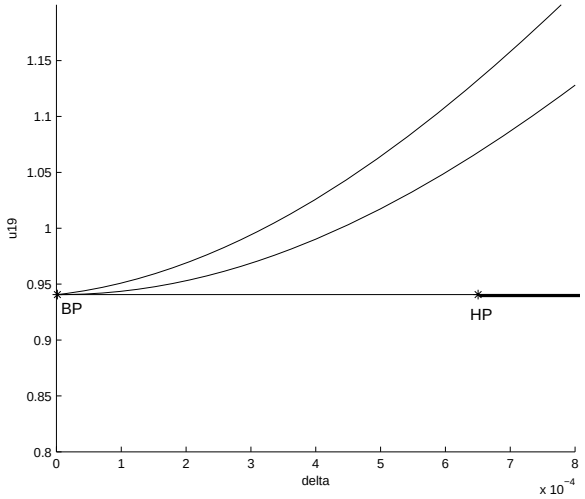

Fig. 4.19: Equilibrium solutions for Chebyshev spectral solution of Burgers equation for $N = 51$. HP represents the point where the Hopf Bifurcation takes place. BP represents a branch point. The bold segments represent the stable solutions.

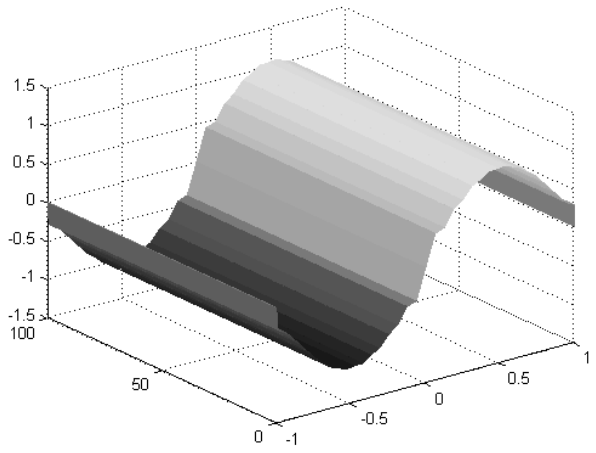

Fig. 4.20: For $N = 50$, a spurious solution for $\delta = 0.0007$, a value for the viscosity above the value for the Hopf bifurcation.

Observing these figures, one must emphasize the existence, for $N = 50$, of equilibrium points asymptotically stable not corresponding to the asymptotic solution of Burgers equation. These points are marked on bold in figure 4.18. These stable equilibrium points appear for values of δ before and after the Hopf bifurcation has occurred. If one could think that for values of δ greater than the one at which the Hopf bifurcation occurs no spurious solution would appear, this example shows the opposite. As an example of one of these stable equilibrium for a value of δ greater than the one corresponding to the Hopf bifurcation, figure 4.20 shows the spurious solution for $\delta = 0.0007$ and for the following initial condition satisfying the symmetry $u_i = -u_{N-i}$, $0 \leq i \leq N$:

$u_0(1) = 0.120007$ $u_0(2) = 0.290866$ $u_0(3) = 0.304056$
$u_0(4) = 0.322525$ $u_0(5) = 0.333680$ $u_0(6) = 0.375896$
$u_0(7) = 0.415379$ $u_0(8) = 0.487166$ $u_0(9) = 0.551368$
$u_0(10) = 0.643676$ $u_0(11) = 0.718378$ $u_0(12) = 0.814980$
$u_0(13) = 0.881280$ $u_0(14) = 0.962716$ $u_0(15) = 0.999279$
$u_0(16) = 1.045659$ $u_0(17) = 1.032028$ $u_0(18) = 1.028031$
$u_0(19) = 0.949750$ $u_0(20) = 0.891824$ $u_0(21) = 0.745570$
$u_0(22) = 0.652637$ $u_0(23) = 0.449124$ $u_0(24) = 0.405714$

As for the previous cases, for these values of N, a supercritical Hopf bifurcation also takes place and a stable periodic orbit emerges. For both cases there is a value of the parameter δ where the limit cycle loses its stability by a Neimark-Sacker bifurcation and where a new stable attractor comes out.

Keeping the decrease of the value of δ, other bifurcations occur and new stable attractors arise. This behavior drives to new phenomena of bistability where, besides the ones already described, a new one of bistability with two nonperiodic attractors is observed for both cases. Besides the stable periodic attractors well identified, other attractors are found. As in the previous cases, the improvement in the calculation of the largest Lyapunov exponent shows that this value is compatible with the zero value for the cases studied. This fact, together with the observation of the orbits and the calculation of Poincaré diagrams indicate that the majority of these attractors seem to be of the torus type nonchaotic. Moreover it seems that the system can also generate long periodic cycles instead of dense orbits. However, the presence of strange attractors, among those attractors, should not be excluded. It is also possible, that for some values of the parameter δ, the largest Lyapunov may be positive, or compatible with the nil value, but in finite periods with the maximum exponent Lyapunov positive. This last case would suggest a strange nonchaotic attractor (SNA). The fundamental property of a strange nonchaotic attractor (SNA) is the existence of regions in phase space where there is a finite probability for the maximum exponent Lyapunov to be temporally positive, although possessing an asymptotic nonpositive largest Lyapunov exponent. This exponent can be regarded as the weighted sum of the temporally positive exponent when the orbit is in expanding regions and the temporally negative exponent when the orbit is in contracting regions [265]. To completely identify all those attractors, further investigations are needed.

Figure 4.21 shows, for $\delta = 0.00062$, the attractor and a Poincaré map projected onto different coordinates. As before, the Poincaré maps have been computed by allowing an error below 10^{-6} between any point of the orbit and the hyperplane orthogonal to a vector defined by two close points on the attractor.

Figure 4.22 shows for $N = 50$ and $\delta = 0.000648$ a situation of bistability with a periodic stable attractor and a torus type one. Figure 4.23 shows for $N = 51$ and $\delta = 0.00057$ another similar situation of bistability.

Figures 4.24 and 4.25 show the scheme of the dynamics observed.

For the case $N = 50$, as referred above, there are stable equilibrium not corresponding to the asymptotic solution of Burgers equation (4.18). Between the fold point at δ around 0.000740995 and an Hopf bifurcation occurring at δ around 0.000578 there is a branch of stable equilibria. After this new Hopf point, not corresponding to the asymptotic equilibrium, keeping the decrease of δ, a stable periodic orbit arises followed by its loss of stability at $\delta \simeq 0.000572$ by a Neimark-Sacker bifurcation and by the appearance of a torus type attractor. These part of the dynamics is not represented in figure

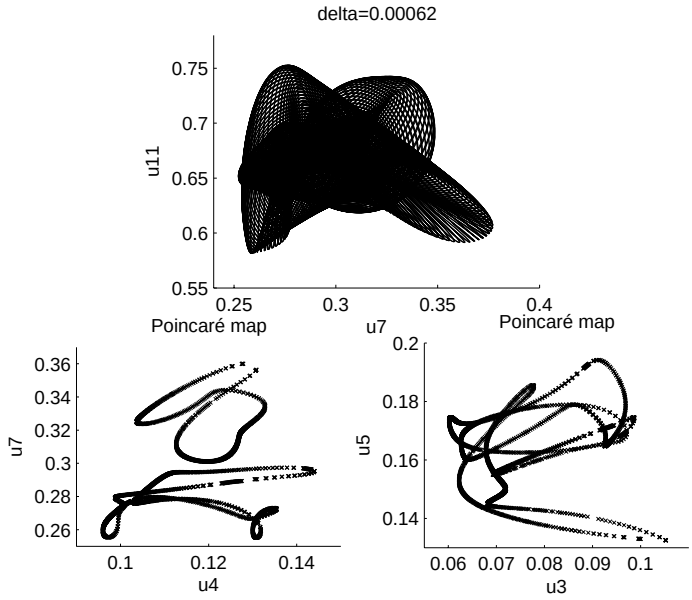

Fig. 4.21: $N = 50$. The attractor for $\delta = 0.00062$ and a Poincaré map projected onto different coordinates.

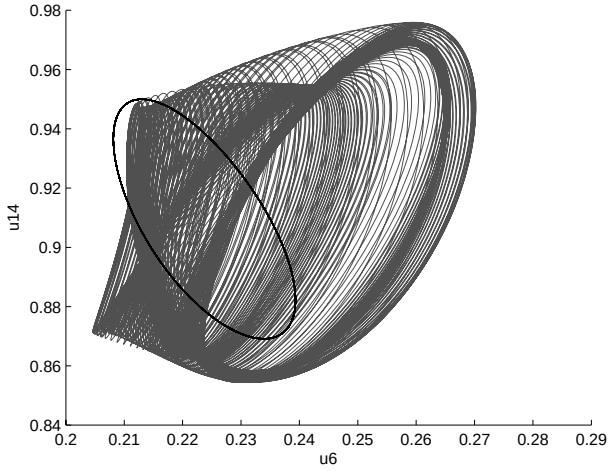

Fig. 4.22: $N = 50$. Bistability for $\delta = 0.000648$.

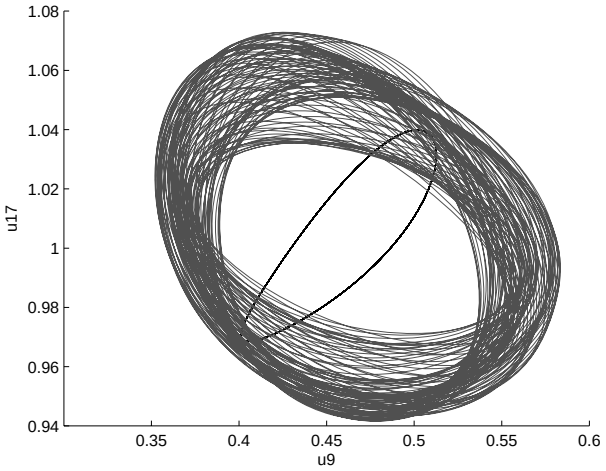

Fig. 4.23: $N = 51$. Bistability for $\delta = 0.00057$.

4.18.

4.4.2 Discussion

Next, it will be discussed which conditions facilitate the spectral solutions of Burgers equation to behave as described above. To perform it some others simulations for another examples are made. However, it seems clear that the loss of stability of the asymptotic solution must occur by means of a supercritical Hopf bifurcation and not by a subcritical Hopf bifurcation or by a change of the signal of a real eigenvalue of the jacobian, so that stable limit cycles can emerge. Also, the torus type attractors seem to appear mainly due to the loss of stability of the periodic solutions by Neimark-Sacker bifurcations.

Let one begin by discussing the forced Burgers equation of the example studied, equation (4.18), with $f(x) = \pi \sin(\pi x)[\cos(\pi x) + \delta\pi]$. In this case f is odd, which means that for Chebyshev and Fourier spectral solutions, there is an invariant transformation of coordinates $T : u_i \rightsquigarrow -u_{N-i}$, $i = 0, ..., N$. In other words, the evolution equations for u_i and $-u_{N-i}$ are invariant under T, $\frac{du_i}{dt} = -\frac{du_{N-i}}{dt}$, with the respectively invariant subspace given by

$$u_i = -u_{N-i}, \quad 0 \leq i \leq N \tag{4.20}$$

Hence, the orbits arising from all the initial conditions satisfying (4.20) do not leave that subspace.

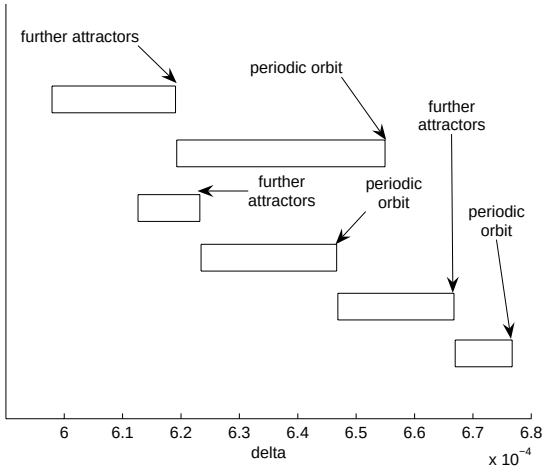

Fig. 4.24: Dynamics for $N = 50$.

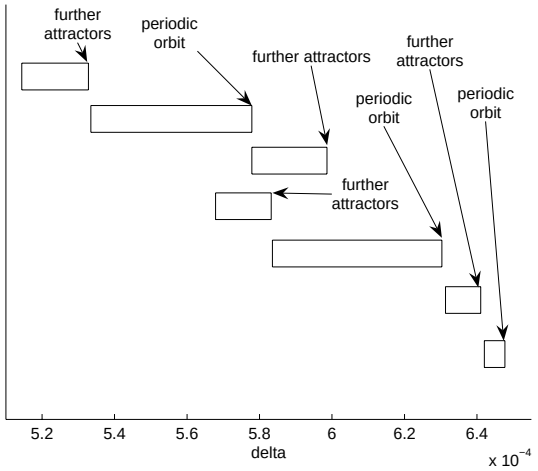

Fig. 4.25: Dynamics for $N = 51$.

The Chebyshev differentiation matrix $D^{(1)}$ satisfies the antisymmetric condition $\left(D^{(1)}\right)_{i,j} = -\left(D^{(1)}\right)_{N-i,N-j}$ [255]. To compute the second derivative one can square $D^{(1)}$, which costs $O\left(N^3\right)$ floating point operations or, alternatively, by explicit formulas or recurrences [296], which may cost only $O\left(N^2\right)$ floating point operations. For Chebyshev spectral solution, one has for $1 \leq i \leq N-1$:

$$\begin{aligned}
\frac{du_i}{dt} =& - u_i D_i^{(1)} u + \delta D_i^{(2)} u + f\left(x_i\right) = \\
=& - u_i \sum_{j=0}^{N} \left(D^{(1)}\right)_{i,j} u_j + \delta \sum_{j=0}^{N} \left(D^{(2)}\right)_{i,j} u_j + f\left(x_i\right) = \\
=& u_{N-i} \sum_{j=0}^{N} \left(-D^{(1)}\right)_{N-i,N-j} \left(-u_{N-j}\right) + \\
&+ \delta \sum_{j=0}^{N} \left(\sum_{j=0}^{N} \left(D^{(1)}\right)_{N-i,N-k} \left(D^{(1)}\right)_{N-k,N-j} \right) \left(-u_{N-j}\right) - f\left(x_{N-i}\right) = \\
=& u_{N-i} \sum_{j=0}^{N} \left(D^{(1)}\right)_{N-i,j} u_j - \delta \sum_{j=0}^{N} \left(D^{(2)}\right)_{N-i,j} u_j - f\left(x_{N-i}\right) = -\frac{du_{N-i}}{dt}
\end{aligned} \tag{4.21}$$

For the Fourier spectral differentiation matrices, the relation $D^{(m)} = \left(D^{(1)}\right)^m$ holds for N odd or it can held for N even when m is odd. The formulae can be consulted in [296] [255].

For N even, $0 \leq i \leq N-1$, one has:

$$\begin{aligned}
\frac{du_i}{dt} =& - u_i D_i^{(1)} u + \delta D_i^{(2)} u + f\left(x_i\right) \\
=& - u_i \sum_{j=0}^{N-1} \left(D^{(1)}\right)_{i,j} u_j + \delta \sum_{j=0}^{N-1} \left(D^{(2)}\right)_{i,j} u_j + f\left(x_i\right) = \\
=& u_{N-i} \sum_{j=0, i\neq j}^{N-1} \frac{1}{2} (-1)^{i-j} \cot\left(\frac{(j-i)\,\pi}{N}\right) u_{N-j} \\
& - \delta \left[\sum_{j=0, i\neq j}^{N-1} \frac{1}{2} (-1)^{i-j+1} \csc^2\left(\frac{(i-j)\,\pi}{N}\right) u_{N-j} \right. \\
& \left. - \frac{N^2}{12} u_{N-i} - \frac{1}{6} u_{N-i} \right] - f\left(x_{N-i}\right) = \\
=& u_{N-i} \sum_{j=0, i\neq N-1-j}^{N-1} \frac{1}{2} (-1)^{i-(N-1-j)} \cot\left(\frac{(N-1-j-i)\,\pi}{N}\right) u_{N-(N-1-j)} \\
& - \delta \left[\sum_{j=0, i\neq N-1-j}^{N-1} \frac{1}{2} (-1)^{i-(N-1-j)+1} \csc^2\left(\frac{(i-(N-1-j))\,\pi}{N}\right) u_{N-(N-1-j)} \right. \\
& \left. - \frac{N^2}{12} u_{N-i} - \frac{1}{6} u_{N-i} \right] - f\left(x_{N-i}\right) = \\
=& u_{N-i} \sum_{j=0, N-i\neq j+1}^{N-1} \frac{1}{2} (-1)^{(N-i)-(j+1)} \cot\left(\frac{[N-i-j-1]\,\pi}{N}\right) u_{j+1} \\
& - \delta \left[\sum_{j=0, N-i\neq j+1}^{N-1} \frac{1}{2} (-1)^{(N-i)-(j+1)+1} \csc^2\left(\frac{(N-i-j-1)\,\pi}{N}\right) u_{j+1} \right. \\
& \left. - \frac{N^2}{12} u_{N-i} - \frac{1}{6} u_{N-i} \right] - f\left(x_{N-i}\right) = -\frac{du_{N-i}}{dt}
\end{aligned} \tag{4.22}$$

For N odd the result $\frac{du_i}{dt} = -\frac{du_{N-i}}{dt}$ is also easily verified.

One can see that, the example studied, being invariant under T, is a dynamical system with symmetry. Multistability is frequently observed in dynamical systems with symmetry [173] [106] [104], but the symmetry does not explain the bistability observed. Additionally, in this case, symmetry does not even facilitate the appearance of bistability, which could be the case for the example worked out in the previous subsection when there was an even number of degrees of freedom, where the symmetry was somehow broken and the motion was not restricted to the invariant subspace. As

explained below, the bistability observed did not emerged from this break of symmetry.

If there is an asymptotic stable solution, such as a limit cycle, a torus type or a strange attractor, the invariant transformation T must apply the initial conditions belonging to its basin of attraction into a second set of initial conditions, symmetric to the first one and belonging to a basin of attraction of a second symmetric asymptotic stable solution. Suppose that $f_1 = f$ is any function of equation (4.19). Consider a second Chebyshev discretized equation for the Dirichlet problem with homogeneous boundary conditions, given by adding a second set of $N-1$ equations with $f_2 = f$ in equation (4.19) being a function obtained by substituting $f_1(x_i)$ by $-f_1(x_{N-i})$. Therefore, one arrives to the relation $f_2(x_i) = -f_1(x_{N-i})$ and gets one set of equations with twice the equations, constituted by the union of the two following set of equations:

$$\frac{du_i}{dt} = -u_i D^{(1)} u + \delta D^{(2)} u + f_1(x_i), \quad 0 \leq i \leq N \tag{4.23}$$

$$\frac{dv_i}{dt} = -v_i D^{(1)} v + \delta D^{(2)} v + f_2(x_i), \quad 0 \leq i \leq N \tag{4.24}$$

The transformation $H : u_i \rightarrow -v_{N-i}$, $i = 0, ..., N$, is invariant for this new set of $2N-2$ equations:

$$\begin{aligned}\frac{du_i}{dt} =& - u_i D_i^{(1)} u + \delta D_i^{(2)} u + f_1(x_i) = \\ =& v_{N-i} \sum_{j=0}^{N} \left(D^{(1)}\right)_{N-i,j} v_j - \delta \sum_{j=0}^{N} \left(D^{(2)}\right)_{N-i,j} v_j - f_2(x_{N-i}) = -\frac{dv_{N-i}}{dt}\end{aligned} \tag{4.25}$$

One can conclude that all the asymptotic stable solutions, such as limit cycles, the torus type or the strange attractors observed for the first set of equations (4.23) must have the corresponding identical symmetric attractor for the second set of equations (4.24). In other words, if one finds an asymptotic stable attractor for the Chebyshev solution of Burgers equation (4.18), one has also to find a symmetric one for the same equation by substituting $f(x)$ by $-f(-x)$. This enlarges the set of functions f where all the phenomena described above could be observed.

For the example studied, the function f is an odd function, $f(x) = -f(-x)$, and due to that, for attractors possessing the symmetry propriety, no other symmetric attractor has to show up. The possible exceptions arise if the symmetry is broken, and as referred above, this is the case when N is odd and there is an even number of degrees of freedom. In these cases, where

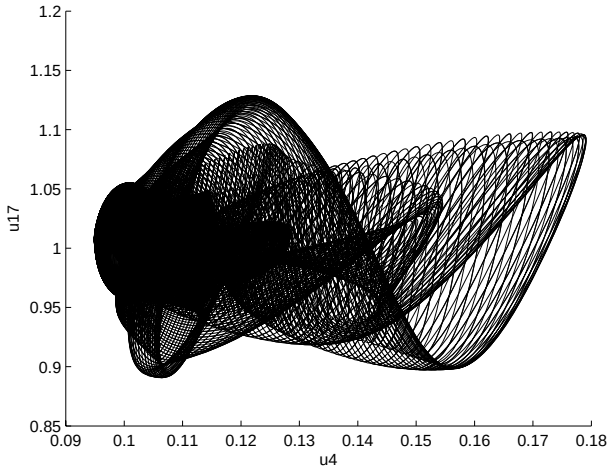

Fig. 4.26: $N = 50$. Attractor for $\delta = 0.000615$.

the asymptotic attractor breaks the symmetric property, new symmetric attractors should appear. This is not the case, because although the motion is no longer restricted to the invariant subspace, looking to the attractor as an entire entity, the symmetry is preserved. To see that, let one consider an asymptotic stable attractor A. If $p \in A$ is a point belonging to A with coordinates $p \curvearrowright (0, u_1, \ldots, u_i, \ldots, u_{N-i}, \ldots, u_{N-1}, 0)$, then the symmetric point $q \curvearrowright (0, -u_{N-1}, \ldots, -u_{N-i}, \ldots, -u_i, \ldots, -u_1, 0)$ also belongs to A for the example studied. If the motion is restricted to the invariant subspace, then p must be equal to q. If not, and q does not belong to A, then the symmetric point q has to evolve to a symmetric attractor of A, which does not happen. Both points p and q belong to A. This can be shown by the superposition of the attractors with initial conditions p and q or by superposition of the symmetric images for $x > 0$ and $x < 0$. The plots of symmetric points when the motion is inside the attractor also show this. Figure 4.26 shows an attractor for $N = 50$ and $\delta = 0.000615$ and figure 4.27 shows that its motion is made without leaving the invariant subspace, while figure 4.28 shows an attractor for $N = 51$ and $\delta = 0.00059$ and figure 4.29 shows that its motion is not restricted to the invariant subspace but, globally, the attractor preserves the symmetry. Everything occurs as the the dynamics for $x > 0$ and the one for $x < 0$ evolve in a symmetric manner but with a time delay.

To further investigate the dynamical behavior of spectral discretization of Burgers equation, more studies are made involving different functions f. It is known that for low values of the viscosity coefficient, Burgers equation can

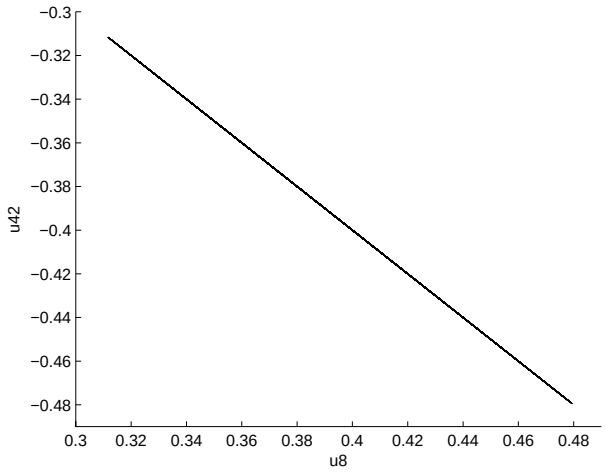

Fig. 4.27: $N = 50$. Attractor in symmetric coordinates, for $\delta = 0.000615$.

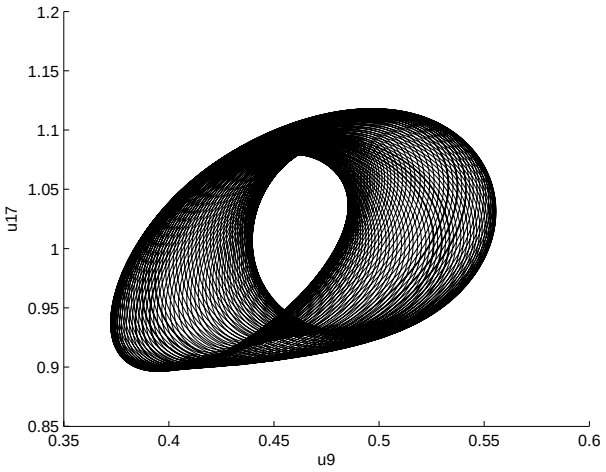

Fig. 4.28: $N = 51$. Attractor for $\delta = 0.00059$.

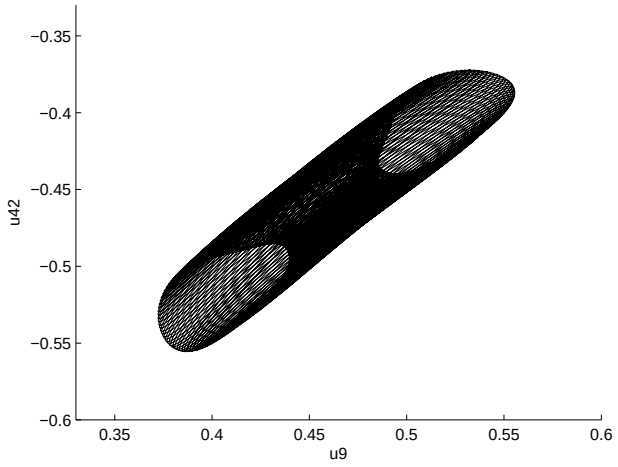

Fig. 4.29: $N = 51$. Attractor in symmetric coordinates, for $\delta = 0.00059$.

develop sharp discontinuities, which are difficult to simulate numerically. Oscillations can occur by discretization through spectral collocation methods, due to Gibbs phenomenon. The Gibbs phenomenon occurs at simple discontinuities, and is an overshoot with large oscillations, near the endpoints of the jump discontinuity, exhibited by the partial sums S_n of an eigenfunction series. With an increase of n, number of terms of the series approximation, the amplitude of the overshoot will not diminish, occurring only over smaller intervals. It can be removed with the Lanczos sigma factor. At low viscosity, the tendency for Burgers equation to develop discontinuities, together with these oscillations, must be responsible to this dynamic behavior. But although necessary, it is evident that it can not be a sufficient condition because, otherwise, it would be a common phenomenon. Burgers equation is a wave nonlinear equation where the convection u is active since it depends on the solution of the equation. As the speed of the wave is given by the solution itself, it increases when u increases and decreases when u decreases. The higher points of the nonlinear wave will travel at a higher speed and shocks and discontinuities for low values of δ will tend to appear in the intervals where u is decreasing. The instabilities observed in the forced Burgers equation will then tend to appear first at intervals where the asymptotic solution is decreasing, which are, for the example studied above with an asymptotic solution given by $u(x,t) = \sin(\pi x)$, the intervals $(-1, 0.5)$ and $(0.5, 1)$. These branches of the solution are the ones that are fixed by one extremity to each fixed boundary for the Dirichlet problem. By numerically studying several

examples, one argues that this fact, together with the nonexistence of such branches where discontinuities tend to appear not fixed to the boundaries, is a necessary condition to keep the asymptotic equilibrium solution stable for lower values of δ. Consequently, this gives time for the first loss of stability to be signed by the emergency of a supercritical Hopf bifurcation. Intervals where the asymptotic solution is decreasing and are not fixed to any of the boundaries lead to a lost of stability of the asymptotic equilibrium solution for higher values of δ, by means of a real eighenvalue becoming positive and not by an Hopf bifurcation. In these cases, supercritical Hopf bifurcations and the followers stable limit cycles for lower values of the parameter δ were observed, but for an equilibrium not belonging to the asymptotic solution.

To show this, several function f for equation (4.18) are then studied.

Consider Burgers equation (4.18) with $f(x) = 3x^5 - 4x^3 + (6\delta + 1)x$, so an asymptotic solution is given by $u(x,t) = x - x^3$. This example is similar to the one studied in terms of monotony and symmetry of the asymptotic solution. The discretized Dirichlet problem with homogeneous boundary conditions (4.19) has also a rich behavior. For example, for $N = 16$, the supercritical Hopf bifurcation takes place at $\delta \simeq 0.002281352$, where a stable limit cycle emerges with a period around 1.3490472 at the onset of the bifurcation. For lower values of the parameter, at $\delta \simeq 0.002243689$, a period doubling bifurcation takes place with the emerging of a stable periodic solution with twice its period. For even lower values of δ, for $0.0019895707 \lesssim \delta \lesssim 0.0021712447$, a stable period orbit is present with a period similar to the one of the cycles arising from the Hopf bifurcation. At $\delta \simeq 0.0021712447$, a period doubling bifurcation takes place. Therefore, from the Hopf point, decreasing δ, the cycle double its period and keeping decreasing δ it retakes approximately its original period. Eventually, for $\delta \simeq 0.0019895707$ the periodic orbit looses its stability by a Neimark-Sacker bifurcation with a negative normal form coefficient, which drives the appearance of a stable torus type attractor.

For the cases where the asymptotic solution is symmetric, related to the x-axis, for the previous two examples, which means that the asymptotic solutions are $u(x,t) = -\sin(\pi x)$ and $u(x,t) = -x + x^3$, the descendent branches of the solution are no longer fixed to the boundaries, and the asymptotic solutions loose their stability at a value more than ten folder higher the previous value of δ. No attractors, limit cycles, torus type or strange ones, were found for these cases.

To increase the height of the waves of the asymptotic solution, consider the case where $f(x) = \alpha\pi \sin(\pi x)[\alpha \cos(\pi x) + \delta\pi]$, so an asymptotic solution is given by $u(x,t) = \alpha \sin(\pi x)$. The solution is still odd, so the function f is odd too and the symmetry is present in the system. The only difference

between this case and the first example studied is the asymptotic solution multiplied by a factor α. In this example the waves are higher, the path where the solution may develop discontinuities has increased and equally do the instabilities. To corroborate the theory exposed, it is expected a loss of stability for the asymptotic solution to occur at higher values of δ. Not only this happened, but also a linear relation could be established between the value of δ corresponding to the point where the asymptotic equilibrium looses its stability and the absolute value of α. So, for $\alpha > 0$, a Hopf bifurcation related to the asymptotic solution occurs for a value of δ satisfying approximately the linear equation $HP(\alpha) = |\alpha| HP(1)$, where $HP(1)$ is the value of δ at the Hopf point for the first example studied and $HP(\alpha)$ the the value of δ at the Hopf point for the new example. For $\alpha < 0$ a similar relation helds for the value of δ corresponding to the loss of stability of the asymptotic solution.

Consider now an increase on the frequency of the nonlinear waves, with $f(x) = \alpha\pi \sin(\alpha\pi x)[\cos(\alpha\pi x) + \alpha\delta\pi]$, so an asymptotic solution is given by $u(x,t) = \sin(\alpha\pi x)$, $\alpha \in \mathbb{Z}\backslash\{-1,0,1\}$. The function f is odd, so the symmetry is kept present in the system. Due to the presence of decreasing intervals in the asymptotic solution not fixed to boundaries, it is expected a loss of the asymptotic equilibrium for higher values of δ by one real eigenvalue. This is what really happens and so, around asymptotic equilibrium, no periodic, torus type or strange attractors are observed. However, other stable equilibria are observed and, for those equilibria, supercritical Hopf bifurcations are also observed with the corresponding periodic orbits. The stable attractors found break the symmetry of the system and new symmetric attractors arise, leading to the presence of bistability. Figure 4.30 shows two periodic orbits for $\alpha = 2$, $\delta = 0.0363$ and $N = 16$, projected onto the space $u_3 - u_7$, and figure 4.31 shows the same two period attractors for symmetric points where the overall symmetry is patent. These periodic orbits loose their stability for δ around 0.03531646 by a Neimark-Sacker bifurcation with a normal form coefficient very slightly negative. No stable attractors were observed for lower values of the parameter δ.

The symmetry is not a necessary condition for the phenomena observed to show up, as shown by the next examples. Consider Burgers equation (4.18) with

$$\begin{aligned} f(x) = {} & e^{2x}\sin^2(\pi x) + \pi e^{2x}\sin(\pi x)\cos(\pi x) - \delta e^x \sin(\pi x) \\ & - 2\delta\pi e^x \cos(\pi x) + \delta\pi^2 e^x \sin(\pi x) \end{aligned} \tag{4.26}$$

In this case an asymptotic solution is given by $u(x,t) = e^x \sin(\pi x)$. It is clear that this is not an odd function and consequently the transformation

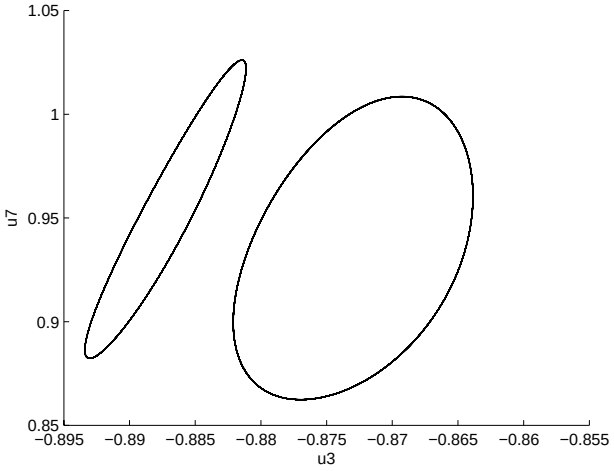

Fig. 4.30: Two stable periodic orbits for forced Burgers equation with asymptotic solution $u(x,t) = \sin(2\pi x)$, for $N = 16$ and $\delta = 0.0363$.

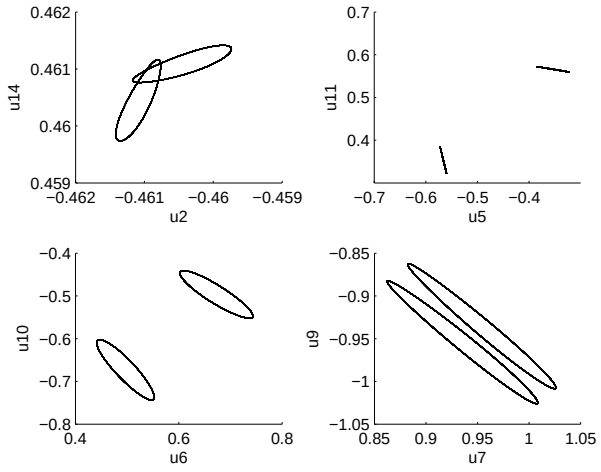

Fig. 4.31: Two symmetric stable periodic orbits for forced Burgers equation with asymptotic solution $u(x,t) = \sin(2\pi x)$, for $N = 16$ and $\delta = 0.0363$, viewed over symmetric coordinates.

T is no longer invariant. Although no symmetry is present in this example, a supercritical Hopf bifurcation takes place at $\delta \simeq 0.00753$. For lower values of $\delta \simeq 0.00740813$ the periodic orbit duplicates its period and for $\delta \simeq 0.00694054$ it looses its stability by a Neimark-Sacker bifurcation with a normal form coefficient positive. No other attractors were found for this case. Notice that the same behavior for symmetric coordinates must be present when

$$f(x) = -e^{-2x}\sin^2(\pi x) + \pi e^{-2x}\sin(\pi x)\cos(\pi x) - \delta e^{-x}\sin(\pi x) + 2\delta\pi e^{-x}\cos(\pi x) + \delta\pi^2 e^{-x}\sin(\pi x) \tag{4.27}$$

where an asymptotic solution is given by $u(x,t) = e^{-x}\sin(\pi x)$.

Another case without symmetry is that for

$$f(x) = \frac{\pi}{4}\cos\left(\frac{\pi x}{2}\right)\left(\delta\pi - 2\sin\left(\frac{\pi x}{2}\right)\right) \tag{4.28}$$

where an asymptotic solution is given by $u(x,t) = \cos\left(\frac{\pi x}{2}\right)$. In this case there is only one descent branch fixed to one boundary and an ascendent branch fixed to the other. The loss of stability of the asymptotic solution seems to be done by a subcritical Hopf bifurcation and no stable attractors were found.

All these examples show the importance of the descendent branches of the asymptotic solution to be fixed to the boundaries, so that a supercritical Hopf bifurcation, followed by periodic orbits and perhaps other attractors may arise. This is also supported by examples performed with Fourier spectral collocation where the solution is not fixed to boundaries and none of this phenomena was observed.

The previous studies yield the conclusions described below.

For Chebyshev spectral solutions of forced Burgers equation several phenomena and bifurcation can be observed for low values of the viscosity coefficient. Besides the attractors found by Dang-Vu and Delcarte [77], arising from the loss of stability of the periodic orbits arising themselves from Hopf bifurcations, other phenomena were observed: existence of other attractors, such as periodic orbits, torus type attractors and strange attractors. Bistability with the coexistence of two periodic attractors, a periodic and a non-periodic one (torus type or strange attractor), and even two nonperiodic attractors seeming to be quasiperiodic ones, were also observed.

For the examples where attractors possess the symmetry propriety, no other symmetric attractor has to show up. The possible exceptions arise when the symmetry is broken, and that is what occurred in some cases studied. In such cases, where the asymptotic attractor breaks the symmetric property,

new symmetric attractors could appear. One saw that these new attractors did not appear in some cases described, particularly when an asymptotic solution was given by $u(x,t) = \sin(\pi x)$ and there was an even number of degrees of freedom. The motion inside the attractors was no longer restricted to the invariant subspace but, looking to the attractor as an entire entity, the symmetry was preserved. Everything occurred as the dynamics evolve in a symmetric manner but with a time delay.

The instabilities observed in the forced Burgers equation tend to appear first at the intervals where the asymptotic solution is decreasing, since such intervals are the ones where the discontinuities will tend to emerge. These branches of the solution are the ones that are fixed by one extremity to each fixed boundary of the Dirichlet problem. By numerically studying several examples, one argued that the existence of these intervals fixed to the extremities, together with the nonexistence of similar decreasing intervals not fixed to the boundaries, was a necessary condition to keep the asymptotic equilibrium solution stable for lower values of δ, allowing the first loss of stability to be signed by the appearance of a supercritical Hopf bifurcation. Intervals where the asymptotic solution is decreasing and not fixed to any of the boundaries led to a lost of stability of the asymptotic equilibrium solution for higher values of δ, by means of a real eigenvalue turning positive and not by an Hopf bifurcation. In these cases, Hopf bifurcations and the followers stable limit cycles for lower values of the parameter δ were observed, but for equilibria not belonging to the asymptotic solution. The existence of only one interval where the asymptotic solution is decreasing and fixed to only one of the boundaries and the nonexistence of such decreasing intervals not fixed to any of the boundaries, led to the loss of stability for lower values of the viscosity coefficient but not by a supercritical Hopf bifurcation and no stable attractors were observed.

Also stable points were observed for values of the viscosity coefficient above the supercritical Hopf bifurcation, which means that spurious solutions can occur even when the value of viscosity coefficient did not suggest it.

5. SYNCHRONIZATION OF COUPLED BURGERS EQUATIONS

5.1 Dynamics in coupled Burgers equations

Many nonlinear phenomena are modeled by spatiotemporal systems of infinite or very high dimension, denominated as *spatially extended dynamical systems*. Coupling and synchronization of spatially extended dynamical systems is an area of present intensive research, concerning communications systems, chaos control, estimation of model parameters and model identifications. Besides synchronization of periodic signals which is a phenomenon already well-known, it has been shown in the literature that it is also possible to synchronize both low-dimensional chaotic dynamical systems and high-dimensional ones [166] [167] [168] [254].

To determine the threshold for chaos synchronization, the stability of the synchronized trajectories as a function of the coupling parameter has to be studied. Two most frequently used criteria for this study of stability are the Lyapunov functions and the transversal conditional Lyapunov exponents calculated from the linearized equations for the perturbations transversal to the synchronization manifold [99] [121] [227] [102]. Lyapunov functions for the vector field of perturbations transversal to the manifold generally allow one to prove stability and also that all trajectories in the phase space are attracted by the synchronization manifold. It is not a general method since there is no established procedure for constructing a Lyapunov function for an arbitrary system. In many practical cases, Lyapunov functions cannot be found, even for systems that possess a strong stable manifold of synchronized motions. Unlike Lyapunov functions, the calculation of the transversal Lyapunov exponents is quite simple, although the negativeness of all Lyapunov exponents do not guarantee the stability. The robustness of the identical synchronized manifold implies that small perturbations of the parameters of the coupled systems lead to small deviations from the identical oscillations.

In the next section sufficient conditions for identical synchronization of a linear coupling for both unidirectionally and bidirectionally coupled Burgers equation is discussed by means of a Lyapunov function. In the last section, the dynamics and synchronization of unidirectionally coupling of Chebyshev spectral solutions of Burgers equations, by means of a linear and nonlinear coupling, is described and discussed.

5.1.1 Coupled Burgers equations

Consider two unidirectionally coupled Burgers equations and a linear coupling between them for $a < x < b$:

$$\begin{aligned}\frac{\partial u}{\partial t} &= -u\frac{\partial u}{\partial x} + \delta\frac{\partial^2 u}{\partial x^2} \\ \frac{\partial v}{\partial t} &= -v\frac{\partial v}{\partial x} + \delta\frac{\partial^2 v}{\partial x^2} + \alpha\left(u - v\right)\end{aligned} \tag{5.1}$$

Lyapunov functions can help finding sufficient conditions for identical synchronization. For $w = (u - v)$, one gets equation (5.2)

$$\begin{aligned}\frac{\partial w}{\partial t} &= -\left(u\frac{\partial u}{\partial x} - v\frac{\partial v}{\partial x}\right) + \delta\frac{\partial^2 w}{\partial x^2} - \alpha w \\ &= -\left(u\frac{\partial u}{\partial x} - v\frac{\partial u}{\partial x} + v\frac{\partial u}{\partial x} - v\frac{\partial v}{\partial x}\right) + \delta\frac{\partial^2 w}{\partial x^2} - \alpha w \\ &= -\left(w\frac{\partial u}{\partial x} + v\frac{\partial w}{\partial x}\right) + \delta\frac{\partial^2 w}{\partial x^2} - \alpha w\end{aligned} \tag{5.2}$$

Consider the well known Lyapunov function:

$$V = \frac{1}{2}\int_a^b w^2 dx \tag{5.3}$$

By computing the time derivative of the Lyapunov function (5.3) one gets:

$$\begin{aligned}\dot{V} &= \int_a^b w\frac{\partial w}{\partial t}dx \\ &= \int_a^b w\left(-w\frac{\partial u}{\partial x} - v\frac{\partial w}{\partial x} + \delta\frac{\partial^2 w}{\partial x^2} - \alpha w\right)dx \\ &= -\int_a^b w^2\frac{\partial u}{\partial x}dx - \int_a^b vw\frac{\partial w}{\partial x}dx + \delta\int_a^b w\frac{\partial^2 w}{\partial x^2}dx - \int_a^b \alpha w^2 dx\end{aligned} \tag{5.4}$$

Computing the first and third integrals of equation (5.4) one obtains the two following equations:

$$\begin{aligned}\int_a^b w^2\frac{\partial u}{\partial x}dx &= \frac{1}{2}\int_a^b w^2\frac{\partial u}{\partial x}dx + \frac{1}{2}\int_a^b w^2\frac{\partial u}{\partial x}dx \\ &= \frac{1}{2}\,w^2 u\Big]_a^b - \int_a^b uw\frac{\partial w}{\partial x}dx + \frac{1}{2}\int_a^b w^2\frac{\partial u}{\partial x}dx\end{aligned} \tag{5.5}$$

$$\int_a^b w\frac{\partial^2 w}{\partial x^2}dx = w\frac{\partial w}{\partial x}\Big]_a^b - \int_a^b \left(\frac{\partial w}{\partial x}\right)^2 dx \tag{5.6}$$

Substituting these results into equation (5.4) yields:

$$\begin{aligned}\dot{V} =& \int_a^b uw\frac{\partial w}{\partial x}dx - \frac{1}{2}\int_a^b w^2\frac{\partial u}{\partial x}dx - \int vw\frac{\partial w}{\partial x}dx - \delta\int_a^b\left(\frac{\partial w}{\partial x}\right)^2 dx - \int_a^b \alpha w^2 dx \\ &+ \delta w\frac{\partial w}{\partial x}\Big]_a^b - \frac{1}{2}\,w^2u\Big]_a^b \\ =& -\frac{1}{2}\int_a^b w^2\frac{\partial u}{\partial x}dx - \int_a^b \alpha w^2 dx - \delta\int_a^b\left(\frac{\partial w}{\partial x}\right)^2 dx \\ &+ \frac{w^3}{3}\Big]_a^b + \delta w\frac{\partial w}{\partial x}\Big]_a^b - \frac{1}{2}\,w^2u\Big]_a^b \\ =& -\delta\int_a^b\left(\frac{\partial w}{\partial x}\right)^2 dx - \int_a^b w^2\left(\frac{1}{2}\frac{\partial u}{\partial x}+\alpha\right)dx \\ &+ \frac{w^3}{3}\Big]_a^b + \delta w\frac{\partial w}{\partial x}\Big]_a^b - \frac{1}{2}\,w^2u\Big]_a^b \end{aligned} \tag{5.7}$$

By observation of equation (5.7), one can get sufficient conditions for synchronization of coupled Burgers equations. It must be noticed that these conditions are sufficient but not necessary. If the time derivative of the Lyapunov function (5.3) is negative, one has $\int_a^b w^2dx$ converging to zero, meaning that the nil point $w(x,t)=0$, corresponding to the identical synchronization manifold, is achieved for almost all $x\in[a,b]$ as t tends to infinity, and synchronization is reached except perhaps for a set of nil measure. Adding the condition of convergence or merely bounded of the function $t\rightsquigarrow\int_a^b\left(\frac{\partial w(x,t)}{\partial x}\right)^2dx$, $\lim_{t\to\infty}w(x,t)=0$ for all $x\in[a,b]$, eliminating those $x\in[a,b]$ belonging to a set of nil measure, where $w(x,t)$ could not converge to zero as t tends to infinity.

By integration, one has for all $x_1,x_2\in[a,b]$:

$$\int_{x_1}^{x_2} w(x,t)\,\frac{\partial w(x,t)}{\partial x}dx = w(x_2,t)^2 - w(x_1,t)^2 - \int_{x_1}^{x_2} w(x,t)\,\frac{\partial w(x,t)}{\partial x}dx \tag{5.8}$$

Applying the Cauchy-Schwarz inequality one obtains:

$$\begin{aligned} w(x_2,t)^2 &= w(x_1,t)^2 + 2\int_{x_1}^{x_2} w(x,t)\,\frac{\partial w(x,t)}{\partial x}dx \\ &\le w(x_1,t)^2 + 2\sqrt{\int_a^b w(x,t)^2\,dx}\sqrt{\int_a^b\left(\frac{\partial w(x,t)}{\partial x}\right)^2 dx} \end{aligned} \tag{5.9}$$

As in the previous equations there were no restrictions on the choice of x_1 and x_2 in the interval $[a, b]$, one gets the Agmon inequality:

$$\max_{x\in[a,b]} w(x,t)^2 \leq \min_{x\in[a,b]} w(x,t)^2 + 2\sqrt{\int_a^b w(x,t)^2\,dx}\sqrt{\int_a^b \left(\frac{\partial w(x,t)}{\partial x}\right)^2 dx} \tag{5.10}$$

which means that, for all $x \in [a, b]$, $\lim_{t\to\infty} w(x,t) = 0$.

For the bidirectionally case, the results are similar if one replaces α by $\alpha + \beta$:

$$\begin{aligned}\frac{\partial u}{\partial t} &= -u\frac{\partial u}{\partial x} + \delta\frac{\partial^2 u}{\partial x^2} + \beta(v-u)\\ \frac{\partial v}{\partial t} &= -v\frac{\partial v}{\partial x} + \delta\frac{\partial^2 v}{\partial x^2} + \alpha(u-v)\end{aligned} \tag{5.11}$$

Returning to the coupled Burgers equation (5.1) and considering periodic boundary conditions or Dirichlet boundary conditions with the boundaries of the drive and driven equations equal, and supposing $\frac{\partial u}{\partial x}$ continuous, by the mean value theorem equation (5.7) becomes for $\xi \in [a, b]$:

$$\begin{aligned}\dot{V} &= -\delta\int_a^b \left(\frac{\partial w}{\partial x}\right)^2 dx - \int_a^b w^2\left(\frac{1}{2}\frac{\partial u}{\partial x} + \alpha\right)dx\\ &= -\delta\int_a^b \left(\frac{\partial w}{\partial x}\right)^2 dx - \left(\frac{1}{2}\frac{\partial u}{\partial x}(\xi,t) + \alpha\right)\int_a^b w^2 dx\end{aligned} \tag{5.12}$$

As one can conclude by observation of equation (5.12), synchronization must be reached for sufficient large values of the dissipation coefficient δ, and for sufficient large values of the coupling parameter α. For low values of the dissipation coefficient δ, Burgers equation presents sharp slopes with big negative values for $\frac{\partial u}{\partial x}$. Hence equation (5.12) shows that one may have to increase more the value of the coupling parameter α for these cases. A more intense coupling parameter is required for the time derivative of the Lyapunov function (5.3) to be negative, when shocks are present. Also, a sufficient condition for the time derivative to ensure the Lyapunov function (5.3) to be negative is

$$\alpha > -\frac{1}{2}\frac{\partial u}{\partial x} \tag{5.13}$$

Consider the synchronization error obtained for instant t as given by:

$$e(t) = \sqrt{\frac{1}{b-a}\int_a^b |u(x,t) - v(x,t)|^2\,dx} \tag{5.14}$$

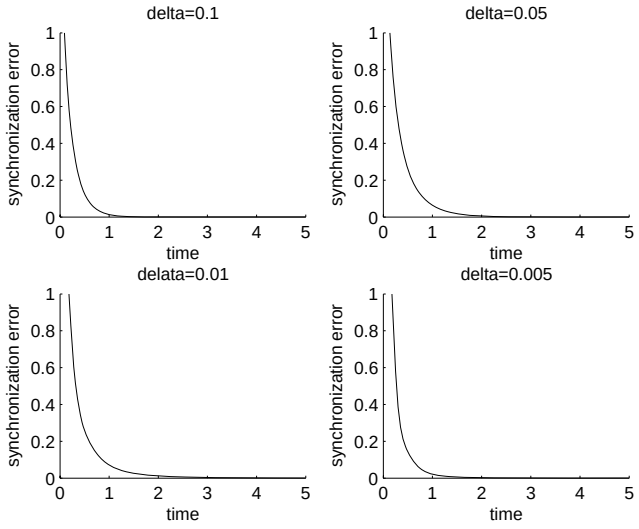

Fig. 5.1: Synchronization error in function of time for different values of δ and $\alpha = \max\left(-\frac{1}{2}\frac{\partial u}{\partial x_i}\right) + 0.5$.

For coupled Burgers equation (5.1) with periodic boundary conditions, $a = 0$ and $b = 1$, and for $\alpha = \max\limits_{x\in[0,1]}\left(-\frac{1}{2}\frac{\partial u}{\partial x_i}\right) + 0.5$ at each instant time t, figure 5.1 shows the evolution of the synchronization error given by equation (5.14) with the time t, for $\delta = 0.1$, $\delta = 0.05$, $\delta = 0.01$ and $\delta = 0.005$. At each time t, the value of α is adapted to the slopes presented in the x direction of the curve u.

For the same example, and for $\alpha = \left(-\frac{1}{2}\frac{\partial u}{\partial x_i}\right) + 0.5$ at each instant time t, figure 5.2 shows the evolution of the synchronization error given by equation (5.14) with the time t, for $\delta = 0.1$, $\delta = 0.05$, $\delta = 0.01$ and $\delta = 0.005$. In this case, for each time t, α is not a constant, but an adaptative value depending on the slopes in the x direction of the curve u, which can take different values at different spatial points. As it can be seen synchronization is reached slower with the reduction of δ. In the previous case, the reduction of δ does not affect so significantly the speed of synchronization.

For the case of Dirichlet boundary conditions, where the boundaries of the drive and driven equations are different, $u(a) \neq v(a)$ or $u(b) \neq v(b)$, complete synchronization can not be reached. For this case, synchronization near the different boundaries can not be achieved, although by observation of equation (5.7) one can expect that increasing α and δ the degree of synchronization may increase.

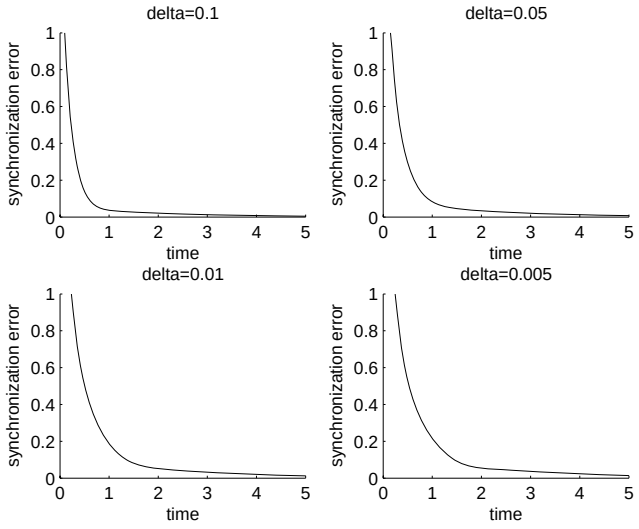

Fig. 5.2: Synchronization error in function of time for different values of δ and $\alpha = \left(-\frac{1}{2}\frac{\partial u}{\partial x_i}\right) + 0.5$.

As an example, numerical simulations for the case where $0 < x < 1$, and boundary conditions given by $u_0(0) = u_0(1) = k_1$ and $v_0(0) = v_0(1) = k_2$, are performed by using Chebyshev spectral collocation method. For the sake of clarity, to enforce the boundary conditions, one can restrict the solution to interpolants that satisfy these ones, or add additional equations to enforce the boundary conditions [255] [50]. Applying the first condition, one must first perform a change of coordinates to the interval $[-1, 1]$ so Chebyshev polynomials can be applied, and one must also convert the inhomogeneous boundary conditions into homogeneous ones. Hence, by applying the change of variables expressed by equations (5.15), (5.16) and (5.17):

$$u^* = u - k_1 \tag{5.15}$$

$$v^* = v - k_2 \tag{5.16}$$

$$x^* = 2x - 1 \tag{5.17}$$

the following equations are obtained from equation (5.1) with homogeneous Dirichlet boundary conditions:

$$\begin{aligned} \frac{\partial u^*}{\partial t} &= -2u^*\frac{\partial u^*}{\partial x^*} - 2k_1\frac{\partial u^*}{\partial x^*} + 4\delta\frac{\partial^2 u^*}{\partial x^{*2}} \\ \frac{\partial v}{\partial t} &= -2v^*\frac{\partial v^*}{\partial x^*} - 2k_2\frac{\partial v^*}{\partial x^*} + 4\delta\frac{\partial^2 v^*}{\partial x^{*2}} + \alpha\left(u^* - v^* + k_1 - k_2\right) \end{aligned} \tag{5.18}$$

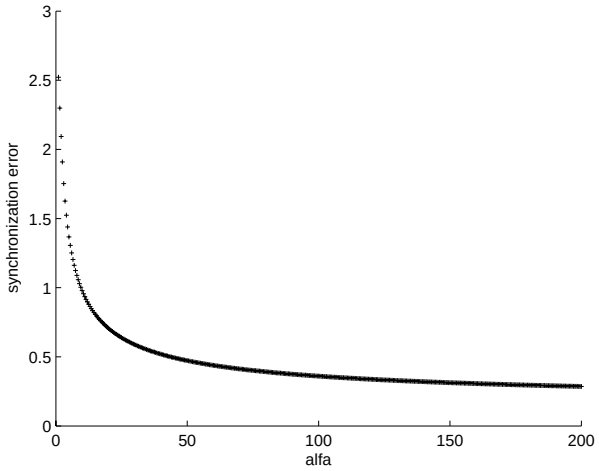

Fig. 5.3: Error at instant $t = 5$ as a function of α, for two unidirectionaly coupled Burgers equation, u and v, with Dirichlet boundary conditions $u(0) = u(1) = 0$ and $v(0) = v(1) = 3$.

Increasing α, the degree of synchronization increases initially and for higher values of α the synchronization improves only slightly, because identical synchronization cannot be achieved. Figure 5.3 shows the synchronization error given by equation (5.14) as a function of the coupling strength α, obtained for $\delta = 0.01$, with boundary conditions given by $u(0) = u(1) = 0$, $v(0) = v(1) = 3$ at $t = 5$.

5.1.2 Coupled spectral solutions of Burgers equation

The low viscosity value is the main responsible for the different dynamical behavior of the spectral solutions of the forced Burgers equation. The dynamics and synchronization of a pair of unidirectionally coupled spectral solutions of Burgers equation under different asymptotic regimes are present, specially with parameter mismatch.

The Dirichlet problem with homogeneous boundary conditions for the forced Burgers equation (4.18) is considered:

$$\frac{\partial u}{\partial t} + u\frac{\partial u}{\partial x} = \delta\frac{\partial^2 u}{\partial x^2} + f(x), \quad -1 \leq x \leq 1$$

Equation (4.19) with $N-1$ degrees of freedom is obtained by discretization of equation (4.18) with $N+1$ points x_j, $0 \leq j \leq N$, by Chebyshev

collocation method:

$$\frac{du_i}{dt} = -u_i D^{(1)} u + \delta D^{(2)} u + f_i, \quad 1 \leq i \leq N-1$$

where $u_1 = u(x_1, t)$, $u_2 = u(x_2, t)$, ..., $u_{N-1} = u(x_{N-1}, t)$, $u = [u_1, u_2, ..., u_{N-1}]^T$, $f_i = f(x_i)$ and $D^{(i)}$, $1 \leq i \leq 2$ are the Chebyshev differentiation matrices of order i. The problem is reduced to a system of ordinary differential equations of order $N-1$, and the study of the dynamics and synchronization is made for an unidirectionally coupling of pair of equations (4.19).

Linear coupling

Consider the linear unidirectionally coupling of the discretized equation (4.19):

$$\begin{aligned} \frac{du_i}{dt} &= -u_i D^{(1)} u + \delta D^{(2)} u + f_i \\ \frac{dv_i}{dt} &= -v_i D^{(1)} v + \delta D^{(2)} v + f_i + \alpha (u_i - v_i) \end{aligned} \tag{5.19}$$

For the case where a parameter mismatch is present between the drive and driven equations, generalized synchronization is observed.

Before discussing synchronization, let one consider the drive system in asymptotic stable regime and describe the dynamics of the coupled equations. Numerical simulations show that, for all the cases studied and independently of the value of N, as the coupling increases starting from zero, there is a threshold value of the coupling parameter α above which one has the driven equation stabilized around the asymptotic solution for any regime of the driven equation.

Before reaching the asymptotic regime, as the coupling increases, several other regimes can be found: from periodic, quasiperiodic or strange regimes to the presence of bistability. These regimes possess patterns that exhibit some similarities with that of the uncoupled equation. Hence, with the driven equation in strange regime and increasing α from zero, it exists a threshold above which the strange motion is suppressed. However, further increasing of the coupling parameter α, may drive the response equation to several other regimes. Similarly, with the driven equation in periodic regime, increasing α from zero may drive the response equation to other regimes. The behavior depends on N, on the function f and on the value of the dissipative coefficient δ of the driven equation, which determine its regime when uncoupled.

An example can illustrate this. Let one consider equation (4.19) for $N = 16$, with $f(x) = \pi \sin(\pi x) [\cos(\pi x) + \delta\pi]$. As already mentioned an

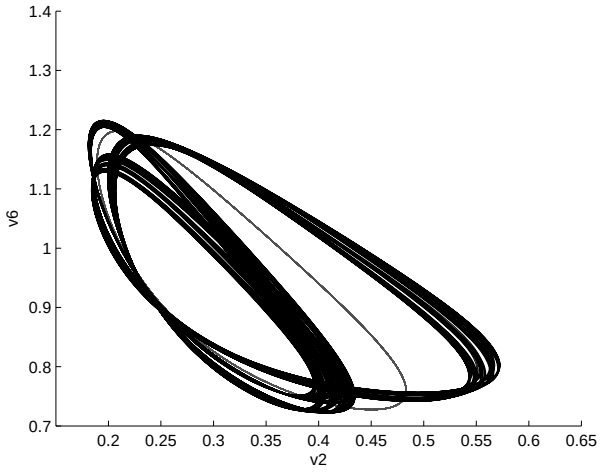

Fig. 5.4: Bistability in the driven equation with a torus type and a stable periodic atractors, for $\alpha = 0.02$.

asymptotic solution is given by $u(x,t) = \sin(\pi x)$. Let the drive equation be in asymptotic stable regime with $\delta > \delta_H \simeq 0.0076389032$ and the driven equation be in strange chaotic regime with $\delta = 0.00576$. The largest Lyapunov exponent for this case has been estimated to be around 0.147. Increasing the coupling α from zero, the driven equation passes through periodic to quasiperiodic motions before achieving complete synchronization with the drive one. The largest Lyapunov exponent diminishes with the increase of α (for instance, this exponent has a value of around 0.047 for $\alpha = 0.01$) till the strange motion is completely suppressed, being substituted by torus type orbits. For a value of $\alpha \simeq 0.0215$ a bifurcation occurs and a stable periodic orbit with a period of approximately 1.72 arises, loosing its stability at $\alpha \simeq 0.02828033$. For $\alpha \gtrsim 0.01300439$, another stable periodic orbit can be found with a period of approximately 0.57, 1/3 of the one previous mentioned cycle. These situations of bistability for the driven equation, with a torus type attractor and a periodic orbit, and with two stable periodic orbits, are illustrated in figures 5.4 and 5.5, for $\alpha = 0.02$ and for $\alpha = 0.026$ respectively.

This new periodic orbit looses its stability at $\alpha \simeq 0.23405706$ through the appearance of a period doubling bifurcation and a new attractor appears as it can be seen in figure 5.6 for $\alpha = 0.26$. This new or news attractors have a largest Lyapunov exponent compatible with zero, seeming to be of torus type.

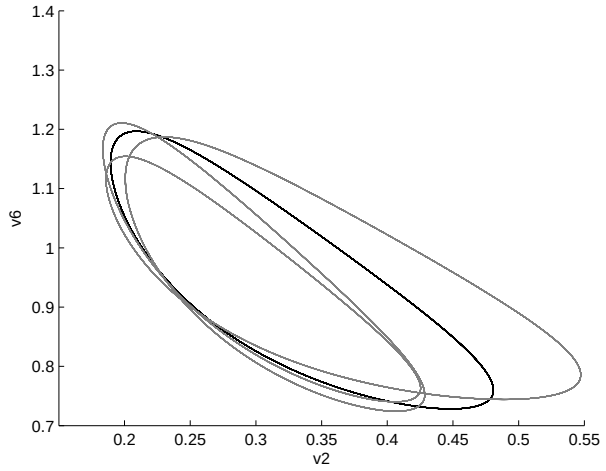

Fig. 5.5: Bistability in the driven equation with two stable periodic orbits, for $\alpha = 0.026$.

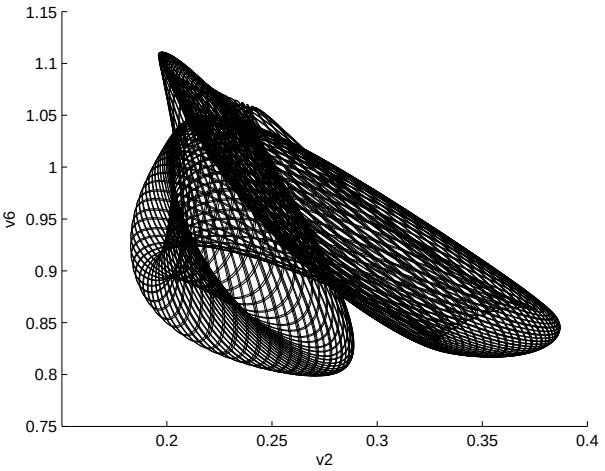

Fig. 5.6: Attractor of torus type for the driven system for $\alpha = 0.26$.

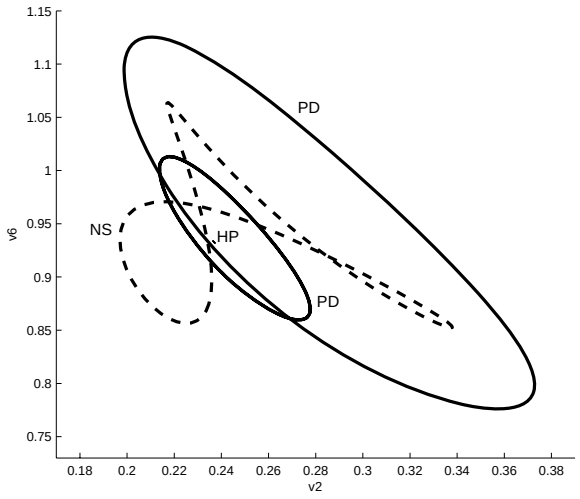

Fig. 5.7: The cycle bifurcations on the driven system, from the period doubling bifurcation at $\alpha \simeq 0.23405706$, till the Hopf bifurcation, as α is increased, projected onto the $v2 - v6$ space.

Keeping α increasing, a Neimark-Sacker bifurcation takes place at $\alpha \simeq 0.28326382$ with a negative normal form coefficient, and a periodic orbit shows up, with the period approximately twice the one of the last cycle. At $\alpha \simeq 0.35728447$, a period doubling bifurcation takes place and a periodic orbit of half the period appears and keeps present till the Hopf bifurcation is reached at $\alpha \simeq 0.3805$, above which stable identical synchronization is observed. The cycle bifurcations on the driven system, from the period doubling bifurcation at $\alpha \simeq 0.23405706$, till the Hopf bifurcation, are shown in figures 5.7 and 5.8, as α is increased. The summary of the dynamics described above is presented in figure 5.9

For the cases where the drive equation is not in asymptotic stable regime and there is a parameter mismatch between the drive and driven equations, generalized synchronization can be achieved. To detect the presence of this type of synchronization some methods have been described in literature. In the work of [244] a numerical method called *mutual false nearest neighbors*, to detect the presence of a continuous transformation ϕ between the drive and driven system was described. The method relies on the technique of time delay phase space reconstruction, based on the continuity of the function ϕ and requires some grade of smoothness [244] [226]. This method can be applied to temporal series where the underlying evolution equations are unknown. For the present case, an adequate method to detect this type of

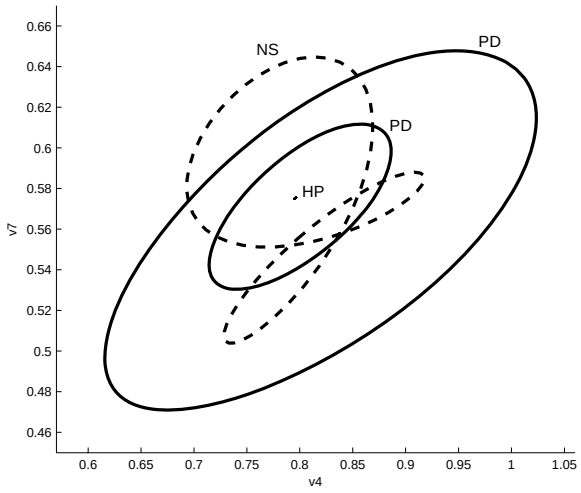

Fig. 5.8: The cycle bifurcations on the driven system, from the period doubling bifurcation at $\alpha \simeq 0.23405706$ till the Hopf bifurcation, as α is increased, projected onto the $v4 - v7$ space.

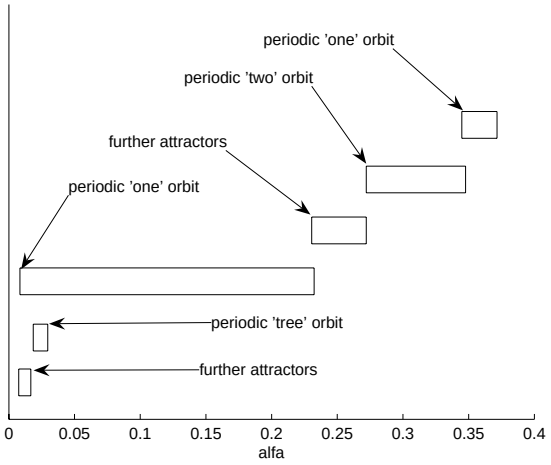

Fig. 5.9: Summary of the dynamics of a linear coupled equation for $N = 16$, with the drive equation in stable asymptotic regime and the driven equation in chaotic regime.

generalized synchronization between the drive and driven systems, is the *auxiliar system approach* described by [3]. It considers the dynamics of another system identical to the response system, but starting with different initial conditions, called *auxiliary system*. In the presence of generalized synchronization, the trajectories of the response and the auxiliary system become identical after a transient period, otherwise the orbits keep unrelated even if they are in the same attractor. Moreover, the negativeness of the conditional Lyapunov exponents of the response system can be used to detect this kind of synchronization [160] [165] [161]. The Jacobian matrix of the coupled discretized equation (5.19) needed to perform the calculation of the conditional Lyapunov exponents is given by

$$J_{ij} = -v_i D_{ij}^{(1)} - \delta_{ij} \sum_{k=1}^{N-1} D_{ik}^{(1)} v_k + \delta D_{ij}^{(2)} - \delta_{ij}\alpha, \quad 1 \leq i, j \leq N-1 \qquad (5.20)$$

where δ_{ij} is the Kronecker symbol.

Numerical experiments for synchronization with parameter mismatch between drive and driven equations, by means of the auxiliar system approach and the negativeness of the conditional Lyapunov exponents of the response equation, confirm for this case the possibility of generalized synchronization for an adequate coupling strength α, for all the values of N tested. For a sufficient strength of the coupling parameter α, it is possible to achieve a state of almost identical synchronization. An example with the drive and driven equations in different asymptotic regimes is describe below.

Consider the case for $N = 16$, with $f(x) = \pi \sin(\pi x)[\cos(\pi x) + \delta\pi]$, where the drive equation (4.19) is in periodic stable regime, with $\delta = 0.007$, the one that arose from the Hopf bifurcation, and the driven equation is in strange chaotic regime with $\delta = 0.00576$. As α increases, the largest Lyapunov exponent of the coupled system decreases its value till zero. For some values of α around 0.02 a first situation of bistability of two torus type attractors can be observed, remaining only one of them stable as α increases further. This situation of bistability is shown in figure 5.10.

For $\alpha \gtrsim 0.1840654$ a second situation of bistability is observed, due to the appearance of a stable periodic orbit, which, for lower α values (at $\alpha \simeq 0.1840654$) looses its stability by a Neimark-Sacker bifurcation. This second situation of bistability is shown in figure 5.11.

For higher values of α ($\alpha \gtrsim 0.22$) the torus type attractor looses its stability, keeping the periodic orbit stable that achieve almost identical synchronization with the drive for a sufficient strength of the coupling parameter α. Generalized synchronization is only achieved for values of α for which the motion of the driven equation is periodic as in the drive equation. In this

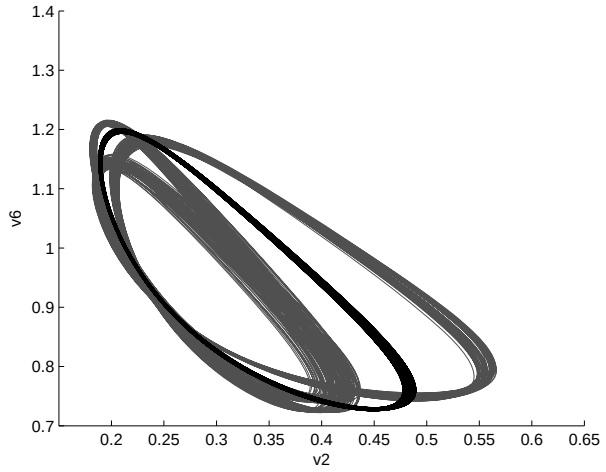

Fig. 5.10: Bistability in the driven equation with two torus type attractors for $\alpha = 0.02$. The drive equation is in periodic regime and the driven one is in strange regime.

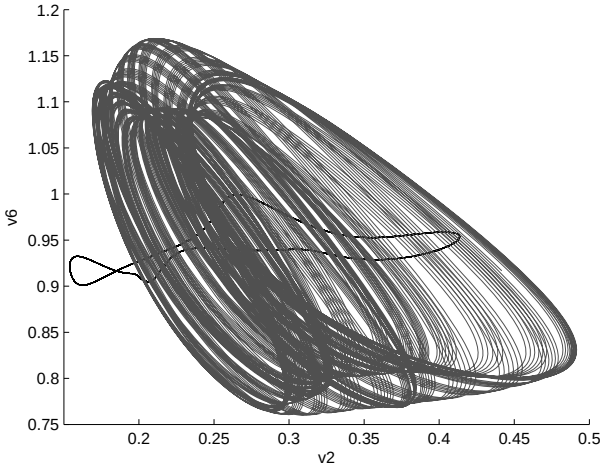

Fig. 5.11: Bistability in the driven equation with a torus type attractor and a periodic orbit for $\alpha = 0.2$. The drive equation is in periodic regime and the driven one is in strange regime.

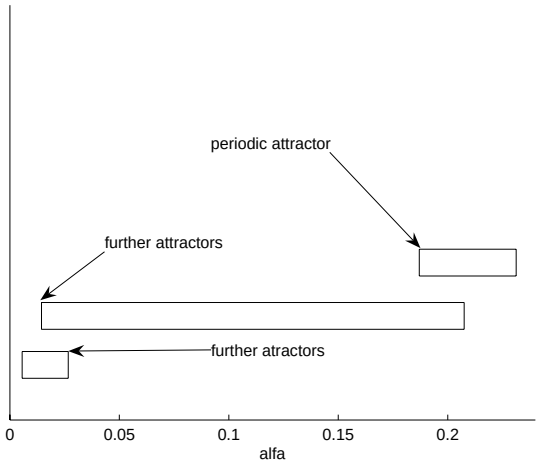

Fig. 5.12: Summary of the dynamics of a linear coupled equation for $N = 16$, with the drive equation in periodic stable regime and the driven equation in chaotic regime.

example the value of the coupling parameter must be above 0.1840654, which is the value where a stable periodic orbit in the driven equation arises. The dynamics described is summarized in figure 5.12.

Changing the drive and driven equations, now the drive equation being in chaotic regime and the driven one in periodic regime, by means of the auxiliar system approach and of the conditional Lyapunov exponents of the response equation, generalized synchronization is achieved for $\alpha \gtrsim 0.05$.

Consider now the case for $N = 17$, with the same function f as above, where the drive and driven equations are both in chaotic regime. For the drive equation with $\delta = 0.00472$ and the driven one with $\delta = 0.0046$, generalized synchronization is achieved for $\alpha \gtrsim 0.3$ and for the case where the coupling is made with $\delta = 0.0046$ for the drive equation and $\delta = 0.00472$ for the driven one generalized synchronization is achieved for $\alpha \gtrsim 0.2$.

For the case of linear coupling of two identical equations (4.19), without parameter mismatch, numerical calculations show that stable identical synchronization is achieved for an adequate value of the coupling parameter α, marked by all the transverse Lyapunov exponents negative.

Nonlinear coupling

Coupling can be done by replacement of one or more components of the response system by the correspondent components of the drive system, as in

the *complete replacement* of Pecora and Carroll [224] [225] [227] being the dimension of the response system reduced. The replacement of one or more components from the drive system into the driven one, can also be done in a partial way, as described by [109] [108] [227], procedure that is called *partial replacement*. In the partial replacement approach a response variable is replaced with the drive counterpart only in certain locations, depending on which will cause stable synchronization and which are accessible in the physical device one is interested in building. In the work of [117] a nonlinear coupling for discrete chaotic systems is discussed using the example of two coupled skew tent maps. Combining herein the partial replacement and nonlinear coupling, one presents a nonlinear coupling for all the discretized variables but only in one of the three locations of the response discretized equation (4.19), namely, waves velocity v, $\frac{\partial v}{\partial x}$ or $\frac{\partial^2 v}{\partial x^2}$. The procedure consists of replacing the discretized response variable v by $v + \alpha\,(u - v)$, where u represents the drive and α the coupling parameter. For $\alpha = 1$ one reaches a situation of partial replacement. It is observed that coupling at the position corresponding to the waves velocity v can lead to identical or generalized synchronization, but generally not allowing values of $\alpha = 1$. This means that the partial replacement in certain locations may not lead to synchronization, but the convex linear combination of the variables of the drive and driven equations in that location do. When coupling at $\frac{\partial v}{\partial x}$, generalized synchronization can only be achieved in quite few cases, specially periodic cases, and only for low values of α. Identical synchronization for identical systems seems only possible for periodic regimes. For the nonlinear coupling at $\frac{\partial^2 v}{\partial x^2}$, no synchronization was observed. This is observed for all the cases studied independently of the dimension of the systems given by the discretized spatial points.

The equations for the case where the nonlinear unidirectionally coupling of the discretized equation (4.19) is made in the waves velocity v are as follows:

$$\begin{aligned} \frac{du_i}{dt} &= -u_i D^{(1)} u + \delta D^{(2)} u + f_i \\ \frac{dv_i}{dt} &= -\left[v_i + \alpha\,(u_i - v_i)\right] D^{(1)} v + \delta D^{(2)} v + f_i \end{aligned} \tag{5.21}$$

The Jacobian matrix must be computed in order to perform the calculation of the conditional Lyapunov exponents of the coupled discretized equation (5.21). The Jacobian matrix for the nonlinear coupling in the waves velocity v is given by equation (5.22) and, for the nonlinear coupling in $\frac{\partial v}{\partial x}$

and in $\frac{\partial^2 v}{\partial x^2}$, is given by equations (5.23) and (5.24) respectively.

$$J_{ij} = -(1-\alpha)\, v_i D^{(1)}_{ij} - \delta_{ij}(1-\alpha) \sum_{k=1}^{N-1} D^{(1)}_{ik} v_k + \delta D^{(2)}_{ij} - \alpha u_i D^{(1)}_{ij} \qquad (5.22)$$
$$1 \leq i, j \leq N-1$$

$$J_{ij} = -(1-\alpha)\, v_i D^{(1)}_{ij} - \delta_{ij}(1-\alpha) \sum_{k=1}^{N-1} D^{(1)}_{ik} v_k + \delta D^{(2)}_{ij} - \alpha \delta_{ij} \sum_{k=1}^{N-1} D^{(1)}_{ik} u_k \qquad (5.23)$$
$$1 \leq i, j \leq N-1$$

$$J_{ij} = -v_i D^{(1)}_{ij} - \delta_{ij} \sum_{k=1}^{N-1} D^{(1)}_{ik} v_k + \delta(1-\alpha) D^{(2)}_{ij} \qquad (5.24)$$
$$1 \leq i, j \leq N-1$$

Similarly to what was done for the linear coupling and for the sake of comparison, one starts considering the example given for linear coupling with $N = 16$ with the drive system in asymptotic stable regime and the driven one in strange chaotic regime with $\delta = 0.00576$.

For the nonlinear coupling in the waves velocity v, the dynamics before reaching the asymptotic regime, as the coupling increases from zero, passes through the following regimes: periodic orbit, torus type attractor and periodic motion again. Between the first periodic orbit and the torus type attractor there is a situation of bistability with both attractors coexisting for a small range of α values. The asymptotic regime is achieved for values of α in the range $0.46 \lesssim \alpha \lesssim 1$. Figure 5.13 shows the different attractors observed for different values of the coupling parameter α.

For the nonlinear coupling in $\frac{\partial v}{\partial x}$ as the coupling increases from zero, the following regimes are observed: periodic orbit, bistability with two periodic orbits, bistability with a torus type attractor and a periodic orbit, bistability with two torus type attractors, torus type attractor and periodic orbit. The dynamics does not converge to the asymptotic solution rather it converges to a spurious stable fixed point at $\alpha \approx 0.48$. Figure 5.14 shows the different attractors and situations of bistability observed.

The nonlinear coupling in $\frac{\partial^2 v}{\partial x^2}$ is very unstable becoming the dynamics unbounded with a very low value of the coupling parameter α.

For the nonlinear coupling in the waves velocity v, and as done previously for the example $N = 16$ with $f(x) = \pi \sin(\pi x)[\cos(\pi x) + \delta\pi]$, where the

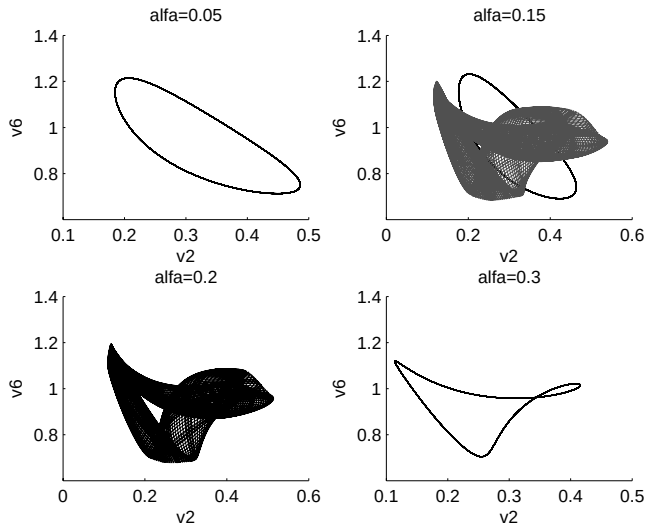

Fig. 5.13: Nonlinear coupling in the waves velocity v with the drive equation in asymptotic stable regime and the driven one in strange chaotic regime with $\delta = 0.00576$. Attractors from left to right and from top to bottom: periodic orbit, bistability with a torus type attractor and a periodic orbit, torus type attractor and periodic orbit.

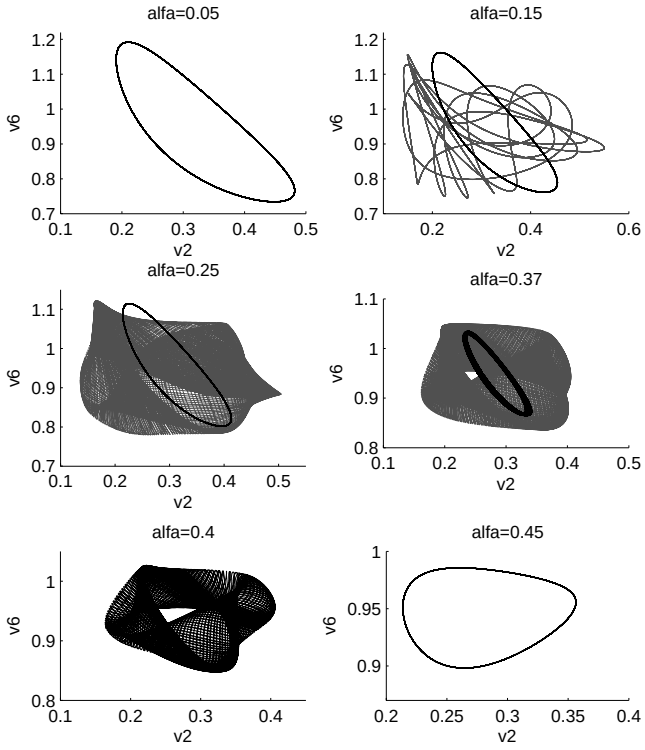

Fig. 5.14: Nonlinear coupling in $\frac{\partial v}{\partial x}$ with the drive equation in asymptotic stable regime and the driven one in strange chaotic regime with $\delta = 0.00576$. Attractors from left to right and from top to bottom: periodic orbit, bistability with two periodic orbits, bistability with a torus type attractor and a periodic orbit, bistability with two torus type attractors, torus type attractor and periodic orbit.

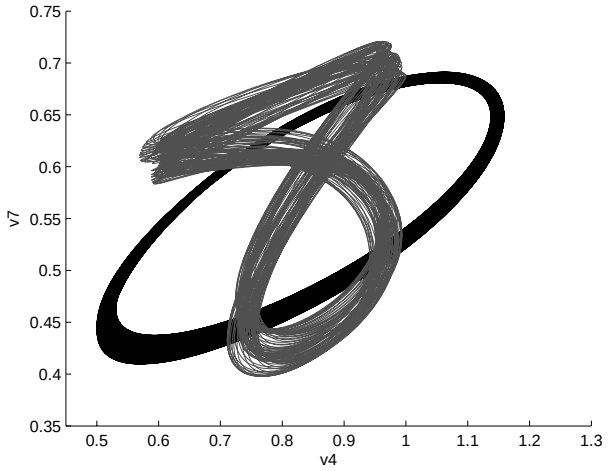

Fig. 5.15: Bistability for nonlinear coupling in the waves velocity v with the drive equation in periodic stable regime with $\delta = 0.007$ and the driven one in strange chaotic regime with $\delta = 0.00576$.

drive equation (4.19) is in periodic stable regime with $\delta = 0.007$, and the driven equation is in strange chaotic regime with $\delta = 0.00576$, a similar but simpler behavior (in relation to the linear case) is observed. In fact, as α increases, for values of α in the range $0.07 \lesssim \alpha \lesssim 0.18$ a bistability situation of two attractors with maximum Lyapunov exponent compatible with the nil value is observed, remaining only one of them stable as α increases further, giving rise to the appearance of a stable periodic orbit for higher values of α in the range $0.25 \lesssim \alpha \lesssim 1$. Figure 5.15 shows the bistability situation for $\alpha = 0.17$.

For the other two types of nonlinear coupling, no generalized synchronization was observed with the response system becoming very unstable and allowing only very small values of α.

For the same example, but now with the drive equation in chaotic regime and the driven one in periodic regime, by means of the auxiliar system approach and of the conditional Lyapunov exponents of the response equation, generalized synchronization is achieved for the nonlinear coupling in the waves velocity v for $0.05 \lesssim \alpha \lesssim 1$ and for the nonlinear coupling in $\frac{\partial v}{\partial x}$ for $0.02 \lesssim \alpha \lesssim 0.15$.

For the case $N = 17$, where the drive and driven equations are both in chaotic regime with the drive equation with $\delta = 0.00472$ and the driven one with $\delta = 0.0046$ and vice-versa, generalized synchronization is achieved for

nonlinear coupling in the waves velocity v for values of $0.2 \lesssim \alpha \lesssim 0.95$. For the other cases of nonlinear coupling it appears not to be possibly to achieve synchronization, except when the coupling is the nonlinear one in $\frac{\partial v}{\partial x}$, with $\delta = 0.0046$ for the drive equation and $\delta = 0.00472$ for the driven one, and the value of α is very small. In this case a maximum negative conditional Lyapunov exponent is observed for values of $\alpha \simeq 0.04$.

For the case of nonlinear coupling of two identical equations (4.19), without parameter mismatch, numerical calculations show that stable identical synchronization is achieved only for the case where the nonlinear coupling is in the waves velocity v, and in periodic cases for the nonlinear coupling in $\frac{\partial v}{\partial x}$.

6. CONCLUSIONS

6.1 Conclusions

6.1.1 Concluding remarks

Nonlinear phenomena is present in every science field and therefore, it is of fundamental importance to develop efficient methods to solve nonlinear equations and nonlinear differential equations. Unfortunately, in most cases, only numerical solutions can are obtainable. This makes evident the importance of analytical techniques, such Adomian's decomposition method [15] [17] [16] [19] [22], since it searches for solutions under a series form, not requiring any discretization or assumption for a small parameter to be present in the problem, which, in fact, may not exist at all [**119**]. The application of this method to partial differential equations poses some obstacles, as the computational effort that is heavier than the one required to solve ordinary differential equations and the possible convergence to a solution that does not satisfy all the boundary conditions. Anyway, as the exact analytical solution is probably not recognized from the solution series, truncated series must be used to represent the solution. A disadvantage of such approach is that the truncated series may have a small convergence radius. To overcome this drawback when applying Adomian's method to ordinary differential equations, some authors have used an aftertreatment with Padé approximants [**29**] [**274**] [273] [132]. Only recently, and simultaneously to the development of the thesis, this technique was applied to partial differential equations [4] [5] where graphical illustrations were used to show that the domain of convergence of Adomian's solution was improved by the application of this technique. In this thesis, it is shown not only graphically but also numerically, that this technique can enlarge the domain of convergence of the solution and that the accuracy is generally also improved inside the domain of convergence of Adomian's series solution as the numerical results show [43]. Also, and not referred by [4] [5], is the disadvantage of representing the series solution as a ratio of two polynomials when poles not existing in the actual solution appear in the Padé approximants. Close to these poles the solution can become inaccurate [43]. This drawback indicates that sometimes it is not advised to increase the order of the Padé approximants to improve the solution, but instead one should search to find the optimal order of the Padé approximants to be used. Other authors tried a different approach to overcome the small converge radius of the solution series: they divided the time horizon in subintervals and applied in a recursive form the Adomian's method, the so called multistage Adomian's decomposition method (MADM) [65] [93], in order to make possible to approach the solution in the entire time interval. To increase the accuracy of the solution, some authors

proposed the choice of a smaller time interval and/or to add more terms to the solution series. Hence, another approach not yet referred in the open literature that one could use to overcome the small convergence radius of the solution series of PDEs would be the application of the Adomian's method to the spatial discretized PDE through finite differences, followed by the application of the MADM to improve the convergence radius. Such approach is used in this thesis. By applying Adomian's method to an example of a spatial discretized Burgers equation through finite differences, one observed that the convergence domain decreased with the number of discretized points, so this approach became useless [43]. This behavior seems to be related to the powers of the terms $\frac{1}{\Delta x}$ that appear in the solution, which are larger when the spatial interval grid is smaller [43]. Another possible approach is to use Padé approximants to the solution series applied to the lines obtained by the spatial discretization of the PDE. Again, in this case, this technique revealed useless since, as expected, the convergence radius also decreased with the number of spatial discretization points [43].

Adomian's decomposition method can also be used to solve nonlinear equations. Due to the nonlinearity of the equations, analytical solutions are only reachable for very few cases. The need to construct efficient numerical methods is essential to solve nonlinear problems. In spite of the importance of the solution series given by Adomian's method, the convergence rate is in this case sometimes slow. Some modifications were made by several authors to solve this flaw, trying to improve Adomian's method applied to those type of equations [33] [12] [35]. This approach was also performed in this thesis and a new iterative method to compute nonlinear equations was developed [40]. This new method has an order of convergence three and comparisons against Adomian's method and other methods based on it were made. Also comparisons were made against Newton-Raphson method, a method of second order, and the Househölder and Halley methods, methods of third order. This new method revealed to be one of the best ones derived from Adomian's method and also a very good alternative to the other referred well known methods, such the Newton-Raphson or the Househölder and Halley methods [40].

Burgers equation ([55]) is one of the simplest nonlinear partial differential equations, and due to its quadratic term, the nonlinear term of convection, it can exhibit sharp discontinuities under a low viscosity coefficient, which are difficult to simulate numerically.

By using Chebyshev spectral methods, Dang-Vu and Delcarte [77] found out the existence of a critical value for the viscosity coefficient, where a Hopf bifurcation occurred to the spectral spatially discretized driven Burgers equation. Bellow that value, after the loss of stability of the periodic orbits, a strange attractor seemed to appear, due to the positive largest Lyapunov ex-

ponent [77]. To the author's knowledge, no other studies on such motions for the spectral solutions of Burgers equations have been published in the open literature. In this work, new behaviors were found for the collocation spectral solutions of the driven Burgers equation [42] [41]. Hence, several bifurcations occur as one decreases the value of the viscosity coefficient and several attractors appear. It was observed the existence of nonperiodic attractors, torus type attractors and strange attractors, for lower values of that parameter below the Hopf point. Bistability with two periodic attractors, with a periodic attractor and a nonperiodic one (torus or strange attractor) and even with two nonperiodic attractors that seem to correspond to quasiperiodic motions, were also observed. Stable equilibrium and new Hopf bifurcations different from the ones that correspond to the asymptotic stationary solution were found out [42] [41].

This dynamic behavior must be related to the discontinuities that Burgers equation can develop and to the Gibbs phenomenon that occurs near these points [42] [41]. For the forced Burgers equation, as the higher points of the nonlinear waves travel at a higher speed, shocks and discontinuities will tend to appear in the intervals where the asymptotic solution is decreasing. Numerical results indicate that these branches of the solution must be fixed to the boundaries. Moreover, such branches where discontinuities tend to appear must not exist not fixed to the boundaries. This seems to be related to that observed in the numerical experiments: in these cases, the asymptotic solution keeps its stability for lower values of the viscosity coefficient, giving time to the equilibrium to loose stability by a supercritical Hopf bifurcation [41]. Indeed, the numerical simulations made over several examples with different Burgers equation drive function, show that the loss of stability of the equilibrium point corresponding to the asymptotic solution must occur by means of a supercritical Hopf bifurcation so that stable limit cycles can emerge, followed by the other phenomena described. However, Hopf bifurcations and limit cycles were observed for cases not satisfying the above premise, but for an equilibrium not belonging to the asymptotic solution. For the case where there is only one interval where the asymptotic solution is decreasing and is fixed to only one of the boundaries, the loss of stability was also done for lower values of the viscosity coefficient but not by a supercritical Hopf bifurcation and no stable attractors were observed. Also, for the Fourier spectral collocation solutions where the solution is not fixed to boundaries, no phenomenon of this kind was observed [41].

Concerning the bistability observed, for almost all the cases, is not related to the symmetry that is exhibited in several examples, as bistability is present even when the motion at the attractors does not break the system symmetry. Even when the motion at the attractors apparently breaks the symmetry, as

for an example studied, the same behavior was observed [42] [41]. A deeper look into the attractor, viewing it as an entire entity, allows to conclude that the symmetry is preserved. Everything occurs as the dynamics evolve in a symmetric manner but with a time delay [41].

This rich dynamical behavior shows that the spectral solution of Burgers equation can be used as a model for the study of dynamical systems and for the implementation of new techniques of synchronization of high dimensional systems, since this is an area with several applications, such as chaotic synchronization in communications. Hence, discussion of sufficient conditions for identical synchronization of coupled Burgers equations, by means of a Lyapunov function, was presented in this work and a nonlinear coupling to synchronize coupled spectral solutions of forced Burgers equations was proposed and studied [41]. The results showed that this kind of coupling must be done at the position corresponding to the waves velocity in the response equation, and generally not by partial replacement, but by a convex linear combination between the drive and driven equations. This applies for both generalized or identical synchronization, with or without parameter mismatch respectively. The results found for the linear coupling show that it is always possible to reach some kind of synchronization, identical or generalized. Also some dynamical behaviors were described which were mainly related to the coupling with the asymptotic solution [41].

There is still work that can be done. Some is presented in the following section.

6.1.2 Future work

The problem of solving initial-boundary value problems using the Adomian's decomposition method, and particularly Burgers equation, is still not resolved and poses still difficulties when one deals with it. This type of problems has been usually solved based only on the imposition of the initial conditions, with the nonimposed boundary conditions being naturally satisfied. When initial and boundary conditions have to be imposed, the Adomian's solution may not be a valid solution. On this subject, there is a strong lack of published work in the open literature. The only works found out are pointed out again in order to illustrate such lack. Ngarhasta *et al.* [211] proposed a search of each term of the Adomian's series to choose the first term verifying both initial and boundary conditions. Wazwaz [281], on the formulation of some boundary value problems, used an unknown function or parameter that was determined later by imposing the other boundary conditions. Adomian [16] and Lesnic [182] [183] [184] proposed a method to solve linear initial-boundary problems, with possible extensions to higher-dimensional,

inhomogeneous and nonlinear problems. The approach proposed by Adomian [16] and later improved by Lesnic [182] [183] [184] consists of applying Adomian's method to linear initial boundary problems, where the starting term and the inverse operators incorporate both the initial and the boundary conditions. To solve the linear heat equation (6.1), namely

$$\frac{\partial u}{\partial t} = \frac{\partial^2 u}{\partial x^2}, \quad 0 < x < 1, \quad t > 0 \tag{6.1}$$

the following equations (6.2) and (6.3) are added, and equation (6.4) is obtained:

$$L_t^{-1} L_t u = L_t^{-1} L_{xx} u \tag{6.2}$$

$$L_{xx}^{-1} L_{xx} u = L_{xx}^{-1} L_t u \tag{6.3}$$

$$u(x,t) = \frac{1}{2}\left[L_t^{-1} L_{xx} + L_{xx}^{-1} L_t\right] u(x,t) \tag{6.4}$$

Lesnic [182] proposed defining the inverse operators L_t^{-1} and L_{xx}^{-1} as definite integrals such as to incorporate the initial and boundary conditions. Hence, for the Dirichlet problem, the inverse operators were defined as follows:

$$L_t^{-1}(\cdot) = \int_0^t (\cdot)\, dt' \tag{6.5}$$

$$L_{xx}^{-1}(\cdot) = \int_0^x dx' \int_0^{x'} (\cdot)\, dx'' - x \int_0^1 dx' \int_0^{x'} (\cdot)\, dx'' \tag{6.6}$$

For the mixed heat equation, Lesnic proposed the following inverse operators:

$$L_t^{-1}(\cdot) = \int_0^t (\cdot)\, dt' \tag{6.7}$$

$$L_{xx}^{-1}(\cdot) = \int_0^x dx' \int_1^{x'} (\cdot)\, dx'' \tag{6.8}$$

with mixed boundary conditions given by:

$$u(0,t) = f_0(t), \quad \frac{\partial u}{\partial x}(1,t) = g_1(t) \tag{6.9}$$

And for the Newmann heat problem, Lesnic proposed the inverse operators:

$$L_t^{-1}(\cdot) = \int_0^t (\cdot)\, dt' \tag{6.10}$$

$$L_{xx}^{-1}(\cdot) = \int_0^x dx' \int_0^{x'} (\cdot)\, dx'' - \frac{x^2}{2} \int_0^1 (\cdot)\, dx' \tag{6.11}$$

with boundary conditions given by:

$$\frac{\partial u}{\partial x}(0,t) = g_0(t), \quad \frac{\partial u}{\partial x}(1,t) = g_1(t) \tag{6.12}$$

The application of this method to nonlinear problems has not yet been done. Although referred by Lesnic [182], it is not an easy task to extend this procedure to higher-dimensional and nonlinear problems, due to the excessive computational effort that it would bring. Intensive research work accounting for some modifications to the above method has to be done. Besides, the study of the convergence to the real solution satisfying both initial and boundary conditions has also to be done. Moreover, the approach suggested by those authors includes writing the equation in two different forms and defining two different inverse operators. The solution is then the arithmetic mean of these two solutions. The possible addition of these equations with weighed coefficients, which could drive to a solution with a different starting term and a recursive relation, can be investigated to minimize the nonlinear effects in the computational work. The proposals of Ngarhasta *et al.* [211], taking into account both initial and boundary conditions by choosing the first term of Adomian's series verifying both initial and boundary conditions, is also worth of further investigation.

A more complete description of the bifurcations and attractors observed for spectral solutions of Burgers equation is still possibly to be done. To completely identify all the bifurcations and attractors implicated, further investigations are needed. Also, the different attractors observed for Chebyshev spectral solutions of Burgers equation may be not a phenomenon exclusive of this equation. Further spectral solutions of Burgers type equations may also exhibit a rich dynamical behavior under certain parameters variation, such as possible chaotic motions. These phenomena could be prospected and explored, so studies like dynamical behavior and chaotic synchronization in extended dynamical systems could be further investigated. Other similar equations are described in the literature relating to various physical phenomena including hydrodynamic processes, possessing the same nonlinearity $u\frac{\partial u}{\partial x}$, which takes, in the generalized meaning, the form $\frac{\partial F(u)}{\partial x}$. Some of such equations are those presented below.

The *Korteweg-de-Vries equation* (KdV), which incorporates dispersion, describes long waves in water of relatively shallow depth, possessing steady progressing wave solutions [297].

$$\frac{\partial u}{\partial t} + u\frac{\partial u}{\partial x} + \beta\frac{\partial^3 u}{\partial x^3} = 0 \tag{6.13}$$

The *Korteweg-de-Vries-Burgers equation* (KdVB), which incorporates dispersion and dissipation, was first proposed for the study of the flow of viscous

fluids down an inclined plane, exhibiting a soliton in the solution.

$$\frac{\partial u}{\partial t} + u\frac{\partial u}{\partial x} + \delta\frac{\partial^2 u}{\partial x^2} + \beta\frac{\partial^3 u}{\partial x^3} = 0 \tag{6.14}$$

The *Kuramoto-Sivashinski equation* (K-S) [169], a model to describe long-wave motions of a liquid thin film over a vertical plane.

$$\frac{\partial u}{\partial t} + u\frac{\partial u}{\partial x} + \delta\frac{\partial^2 u}{\partial x^2} + \gamma\frac{\partial^4 u}{\partial x^4} = 0 \tag{6.15}$$

The *Nikolaevskii equation* [301].

$$\frac{\partial u}{\partial t} + \frac{\partial^2}{\partial x^2}\left[\varepsilon - \left(1 + \frac{\partial^2}{\partial x^2}\right)^2\right] u + u\frac{\partial u}{\partial x} = 0 \tag{6.16}$$

The *modified Korteweg-de-Vries equation* (MKdV) with $m = 0, 1, 2$,

$$\frac{\partial u}{\partial t} + cu^m\frac{\partial u}{\partial x} + \beta\frac{\partial^3 u}{\partial x^3} = 0 \tag{6.17}$$

which, for $m = 0$ becomes the linear KdV equation and for $m = 1$ becomes the nonlinear KdV equation.

The *Fifth-order KdV equation* (FKdV),

$$\frac{\partial u}{\partial t} - \frac{\partial^5 u}{\partial x^5} = F\left(x, t, u, u^2, \frac{\partial u}{\partial x}, \frac{\partial^2 u}{\partial x^2}, \frac{\partial^3 u}{\partial x^3}\right) \tag{6.18}$$

occurs, for example, in the theory of shallow water waves with surface tension.

The *coupled Korteweg-de-Vries equation*, known as *Hirota-Satsuma equation*, was introduced by Hirota and Satsuma [124] and can take the form:

$$\frac{\partial u}{\partial t} = a\left(\frac{\partial^3 u}{\partial x^3} + 6u\frac{\partial u}{\partial x}\right) + 2bv\frac{\partial v}{\partial x} \tag{6.19}$$

$$\frac{\partial v}{\partial t} = -\frac{\partial^3 v}{\partial x^3} - 3u\frac{\partial v}{\partial x} \tag{6.20}$$

BIBLIOGRAPHY

[1] *MATLAB, The Mathworks Inc.* http://www.mathworks.com.

[2] B. A.-Hamid. Exact Solutions of some Nonlinear Evolution Equations Using Symbolic Computations. *Computers & Mathematics with Applications*, 40:291–302, 2000.

[3] H. D. I. Abarbanel, N. F. Rulkov, and M. M. Sushchik. Generalized Synchronization of Chaos: The Auxiliary System Approach. *Physical Review E*, 53(5):4528–4535, 1996.

[4] T. A. Abassy, M. A. El-Tawil, and H. K. Saleh. The Solution of KdV and mKdV Equations Using Adomian Padé Approximation. *International Journal of Nonlinear Sciences and Numerical Simulation*, 5(4):327–339, 2004.

[5] T. A. Abassy, M. A. El-Tawil, and H. K. Saleh. The Solution of Burgers' and Good Boussinesq Equations Using ADM-Padé Technique. *Chaos Solitons & Fractals*, to appear.

[6] K. Abbaoui and Y. Cherruault. Convergence of Adomian's Method Applied to Differential Equations. *Computers and Mathematics with Applications*, 28(5):103–109, 1994.

[7] K. Abbaoui and Y. Cherruault. Convergence of Adomian's Method Applied to Nonlinear Equations. *Mathematical and Computer Modelling*, 20(9):69–73, 1994.

[8] K. Abbaoui and Y. Cherruault. New Ideas for Proving Convergence of Decomposition Methods. *Computers and Mathematics with Applications*, 29(7):103–108, 1995.

[9] K. Abbaoui and Y. Cherruault. The Decomposition Method Applied to the Cauchy Problem. *Kybernetes*, 28(1):68–74, 1999.

[10] K. Abbaoui, Y. Cherruault, and V. Seng. Practical Formulae for the Calculus of Multivariable Adomian Polynomials. *Mathematical and Computer Modelling*, 22(1):89–93, 1995.

[11] K. Abbaoui, M. J. Pujol, Y. Cherruault, N. Himoun, and P. Grimalt. A New Formulation of Adomian Method. *Kybernetes*, 30:1183–1191, 2001.

[12] S. Abbasbandy. Improving Newton-Raphson Method for Nonlinear Equations by Modified Adomian Decomposition Method. *Applied Mathematics and Computation*, 145:887–893, 2003.

[13] S. Abbasbandy and M. T. Darvishi. A Numerical Solution of Burgers' Equation by Modified Adomian Method. *Applied Mathematics and Computation*, page in press, 2004.

[14] M. J. Ablowitz and P. A. Clarkson. *Solitons, Nonlinear Evolution and Inverse Scattering*. Cambridge University Press, Cambridge, 1991.

[15] G. Adomian. A New Approach to Nonlinear Partial Differential Equations. *Journal of Mathematical Analysis and Applications*, 102:420–434, 1984.

[16] G. Adomian. A New Approach to the Heat Equation - An Application of the Decomposition Method. *Journal of Mathematical Analysis and Applications*, 113:202–209, 1986.

[17] G. Adomian. *Nonlinear Stochastic Operator Equations*. Academic Press, New York, 1986.

[18] G. Adomian. Modification of the Decomposition Approach to the Heat Equation. *Journal of Mathematical Analysis and Applications*, 124:290–291, 1987.

[19] G. Adomian. *Solving Frontier Problems of Physics: The Decomposition Method*. Boston, 1994.

[20] G. Adomian. Random Volterra Integral Equations. *Mathematical and Computer Modelling*, 22(8):101–102, 1995.

[21] G. Adomian. Stochastic Burgers Equation. *Mathematical and Computer Modelling*, 22(8):103–105, 1995.

[22] G. Adomian. Explicit Solutions of Nonlinear Partal Differential Equations. *Applied Mathematics and Computation*, 88:117–126, 1997.

[23] G. Adomian. On KdV Type Equations. *Applied Mathematics and Computations*, 88:131–135, 1997.

[24] G. Adomian. Solution of the Thomas-Fermi Equation. *Applied Mathematics Letters*, 11(3):131–133, 1998.

[25] G. Adomian and R. Rach. Noise Terms in Decomposition Solution Series. *Computers and Mathematics with Applications*, 24(11):61–64, 1992.

[26] V. S. Afraimovich, N. N. Verichev, and M. I. Rabinovich. Stochastically Synchronized Oscillations in Dissipative Systems. *Radiophysics*, 29(9):1050–1060, 1986.

[27] F. R. D. Agudo. Análise Real, 1992.

[28] J. C. Alexander, I. Kan, J. A. Yorke, and Z.-P. You. Riddled Basins. *International Journal of Bifurcation and Chaos*, 2:795–813, 1992.

[29] I. V. Andrianov, V. I. Olevskii, and S. Tokarzewski. A Modified Adomian's Decomposition Method. *Journal of Applied Mathematics and Mechanics*, 62(2):309–314, 1998.

[30] A. R. A. Arafa. Analytical Numerical Method for Solving Nonlinear Partial Differential Equations. *Applied Mathematical Letters*, 9(4):115–122, 1996.

[31] P. Ashwin. Riddled Basins and Coupled Dynamical Systems. *Lecture Notes in Physics*, 671, 2005.

[32] E. Babolian and J. Biazar. On the Order of Convergence of Adomian Method. *Applied Mathematics and Computation*, 130:383–387, 2002.

[33] E. Babolian and J. Biazar. Solution of Nonlinear Equations by Modified Adomian Decomposition Method. *Applied Mathematics and Computation*, 132:167–172, 2002.

[34] E. Babolian and A. Davari. Numerical Implementation of Adomian Decomposition Method. *Applied Mathematics and Computation*, 153:301–305, 2004.

[35] E. Babolian and S. Javadi. Restarted Adomian Method for Algebraic Equations. *Applied Mathematics and Computation*, 146:533–541, 2003.

[36] T. Badredine, K. Abbaoui, and Y. Cherruault. Convergence of Adomian's Method Applied to Integral Equations. *Kybernetes*, 28(5):557–564, 1999.

[37] A. Bahadir and M. Saglam. A Mixed Finite Difference and Boundary Element Approach to One-Dimensional Burgers' Equation. *Applied Mathematics and Computation*, 160(3):663–673, 2005.

[38] A. R. Bahadir. A Fully Implicit Finite-Difference Scheme for Two-Dimensional Burgers' Equations. *Applied Mathematics and Computation*, 137:131–137, 2003.

[39] G. A. Baker. *Essentiald of Padé Approximants*. Academic Press, London, 1975.

[40] M. Basto, V. Semiao, and F. Calheiros. A New Iterative Method to Compute Nonlinear Equations. *Applied Mathematics and Computation*, 173:468–483, 2006.

[41] M. Basto, V. Semiao, and F. Calheiros. Dynamics and Synchronization of Numerical Solutions of Burgers Equation. *to be submitted to Journal of Computational and Applied Mathematics*, 2006.

[42] M. Basto, V. Semiao, and F. Calheiros. Dynamics in Spectral Solutions of Burgers Equation. *Journal of Computational and Applied Mathematics, in press*, 2006.

[43] M. Basto, V. Semiao, and F. Calheiros. Numerical Study of Modified Adomians Method Applied to Burgers Equation. *Journal of Computational and Applied Mathematics, in press*, 2006.

[44] N. Bellomo, E. Angelis, L. Graziano, and A. Romano. Solution of Non-Linear Problems in Applied Sciences by Generalized Collocation Methods and Mathematica. *Computers & Mathematics with Applications*, 41:1343–1363, 2001.

[45] N. Bellomo and R. A. Monaco. Comparison Between Adomian's Decomposition Methods and Perturbation Techniques for Nonlinear Random Differential Equations. *Journal of Mathematical Analysis and Applications*, 110:495–502, 1985.

[46] M. Berzins. Varible-Order Finite Elements and Positivity Preservation for Hyperbolic PDEs. *Applied Numerical Mathematics*, 48:271–292, 2004.

[47] J. Biazar and R. Islam. Solution of Wave Equation by Adomian Decomposition Method and the Restrictions of the Method. *Applied Mathematics and Computation*, 149:807–814, 2004.

[48] G. Biondini and S. Lillo. Semiline Solutions of the Burgers Equation with Time Dependent Flux at the Origin. *Physics Letters A*, 220:201–204, 1996.

[49] A. N. Boules. On the Least-Squares Conjugate-Gradient Solution of the Finite Element Approximation of Burgers' Equation. *Applied Mathematical Modelling*, 25:731–741, 2001.

[50] J. P. Boyd. *Chebyshev and Fourier Spectral Methods*. Dover Publications, Inc., New York, 2 edition, 2000.

[51] H. F. Bremen, F. E. Udwadia, and W. Proskurowski. An Efficient QR Based Method for the Computation of Lyapunov Exponents. *Physica D*, 101:1–16, 1997.

[52] M. Brin and G. Stuck. *Introduction to Dynamical Systems*. Cambridge University Press, United Kingdom, 1 edition, 2002.

[53] R. Brown and N. F. Rulkov. Designing a Coupling that Guarantees Synchronization between Identical Chaotic Systems. *Physical Review Letters*, 78(22):4189–4192, 1997.

[54] R. Brown and N. F. Rulkov. Synchronization of Chaotic Systems: Transverse Stability of Trajectories in Invariant Manifolds. *Chaos*, 7(3):395–413, 1997.

[55] J. M. Burgers. A Mathematical Model Illustrating the Theory of Turbulence. *Advanced in Applied Mechanics*, 1:171–199, 1948.

[56] R. C.-González and M. J. Bünner. Lyapunov length scale in spatially extended systems. unpublished, 2002.

[57] R. C.-González, S. Ørstavik, J. Huke, D. S. Broomhead, and J. Stark. Scalling and Interleaving of Subsystem Lyapunov Exponents for Spatio-Temporal Systems. *Chaos*, 9(2):466–482, 1999.

[58] D. Cai and D. W. McLaughlin. Chaotic and Turbulent Behavior of Unstable One-Dimensional Nonlinear Dispersive Waves. *Journal of Mathematical Physics*, 41(6):4125–4153, 2000.

[59] W. Cai, D. Gottlieb, and A. Harten. Cell Averaging Chebyshev Methods for Hyperbolic Problems. *Computers and Mathematics with Applications*, 24(516):37–49, 1992.

[60] W. Cai, D. Gottlieb, and C. W. Shu. Essentially Non-Oscillatory Spectral Fourier Method for Shock Wave Calculations. *Mathematics of Computation*, 52(186):389–410, 1989.

[61] W. Cai and C.-W. Shu. Uniforme High Order Spectral Methods for One and Two Dimensional Euler Equations. *Journal of Computational Physics*, 104(2):427–443, 1993.

[62] V. Candela and A. Marquina. Recurrence Relations for Rational Cubic Methods I: The Halley Method. *Computing*, 44:169, 1990.

[63] L. Casasús and W. Al-Hayani. The Decomposition Method for Ordinary Differential Equations with Discontinuities. *Applied Mathematics and Computation*, 131:245–251, 2002.

[64] W. Chen and Z. Lu. An Algorithm for Adomian Decomposition Method. *Applied Mathematics and Computation*, 159:221–235, 2004.

[65] M. Cheng, K. Scott, Y. Sun, and B. Wu. Explicit Solution of Nonlinear Electrochemical Models by the Decomposition Method. *Chemical Engineering & Technology*, 25:1155–1160, 2002.

[66] Y. Cherruault. Convergence of Adomian's Method. *Kybernetes*, 18(2):31–38, 1989.

[67] Y. Cherruault and K. Abbaoui. A Computational Approach to the Wave Equations, an Application of the Decomposition Method. *Kybernetes*, 33(1):80–97, 2004.

[68] Y. Cherruault and G. Adomian. Decomposition Method: A New Proof of Convergence. *Mathematical and Computer Modelling*, 18(12):103–106, 1993.

[69] Y. Cherruault, G. Adomian, K. Abbaoui, and R. Rach. Further Remarks on Convergence of Decomposition Method. *International Journal of Bio-Medical Computing*, 38:89–93, 1995.

[70] Y. Cherruault, G. Saccomandi, and B. Some. New Results for Convergence of Adomian's Method Applied to Integral Equations. *Mathematical and Computer Modelling*, 16(2):85–93, 1992.

[71] H.-W. Choi and J.-G. Shin. Symbolic Implementation of Th Algorithm for Calculating Adomian Polynomials. *Applied Mathematics and Computation*, 146:257–271, 2003.

[72] J. D. Cole. On a Quasi-Linear Parabolic Equation Occuring in Aerodynamics. *Quarterly Applied Mathematics*, 9(3):225–236, 1951.

[73] M. Cross. Chaos on the Web, Physics 161: Introduction to Chaos. http://www.cmp.caltech.edu/∼mcc/Chaos_Course/Outline.html, March 2000.

[74] P. S. Crossley, R. Saunders, D. M. Causon, and C. G. Mingham. A Spectral Method with Subcell Resolution for Shock Wave Calculations. *Applied Numerical Mathematics*, 21:141–153, 1996.

[75] J. A. Cuminato and M. M. Junior. *Discretização de Equações Diferenciais Parciais*. Laboratório de Computação de Alto Desempenho, http://www.lcad.imcm.sc.usp.br (consulted in 08/2004), 2002.

[76] I. Dag, D. Irk, and B. Saka. A Numerical Solution of the Burgers' Equation Using Cubic B-Splines. *Applied Mathematics and Computation*, 163(1):199–211, 2005.

[77] H. Dang-Vu and C. Delcarte. Hopf Bifurcation and Strange Attractors in Chebyshev Spectral Solutions of the Burgers Equation. *Applied Mathematics and Computation*, 73:99–113, 1995.

[78] L. Debnath. *Nonlinear Partial Differential Equations for Scientists and Engineers*. Birkhäuser, Boston, 2 edition, 2004.

[79] H. Demiray. A Travelling Wave Solution to the KdV-Burgers Equation. *Applied Mathematics and Computation*, 154(3):665–670, 2004.

[80] H. Demiray. Complex Travelling Wave Solutions to the KdV and Burgers Equations. *Applied Mathematics and Computation*, 162(2):925–930, 2005.

[81] R. G. Derickson and R. A. Pielke. A Preliminary Study of the Burgers Equation with Symbolic Computation. *Journal of Computational Physics*, 162:219–244, 2000.

[82] R. L. Devaney. *An Introduction to Chaotic Dynamical Systems*. Addison-Wesley Publishing Company, Inc., 2 edition, 1987.

[83] A. Dhooge, W. Govaerts, and Y. A. Kuznetsov. *MATCONT*. http://allserv.UGent.be/∼ajdhooge.

[84] A. Dhooge, W. Govaerts, and Y. A. Kuznetsov. MATCONT: A MATLAB Package for Numerical Bifurcation Analysis of ODEs. *ACM Transactions on Mathematical Software (TOMS)*, 29(2):141–164, 2003.

[85] M. Ding and W. Yang. Observation of Intermingled Basins in Coupled Oscillators Exhibiting Synchronized Chaos. *Physical Review E*, 54(3):2489–2494, 1996.

[86] P. Dita and N. Grama. On Adomian's Decomposition Method for Solving Differential Equations. arXiv.org: solv-int/9705008, Julho 2004.

[87] A. Dogan. A Galerkin Finite Element Approach to Burger' Equation. *Applied Mathematics and Computation*, 2003. article in press.

[88] P. DuChateau. Introduction to Nonlinear Partial Differential Equations. http://www.math.colostate.edu/∼pauld/M546.html (consulted in 01/2004), 2002.

[89] Efunda. Fluid Mechanics. http://www.efunda.com/formulae/fluids (consulted in 03/2003).

[90] M. B. Abd el Malek and S. M. A. El-Mansi. Group Theoretic Methods Applied to Burgers' Equation. *Journal of Computational and Applied Mathematics*, 115:1–12, 2000.

[91] S. M. El-Sayed and M. R. Abdel-Aziz. A Comparison of Adomian's Decomposition Method and Wavelet-Galerkin Method for Solving Integro-Differential Equations. *Applied Mathematics and Computation*, 136:151–159, 2003.

[92] S. M. El-Sayed and D. Kaya. On the Numerical Solution of the System of Two-Dimensional Burgers' Equations by the Decomposition Method. *Applied Mathematics and Computation*, 158:101–109, 2004.

[93] M. A. El-Tawil, A. A. Bahnasawi, and A. A.-Naby. Solving Riccati Differential Equation Using Adomian's Decomposition Method. *Applied Mathematics and Computation*, 157:503–514, 2004.

[94] S. E. Esipov. Coupled Burgers Equations. A Model of Polydispersive Sedimentation. *Physical Review E*, 52:3711–3718, 1995.

[95] D. G. Figueiredo. *Análise de Fourier e Equações Diferenciais Parciais*. Projecto Euclides - IMPA, 2 edition, 1986.

[96] C. A. J. Fletcher. *Numerical Solution of Partial Differential Equations*. North-Holland, Amsterdam, 1982.

[97] C. A. J. Fletcher. *Computational Galerkin Methods*. Springer-Verlag, New York, 1984.

[98] Z. Fu, S. Liu, and S. Liu. New Exact Solutions to the KdV-Burgers-Kuramoto Equation. *Chaos, Solitons & Fractals*, 23(2):609–616, 2005.

[99] H. Fujisaka and T. Yamada. Stability Theory of Synchronized Motion in Coupled-Oscillator Systems. *Progress of Theorical Physics*, 69(1):32–47, 1983.

[100] L. Gabet. The Theoretical Foundation of the Adomian Method. *Computers and Mathematics with Applications*, 27(12):41–52, 1994.

[101] A. L. Garcia. *Numerical Methods for Physics*. Prentice-Hall, Inc., 2 edition, 2000.

[102] D. J. Gauthier and J. C. Bienfang. Intermittent Loss of Synchronization in Coupled Chaotic Oscillators: Toward a New Criterion for High-Quality Synchronization. *Physical Review Letters*, 77(9):1751–1754, 1996.

[103] K. Geist, U. Parlitz, and W. Lauterborn. Comparison of Different Methods for Computing Lyapunov Exponents. *Progress of Theorical Physics*, 83(5):875–893, 1990.

[104] J. M. González-Miranda. Synchronization of Symmetric Chaotic Systems. *Physical Review E*, 53(6):5656–5669, 1996.

[105] D. Gottlieb and S. A. Orszaq. *Numerical Analysis of Spectral Methods: Theory and Applications*. CBMS-NSF Regional Conference Series in Applied Mathematics (n26), Philadelphia, USA, 1987.

[106] S. Guan, C.-H. Lai, and G. W. Wei. Bistable Chaos Without Symmetry in Generalized Synchronization. *Physical Review E*, 71:036209 (11 pages), 2005.

[107] S. Guellal, P. Grimalt, and Y. Cherruault. Numerical Study of Lorenz's Equation by the Adomian Method. *Computers and Mathematics with Applications*, 33(3):25–29, 1997.

[108] J. Guémez, C. Martin, and M. A. Matias. Approach to the Chaotic Synchronized State of some Driving Methods. *Physical Review E*, 55(1):124–134, 1997.

[109] J. Guémez and M. A. Matías. Modified Method for Synchronizing and Cascading Chaotic Systems. *Physical Review E*, 52:2145, 1995.

[110] J. M. Gutiérrez and A. Iglesias. Synchronizing Chaotic Systems with Positive Conditional Lyapunov Exponents by Using Convex Combinations of the Drive and Response Systems. *Physics Letters A*, 239:174–180, 1998.

[111] M. Hadizadeh and K. Maleknejad. On the Decomposition Method to the Heat Equation with Non-Linear and Non-Local Boundary Conditions. *Kybernetes*, 27(4):426–434, 1998.

[112] K. Haldar and B. K. Datta. Integrations by Asymptotic Decomposition. *Applied Mathematics Letters*, 9(2):81–83, 1996.

[113] R. W. Hamming. *Numerical Methods for Scientists and Engineers*. Dover Publications, New York, 1973.

[114] A. Harten. High Resolution Scheme for Hyperbolic Conservation Laws. *Journal of Computational Physics*, 49:357–393, 1983.

[115] A. Harten. ENO Schemes with Subcell Resolution. *Journal of Computational Physics*, 83(1):148–184, 1989.

[116] A. Harten, B. Engquist, S. Osher, and S. Chakravarthy. Uniformly High Order Accurate Essentially Non-Oscillatory Schemes III. *Journal of Computational Physics*, 71(2):231–303, 1987.

[117] M. Hasler and Y. Maistrenko. An Introduction to the Synchronization of Cahotic Systems: Coupled Skew Tent Maps. Technical report, École Polytechnique Fédérale de Lausanne, http://icwww.epfl.ch/publications/documents/IC_TECH_REPORT_199704.pdf, 1997.

[118] J. H. He. A New Approach to Nonlinear Partial Differential Equations. *Communications in Nonlinear Sciences and Numerical Simulations*, 2(4):230–240, 1997.

[119] J.-H. He. Some Asymptotic Methods for Strongly Nonlinear Equations. *International Journal of Modern Physics B*, 20(10):1141–1199, 2006.

[120] J. F. Heagy, T. L. Carroll, and L. M. Pecora and. Desynchronization by Periodic Orbits. *Physical Review E*, 52:1253, 1995.

[121] J. F. Heagy, T. L. Carroll, and L. M. Pecora. Syncronous Chaos in Coupled Oscillator Systems. *Physical Review E*, 50:1874–1885, 1994.

[122] J. F. Heagy, L. M. Pecora, and T. L. Carroll. Short Wavelength Bifurcations and Size Instabilities in Coupled Oscillator Systems. *Physical Review Letters*, 74:4185–4188, 1995.

[123] N. Himoun, K. Abbaoui, and Y. Cherruault. New Results on Adomian Method. *Kubernetes*, 32(4):523–539, 2003.

[124] R. Hirota and J. Satsuma. Soliton Solutions of a Coupled Kortweg-de-Vries Equation. *Physics Letters A*, 85:407–408, 1981.

[125] Y. C. Hon and X. Z. Mao. An Efficient Numerical Scheme for Burgers' Equation. *Applied Mathematics and Computation*, 95:37–50, 1998.

[126] E. Hopf. The Partial Differential Equation $u_t + uu_x = \mu\ u_{xx}$. *Communications on Pure and Applied Mathematics*, 9:201–230, 1950.

[127] A. S. Householder. *The Numerical Treatment of a Single Equation.* McGraw-Hill, New York, 1970.

[128] A. E. Hramov and A. A. Koronovskii. Intermittent Generalized Synchronization in Unidirectionally Coupled Chaotic Oscillators. *Europhysics Letters*, 70(2):169–175, 2005.

[129] L. Illing, J. Bröcker, L. Kocarev, U. Parlitz, and H. D. I. Abarbanel. When are Synchronization Errors Small? *Physical Review E*, 66:036229 (8 pages), 2002.

[130] H. N. A. Ismail, K. Raslan, and A. A. A. Rabboh. Adomian Decomposition Method for Burger's-Huxley and Burger's-Fisher Equations. *Applied Mathematics and Computation*, 159:291–301, 2004.

[131] A. Jalnine and S.-Y. Kim. Characterization of the Parameter-Mismatching Effect on the Loss of Chaos Synchronization. *Physical Review E*, 65:026210 (7 pages), 2002.

[132] Y. C. Jiao, Y. Yamamoto, C. Dang, and Y. Hao. An Aftertreatment Technique for Improving the Accuracy of Adomian's Decomposition Method. *Computers and Mathematics with Applications*, 43:783–798, 2002.

[133] G. A. Johnson, D. J. Mar, T. L. Carroll, and L. M. Pecora. Synchronization and Imposed Bifurcations in the Presence of Large Parameter Mismatch. *Physical Review Letters*, 80(18):3956–3959, 1998.

[134] K. Josic. Invariant Manifolds and Synchronization of Coupled Dynamical Systems. *Physical Review Letters*, 80(14):3053–3056, 1998.

[135] L. Junge and U. Parlitz. Control and Synchronization of Spatially Extended Systems. Crans-Montana, Switzerland, September 1998. International Symposium on Nonlinear Theory and its Applications.

[136] L. Junge and U. Parlitz. Synchronization and Control of Coupled Ginzburg-Landau Equations Using Local Coupling. *Physical Review E*, 61(4):3736–3742, 2000.

[137] L. Junge and U. Parlitz. Synchronization Using Dynamic Coupling. *Physical Review E*, 64:055204 (4 pages), 2001.

[138] L. Junge, U. Parlitz, Z. Tasev, and L. Kocarev. Synchronization and Control of Spatially Extended Systems Using Sensor Coupling. *International Journal of Bifurcation and Chaos*, 9(12):2265–2270, 1999.

[139] A. Y. Kamenshchik, I. M. Khalatnikov, and M. Martellini. Singularities in Solutions of Burger's Equation. *Physics Letters A*, 232:87–90, 1997.

[140] J. L. Kaplan and J. A Yorke. Chaotic Behaviour of Multidimensional Difference Equations. *Lecture Notes in Mathematics*, 730:204–227, 1979.

[141] S. Katsuhiro. A New Finite Variable Difference Method with Application to Locally Exact Numerical Scheme. *Journal of Computational Physics*, 124:301–308, 1996.

[142] S. Katsuhiro. A New Finite Variable Difference Method with Application to Nonlinear Burgers Equation. *Nonlinear Analysis, Theory, Methods & Applications*, 30(4):2169–2180, 1997.

[143] D. Kaya. On the Solution of a Korteweg-de Vries Like Equation by the Decomposition Method. *International Journal of Computer Mathematics*, 72:531–539, 1999.

[144] D. Kaya. An Explicit and Numerical Solutions of some Fifth-Order KdV Equation by Decomposition Method. *Applied Mathematics and Computation*, 144:353–363, 2003.

[145] D. Kaya and M. Aassila. An Application for a Generalized KdV Equation by the Decomposition Method. *Physics Letters A*, 299:201–206, 2002.

[146] D. Kaya and S. M. El-Sayed. On the Solution of the Coupled Schrödinger-Kdv Equation by the Decomposition Method. *Physics Letters A*, 313:82–88, 2003.

[147] D. Kaya and I. E. Inan. A Convergence Analysis of the ADM and an Application. *Applied Mathematics and Computation*, 161(3):1015–1025, 2005.

[148] D. Kaya and I. E. Inan. A numerical application of the decomposition method for the combined KdV-MKdV equation. *Applied Mathematics and Computation*, 168(2):915–926, 2005.

[149] D. Kaya and A. Yokus. A Numerical Comparison of Partial Solutions in the Decomposition Method for Linear and Nonlinear Partial Differential Equations. *Mathematics and Computers in Simulation*, 60:507–512, 2002.

[150] D. Kaya and A. Yokus. A Decomposition Method for Finding Solitary and Periodic Solutions for a Coupled Higher Dimensional Burgers Equation. *Applied Mathematis and Computation*, page in press, 2004.

[151] H. Kielhöfer. *Bifurcation Theory An Introduction with Applications to PDEs*, volume 156. Applied Mathematical Sciences, New York, 2000.

[152] S.-Y. Kim and W. Lim. Effect Os Asymmetry on the Loss of Chaos Synchronization. *Physical Review E*, 64:016211 (12 pages), 2001.

[153] S.-Y. Kim and W. Lim. Mechanism for the Riddling Transition in Coupled Chaotic Systems. *Physical Review E*, 63:026217 (7 pages), 2001.

[154] S.-Y. Kim, W. Lim, A. Jalnine, and S. P. Kuznetsov. Characterization of the Noise Effect on Weak Synchronization. *Physical Review E*, 67:016217 (8 pages), 2003.

[155] S.-Y. Kim, W. Lim, and Y. Kim. New Riddling Bifurcation in Asymmetric Dynamical Systems. *Progress of PhysicsTheoretical*, 105(2):187–196, 2001.

[156] S.-Y. Kim, W. Lim, and Y. Kim. Effect of Parameter Mismatch and Noise on Weak Synchronization. *Progress of Theoretical Physics*, 107(2):239–252, 2002.

[157] S.-Y. Kim, W. Lim, E. Ott, and B. Hunt. Dynamical Origin for the Occurence of Asynchronous Hyperchaos and Chaos Via Blowout Bifurcation. *Physical Review E*, 68:066203 (10 pages), 2003.

[158] L. Kocarev, P. Janjic, and T. Stojanovski. Controlling Spatio-Temporal Chaos in Coupled Oscillators by Sporadic Driving. *Chaos, Solitons & Fractals*, 9:283–293, 1998.

[159] L. Kocarev and U. Parlitz. General Approach for Chaotic Synchronization with Applications to Communication. *Physical Review Letters*, 74(25):5028–5031, 1995.

[160] L. Kocarev and U. Parlitz. Generalized Synchronization in Chaotic Systems. *SPIE*, 2612:57–61, 1995.

[161] L. Kocarev and U. Parlitz. Generalized Synchronization, Predictability, and Equivalence of Unidirectionally Coupled Dynamical Systems. *Phyical Review Letters*, 76(11):1816–1819, 1996.

[162] L. Kocarev and U. Parlitz. Synchronizing Spatiotemporal Chaos in Coupled Nonlinear Oscillators. *Physical Review Letters*, 77(11):2206–2209, 1996.

[163] L. Kocarev, U. Parlitz, and R. Brown. Robust Synchronization of Chaotic Systems. *Physical Review E*, 61(4):3716–3720, 2000.

[164] L. Kocarev, U. Parlitz, and B. Hu. Lie Derivatives and Dynamical Systems. *Chaos, Solitons & Fractals*, 9(8):1359–1366, 1998.

[165] L. Kocarev, U. Parlitz, and T. Stojanovski. Generalized Synchronization of Chaotic Signals. pages 953–956, Las Vegas, USA 10-14, December 1995. International Symposium on Nonlinear Theory and its Applications.

[166] L. Kocarev, U. Parlitz, T. Stojanovski, and P. Janjic. Controlling Spatiotemporal Chaos in Coupled Nonlinear Oscillators. *Physical Review E*, 56(1):1238–1241, 1997.

[167] L. Kocarev, Z. Tasev, and U. Parlitz. Synchronizing Spatiotemporal Chaos of Partial Differential Equations. *Physical Review Letters*, 79(1):51–54, 1997.

[168] L. Kocarev, Z. Tasev, T. Stojanovski, and U. Parlitz. Synchronizing Spatiotemporal Chaos. *Chaos*, 7(4):635–643, 1997.

[169] Y. Kuramoto and T. Tsuzuki. Persistent Propagation of Concentration Waves in Dissipative Media for from Thermal Equilibrium. *Progress of Theorical Physics*, 55(2):356–369, 1976.

[170] S. Kutluay, A. R. Bahadir, and A. Özdes. Numerical Solution of One-Dimensional Burgers Equation: Explicit and Exact-Explicit Finite Difference Methods. *Journal of Computational and Applied Mathematics*, 103:251–261, 1999.

[171] S. Kutluay and A. Esen. A Linearized Numerical Scheme for Burgers-Like Equations. *Applied Mathematics and Computation*, 156(2):295–305, 2004.

[172] Y. A. Kuznetsov. *Elements of Applied Bifurcation Theory*, volume 112. Applied Mathematical Sciences, New York, 3 edition, 2004.

[173] Y.-C. Lai. Symmetry-Breaking Bifurcation with on-Off Intermittency in Chaotic Dynamical Systems. *Physical Review E*, 53(5):R4267–R4270, 1996.

[174] Y.-C. Lai. Pseudo-Riddling in Chaotic Systems. *Physica D*, 150:1–13, 2001.

[175] Y.-C. Lai, E. M. Bollt, and Z. Liu. Low-Dimensional Chaos in High-Dimensional Phase Space: How Does It Occur? *Chaos, Solitons and Fractals*, 15:219–232, 2003.

[176] Y.-C. Lai and C. Grebogi. Modeling of Coupled Chaotic Oscillators. *Physical Review Letters*, 82(24):4803–4806, 1999.

[177] Y.-C. Lai and C. Grebogi. Riddling of Chaotic Sets in Periodic Windows. *Physical Review Letters*, 83(15):2926–2929, 1999.

[178] Y.-C. Lai, C. Grebogi, J. A. Yorke, and S. C. Venkataramani. Riddling Bifurcation in Chaotic Dynamical Systems. *Physical Review Letters*, 77(1):55–58, 1996.

[179] Y.-C. Lai, D. Lerner, K. Williams, and C. Grebogi. Unstable Dimension Variability in Coupled Chaotic Systems. *Physical Review E*, 60(5):5445–5454, 1999.

[180] Y.-C. Lai and R. L. Winslow. Riddled Parameter Space Spatiotemporal Chaotic Dynamical Systems. *Physical Review Letters*, 72(11):1640–1643, 1994.

[181] P. D. Lax. Integrals of Nonlinear Equations of Evolution and Solitary Waves. *Communications on Pure and Applied Mathematics*, 21(5):467–490, 1968.

[182] D. Lesnic. A Computational Algebraic Investigation of the Decomposition Method for Time-Dependent Problems. *Applied Mathematics and Computation*, 119:197–206, 2001.

[183] D. Lesnic. Convergence of Adomian's Decomposition Method: Periodic Temperatures. *Computers and Mathematics with Applications*, 44:13–24, 2002.

[184] D. Lesnic. The Decomposition Method for Forward and Backward Time-Dependent Problems. *Journal of Computational and Applied Mathematics*, 147:27–39, 2002.

[185] W. Lim and S.-Y. Kim. On the Consequence of Blow-Out Bifurcations. *Journal of Korean Physical Society*, 43(2):202–206, 2003.

[186] W. Lim and S.-Y. Kim. Noise Effect on Weak Chaotic Synchronization in Coupled Invertible Systems. *Journal of Korean Physical Society*, 45(2):287–294, 2004.

[187] W. Lim and S.-Y. Kim. Parameter-Mismatching on the Attractor Bubbling in Coupled Chaotic Systems. *Journal of the Korean Physical Society*, 44(3):510–513, 2004.

[188] W. W. Lin, C. C. Peng, and C. S Wang. Synchronization in Coupled Map Lattices with Periodic Boundary Conditions. *International Journal of Bifurcation and Chaos*, 9:1635–1652, 1999.

[189] W.-W. Lin and Y.-Q. Wang. Chaotic Synchronization in Coupled Map Lattices with Periodic Boundary Conditions. *SIAM Journal on Applied Dynamical Systems*, 1(2):175–189, 2002.

[190] G. L. Liu. Weighted Residual Decomposition Method in Nonlinear Applied Mathematics. pages 643–648, Suzhou, China, 1995. 6th Congress of Modern Mathematics and Mechanics (MM M-VI).

[191] X. D. Liu, S. Osher, and T. Chan. Weighted Essencially Non-Oscillatory Schemes. *Journal of Computational Physics*, 115:200, 1994.

[192] Z. Liu, Y.-C. Lai, L. Billings, and I. B. Schwartz. Transition to Chaos in Continuous-Time Random Dynamical Systems. *Physical Review Letters*, 88(12):124101 (4 pages), 2002.

[193] Z. Liu, Y.-C. Lai, and M. A. Matias. Universal Scaling of Lyapunov Exponents in Coupled Chaotic Oscillators. *Physical Review E*, 67:045203 (4 pages), 2003.

[194] W. Malfliet. Solitary Wave Solutions of Nonlinear Wave Equations. *American journal of physics*, 60:650–654, 1992.

[195] R. Mañé. *Introdução a Teoria Ergódica*. IMPA, Rio de Janeiro, 1983.

[196] M. A. Matías and J. Guémez. Stabilization of Chaos by Proportional Pulses in the System Variables. *Physical Review Letters*, 72:1455–1458, 1994.

[197] J. P. Matos. Introdução às Equações Diferenciais Parciais. IST, Lisboa, 1999.

[198] T. Mavoungou and Y. Cherruault. Convergence of Adomian's Method and Applications to Non-Linear Partial Differential Equations. *Kybernetes*, 21(6):13–25, 1992.

[199] T. Mavoungou and Y. Cherruault. Numerical Study of Fisher's Equation by Adomian's Method. *Mathematical and Computer Modelling*, 19(1):89–95, 1994.

[200] L. A. Medeiros, J. L. Ferrel, and A. C. Biazutti. *Métodos Clássicos Em Equações Diferenciais Parciais*. UFRJ, Rio de Janeiro, 2000.

[201] L. A. Medeiros and M. M. Miranda. *Espaços de Sobolev*. UFRJ, Rio de Janeiro, 2 edition, 2000.

[202] M. Meneguzzi, H. Politano, A. Pouquet, and M. Zolver. A Sparse-Mode Spectral Methods for the Simulation of Turbulent Flows. *Journal of Computational Physics*, 123:32–44, 1996.

[203] R. Mickens. A Nonstandard Finite Difference Scheme for the Diffusionless Burgers Equation with Logistic Reaction. *Mathematics and Computers in Simulation*, 62:117–124, 2003.

[204] J. Milnor. On the Concept of Attractor. *Communications in Mathematical Physics*, 99(2):177–195, 1985.

[205] J. Milnor. On the Concept of attractor: Correction and Remarks. *Communications in Mathematical Physics*, 102(3):517–519, 1985.

[206] S. V. Muniandy and I. M. Moroz. Galerkin Modelling of the Burgers Equation Using Harmonic Wavelets. *Physics Letters A*, 235:352–356, 1997.

[207] M. A. Murison. Notes on How to Numerically Calculate the Maximum Lyapunov Exponent. http://arnold.usno.navy.mil/murison/papers/Notes/LyapCalc/LyapCalc.pdf (consulted in 03/2003), September 1995.

[208] A. H. Nayfeh. *Perturbation Methods*. Jonh Wiley and Sons, 1973.

[209] F. Ndeges. Non-Oscillatory Spectral Analysis. Technical report, Polytechnic Institute and State University, Virginia, March 2004.

[210] J. Nee and J. Duan. Limit Set of Trajectories of the Coupled Viscous Burgers' Equations. *Applied Mathematical Letters*, 11(1):57–61, 1998.

[211] N. Ngarhasta, B. Some, K. Abbaoui, and Y. Cherruault. New Numerical Study of Adomian Method Applied to a Diffusion Model. *Kybernetes*, 31(1):61–75, 2002.

[212] A. V. Oppenheim and R. W. Schafer. *Discrete-Time Signal Processing*. Prentice-Hall, 1989.

[213] R. Z. Ouedraogo, Y. Cherruault, and K. Abbaoui. Convergence of Adomians Method Applied to Algebraic Equations. *Kybernetes*, 29(9/10):1298–1305, 2000.

[214] T. Özis, E. N. Aksan, and A. Özdes. A Finite Element Approach for Solution of Burgers' Equation. *Applied Mathematics and Computation*, 139:417–428, 2003.

[215] T. Ozis and A. Özdes. A Direct Variational Method Applied to Burgers Equation. *Journal of Computational and Applied Mathematics*, 71:163–175, 1996.

[216] E. J. Parkes and B. R. Duffy. Travelling Solitary Wave Solutions to a Computed KdV-Burgers Equation. *Physics Letters A*, 229:217–220, 1997.

[217] L. Junge, U. Parlitz. Dynamic Coupling in Partitioned State Space. pages 245–248, Dresden, Germany, September 2000. International Symposium on Nonlinear Theory and its Applications (NOLTA2000).

[218] L. Kocarev, J. Bröcker, U. Parlitz. Normal Hyperbolicity and Robust Synchronization. pages 37–40, Hawaii, USA, November 1999. International Symposium on Nonlinear Theory and its Applications (NOLTA99).

[219] U. Parlitz and L. Junge. Synchronization of Chaotic Systems. Karsruhe, Germany, September 1999. Proceedings of the European Control Conference ECC'99. Paper F1056-5.

[220] U. Parlitz, L. Junge, and L. Kocarev. Subharmonic Entrainment of Unstable Period Orbits and Generalized Synchronization. *Physical Review Letters*, 79(17):3158–3161, 1997.

[221] U. Parlitz, L. Junge, and L. Kocarev. Nonidentical Synchronization of Identical Systems. *International Journal of Bifurcation and Chaos*, 9(12):2305–2309, 1999.

[222] U. Parlitz, L. Yunge, and W. Lauterborn. Experimental Observation of Phase Synchronization. *Physical Review E*, 54(2):2115–2117, 1996.

[223] L. M. Pecora. Synchronization Conditions and Desynchronization Patterns in Coupled Limit-Cycle and Chaotic Systems. *Physical Review E*, 58(1):347–360, 1998.

[224] L. M. Pecora and T. L. Carroll. Synchronization in Chaotic Systems. *Physical Review Letters*, 64:821–823, 1990.

[225] L. M. Pecora and T. L. Carroll. Driving Systems with Chaotic Signals. *Physical Review A*, 44:2374, 1991.

[226] L. M. Pecora, T. L. Carroll, and J. F. Heagy. Statistics for Mathematical Properties of Maps Between Time Series Embeddings. *Physical Review E*, 52(4):3420–3439, 1995.

[227] L. M. Pecora, T. L. Carroll, G. A. Johnson, D. J. Mar, and J. F. Heagy. Fundamentals of Synchronization in Chaotic Systems, Concepts, and Applications. *Chaos, an Interdisciplinary Journal of Nonlinear Science*, 7(4):520–543, 1997.

[228] J. H. Peng, E. J. Ding, M. Ding, and W. Yang. Synchronizing Hyperchaos with a Scalar Transmitted Signal. *Physical Review Letters*, 76:904–907, 1996.

[229] A. Pikovsky and A. Politi. Dynamic Localization of Lyapunov Vectors in Spacetime Chaos. *Nonlinearity*, 11:1049–1062, 1998.

[230] A. Pikovsky, M. Rosenblum, and J. Kurths. Phase Synchronization in Regular and Chaotic Systems. *International Journal of Bifurcation and Chaos*, 10(10):2291–2305, 2000.

[231] H. Pina. *Métodos Numéricos*. McGraw-Hill, 1995.

[232] A. D. Polyanin and V. F. Zaitsev. *Handbook of Nonlinear Partial Differential Equations*. Chapman & Hall/CRC, 2004.

[233] J. Qiu and C.-W. Shu. Finite Difference Weno Schemes with Lax-Wendroff Type Time Discretizations. *Society for Industrial and Applied Mathematics*, 24(6):2185–2198, 2003.

[234] R. Rach. On the Adomian (Decomposition) Method and Comparisons with Picard's Method. *Journal of Mathematical Analysis and Applications*, 128:480–483, 1987.

[235] P.-A. Raviart and J.-M. Thomas. *Introduction À L'Analyse Numérique Des Équations Aux Dérivées Partielles*. Dunod, Paris, 1998.

[236] A. J. Roberts. Holistic Discretization Ensures Fidelity to Burger's Equation. *Applied Numerical Mathematics*, 37:371–396, 2001.

[237] M. Rosenblum, A. S. Pikovsky, and J.Kurths. Phase Synchronization of Chaotic Oscillators. *Physical Review Letters*, 76:1804–1807, 1996.

[238] M. G. Rosenblum, A. S. Pikovsky, and J. Kurths. From Phase to Lag Synchronization in Coupled Chaotic Oscillators. *Physical Review Letters*, 78(22):4193–4196, 1997.

[239] M. G. Rosenblum, A. S. Pikovsky, and J. Kurths. Phase Synchronization in Driven and Coupled Chaotic Oscillators. *IEEE Transactions on circuits and systems-I*, 44(10):874–881, 1997.

[240] J. Ruan and L. Li. An Improved Method in Synchronization of Chaotic Systems. *Communications in Nonlinear Science & Numerical Simulation*, 3(3):140–143, 1998.

[241] N. F. Rulkov. Images of Synchronized Chaos: Experiments with Circuits. *Chaos*, 6(3):262–279, 1996.

[242] N. F. Rulkov, V. S. Afraimovich, C. T. Lewis, J.-R. Chazottes, and A. Cordonet. Multivalued Mappings in Generalized Chaos Synchronization. *Physical Review E*, 64:016217 (11 pages), 2001.

[243] N. F. Rulkov and C. T. Lewis. Subharmonic Destruction of Generalized Chaos Synchronization. *Physical Review E*, 63:065204 (4 pages), 2001.

[244] N. F. Rulkov, M. M. Sushchik, L. S. Tsimring, and H. D. I. Abarbanel. Generalized Synchronization of Chaos in Directionally Coupled Chaotic Systems. *Physical Review E*, 51:980–994, 1995.

[245] L. I. Sedov. *Similarity and Dimensional Methods in Mechanics*. CRC Press, Boca Raton, 1993.

[246] N. Shawagfeh and D. Kaya. Comparing Numerical Methods for the Solutions of Systems of Ordinary Differential Equations. *Applied Mathematics Letters*, 17:323–328, 2004.

[247] C.-W. Shu. Essentially Non-Oscillatory and Weighted Essentially Non-Oscillatory Schemes for Hyperbolic Conservation Laws. Technical Report 97-65, Institute for Computer Applications in Science and Engineering, Hampton Virginia, Novembre 1997.

[248] C.-W. Shu and S. Osher. Efficient Implementation of Essentially Nonoscillatory Shock-Capturing Schemes, II. *Journal of Computational Physics*, 83(1), 1989.

[249] Y. G. Sinai. A Remark Concerning the Thermodynamic Limit of the Lyapunov Spectrum. *International Journal of Bifurcation and Chaos*, 6(6):1137–1142, 1996.

[250] P. So, E. Brreto, K. Josic, E. Sander, and S. J. Schiff. Limits to the Experimental Detection of Nonlinear Synchrony. *Physical Review E*, 65:046225 (5 pages), 2002.

[251] J. C. Sprott. Numerical Calculation of Largest Lyapunov Exponent. http://sprott.physics.wisc.edu/chaos/lyapexp.htm, 13 de Outubro 1998.

[252] S. Taherion and Y.-C. Lai. Observability of Lag Synchronization of Coupled Chaotic Oscillators. *Physical Review E*, 59(6):R6247 (4 pages), 1999.

[253] S. Tajima and H. S. Greenside. Microextensive Chaos of a Spatially Extended System. *Physical Review E*, 66:017205 (4 pages), 2002.

[254] Z. Tasev, L. Kocarev, L. Junge, and U. Parlitz. Synchronization of Kuramoto-Sivashinsky Equations Using Spatially Local Coupling. *International Journal of Bifurcation and Chaos*, 10(4):869–873, 2000.

[255] L. N. Trefethen. *Spectral Methods in Matlab*. SIAM, Society for Industrial and Applied Methematics, Philadelphia, 2000.

[256] C. Tresser and P. A. Worfolk. Resynchronizing Dynamical Systems. *Physics Letters A*, 229(5):293–298, 1997.

[257] C. Tresser, P. A. Worfolk, and H. Bass. Master-Slave Synchronization from the Point of View of Global Dynamics. *Chaos*, 5(4):693–699, 1995.

[258] F. E. Udwadia and H. F. Bremen. An Efficient and Stable Approach for Computation of Lyapunov Characteristic Exponents of Continuous Dynamical Systems. *Applied Mathematics and Computation*, 121:219–259, 2001.

[259] F. E. Udwadia and H. F. Bremen. Computation of Lyapunov Characteristic Exponents for Continuous Dynamical Systems. *Zeitschrift für Angewandte Mathematik und Physik*, 53:123–146, 2002.

[260] F. E. Udwadia, H. F. Bremen, and W. Proskurowski. A Note on the Computation of the Largest P LCEs of Discrete Dynamical Systems. *Applied Mathematics and Computation*, 114:205–214, 2000.

[261] P. Vadasz and S. Olek. Convergence and Accuracy of Adomian's Decomposition Method for the Solution of Lorenz Equations. *International Journal of Heat and MassTransfer*, 43:1715–1734, 2000.

[262] S. C. Venkataramani, B. R. Hunt, and E. Ott. Transitions to Bubbling of Chaotic Systems. *Physical Review Letters*, 77(27):5361–5364, 1996.

[263] S. N. Venkatarangan and K. Rajalakshmi. Modification of Adomian's Decomposition Method to Solve Equations Containing Radicals. *Computers and Mathematics with Applications*, 29(6):75–80, 1995.

[264] P. Walters. *An Introduction to Ergodic Theory*. Springer-Verlag New York Inc., 1982.

[265] X. Wang, M. Zhan, C.-H. Lai, and Y.-C. Lai. Strange Nonchaotic Attractors in Random Dynamical Systems. *Physical Review Letters*, 92(7):074102 (4 pages), 2004.

[266] Z. J. Wang and R. F. Chen. Optimized Weighted Essencially Nonoscillatory Schemes for Linear Waves with Discontinuity. *Journal of Computational Physics*, 174:381–404, 2001.

[267] A.-M. Wazwaz. A New Approach to the Nonlinear Advection Problem: An Application of the Decomposition Method. *Applied Mathematics and Computation*, 72:175–181, 1995.

[268] A.-M. Wazwaz. The Decomposition Method for Approximate Solution of the Goursat Problem. *Applied Mathematics and Computation*, 69:299–311, 1995.

[269] A.-M. Wazwaz. Necessary Conditions for the Appearance of Noise Terms in Decomposition Solution Series. *Applied Mathematics and Computation*, 81:265–274, 1997.

[270] A.-M. Wazwaz. A Comparison Between Adomian Decomposition Method and Taylor Series Method in the Series Solutions. *Applied Mathematics and Computation*, 97:37–44, 1998.

[271] A.-M. Wazwaz. A Reliable Technique for Solving the Wave Equation in an Infinite One-Dimensional Medium. *Applied Mathematics and Computation*, 92:1–7, 1998.

[272] A.-M. Wazwaz. A Reliable Modification of Adomian Decomposition Method. *Applied Mathematics and Computation*, 102:77–86, 1999.

[273] A.-M. Wazwaz. Analytica Approximations and Padé Approximants for Volterra's Population Model. *Applied Mathematics and Computation*, 100:13–25, 1999.

[274] A.-M. Wazwaz. The Modified Decomposition Method and Padé Approximants for Solving the Thomas-Fermi Equation. *Applied Mathematics and Computation*, 105:11–19, 1999.

[275] A.-M. Wazwaz. A New Algorithm for Calculating Adomian Polynomials for Nonlinear Operators. *Applied Mathematics and Computation*, 111:53–69, 2000.

[276] A.-M. Wazwaz. A Note on Using Adomian Decomposition Method for Solving Boundary Value Problems. *Foundations of Physics Letters*, 13(5):493–498, 2000.

[277] A.-M. Wazwaz. Approximate Solutions to Boundary Value Problems of Higher Order by the Modified Decomposition Method. *Computers and Mathematics with Applications*, 40:679–691, 2000.

[278] A.-M. Wazwaz. The Decomposition Method Applied to Systems of Partial Differential Equations and to the Reaction-Diffusion Brusselator Model. *Applied Mathematics and Computation*, 110:251–264, 2000.

[279] A.-M. Wazwaz. A Computational Approach to Soliton Solutions of the Kadomtsev-Petviashvili Equation. *Applied Mathematics and Computation*, 123:205–217, 2001.

[280] A.-M. Wazwaz. A New Algorithm for Solving Differential Equations of Lane-Emden Type. *Applied Mathematics and Computation*, 118:287–310, 2001.

[281] A. M. Wazwaz. A Reliable Algorithm for Obtaining Positive Solutions for Nonlinear Boundary Value Problems. *Computers & Mathematics with Applications*, 41:1237–1244, 2001.

[282] A-M. Wazwaz. A Reliable Algorithm for Solving Boundary Value Problems for Higher-Order Integro-Differential Equations. *Applied Mathematics and Computation*, 118:327–342, 2001.

[283] A.-M. Wazwaz. A Study of Nonlinear Dispersive Equations with Solitary-Wave Solutions Having Compact Support. *Mathematics and Computers in Simulation*, 56:269–276, 2001.

[284] A.-M. Wazwaz. Construction of Solitary Wave Solutions and Rational Solutions for the KdV Equation by Adomian Decomposition Method. *Chaos Solitons & Fractals*, 12:2283–2293, 2001.

[285] A.-M. Wazwaz. Construction of Soliton Solutions and Periodic Solutions of the Boussinesq Equation by the Modified Decomposition Method. *Chaos Solitons & Fractals*, 12:1549–1556, 2001.

[286] A.-M. Wazwaz. A New Method for Solving Singular Initial Value Problems in the Second-Order Ordinary Differential Equations. *Applied Mathematics and Computation*, 128:45–57, 2002.

[287] A.-M. Wazwaz. A Reliable Treatment for Mixed Volterra-Fredholm Integral Equations. *Applied Mathematics and Computation*, 127:405–414, 2002.

[288] A.-M. Wazwaz. The Existence of Noise Terms for Systems of Inhomogeneous Diferential and Integral Equations. *Applied Mathematics and Computation*, 146:81–92, 2003.

[289] A.-M. Wazwaz and S. M. El-Sayed. A New Modification of the Adomian Decomposition Method for Linear and Nonlinear Operators. *Applied Mathematics and Computation*, 122:393–405, 2001.

[290] A.-M. Wazwaz and A. Gorguis. An Analytic Study of Fisher's Equation by Using Adomian Decomposition Method. *Applied Mathematics and Computation*, 154:609–620, 2004.

[291] A.-M. Wazwaz and A. Gorguis. Exact Solutions for Heat-Like and Wave-Like Equations with Variable Coefficients. *Applied Mathematics and Computation*, 149:15–29, 2004.

[292] A.-M. Wazwaz and S. A. Khuri. A Reliable Technique for Solving the Weakly Singular Second-Kind Volterra-Type Integral Equations. *Applied Mathematics and Computation*, 80:287–299, 1996.

[293] G. W. Wei. Synchronization of Single-Side Locally Averaged Adaptative Coupling and Its Application to Shock Capturing. *Physical Review Letters*, 86(16):3542–3545, 2001.

[294] G. W. Wei, D. S. Zhang, D. J. Kouri, and D. K. Hoffman. A Robust and Reliable Approach to Nonlinear Dynamical Problems. *Computer Physics Communications*, 111:87–92, 1998.

[295] G. W. Wei, D. S. Zhang, D. J. Kouri, and D. K. Hoffman. Distributed Approximation Functional Approach to Burgers' Equation in One and Two Space Dimensions. *Computer Physics Communications*, 111:93–109, 1998.

[296] J. A. C. Weideman and S. C. Reddy. A Matlab Differentiation Matrix Suite. *ACM Transactions on Mathematical Software*, 26(4):465–519, 2000.

[297] G. B. Whitham. *Linear and Nonlinear Waves*. Wiley, New York, 1974.

[298] A. Wolf, J. B. Swift, H. L. Swinney, and J. A. Vastano. Determining Lyapunov Exponents from a Time Series. *Physica D*, 16:285–317, 1985.

[299] WolframResearch. Soliton. http://www.mathworld.wolfram.com/soliton.html (consulted in 03/2004).

[300] Y. Wun and X. Wu. Linearized and Rational Approximation Method for Solving Non-Linear Burgers' Equation. *International Journal for Numerical Methods in Fluids*, 45:509–525, 2004.

[301] H. Xi, R. Toral, J. D. Gunton, and M. I. Tribelsky. Extensive Chaos in the Nikolaevskii Model. *Physical Review E*, 62:R17–R20, 2000.

[302] H. Y. Xu, M. D. Matovic, and A. Pollard. Finite Difference Schemes for Three-Dimensional Time-Dependent Convection-Diffusion Equation Using Global Discretization. *Journal of Computational Physics*, 130:109–122, 1997.

[303] M. Zhan, G. Hu, D.-H. He, and W.-Q. Ma. Phase Locking in on-Off Intermittency. *Physical Review E*, 64:066203 (4 pages), 2001.

[304] L. Zhu and Y.-C. Lai. Experimental Observation of Generalized Time-Lagged Chaotic Synchronization. *Physical Review E*, 64:045205 (4 pages), 2001.